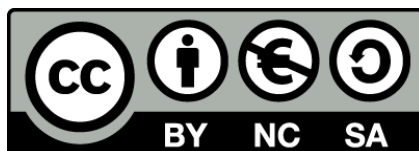




UNIVERSITAT DE  
BARCELONA

**High throughput determination  
of relevant physicochemical parameters  
in the drug discovery and HPLC processes.  
Microfluidic devices**

Abdulkarim Khalaf Albishri



Aquesta tesi doctoral està subjecta a la llicència **Reconeixement- NoComercial – Compartir Igual 4.0. Espanya de Creative Commons.**

Esta tesis doctoral está sujeta a la licencia **Reconocimiento - NoComercial – Compartir Igual 4.0. España de Creative Commons.**

This doctoral thesis is licensed under the **Creative Commons Attribution-NonCommercial-ShareAlike 4.0. Spain License.**

2024

Tesi doctoral

Abdulkarim Khalaf Albishri

---

High throughput determination of relevant physicochemical parameters in the drug discovery and HPLC processes. Microfluidic devices

---

Abdulkarim Khalaf Albishri



UNIVERSITAT DE  
BARCELONA

**Doctoral program in Analytical Chemistry and the Environment**

**Department of Chemical Engineering and Analytical Chemistry**

**Faculty of Chemistry**

**High throughput determination of relevant physicochemical  
parameters in the drug discovery and HPLC processes.**

**Microfluidic devices**

**Abdulkarim Khalaf Albishri**

**Prof. Martí Rosés Pascual, Catedràtic D'Universitat al Departament  
D'Enginyeria Química I Química Analítica De La Universitat De Barcelona**

**Dr. Joan Marc Cabot Canyelles , Principal Investigator at Leitat Technology  
Center, Innovació 2, 08225 Terrassa, Spain**

Prof. Martí Rosés Pascual, Catedràtic d'Universitat at the Chemical Engineering and Analytical Chemistry Department of University of Barcelona

Dr. Joan Marc Cabot Canyelles , Principal Investigator at Leitat Technology Center, Innovació 2, 08225 Terrassa, Spain

## **Declare:**

That the present work entitled

“High throughput determination of relevant physicochemical parameters in the drug discovery and HPLC processes. Microfluidic devices”

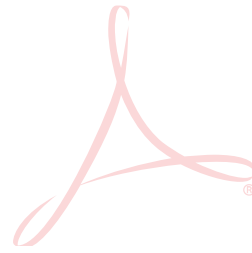
has been achieved by **Abdulkarim Khalaf Albishri** at the laboratories of the Analytical Chemical Section of University of Barcelona under their supervision.

And for this to be recorded, we issue this certificate.

Barcelona, January , 2024



Prof. Martí Rosés Pascual



Dr. Joan Marc Cabot Canyelles

## Acknowledgement

I would like to express my deepest gratitude to the divine for the countless blessings bestowed upon me. Additionally, I would like to extend my immense appreciation to Prof. Martí Rosés and Dr. Joan Marc Cabot for their exceptional guidance, unwavering support, valuable insights, constructive feedback, and insightful criticism throughout the entirety of my research journey. Their expertise has been invaluable in shaping the outcome of my work.

My deepest regards and my heartfelt gratitude to Dr. Elisabet Fuguet for her invaluable contributions to my journey. Her wealth of experience and knowledge have been a constant source of enlightenment throughout my PhD.

I would also like to express my appreciation to all my colleagues, both in the lab and beyond, who have become dear friends and companions on this academic path. Together, we have shared incredible moments and created memories that I will cherish for a lifetime. Their camaraderie and support have made this journey all the more meaningful and enjoyable.

To each of these individuals, I am truly grateful for the impact they have had on my personal and academic development. Their guidance, friendship, and encouragement have been invaluable, and I am honored to have had the opportunity to work alongside them.

I am extremely thankful to my parents and brothers for their continuous support, my beloved wife (Rawan) for her constant encouragement, and my lovely kids Wajd and Abdulmohsen for staying with me and keeping me strong, which has been instrumental in my success.

Leitat will always have a special place in my heart for hosting me for three wonderful months during my PhD. Their fantastic team was crucial in increasing my understanding of microfluidic systems, as well as their assistance and collaboration in preparing microfluidic plates.

Finally, a special thanks to my sponsor, King Abdulaziz University, for their generous support throughout my PhD journey. Their financial support has been critical in allowing me to continue my studies. I am very appreciative of their commitment to my education and for allowing me to expand my knowledge.



# Acronyms

ACRONYM	Description
A	Coefficient A in activity Debye Hückel equation
a	Activity
AN	Analyte
EP	Equivalent point
B	Coefficient B in activity Debye Hückel equation
BGE	Background electrolyte
CE	Capillary electrophoresis
CZE	Capillary zone electrophoresis
E	Electric field strength
EOF	Electroosmotic flow
IS	Internal standard
I	Ionic strength
IS-CE	Internal standard capillary electrophoresis method
$K_a$	Acid-base dissociation constant
$L_T$	Total length of capillary
$L_D$	Length of the capillary to the detector
$\mu_{ep}$	Electrophoretic mobility
$\mu_{app}$	Apparent mobility
$\mu_A^-$	Limiting mobility of an acid
$\mu_{BH}^+$	Limiting mobility of a base
pH	Negative logarithm of the hydrogen ion
$pK_a$	Negative log of acid-base constant
$pK'_a$	Negative log of working acid-base constant
$pK_{a,A}$	Negative log of dissociation constant of neutral acid
$pK_{a,B}$	Negative log of acid-base constant of neutral base (protonated acid)
T	Temperature
q	Analyte net charge
$t_m$	Migration time of an analyte
$t_o$	Migration time of the electroosmotic flow marker
UV-Vis	Ultraviolet-visible spectroscopy
MS	Mass spectrometers
V	Voltage

---



---

$\gamma$	Activity coefficient
$\alpha$	Radius of the molecule
$v_{\text{app}}$	Velocity of compound in a capillary
$z$	Charge in Debye Hückel equation
DMSO	Dimethyl-sulfoxide
HPLC	High-performance liquid chromatography
RPLC	Reversed phase liquid chromatography
UPLC	Ultra High-Performance Liquid Chromatography
WHO	World health organization
OCED	Organisation for Economic Co-operation and Development
$\log P_{\text{o/w}}$	Octanol-water partition Coefficient
$\log D_{\text{o/w}}$	Octanol-water distribution Coefficient
$C_{\text{o}}$	Concentration of solute in the organic phase
$C_{\text{w}}$	Concentration of solute in the aqueous phase
$r$	Proper standard solution dilution factor
$k$	Retention factor
MCE-CCD	Microchip capillary electrophoresis with contactless conductivity detection
MLLE	Microfluidic liquid-liquid extraction
PDMS	polydimethylsiloxane
PMMA	Poly(methyl methacrylate)
hPET	hydrophilic polyethylene terephthalate
CNC	Computer Numerical Control
STL	Standard triangulation language
3DP	3D printer
ANSI/SLAS	American National Standards Institute/Society for Laboratory Automation and Screening
CAD	Computer-aided design
n.s.	not specified in the reference.

---



---

## Abstract

Determining the acidity ( $pK_a$ ) and lipophilicity ( $\log P_{o/w}$ ) of organic compounds is fundamental in analytical chemistry fields, with potential relevance in drug development, material science, analytical separation, and environmental research. A precise estimation of these physicochemical parameters is important for estimating compound behavior and distribution in different biological and chemical systems. Fast determination of  $pK_a$  of very insoluble drugs has become an essential tool in drug development as it frequently creates compounds that are highly lipophilic and sparingly soluble in water. Also, studying the pharmacokinetics and pharmacodynamics of a proposed drug involves a thorough knowledge of its ionization state and hydrophobicity.

In the first part of the thesis, a high-throughput internal standard capillary electrophoresis (IS-CE) method was established to determine the  $pK_a$  of ISs at different concentrations of methanol and acetonitrile from 0 to 90% (v/v). IS-CE is a  $pK_a$  determination method based on the use of a known  $pK_a$  reference compound as an internal standard (IS), whose nature and  $pK_a$  value are similar to those one of the analytes. Internal standard mobility is measured under the same conditions as analyte mobility when injected at the same time, hence any change in experimental conditions influences both analyte and IS equally. Whereas the traditional CE approach needs potentiometric measurement of the pH of the buffers used, IS-CE uses IS to calculate the true pH in our electrophoretic system and reduces measurement mistakes. Herein, the acid and base scales of methanol-water mixtures and acetonitrile-water mixtures were properly anchored to the potentiometrically obtained  $pK_a$  values of reference compounds to get absolute  $pK_a$  scales. As a consequence, a set of 46 acid-base compounds with changing structures were proposed as internal standards for consistent  $pK_a$  measurements in methanol-water and acetonitrile-water mixtures buffers using capillary electrophoresis. The determined ISs reference set facilitates the determination of analytes  $pK_a$  and measurement of buffer pH in the range 4-11.5 (in water) for any methanol-water and acetonitrile-water composition.

Secondly, to prove its feasibility, the IS-CE approach was successfully used to determine the aqueous  $pK_a$  in methanol-aqueous buffer compositions up to 40% of methanol in volume. The Yasuda-Shedlovsky extrapolation method was utilized to determine seven drugs of different chemical nature with intrinsic water solubilities lower than  $10^{-6}$  M. The results were successfully compared to literature ones obtained by other approaches. It is

concluded then that the IS-CE methodology permits the measurement of aqueous  $pK_a$  values using lower ratios of methanol than the classical method, becoming then more accurate in the extrapolation procedure than other reference methods.

Finally, since methanol-water and acetonitrile-water mixtures are solvents of interest in liquid chromatographic separations because of their use as the mobile phase, the IS-CE method was also applied to measure the  $pK_a$  of eight organic bases in methanol-water and acetonitrile-water mixtures (0-90%,v/v), which are usually used as test compounds in HPLC column evaluation.

As a result of this work, the IS-CE method was proven to be a fast and simple approach for determining the pH of the buffer and the  $pK_a$  of analytes in typical HPLC systems (RPLC, HILIC) in both methanol-water mixtures and acetonitrile-water mixtures. The degree of ionization of the analytes may be easily determined using them, making it easier to choose the mobile phase composition and thus enhance analytical separations.

In the second part of the thesis, a new approach based on microfluidics was developed to determine the octanol-water partition. The octanol-water partition coefficient is crucial in pharmaceutical and biological sciences as it is a vital metric in predicting chemical distribution and behavior in biological systems. However, the current techniques are time consuming and requires high amounts of solvents. From the need to develop a quicker, more cost-effective, and more sustainable method, microfluidics has raised as a powerful miniaturized analytical tool.

As a first step, a design with a perpendicular configuration of the channels was developed using direct 3D printed microfluidics. A gravitational perfusion system was implemented to create a spontaneous flow within the octanol and water channels without the need for external pump. The movement of octanol and water phases was successfully validated using fluorescent dyes. After that, the intensity of the fluorescent dye was used to evaluate the partition dynamics in static and dynamic conditions. The results prove that the proposed design with this microfluidic methodology allows the evaluation of molecule partition, achieving high efficiency partition and reaching the equilibrium of O/W partition faster than conventional techniques.

Later, the design was adapted to a parallel configuration of the channels to be compatible with up-scalable manufacturing techniques and parallelize it for up to 56 simultaneous determinations in a single platform. Finally, both the perpendicular and parallel designs were validated using several drugs with well standardize  $\log P_{o/w}$  values that cover a wide range of lipophilicity.

The microfluidic device was coupled with HPLC to determine their partition coefficients from the peak areas of the compounds in octanol and in water after partition. Good agreement with the literature values was achieved, showing the capability of microfluidic chips for precise and accurate prediction of the partition coefficient. Finally, the progress of a cost-effective and consistent method for predicting partition coefficient via microfluidic chips demonstrated a great advancement in the field of analytical chemistry, with powerful applications in drug discovery and other related fields. The results gotten from this investigation offer an establishment for additional research and advance of this approach.

To summarize, estimating  $pK_a$  and  $\log P_{o/w}$  values is vital in analytical chemistry, with capacity applications in drug development, material science, and environmental research. A precise estimation of these physicochemical parameters is important for predicting compound performance and distribution in diverse biological and chemical systems. The use of innovative analytical techniques for verifying  $pK_a$  values, like the IS-CE method for  $pK_a$  and microfluidics for measuring  $\log P_{o/w}$ , represents valuable advances in the field of analytical chemistry. These methods provide low-reagent-consumption, cost-effective, and reliable determination for evaluating these parameters, for high-throughput analysis.

## RESUM

La determinació de l'acidesa ( $pK_a$ ) i de la lipofilitat ( $\log P_{o/w}$ ) dels compostos orgànics és fonamental en els camps de la química analítica, amb rellevància potencial en el desenvolupament de fàrmacs, la ciència dels materials, la separació analítica i la investigació ambiental. Una estimació precisa d'aquests paràmetres fisicoquímics és important per estimar el comportament i la distribució dels compostos en diferents sistemes biològics i químics. La determinació ràpida de les constants l'acidesa ( $pK_a$ ) de fàrmacs molt insolubles s'ha convertit en una eina essencial en el desenvolupament de fàrmacs, ja que sovint crea compostos altament lipòfils i poc solubles en aigua. A més, l'estudi de la farmacocinètica i la farmacodinàmica d'un determinat fàrmac implica un coneixement exhaustiu del seu estat d'ionització i hidrofobicitat.

En la primera part de la tesi s'estableix un mètode d'electroforesi capil·lar estàndard interna d'alt rendiment (IS-CE) per determinar el  $pK_a$  de l'analit àcid-base en mescles d'aigua amb solvents orgànics. En aquest treball es va establir un mètode d'electroforesi capil·lar estàndard d'alt rendiment (IS-CE) per determinar el  $pK_a$  dels IS a diferents concentracions de metanol i acetonitril del 0 al 90% (v/v). IS-CE és un mètode de determinació de valors de  $pK_a$  basat en l'ús d'un compost de referència de  $pK_a$  conegut com a patró intern (IS), de natura i valor de  $pK_a$  similars als de l'analit. La mobilitat del patró intern es mesura en les mateixes condicions que la mobilitat de l'analit quan s'injecta al mateix temps, per tant, qualsevol canvi en les condicions experimentals influeix tant en l'analit com en l'IS. El mètode de CE tradicional requereix la mesura potenciomètrica del pH dels tampons utilitzats, mentre que IS-CE utilitza IS per calcular el pH real al nostre sistema electroforètic i reduir els errors de mesura. Les escales d'àcid i base de les mescles de metanol-aigua i les mescles d'acetonitril-aigua s'han ancorat correctament als valors de  $pK_a$  obtinguts potenciomètricament dels compostos de referència per obtenir escales de  $pK_a$  absolutes. Com a conseqüència, es proposa un conjunt de 46 compostos àcid-base amb estructures canviantes com a estàndards interns per a mesures coherents de  $pK_a$  en mescles metanol-aigua i acetonitril-aigua mitjançant electroforesi capil·lar. El conjunt establert de patrons interns facilita la determinació dels analits  $pK_a$  i la mesura del pH del tampó en el rang 4-11,5 (en aigua) per a qualsevol composició metanol-aigua i acetonitril-aigua.

En segon lloc, per demostrar la seva viabilitat, l'enfocament IS-CE es va utilitzar amb èxit per determinar el  $pK_a$  aquós en composicions tampó aquoses de metanol fins a un 40% del volum de metanol. El mètode d'extrapolació De Yasuda-Shedlov es va utilitzar per

determinar set fàrmacs de diferent naturalesa química amb solubilitats d'aigua intrínseques inferiors a  $10^{-6}$  M. Els resultats es van comparar amb èxit amb els de la literatura obtinguts per altres enfocaments. Es conclou llavors que la mètode IS-CE permet mesurar valors aquosos de  $pK_a$  utilitzant proporcions més baixes de metanol que el mètode clàssic, convertint-se llavors en més precís en el procediment d'extrapolació que altres mètodes de referència.

Finalment, com que les mescles metanol-aigua i acetonitril-aigua són dissolvents d'interès en separacions per cromatografia de líquid pel seu ús com a fase mòvil, també es va aplicar el mètode IS-CE per mesurar el  $pK_a$  de vuit bases orgàniques en mescles de metanol-aigua (0 -90%, v/v) i d'acetonitril-aigua, que s'utilitzen habitualment en l'avaluació de columnes de HPLC.

Com a resultat d'aquest treball, es va demostrar que el mètode IS-CE era un enfocament ràpid i senzill per determinar el pH del tampó i el  $pK_a$  d'analits en sistemes de HPLC típics (RPLC, HILIC) tant en mescles de metanol-aigua com en mescles d'acetonitril-aigua. El grau d'itització dels analits es pot determinar fàcilment mitjançant ells, cosa que facilita l'elecció de la composició de fase mòvil i, per tant, millora les separacions analítiques.

A la segona part de la tesi, es va desenvolupar un nou mètode basat en la microfluídica per determinar la partició octanol-aigua. El coeficient de partició octanol-aigua és crucial en ciències farmacèutiques i biològiques, ja que és una paràmetre vital per predir la distribució química i el comportament en sistemes biològics. No obstant això, les tècniques actuals requereixen molt de temps i requereixen grans quantitats de dissolvents. A partir de la necessitat de desenvolupar un mètode més ràpid, més rendible i més sostenible, microfluídics s'ha plantejat com una potent eina analítica miniaturitzada.

Com a primer pas, es va desenvolupar un disseny amb una configuració perpendicular dels canals mitjançant microfluídica impresa En 3d Directa. Es va implementar un sistema de perfusió per gravetat per crear flux espontani dins dels canals d'octanol i aigua sense necessitat de bombament extern. El moviment de les fases d'octanol i aigua es va validar amb èxit mitjançant colorants fluorescents. Després d'això, es va utilitzar la intensitat del colorant fluorescent per avaluar la dinàmica de partició en condicions estàtiques i dinàmiques. Els resultats demostren que el disseny proposat amb aquesta metodologia microfluídica permet avaluar el particionament de molècules, aconseguint un

particionament d'alta eficiència i aconseguint un equilibri de particionament o/n més ràpid que les tècniques convencionals.

Posteriorment, el disseny es va adaptar a una configuració paral·lela dels canals per ser compatible amb tècniques de manufacturar up-scalable i parallelitzar-lo fins a 56 determinacions simultànies en una sola plataforma. Finalment, tant els dissenys perpendiculars com els paral·lels es van validar utilitzant diversos fàrmacs amb valors  $\log P_{o/w}$  de registre ben estandarditzats que cobreixen una àmplia gamma de lipofilitat.

El dispositiu microfluídic es va acoblar amb HPLC per determinar els seus coeficients de partició a partir de les àrees dels pics d'HPLC dels compostos en octanol i en aigua després de la partició. Es va aconseguir un bon acord amb els valors de la literatura, mostrant la capacitat dels xips microfluídics per a una predicció precisa del coeficient de partició. Finalment, el desenvolupament d'un mètode rendible i consistent per determinar el coeficient de partició mitjançant xips microfluídics demostra un gran avenç en el camp de la química analítica, amb potents aplicacions en el descobriment de fàrmacs i altres camps relacionats. Els resultats obtinguts en aquesta investigació ofereixen una base per a investigacions addicionals i per a l'avançament en aquesta línia.

En resum, l'estimació dels valors de  $pK_a$  i  $\log P_{o/w}$  és vital en química analítica, amb aplicacions en el desenvolupament de fàrmacs, la ciència dels materials i la investigació ambiental. Una estimació precisa d'aquests paràmetres fisicoquímics és important per predir el rendiment i la distribució dels compostos en diversos sistemes biològics i químics. L'ús de tècniques analítiques innovadores per verificar els valors de  $pK_a$ , com el mètode IS-CE, i el mètode microfluídic-HPLC, per mesurar coeficients de partició, representa valuoses innovacions en el camp. Aquests mètodes proporcionen tècniques de baix consum de reactius, rendibles i fiables per avaluar aquests paràmetres en anàlisis d'alt rendiment.

# Table of contents

<b>ACKNOWLEDGEMENT</b>	<b>III</b>
<b>ACRONYMS</b>	<b>V</b>
<b>ABSTRACT</b>	<b>VII</b>
<b>RESUM</b>	<b>X</b>
<b>LIST OF FIGURES</b>	<b>XVII</b>
<b>LIST OF TABLES</b>	<b>XIX</b>
<b>OBJECTIVES</b>	<b>XXI</b>
<b>1. GENERAL INTRODUCTION</b>	<b>1</b>
1.1. The importance of physico-chemical properties in drug discovery	1
1.2. Relevant physico-chemical properties: acid-base dissociation constants ( $pK_a$ )	6
1.2.1. Definition of acid-base constant	6
1.2.2. Methods for determining acid-base dissociation constant.	9
1.2.2.1. Potentiometric titrations	9
1.2.2.2. Spectrophotometric titrations	10
1.2.2.3. Capillary electrophoresis (CE)	11
1.2.3. Capillary electrophoresis	12
1.2.3.1. Definition and Instrumentation	12
1.2.3.2. Mobility and Migration Time	13
1.2.3.3. Detection	15
1.2.3.4. Joule heating effect	16
1.3. Internal Standard Capillary Electrophoresis (IS-CE) Method for determination of $pK_a$ and pH.	18
1.3.1. IS-CE method guiding principle.	18
1.3.2. IS-CE method for determining the acid-base constant of neutral monoprotic acids.	19
1.3.3. IS-CE method for determining acid-base constant of neutral monoprotic bases.	20
1.3.4. IS-CE method for determining the pH.	21
1.4. Acidity constant in organic solvent and water-organic solvent mixtures.	23
1.4.1. Organic solvents and organic-water solvents in capillary electrophoresis	24
1.4.2. Exploring the effect of organic solvents on the $pK_a$ of very insoluble drugs	25
1.4.3. Exploring the effect of organic-water solvents on the analyte $pK_a$ and buffer pH in common HPLC mobile phase.	26

<b>1.5. Relevant physico-chemical properties: octanol-water partition coefficient (<math>\log P_{o/w}</math>)</b>	<b>29</b>
<b>1.5.1. Methods used to determine the octanol-water partition coefficient</b>	<b>32</b>
<b>1.5.1.1. Shake flask method.</b>	<b>32</b>
<b>1.5.1.1.1. Fundamental of the procedure</b>	<b>36</b>
<b>1.5.1.2. Potentiometric method</b>	<b>39</b>
<b>1.5.1.3. Liquid chromatographic methods</b>	<b>41</b>
<b>1.5.1.4. Microchip capillary electrophoresis with contactless conductivity detection (MCE-CCD)</b>	<b>44</b>
<b>1.5.1.5. Determination of <math>\log D_{o/w}</math> via Automated Microfluidic Liquid-Liquid Extraction</b>	<b>47</b>
<b>1.5.1.6. Continuous Flow Partition Coefficient Measurements Using a Microfluidics Devices</b>	<b>49</b>
<b>1.5.2. Comparison between experimental methods</b>	<b>53</b>
<b>2. EXPERIMENTAL WORK</b>	<b>57</b>
<b>2.1. Experimental part and Methodology (<math>pK_a</math>)</b>	<b>58</b>
<b>2.1.1. Potentiometric titrations - analyte solution</b>	<b>58</b>
<b>2.1.1.1. Apparatus</b>	<b>58</b>
<b>2.1.1.2. Chemicals and solvents</b>	<b>58</b>
<b>2.1.1.3. Work procedure</b>	<b>58</b>
<b>2.1.2. Capillary electrophoresis</b>	<b>61</b>
<b>2.1.2.1. Apparatus</b>	<b>61</b>
<b>2.1.2.2. Chemicals and solvents</b>	<b>61</b>
<b>2.1.2.3. Capillary conditioning</b>	<b>63</b>
<b>2.1.2.4. Preparation of sample</b>	<b>63</b>
<b>2.1.2.5. Buffer solution preparation</b>	<b>64</b>
<b>2.1.2.6. Data Analysis</b>	<b>66</b>
<b>2.1.2.7. Determination of <math>pK_a</math> values by IS-CE</b>	<b>66</b>
<b>2.1.2.8. Establishment of the <math>pK_a</math> scales of the internal standards.</b>	<b>66</b>
<b>2.2. Experimental part and methodology (<math>\log P_{o/w}</math>)</b>	<b>68</b>
<b>2.2.1. Determining octanol-water partition coefficient <math>\log P_{o/w}</math></b>	<b>68</b>
<b>2.2.1.1. Chemicals and solvents</b>	<b>68</b>
<b>2.2.1.2. Microfluidic design and fabrication</b>	<b>68</b>
<b>2.2.1.3. Apparatus</b>	<b>71</b>
<b>2.2.1.4. Work procedure</b>	<b>73</b>
<b>3. RESULTS AND DISCUSSIONS</b>	<b>75</b>
<b>3.1. Potentiometric determination of the <math>pK_a</math> of the anchoring acid-base compounds</b>	<b>76</b>
<b>3.1.1. Determination of <math>pK_a</math> by potentiometric titration at different % of Methanol - water mixture</b>	<b>76</b>
<b>3.1.2. Determination <math>pK_a</math> by potentiometric titration at different % of Acetonitrile- water mixture</b>	<b>79</b>
<b>3.2. Joule heating and ohm's law verification</b>	<b>80</b>
<b>3.3. Determination of the <math>pK_a</math> of acid-base analytes by IS-CE at different % of methanol - water mixture and different % of acetonitrile- water mixture.</b>	<b>83</b>

3.3.1.	Trends in variation of $pK_a$ values of acid ISs with different percentages of methanol	96
3.3.2.	Trends in variation of $pK_a$ values of bases ISs with different percentages of methanol	102
3.3.3.	Trends in variation of $pK_a$ values of acids ISs with different percentages of acetonitrile	108
3.3.4.	Trends in variation of $pK_a$ values of bases ISs with different percentages of acetonitrile	113
3.4.	Determination of the aqueous $pK_a$ of very insoluble drugs by capillary electrophoresis: Internal standards for methanol-water extrapolation	119
3.5.	Application of the Capillary Electrophoresis Internal Standards method to determine the $pK_a$ of HPLC columns test bases.	127
3.6.	Determination of partition coefficient using Microfluidic chip	143
3.6.1.	Design and development of the dynamic microfluidic device	143
3.6.2.	Flow working principle and evaluation of hydrodynamic perfusion	147
3.6.3.	Partition dynamics between octanol and water phases in the microfluidic device	148
3.6.3.1.	Evaluation of the partition dynamics in static condition	149
3.6.3.2.	Evaluation of the partition dynamics in perfusion conditions	151
3.6.4.	Up-scalability and parallelization of the microfluidic device	154
3.6.4.1.	Redesign of the dynamic microfluidic device	154
3.6.4.2.	Molecule partition and influence of initial concentration of molecules in microscale octanol-water equilibrium systems	157
3.6.5.	Determination of the octanol-water partition coefficient ( $\log P_{o/w}$ ) of pharmaceutical drugs by microfluidics and HPLC.	161
3.6.5.1.	Determination of $\log P_{o/w}$ of pharmaceutical drugs	164
4.	CONCLUSION	170
	REFERENCES	174



## List of Figures

Figure 1. Relationship of solubility, lipophilicity, and acid dissociation in the context of a pharmaceutical compound. ....	3
Figure 2. Species distribution diagram for the benzoic acid, $pK_a$ 4.20, $I=0$ . HA. ....	9
Figure 3. Basic configuration of the capillary electrophoresis.....	12
Figure 4. Flowchart of the shake-flask method steps.....	33
Figure 5. Bjerrum plot curves for (A) a monoprotic weak acid (HA) and (B) a monoprotic weak base (B). 39	
Figure 6. Microfluidic liquid-liquid extraction using porous membranes prior to analysis with HPLC.....	48
Figure 7. Schematic illustration of a droplet-based microfluidics system .....	50
Figure 8. Methods of microfluidic continuous flow to determine partition coefficient.....	53
Figure 9. Metrohm 888 Titrando.....	60
Figure 10. The titration curves of strong acid titrated with strong base and strong base titrated with strong acid are inverse of each other. ....	60
Figure 11. A) Washing and post-curing steps of the 3d printed mold for pdms soft lithography. B) Shows the diagram of soft lithography and preparation procedure. ....	69
Figure 12. A) Photograph of a custom-built LCD SLA 3 D printer. B) Step-by-step workflow of the LCD SLA 3 D printer the additive manufacturing process for 3D printed microfluidic devices. C) The CAD file is converted into a STL file and later digitally sliced into individual layers that are sequentially printed to build an object in a layer-by-layer manner.....	70
Figure 13. Draw of the microfluidic chip assembl.....	71
Figure 14. A) Rocking shaker. B) Dino-Lite, RK-06A-Digital microscope (device in use).....	72
Figure 15. Joule heating test for the buffers; A) CAPS and B) KOH at different % of MeOH. ....	82
Figure 16. Trends in variation of $pK_a$ values of neutral acids from 0-90 % methanol. ....	99
Figure 17. Variation of the $pK_a$ values of the reference neutral acids at different methanol percentages .....	101
Figure 18. Trends in variation of $pK_a$ values of neutral bases from 0-90 % methanol.....	105
Figure 19. Variation of the $pK_a$ values of the conjugated cationic acids of the neutral bases at different methanol percentages.....	107
Figure 20. Trends in variation of $pK_a$ values of neutral acids from 0-90 % acetonitrile. ....	110
Figure 21. Variation of the $pK_a$ values of the reference neutral acids at different acetonitrile percentages..	112
Figure 22. Trends in variation of $pK_a$ values of neutral bases from 0-90 % acetonitrile.....	116
Figure 23. Variation of the $pK_a$ values of the reference conjugated cationic acids of the neutral bases at different acetonitrile percentage. ....	118
Figure 24. Chemical structure of the set of highly insoluble drugs.....	121
Figure 25. Electropherograms at 20% meoh for glyburide (TC) and 2,5-dinitrophenol (IS) at pH 5.0 (in blue) for the determination of the effective mobilities and at pH 9.5 for the mobilities of the ionized species. EOF: electroosmotic flow.....	122
Figure 26. Yasuda-Shedlovsky plots for the water insoluble drugs studied by the IS-CE method in methanol-water mixtures.....	123
Figure 27. The trends in variations of $pK_a$ values of the eight organic bases that were determined using the IS-CE method from 0-90% methanol literature value. ....	137
Figure 28. The trends in variations of $pK_a$ values of the eight organic bases that were determined using the IS-CE method from 0-90% acetonitrile. ....	141

Figure 29. Microfluidic device for $\log P_{o/w}$ partition..	145
Figure 30. Picture of the 3DP microfluidic device taken from underneath using a fluorescent microscope..	146
Figure 31. Gravitational flow, pumpless. $\Delta V$ is the difference between the height of the reservoirs and t is time for each cycle.	147
Figure 32. Sequence of pictures of the microfluidic design when the device was tilted $+7^\circ$	148
Figure 33. Average intensity of rhodamine B in the water phase in static conditions..	150
Figure 34. Sequence of pictures (from 0 to 60 min) of the microfluidic device.	152
Figure 35. Effect of the speed of the rocker on the partition efficiency of rhodamine B in the water phase..	153
Figure 36. UP-Scalable version of the microfluidic design.	156
Figure 37. Sequence of pictures (from 0 to 60 min) of the microfluidic device at different concentrations of 1, 10 and 100 mM	158
Figure 38. Intensity of rhodamine B in the water phase depending on the concentration of analyte in dynamic perfusion.	158
Figure 39. Teflon microfluidic plate with parallel design consisting of 56 O/W subunits.	163
Figure 40. The chemical structure of pharmaceutical drugs that were used for the determination of the partition coefficient $\log P_{o/w}$	164

## List of Tables

Table 1. Acidic and basic internal standards used in the experiments. ....	62
Table 2. Insoluble drugs used in the experiments. ....	63
Table 3. Bases used in the test of HPLC column. ....	63
Table 4. Buffers solutions, and their usable pH range were used as background electrolyte for $pK_a$ determination. ....	65
Table 5. Potentiometric $pK_a$ values (standard deviations) of the neutral acids and conjugated cationic acids of the neutral bases selected for anchoring and testing IS-CE relative $pK_a$ scales at different concentrations of MeOH-water mixture. ....	78
Table 6. Potentiometric $pK_a$ values (standard deviations) of the neutral acids and conjugated cationic acids of the neutral bases selected for anchoring and testing IS-CE relative $pK_a$ scales at different concentrations of acn-water mixture. ....	78
Table 7. The $pK_a$ values with (standard deviations) of the acids internal standards at studied methanol-water compositions (v/v), at 25 °C and 0 ionic strength. ....	85
Table 8. Limiting mobility ( $m^2 v^{-1} s^{-1}$ ) of the acids internal standards at studied methanol-water compositions (v/v), at 25 °C and 0 ionic strength. ....	86
Table 9. The $pK_a$ values with (standard deviations) of the bases internal standards at studied methanol-water compositions (v/v), at 25 °C and 0 ionic strength. ....	87
Table 10. Limiting mobility ( $m^2 v^{-1} s^{-1}$ ) of the bases internal standards at studied methanol-water compositions (v/v), at 25 °C and 0 ionic strength. ....	88
Table 11. The $pK_a$ values with (standard deviations) of the acids internal standards at studied acetonitrile-water compositions (v/v), at 25°C and 0 ionic strength. ....	92
Table 12. Limiting mobility ( $m^2 v^{-1} s^{-1}$ ) of the bases internal standards at studied acetonitrile-water compositions (v/v), at 25 °C and 0 ionic strength. ....	93
Table 13. The $pK_a$ values with (standard deviations) of the bases internal standards at studied acetonitrile-water compositions (v/v), at 25 °C and 0 ionic strength. ....	94
Table 14. Limiting mobility ( $m^2 v^{-1} s^{-1}$ ) of the bases internal standards at studied acetonitrile-water compositions (v/v), at 25 °C and 0 ionic strength. ....	95
Table 15. Macroscopic properties of relevant interest for the studied methanol-water mixtures at 25 °C. ..	123
Table 16. Intrinsic solubility ( $mol l^{-1}$ ) as log S, $pK_a$ values obtained in methanol-water media. ....	124
Table 17. Limiting mobility ( $m^2 v^{-1} s^{-1}$ ) of the insoluble drugs at studied methanol-water compositions (v/v), at 25 °C and 0 ionic strength. ....	125
Table 18. Comparison of aqueous $pK_a$ determined by the IS-CE method to the values determined by other methods. ....	126
Table 19. The $^s pK_a$ values of the eight organic bases determined using the IS-CE method from 0-90% MeOH compositions (v/v) ....	132
Table 20. The $^s pK_a$ values of the eight organic bases determined using the IS-CE method from 0-90% ACN compositions (v/v) ....	132
Table 21. Limiting mobility ( $m^2 v^{-1} s^{-1}$ ) of the bases at studied methanol-water compositions (v/v), at 25 °C and 50 ionic strength. ....	133
Table 22. Limiting mobility ( $m^2 v^{-1} s^{-1}$ ) of the bases at studied acetonitrile-water compositions (v/v), at 25 °C and 50 ionic strength. ....	133
Table 23. Shows average values of the intensity of rhodamine B without agitation. ....	151

Table 24. Values of the dye intensity in water phase in under different gravitational flow.....	153
Table 25. Average values of the intensity of rhodamine B in water over the time at different concentration of analyte in dynamic conditions.....	157
Table 26. Results of the log $P_{o/w}$ using the 3DP microfluidic plate with the perpendicular design determined by HPLC. the sample was prepared at the concentration of 1 mM in water saturated octanol.....	165
Table 27. Log $P_{o/w}$ Values determined by HPLC using the Teflon microfluidic plate with the parallel design. The sample was prepared 1 mM in water saturated octanol.. ..	166
Table 28. Log $P_{o/w}$ values determined by HPLC using the Teflon microfluidic plate with the parallel design the drug was prepared at the concentration of 1mM in octanol saturated water .....	167

## OBJECTIVES

Since there is a great necessity for high-throughput determination of relevant physicochemical parameters in drug discovery, the main purpose of this thesis is the development of fast and precise analytical methods for the determination of acid-base constants ( $pK_a$ ) and octanol-water partition coefficients ( $\log P_{o/w}$ ), which are properties of pharmacokinetic interest for potential drug compounds. The results of the PhD thesis are intended to have significant effects on analytical separations and pharmaceutical drug development. The development of automated, high-throughput technologies to determine these factors can greatly speed up drug development and reduce expenses.

To achieve this main objective, the following subobjectives have been established:

- To develop the internal standard capillary electrophoresis method in methanol-water and acetonitrile-water solvent mixtures, establishing the  $pK_a$  scale of internal standards in this relevant area.
- Application of the method for the determination of the aqueous  $pK_a$  value of pharmaceutical drugs that are insoluble or sparingly soluble in water from the  $pK_a$  measurement by IS-CE method in methanol-water mixtures.
- Study of the application of the IS-CE method for the measurement of the  $pK_a$  of the analyte and pH of the buffering solution in methanol-water and acetonitrile-water for HPLC mobile phase.
- Design and manufacture microfluidic prototypes for fast and high-throughput measurement of the octanol-water partition coefficient.



# 1. GENERAL INTRODUCTION

## 1.1. The importance of physico-chemical properties in drug discovery

The increasing pressure on pharmaceutical companies to accelerate the invention and advancement of new drugs and decrease the related costs encourages laboratories to establish efficient methods for the characterization of the emerging products. The literature shows different approaches to addressing the difficulty based on theoretical estimates or in vitro experimental measurements.<sup>1-3</sup> The final goal is to accomplish an effective procedure for the estimation of properties such as absorption, distribution, metabolism, excretion, and toxic activity (ADMET) of compounds with foreseeable pharmacological applications. In practice, it is of the greatest interest to have a fast and consistent prediction of the parameters critical to making well-knowledgeable decisions conducive to the discarding of very early drug candidates with inadequate properties<sup>4-7</sup>. The purpose is to detect those compounds with high activity in vitro, acceptable selectivity, and physico-chemical parameters within the range of appropriate pharmacokinetics and smallest toxicity. In fact, in the past, they very often ignored inadequate values of the physico-chemical properties of the new molecules, and their negative effects were discovered in the final stages of their development, with a consequent negative impact on clinical success and in costs general. Acidity, solubility, and lipophilicity are among the most important parameters to be examined for a new drug candidate and are fundamental parameters for the estimation of the ADMET properties of new molecules<sup>1,7-9</sup>. Its early evaluation during the initial stage of development, known as drug discovery, provides very interesting information that allows to one better interpret the results of screening and contribute to the design of new molecules<sup>8</sup>. Despite this, the fact of obtaining values associated with these unsuitable physico-chemical properties should not be the only reason to refuse a promising compound that offers in vitro, for example, high affinity and selectivity with respect to the inhibitor, although the risk of a bad result must be assumed in the advanced stages of its development<sup>6,10,11</sup>.

The use of theoretical methods and fast and high-quality experimental measurements (high throughput) is important in the process of generating new compounds, in particular when new syntheses are planned to create a library of compounds or when a limited amount of material is available. In any case, the growing popularity of the theoretical estimation of the acidity constant, solubility, and lipophilicity cannot totally replace the experimental measurements of these properties, and, in the case of new drug development, the experimental determination of the physicochemical properties is essential at the initial stages of their development. It should be noted here that high-quality experimental data obtained using reliable methods is especially valuable when it comes to evaluating a new class of compounds. The importance of physico-chemical properties in drug design has been widely recognized, and in fact, some integrated processes for measuring the physico-chemical properties of drug candidates are now routinely incorporated into the drug discovery steps in many pharmaceutical companies <sup>12</sup>.

One of the main objectives of the pharmaceutical industry is to design molecules with therapeutic activity and sufficient absorption. Consequently, an iterative method is usually chosen to improve properties such as solubility, lipophilicity, and permeability, all of which are closely related to the absorption of the compound through biological membranes <sup>9</sup>. However, the parameters mentioned above are only physico-chemical substitutes for *in vivo* absorption, relatively easy to measure. During the last decades, various approaches have been proposed to predict the absorption of molecules with presumed bioactivity from their physico-chemical parameters. It should be borne in mind that the absorption of the drug into the systemic circulation is a prerequisite for all medicines to achieve their target, except for those that are applied to the place where they should act, or those that are injected intravenously. In the most frequent case, that of oral administration (gastrointestinal route), there are many factors that affect the bioavailability (fraction of drug that reaches the systemic circulation). Since only the dissolved drug is able to cross the gastrointestinal membrane, solubility is one such factor. Yet, the metabolism of the drug in the intestinal lumen, intestinal wall, and liver can reduce its bioavailability. In general, it can be stated that the rate of absorption, that is, the onset and extent of clinical effects, are determined by the dissolution of the drug and its later transport through the intestine and liver. All these activities occur at the same time, and the eventual absorption and distribution will be the result of a compromise of the above <sup>8,13-17,15,18,19</sup>.

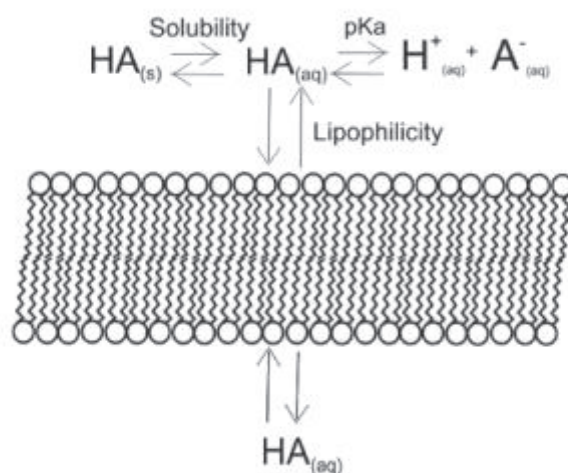


**Figure 1.** Relationship of Solubility, Lipophilicity, and Acid Dissociation in the context of a pharmaceutical compound <sup>13</sup>.

Additionally, drugs may interact with exporter or transporter proteins, which may change the total flux of chemicals into the body. Early in the drug development process, physico-chemical profiling was necessary for this, so, new, efficient techniques have been created. However, because many assays call for the drugs to be in solution while being measured, modern drug discovery techniques frequently result in molecules that are very poorly soluble in water. As a result, assessing physico-chemical properties like ionization and lipophilicity in an aqueous solution can be challenging and problematic. Therefore, only limited use may be made of the previously applied processes. Early drug development greatly benefits from any technique that enables high throughput physico-chemical profiling of several extremely sparingly soluble molecules <sup>8,13-17,20,15,18,19</sup>.

The drug's acid dissociation constant  $pK_a$  is an essential physicochemical parameter that is fundamental to the discovery and development of new pharmaceuticals. It defines the pH range in solution where a drug is both ionized and non-ionized, and it affects a wide range of biological processes, including membrane permeability, solubility, and receptor binding. For this reason, it is essential to have a complete comprehension of the  $pK_a$  of pharmacological compounds in order to predict their pharmacokinetics, effectiveness, and toxicity.  $pK_a$  is employed in drug development to screen and enhance candidate medication compounds. To be effectively absorbed, transported, metabolized, and eliminated from the body, a drug must have the proper  $pK_a$  value and be directed to a specific therapeutic target. Ionization is the main mechanical mechanism that affects how drugs are absorbed and

distributed in the body.  $pK_a$  measurements help identify potential drug-drug interactions, drug-membrane interactions, and potential off-target effects<sup>6,12,19</sup>.

likewise, a crucial physiochemical characteristic that is measured for drug molecules throughout the drug development process is the partition coefficient ( $P$ ). In most cases, a polar and a non-polar solvent are used to represent the distribution of a drug molecule between two immiscible solvents. This parameter is essential to pharmacokinetics since it determines whether a drug can pass through biological membranes and reach its target. Drugs with identical partition coefficients may bind together or to the same receptor, potentially leading to undesirable effects or toxicity. This might assist in forecasting the likelihood of drug-drug interactions. While building and improving therapeutic molecules, knowledge of the partition coefficient is helpful since it enables the development of more specialized, focused, and efficient drug treatments. In conclusion, the partition coefficient is an important physiochemical characteristic in the design of drug molecules and significantly affects the way a drug interacts with biological membranes, as well as its bioavailability, ADME properties, and target binding. As a result, partition coefficient assessments can help find drug candidates that may have lower potential toxicity as well as more effective and efficient treatments<sup>4,15,16,21,22</sup>.

As a result, a principal viewpoint of drug's absorption, distribution, and metabolism is the link between a drug dissociation constant and lipophilicity and its environment. The ability of a drug to dissolve in lipids, or fats, determines its lipophilicity, and the ability to separate into its ionized form determines its dissociation constant. A drug dissociation constant decreases as its lipophilicity increases, and vice versa. The lipophilicity and dissociation constant of the drugs can also be affected by their environment, such as the pH of the medium in which they are present. For instance, at a low pH, the drug lipophilicity will be higher and its dissociation constant will be lower, while at a high pH, the drug lipophilicity will be lower, and its dissociation constant will be higher. Thus, when inspecting candidates that are drug-like in the early stages of drug investigation, physicochemical profiling is a fundamental method<sup>6,12,22,23</sup>.

In a biological system, a compound's performance can be significantly affected by its acidity ( $pK_a$ ), lipophilicity, usually measured by octanol-water partition coefficient ( $\log P_{o/w}$ ), and medium pH. The  $pK_a$  of a compound determines its degree of ionization at a particular pH and thus affects its solubility, permeability, and interaction with other molecules.

Lipophilicity, or the extent to which a compound is soluble in lipids, is critical for determining its ability to cross the biological membrane and reach its target site. Moreover, pH can influence the ionization state of a compound and its interaction with other molecules. Hence, knowing and studying these characteristics is important for designing and optimizing effective compounds in the field of drug discovery and development. These three parameters are connected. The ionization state of a compound is definitely correlated to  $pK_a$ , pH and can influence the lipophilicity of that molecule ( $\log P_{o/w}$ ). This in turn may have an impact on the drug overall efficacy and toxicity, as well as its features related to absorption, distribution, metabolism, and excretion (ADME). The advancement of effective and safe drug molecules can benefit from a knowledge of the relationships between these parameters. In conclusion, the physicochemical properties of pharmaceuticals, such as their  $pK_a$  and lipophilicity, can greatly affect both their pharmacokinetics and pharmacodynamics. Optimizing drug design and dosage methods requires an understanding of these features

14,15,19,24-26

## 1.2. Relevant physico-chemical properties: acid-base dissociation constants ( $pK_a$ )

### 1.2.1. Definition of acid-base constant

The acidity constant, also known as the acid dissociation constant, is a measure of the strength of an acid in solution. It is the equilibrium constant of an acid dissociation reaction and is a measure of the strength of an acid in a solution. The acidity constant ( $pK_a$ ) of a drug molecule is an important parameter for understanding how a drug molecule behaves in different environments. It is a measure of the degree to which a drug molecule can donate or accept a hydrogen atom and is determined by the strength of the hydrogen bonds in the structure of the molecule. In addition, the size and shape of the molecule and the presence of functional groups that can donate or accept hydrogen atoms will also affect the  $pK_a$  of a drug molecule. The  $pK_a$  of a drug molecule can also be affected by the presence of other molecules in the environment, such as solvent molecules. Knowing the  $pK_a$  of a drug molecule can help us understand how it will interact with other molecules in aqueous solution and, therefore, how it will be able to interact with its target. A significant physicochemical factor that affects a huge number of biopharmaceutical features is a drug acid-base dissociation constant ( $pK_a$ ). The most popular technique for determining the  $pK_a$  of compounds that are insoluble in water is the cosolvent approach (also known as the mixed solvent process). Some unionized compounds can become more soluble by combining solvents like acetonitrile, methanol, etc. with water<sup>27-29</sup>. With the  $pK_a$  value known, ionization can be calculated at any pH by using the Henderson-Hasselbalch equation. This is important because of the difference in physicochemical properties between neutral and ionized forms. In general, ionized molecules are more water soluble than neutral ones, which is necessary for passive diffusion of molecules to the site of activity through membranes. Neutral molecules are less water soluble and have higher permeability through biological membranes. The dissociation constant for monoprotic acids and bases is the pH at which half of the molecule is ionized. Thus, the degree of ionization of medicinal molecules has a significant impact on metabolism, absorption, distribution, and excretion<sup>21,30-32</sup>.

The expression of thermodynamic equilibrium constant of any acidic-basic reaction involving the acid ( $HA^z$ ) and a solvent (S), leading to the formation of the solvated species ( $HS^+$ ) and corresponding anion ( $A^{z-1}$ ), as stated in Eq (1), where the equilibrium constant can be presented as Eq (2). The solvent, specific acid, and reaction conditions all affect  $K_a$  value<sup>33-35</sup>.



The equilibrium constant ( $K_a$ ) can be defined as the ratio of concentration of products (HS and  $A^{z-1}$ ) to the concentration of reactants ( $HA^z$  and S) at equilibrium.  $K'_a$  is effective equilibrium constant,  $\alpha_{HS^+}$ ,  $\alpha_{A^{z-1}}$ ,  $\alpha_{HA^z}$  are the activities of species at equilibrium,  $\gamma_{HS^+}$ ,  $\gamma_{A^{z-1}}$ ,  $\gamma_{HA^z}$  are the activity coefficient at the equilibrium.

$$K_a = \frac{\alpha_{HS^+} \alpha_{A^{z-1}}}{\alpha_{HA^z}} = \frac{[HS^+][A^{z-1}]}{[HA^z]} \cdot \frac{\gamma_{HS^+} \gamma_{A^{z-1}}}{\gamma_{HA^z}}, \text{ or } K_a = K'_a \frac{\gamma_{HS^+} \gamma_{A^{z-1}}}{\gamma_{HA^z}} \quad (2)$$

A particular case can be derived for monoprotic neutral acids and monoprotic neutral bases, as shown in the following equations. The charge ( $z = 0$ ) and reaction are simplified for monoprotic neutral acid in the following equation.



The equilibrium constant can be presented as:

$$K_a = \frac{\alpha_{HS^+} \alpha_{A^-}}{\alpha_{HA}} = \frac{[HS^+][A^-]}{[HA]} \cdot \gamma_{HS^+} \gamma_{A^-} = K'_A \gamma_{HS^+} \gamma_{A^-} \quad (4)$$

In the case of monoprotic neutral base, the charge ( $z = 1$ ) and reaction are simplified to



The equilibrium constant can be presented as:

$$K_a = \frac{\alpha_{HS^+} \alpha_A}{\alpha_{HA^+}} = \frac{[HS^+][A]}{[HA^+]} \cdot \frac{\gamma_{HS^+} \gamma_A}{\gamma_{HA^+}} = K'_a \frac{\gamma_{HS^+} \gamma_A}{\gamma_{HA^+}} \quad (6)$$

The dissociation constant of protonated acid can be presented in the following equation.

$$K_a = \frac{\alpha_{A^-} \alpha_{H^+}}{\alpha_{HA}} = \frac{[H^+][A^-]}{[HA]} \cdot \frac{\gamma_{H^+} \gamma_{A^-}}{\gamma_{HA}} = K'_A \gamma_{H^+} \gamma_{A^-} \quad (7)$$

Or

$$pK_a = \text{pH} - \log \frac{[A^-] \gamma_{A^-}}{[HA] \gamma_{HA}} \quad (8)$$

Where  $\gamma_{A^-}$  and  $\gamma_{H^+}$  activity coefficients strongly depend on the ionic strength of the solution and could be defined by Debye-Hückel equation <sup>33-39</sup>.

$$-\log y = \frac{Az^2\sqrt{I}}{1 + a_0B\sqrt{I}} \quad (9)$$

Where,

$$A = \frac{1.8246 \times 10^6}{(\epsilon T)^{3/2}} \quad (10)$$

$$B = \frac{50.2904 \times 10^{-8}}{(\epsilon T)^{3/2}} \quad (11)$$

Coefficients A and B in Eq (5) and (6) are parameters dependent on static dielectric constant of the medium ( $\epsilon$ ), ionic strength (I), and temperature measured in K (T). The Bates–Guggenheim convention ( $a_0 = 4.56 A^0$ ) is commonly adopted, and then, at 25 °C,  $a_0B = 1.5$  and  $A = 0.5$ .

The thermodynamic dissociation constant can be calculated from the effective dissociation constant and from the activity coefficient, Eq (12) for a monoprotic acid and Eq (13) for a monoprotic base.

$$pK_a = pK'_{a,j} - \log \gamma_{A^-} \quad (12)$$

$$pK_a = pK'_{a,j} - \log \gamma_{BH^+} \quad (13)$$

A species distribution diagram can be calculated if the  $pK_a$  is known. Figure 2 illustrates how the molecule will distribute between its acid and the conjugate base as a function of pH, using benzoic acid as an example. A pH lower than  $pK_a$  has higher proportions of the acid species, whereas a pH higher than the  $pK_a$  will have a higher predominance of the ionized species. The  $pK_a$  is equivalent to the pH at which the activities of the acid and its conjugate base are equal <sup>13</sup>.

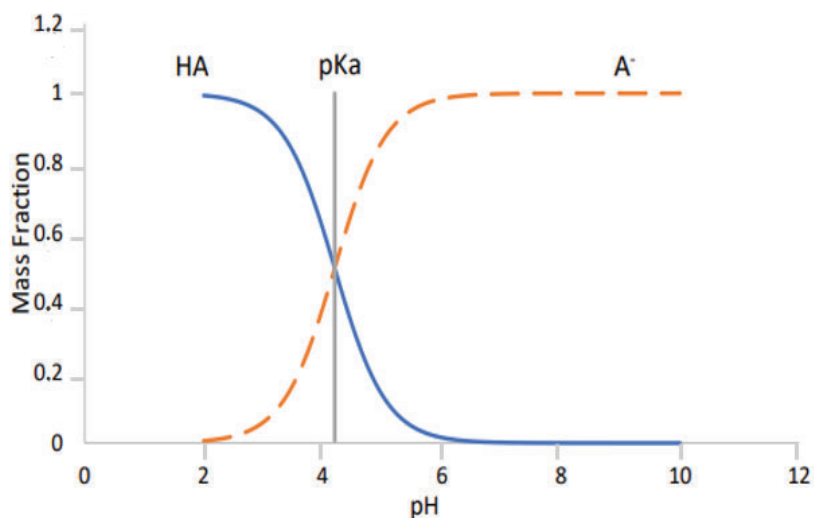


**Figure 2.** Species Distribution Diagram for the Benzoic acid,  $pK_a$  4.20,  $I=0$ . HA represents the acid form, A. corresponds to the dissociated species, according to the equation <sup>13</sup>.

Thus, the  $pK_a$  of a drug will affect its oral availability and absorption in the various compartments of the digestive tract, as aqueous solubility and membrane permeability are both influenced by a molecule's charge state <sup>5,40</sup>. The  $pK_a$  must therefore be determined early in the drug discovery phase in order to maximize the output of a drug development program.

### 1.2.2. Methods for determining acid-base dissociation constant.

There are several methods for predicting the dissociation constant, but historically, potentiometric titration has been the accepted method for determining  $pK_a$  values. Capillary electrophoresis (CE), and spectrophotometric studies were both considered alternatives. Therefore, these three techniques are regarded as the standard approaches for calculating the dissociation constant <sup>40,41</sup>.

#### 1.2.2.1. Potentiometric titrations

The main idea behind potentiometric analysis is that adding a known volume of reagent to a solution containing analyte causes a change in potential, which is then measured by a system comprising two electrodes, an indicator, and a reference electrode. Potential against volume may be plotted to reveal a sigmoidal curve with inflection points that represent current potential at equilibrium, which can be translated into pH and equals  $pK_a$  <sup>30,38,39</sup>. Potentiometric measurement of the  $pK_a$  value offers a trustworthy approach that is

automated, reasonably priced, and easy to use. However, there are certain issues connected to this approach. Comparing this process to a separation technique like capillary electrophoresis, a higher volume of a high purity material is needed. Additionally, it takes longer and is more inaccurate to determine the  $pK_a$  values of compounds that are poorly soluble in water since they need to use a large amount of cosolvent<sup>30,41-44</sup>.

When pH values in the organic-aqueous media were measured in reference to water standards [ ${}_w^S\text{pH}$ ], they can be converted to pH values referring to the same organic-aqueous mixtures [ ${}_S^S\text{pH}$ ], by means of the  $\delta$  term correction, which includes the medium effect and the differences in the liquid junction potentials in the two media<sup>30,33-35</sup>, according to the following Eq (14)

$${}_S^S\text{pH} = {}_w^S\text{pH} - \delta \quad (14)$$

The mass and charge equilibriums of the species in equilibrium were used to calculate  $pK_a$  from the titration results. The calculation must consider the autoprotolysis of the organic-aqueous solvent<sup>45</sup>. Activity corrections at each titration point were done through the mean activity coefficient of each ion ( $\gamma_{\pm}$ ), which was calculated through the Debye-Hückel equation, according to Eq (9).

### 1.2.2.2. Spectrophotometric titrations

The sensitivity of spectrophotometric titrations is better than that of potentiometric titrations, but they can only be used when the chromophore is adjacent to the ionizable group, which is not the case for all compounds. The spectra of the compound in fully ionized and protonated forms must vary and be known in advance. The quantity of each species is determined using the molar absorption coefficient as the titration advances; a diode array detector enables simultaneous measurement of all the wavelengths<sup>40,41</sup>. When just one equilibrium needs to be considered or when the  $pK_a$  to be determined are greater than two  $pK_a$  units apart from one another, the calculations of the  $pK_a$  is straightforward. When these requirements are not satisfied, more complicated techniques like multivariate analysis are necessary, which makes use of the diode array detector high data collection capacity<sup>40,41</sup>. Both procedures are dependable and frequently utilized; specialized devices have even been developed for their everyday usage<sup>46</sup>. The fundamental disadvantage is that exceedingly pure samples are required, because any impurity might change the response and generate a response artifact. In any case, they are the gold standard and absolute procedures for doing

$pK_a$  measurements due to their repeatability and precision <sup>6</sup>.

### **1.2.2.3. Capillary electrophoresis (CE)**

In contrast to earlier approaches, CE is based on physical separation prior to detection, which requires just the migration time for electrophoresis. No quantification is required, which is beneficial since it is no longer limited to compounds of high purity and may be used to work with small volumes of material that may result from a synthesis <sup>47</sup>. This method is based on charged species that are separated by capillary electrophoresis (CE) under the influence of an electric field, with a velocity proportional to their charge-to-mass ratio. This approach makes use of the fact that the mobilities of neutral and ionized species of the same chemical vary. Because of acid-base equilibrium, the amount of ionization of an ionizable chemical varies with the pH of the background solution. When the mobility of the compound is plotted against the pH, a sigmoidal curve is generated, with the inflection point representing the pH at which 50% of the compound is ionized- $pK_a$  value. Furthermore, buffer solutions must be generated with accurate ionic strength, since it has already been demonstrated that  $pK_a$  measured by electrophoretic studies must be adjusted for activity coefficient. Buffers should be carefully chosen since interactions between buffer and analyte might result in false readings <sup>9</sup>. Furthermore, due to the level of heating during the separation caused by the applied high voltage, joule heating might create some error in the  $pK_a$  determination <sup>48</sup>. Despite certain drawbacks, capillary electrophoresis has numerous advantages over reference techniques for determining the dissociation constant.

Conductometric, voltametric, calorimetric, and fluorometric techniques, as well as nuclear magnet resonance, are alternative methods for determining  $pK_a$  values <sup>40,49,50</sup>.

## 1.2.3. Capillary electrophoresis

### 1.2.3.1. Definition and Instrumentation

Capillary electrophoresis (CE) is a type of electrokinetic separation conducted in narrow capillary tubes (typically 10-200  $\mu\text{m}$  i.d.) working under the influence of an applied electric field <sup>51,52</sup>. Capillary zone electrophoresis (CZE) is the most extensively used technique of capillary electrophoresis due to its ease of use and variety. The fact that the capillary is just filled with buffer contributes to its simplicity. The basic capillary electrophoresis instrumental arrangement is simple, consisting of a fused silica capillary with an optical observing window, two electrodes, two buffer containers, a controlled high voltage source, and an ultraviolet (UV), detector as shown in Figure (3). Furthermore, commercial instruments provide completely automated computer control of all operations, such as pressure and injection, autosampler and fraction collector, method and sequence development, temperature management, and a sophisticated heat dissipation system <sup>32,38,47-49,53</sup>.

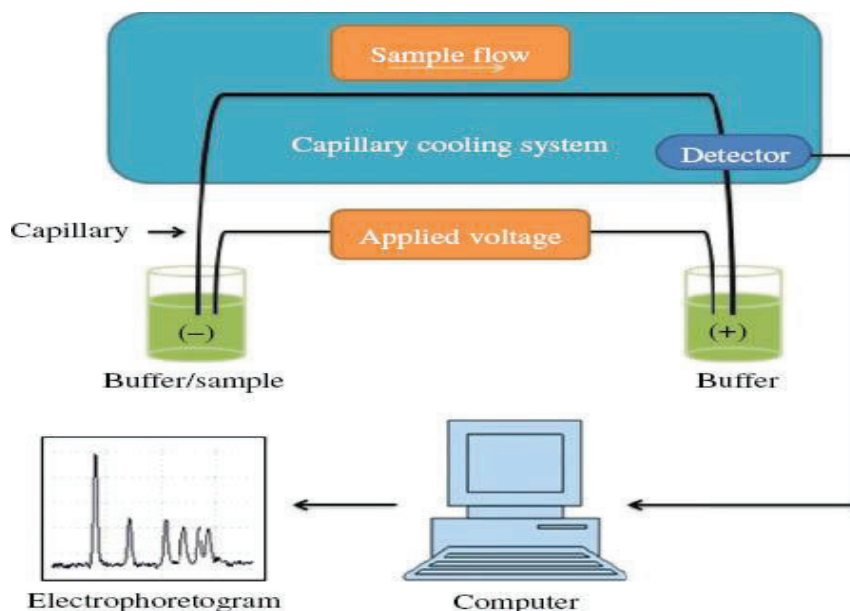


**Figure 3.** Basic configuration of the capillary electrophoresis <sup>54</sup>.

Separation in CE is caused by analytes moving at different speeds under the influence of high voltage. The separation of electrically charged species in a conductive medium is influenced by the electric field in CE. The electroosmotic flow (EOF) of the bulk solution and the electrophoretic mobility of individual analytes are the two basic processes that might affect separation. Because of electro-osmotic flow (EOF), cationic and ionic molecules may be separated in a single run, whereas neutral compounds coelute<sup>51,55</sup>.

Electro-osmotic flow describes electrophoretic processes in which the charged surface of the inner capillary wall causes bulk flow of solvent in the capillary. Silanol groups (SiOH) put on the inner wall create  $\text{SiO}^-$  ions due to pH greater than isoelectric point (pI). Counterions, in this case cations of the background electrolyte, form a double layer on the surface of the capillary and cause a potential difference extremely close to the wall known as the zeta potential. When a voltage is applied, cations forming a diffuse double layer are drawn to the cathode, and because the cations are solvated, their movement draws the bulk solution and solutes towards the cathode<sup>55</sup>.

The feature that characterizes the EOF in the capillary is the flat profile of the flow. In comparison to laminar flow, the driving force of EOF flow is consistently distributed along the capillary, and there is no pressure drop within the capillary, resulting in virtually uniform flow across the capillary. When compared to laminar flow, this flow has far less impact on the dispersion of solute zones.

As a result, it is significant to use narrow-bore capillaries, which reduce thermal dissipation. The current passing through the capillary is lowered by the square of the capillary radius, so heat is dispersed more effectively via narrow capillaries<sup>51,52,56,57</sup>.

### 1.2.3.2. Mobility and Migration Time

Separation in chromatography is based on retention time, but separation in electrophoretic separation is based on migration time, with analytes separate based on their ionic mobilities. The electrophoretic velocity  $V_{ep}$ (cm/s) is the speed at which analytes travel inside the capillary until they reach the detector and is computed as given in Eq (15). The electrophoretic velocity is produced by increasing the intensity of the electric field<sup>51,52,57</sup>.

$$\mu_{ep} = \frac{V_{ep}}{E} = \frac{q}{6\pi r\eta} \quad (15)$$

Electrophoretic mobility  $\mu_{ep}$  is determined by the analytes (shape, electrical charge, and molecular size) and the BGE (pH, additives, viscosity, and ionic strength)<sup>51</sup>. Electrophoretic mobility defines ion migration time and the electrophoretic migration velocity  $V_{ep}$  to electric field ratio  $E$ . Where  $q$  is the analyte net charge,  $r$  is Stoke radius, and  $\eta$  is the buffer viscosity. The electrophoretic mobility  $\mu_{ep}$  may be determined using the preceding equation.

The second phenomenon that influences analyte migration in CE is electroosmotic flow  $\mu_{EOF}$  (cm/s). The bulk motion of the electrolyte solution during electrophoresis is referred to as electroosmotic mobility. The mobility of electroosmotic flow EOF may be computed using the following equation:

$$\mu_{EOF} = \frac{EOF}{E} = \frac{\epsilon\xi}{4\pi\eta} \quad (16)$$

Where  $\xi$  is the zeta potential,  $\epsilon$  is the dielectric constant of the buffers and  $V_{EOF}$  is the EOF velocity which can be determined from the migration time of a neutral marker (e.g., DMSO, acetone, or mesityl oxide).

The migration time is the time it takes the analyte to migrate to the detector in the presence of the EOF marker and is used to calculate mobility, this is referred to as apparent mobility,  $\mu_{app}$ . The apparent mobility may be estimated by moving the analytes at the same velocity as the EOF marker. As a result, apparent mobilities,  $\mu_{app}$  [ $m^2/V \cdot s$ ], may be determined using the following equation:

$$\mu_{app} = \mu_{ep} + \mu_{EOF} \quad (17)$$

Migration time in CE is the fundamental expression in electrophoretic separation, which separates substances based on their ionic mobilities<sup>30</sup>. The equation below is used to calculate the apparent electrophoretic mobility  $\mu_{eff}$  [ $m^2/V \cdot s$ ]:

$$\mu_{eff} = \frac{L_d}{E} \left( \frac{1}{t_m} - \frac{1}{t_{EOF}} \right), \quad E = \frac{V}{L_t} \quad (18)$$

The abbreviation of  $\mu_{eff}$  is the effective mobility,  $L_d$  (cm) is the effective capillary length to the detector,  $t_m$  (min) is the migration time of analyte, and  $t_{EOF}$  (min) is the migration

time of neutral marker. Electrical field E is expressed in Eq (18) and can be calculated from the applied potential (V) and the total capillary length  $L_t$  [cm].

In the case of ionizable substances, several apparent mobilities can be assessed. The first mobility is called limiting mobility, while the second is effective mobility. Both mobilities are estimated using Eq (18), where  $t_m$  is the migration time of the identified chemical. The limiting mobility corresponds to the completely ionized compound, whereas effective mobility represents mobility at varying degrees of ionization of the compound, i.e. mobility of the compound at pH when the material is only partially ionized,  $\mu_{eff}$ <sup>30</sup>.

Each dissociation phase has its own dissociation equilibrium and dissociation constant in acid base equilibrium for each polyprotic chemical, where n represents the number of functional groups and z represents the charge of the completely protonated form. Because the degree of ionization is determined by the dissociation constants, effective mobility of the compound is a function of the dissociation constant of each ionic species and the pH value of the background electrolyte via a general equation.

$$\mu_{eff} = \frac{\mu_{H_n X^z} + \mu_{H_{n-1} X^{z-1}} \sum_{i=1}^n 10^{iPH - \sum_{j=1}^n pK'_{aj}}}{1 + \sum_{i=1}^n 10^{iPH - \sum_{j=1}^n pK'_{aj}}} \quad (19)$$

According to the Debye-Huckel equation (9), adjustment of the activity coefficient is required, and correction is required for each ionic species present in the solution, as discussed in the last part 2.1.

### 1.2.3.3. Detection

CE is usually used in conjunction with various detectors such as UV/Vis, mass spectrometers (MS), laser induced fluorescence (LIF), and capacitively coupled contactless conductivity detectors (C4D). The UV/Vis detector is the most commonly used since it has simpler operation and a lower cost. The presence of a chromophore in the analyte is a primary requirement for UV/Vis detection. Detection wavelengths of 200 nm in the visible zone of the spectrum are possible because of the employment of silica capillaries and buffer solutions. Using low wavelengths results in a significant increase in sensitivity, a lower cost, and a wide range of application<sup>58</sup>. Aside from these advantages, CE has an issue with the sensitivity of low concentration sample analysis due to the short route length for absorbance related detection and limited sample sizes. Fluorometric, conductometric, and electrochemical detectors have the highest sensitivity and are more general and cheaper than

the more common UV detector. Furthermore, mass spectrometry (MS) is ubiquitous, mass sensitive, and costly, and further research is needed to combine it with CE <sup>58,59</sup>.

#### 1.2.3.4. Joule heating effect

The joule heating effect refers to generation of heat by the electric current passing through the conductor with resistance. Joule heating has to be a concern in capillary electrophoresis due to its effect on the separation process, especially when a high electric field is applied, and the temperature stability of the system. The quantity of heat produced ( $P$ ) has a proportional relationship between the current intensity ( $I$ ), the resistance of the conductor ( $R$ ) as shown in Eq (20):

$$P = I^2R \quad (20)$$

The current is squared; by increasing the current intensity inside the resistor while keeping the resistance constant, the heat generated by joule heating will be increased greatly. Similarly, the increase in resistance while maintaining the current intensity constant results in an increase in heat produced due to the joule effect. The resistance can be estimated through the buffer solution and the properties of the capillary, like the current passing through the capillary and the wasted power because of joule heating <sup>56,60-62</sup>.

The equation of Ohm's law can be used to explain the importance of the joule effect in capillary electrophoresis. Ohm's law describes the relation between the current ( $I$ ), voltage ( $V$ ), and resistance ( $R$ ) of the conductor. Ohm's law:

$$I = \frac{V}{R} \quad (21)$$

The voltage passing through a resistor has a proportional relation to the intensity of the current passing and the resistance of the resistor. Ohm's law can help in understanding the relationship between current, voltage, and resistance in a resistive component of the loop, which may be indirectly related to how the joule effect causes heat to dissipate <sup>56,60</sup>.

The conductance ( $G$ ), which is the reverse of the resistance of the capillary filled with a solution, and the potential difference applied can be expressed through the rate of heating produced through the following equation:

$$G = \frac{K \cdot A}{L} = \frac{K \pi d^2}{4L} \quad (22)$$

The conductance of the capillary is based on the buffer solution and its physical dimensions and can be calculated through Equation (22), where  $K$  is the electric conductivity of the buffer,  $A$  is the cross-sectional area of the capillary,  $L$  is total length of the capillary and  $d$  is the inner diameter of the capillary <sup>56,60-66</sup>.

A lower conductivity buffer is preferable for capillary electrophoresis separation due to the decrease in current passing through the capillary and, thus, the heating effect. Moreover, capillaries with a small inner diameter or longer one decreases the joule effect. The capillary conductivity might increase as a result of the inner temperature increase. This increase in conductivity allows more current to be drawn, which increases the temperature even further. Joule heating may disturb the separation process by causing an increase in peak broadening, diffusion, and pH shifts in the buffer solution. Thus, controlling the increase in temperature can help avoid electrolyte boiling and the decomposition of the analyte before separation. In summary, several things have to be considered to avoid the joule effect, including the appropriate temperature, buffer, voltage, and capillary diameter. Understanding and controlling the joule effect can enhance the separation and the results in capillary electrophoresis <sup>56,60-66</sup>.

A practical method to keep the joule heating effect low is to check that Ohm's law is fulfilled, i.e., that, there is a proportionality between the applied voltage and observed current intensity. When there is a significant joule heating effect, the proportionality between the voltage and current is not kept and working in these conditions should be avoided.

## 1.3. Internal Standard Capillary Electrophoresis (IS-CE) Method for determination of $pK_a$ and pH.

### 1.3.1. IS-CE method guiding principle.

The classic CE approach, while considerably used, has the major drawbacks of relying on pH monitoring for BGE. Despite the fact that measuring pH is rather simple, the pH of the solution might fluctuate between runs due to electrolysis,  $CO_2$  absorption into the buffer, or evaporation of buffer components<sup>47,50,67</sup>. For investigating a large number of compounds, many runs will be necessary. It will be challenging to ensure that the pH of the buffer remains constant throughout the run. Changing the electrolyte often is a common recommendation; this choice is provided in the technique description because it will affect the method's longevity. Even if the buffer is modified, this won't reveal the buffer pH level throughout the separation.

Using a reference compound as an internal standard, whose nature and  $pK_a$  value are comparable to those of the compounds whose  $pK_a$  is being evaluated, is the main goal of the capillary electrophoresis with internal standard technique (analyte). Since the reference compound and the analyte must behave identically under identical experimental circumstances for this approach to be valid, the discrepancy in the mobilities of these two compounds can only be explained by variations in the dissociation constants ( $pK_a$ )<sup>38,68</sup>.

As the first step of the method, it is necessary to know the approximate  $pK_a$  value of your analyte. This can be done by searching the literature and getting the values or by doing approximations with the appropriate software (ACD Labs or others). After that, an appropriate IS has to be chosen that has a similar  $pK_a$  value as the analyte. Then, analyte and internal standard are injected together in the capillary, and any alterations in the test conditions, pH, temperature, or ionic strength, affect not only analyte but also IS so any deviation in the mobility of analyte can be compensated with internal standard if both compounds suffer nearly the same alterations. This is an advantage compared to the classical CE method for determination of  $pK_a$  where any alteration of the mobility of the analyte leads to an error in  $pK_a$  determination<sup>67,68</sup>.

In order to evaluate the limiting and effective mobilities of both molecules, it is required to first choose a suitable internal standard for  $pK_a$  measurement of the analyte that has a comparable  $pK_a$  value to our analyte. The limiting mobility of both compounds is measured

at a pH value that is at least two  $pK_a$  units higher or lower than the  $pK_a$  values of the analyte and IS, respectively, for acidic compounds and lower for basic ones. It is required to utilize a buffer with a pH close to the compound  $pK_a$  in order to measure the effective mobilities of both the analyte and the IS in the same run. According to the Henderson-Haselbach equation, a compound ionizes between 1.0 pH units and its  $pK_a$  values<sup>30,38,68</sup>. One of IS-CE criteria is this. According to everything said above, the buffers IS and pH should be correctly selected for the experimental runs.

Like CE, capillary electrophoresis with internal standards is a highly automated method that just needs a small volume of analytes and doesn't require significant purity of those materials because it is a separation method. Capillary electrophoresis with internal standards, in contrast to traditional capillary electrophoresis, does not require an precise measurement of the buffer's pH level<sup>9,47,68</sup>. Since only 2 injections are required to obtain a  $pK_a$  value, the IS-CE method is highly quick. The application is appropriate for high-throughput determination of  $pK_a$  values in the pharmaceutical industry for the drug development process since it has previously been enhanced to be a high-throughput one and only requires a small amount of sample and a brief capillary running routine<sup>9</sup>.

### 1.3.2. IS-CE method for determining the acid-base constant of neutral monoprotic acids.

The bottom Eq (23) is a general expression for calculating effective mobility of a monoprotic neutral acid (HA) and can be represented as a function of the background electrolyte pH and working  $pK_a$  value (BGE), where  $\mu_{A^-}$  and  $\mu_{\text{eff}}$  are limiting and effective mobilities.

$$\mu_{\text{eff}} = \frac{\mu_{A^-}}{1 + 10^{pK'_a - \text{pH}}} \quad (23)$$

Solving Eq (20) for the  $pK'_a$ , Eq (21) can be described for a given analyte:

$$pK'_{a,A^-} = \text{pH} + \log \frac{\mu_{A^-} - \mu_{\text{eff}}}{\mu_{\text{eff}}} = \text{pH} + \log Q_A \quad (24)$$

$pK'_{a,A^-}$  can be correlated with thermodynamic  $pK_a$  through Eq (12). Using Eq (24), we may calculate the pH within the capillary under experimental circumstances using IS, an acid with a known  $pK_a$  value as shown in the following equation.

$$\text{pH} = pK'_{a,IS} - \log Q_{IS} \quad (25)$$

By using equations (24) and (25) with the internal standard, the acidity of the analyte can be determined as shown in the following equation:

$$pK'_{a,AN} - pK'_{a,IS} = \log Q_A - \log Q_{IS} \quad (26)$$

Combining Eq (12) and with Eq (22) can be give:

$$pK_{a,AN} = pK_{a,IS} + \log Q_A - \log Q_{IS} + \log \gamma_{IS} - \log \gamma_{A^-} \quad (27)$$

Eq (27) is a formula for calculating the  $pK_a$  values of acidic analytes. This equation shows that there is no need to measure the pH of the BGE in order to derive the analyte's  $pK_a$  value. Furthermore, If the internal standard is the same type of acid as the analyte (i.e. they have the same charge), activity coefficients are removed and have no effect on the calculated  $pK_a$  value as shown in the next equation.

$$pK_{a,AN} = pK_{a,IS} + \log Q_A - \log Q_{IS} \quad (28)$$

Nonetheless, when we are determining analytes, such as neutral acid, using an internal standard, such as neutral base, we have a different situation.

Activity coefficients have a considerable influence on the calculated  $pK_a$  in these two circumstances and must be included in calculations<sup>47,68</sup>. Then we should use the previous equation (28).

### 1.3.3. IS-CE method for determining acid-base constant of neutral monoprotic bases.

The bottom Eq (29) is a general expression for calculating effective mobility of a monoprotic neutral Base ( $BH^+$ ) and can be represented as a function of the background electrolyte pH and working  $pK_a$  value (BGE), where  $\mu_{A^-}$  and  $\mu_{eff}$  are limiting and effective mobilities.

$$\mu_{eff} = \frac{\mu_{BH^+}}{1 + 10^{pH - pK'_a}} \quad (29)$$

Solving equation (29) for the  $pK'_{aB}$ :

$$pK'_{a,B} = pH - \log \frac{\mu_{BH^+} - \mu_{eff}}{\mu_{eff}} = pH - \log Q_B \quad (30)$$

$pK'_a$  for bases can be correlated with thermodynamic  $pK_a$  through the following equations:

$$pK_a = pK'_{a,IS} + \log \gamma_{BH^+} \quad (31)$$

Using Eq (32), we may calculate the pH within the capillary under experimental conditions using IS, a Base with a known  $pK_a$  value as shown in the following equation:

$$pH = pK'_{a,IS} - \log Q_{IS} \quad (32)$$

Equations (30) and (32) can be used to give Eq (33):

$$pK'_{a,B} - pK'_{a,IS} = \log Q_{IS} - \log Q_B \quad (33)$$

Combining it with (33)

$$pK_{a,B} = pK_{a,IS} + \log Q_{IS} - \log Q_B + \log \gamma_{BH^+} - \log \gamma_{IS} \quad (34)$$

Equation (34) is a formula for calculating the  $pK_a$  values of basic analytes. This equation shows that there is no need to measure the pH of the BGE in order to derive the analyte's  $pK_a$  value. Furthermore, if we use an internal standard of the same charge type as the analyte, we may eliminate activity coefficients because they have the same value.

$$pK_{a,B} = pK_{a,IS} + \log Q_{IS} - \log Q_B \quad (35)$$

However, when we are determining analytes, such as neutral base, using an internal standard, such as neutral acid, we have a different situation<sup>55,69</sup>.

In these two cases, activity coefficients have a considerable influence on the measured  $pK_a$  and must be included in calculations<sup>47,68</sup>. Then we should use the previous equation (35).

#### 1.3.4. IS-CE method for determining the pH.

The effective mobility ( $\mu_{eff}$ ) of a monoprotic neutral acid (HA) can be expressed as the function of its  $pK'_a$  and the pH of the BGE<sup>39,70</sup> by Eq (23):

Solving Eq (23) give the relation between  $pK'_a$  and thermodynamic  $pK_a$  can be shown by the following Eq (36):

$$pK_a = pK'_a + \log \gamma_{A^-} \quad (36)$$

Where  $\gamma$  denotes the activity coefficient of the subscripted species and corrects the effect of the ionic strength on the solute ionization.

Rearranging Eq (23) gives the equation to calculate pH of BGE from effective and limiting mobilities of monoprotic acidic TC shown in Eq (37):

$$pH = pK'_a + \log \frac{\mu_{A^-} - \mu_{eff}}{\mu_{eff}} \quad (37)$$

Similarly, in case of monoprotic neutral base,  $\mu_{\text{eff}}$  of a monoprotic neutral base (B) can be expressed as the function of its  $pK'_a$  and the pH of the BGE by Eq (29):

Solving Eq (29) gives the relation between  $pK'_a$  and thermodynamic  $pK_a$  can be shown by the following Eq (38):

$$pK_a = pK'_a + \log \gamma_{\text{BH}^+} \quad (38)$$

Finally, rearranging Eq (30) leads to the equation that could be used to calculate pH of BGE from effective and limiting mobilities of monoprotic basic TC shown in Eq (39):

$$\text{pH} = pK_a + \log \frac{\mu_{\text{BH}^+} \mu_{\text{eff}}}{\mu_{\text{eff}}} \quad (39)$$

## 1.4. Acidity constant in organic solvent and water-organic solvent mixtures.

Acid dissociation constants, also known as acidity constant, are usually evaluated in aqueous solutions as water is a common solvent and many acid-base interactions occur in aquatic environments. Although acid dissociation constant may be calculated in non-aqueous solvents like organic solvents, aqueous solution is more commonly used because of the predominance of water as a solvent in many chemical and biological developments. Nevertheless, some compounds are not soluble enough in water to determine the  $pK_a$  and extrapolate it to water if needed. In such a case,  $pK_a$  must be established in a nonaqueous solvent or in water-organic mixtures. Likewise, aqueous  $pK_a$  measurements are limited in their use in calculating the results of reactions in non-aqueous solutions. As a result, determining  $pK_a$  and pH in non-aqueous or partially aqueous mediums is often of interest, such as in common HPLC systems mobile phase<sup>37,71-73</sup>.

It is significant to understand the influence of organic solvents on the  $pK_a$  of a compound because it can affect how the compound works in different solvents. Different solvents can induce different degrees of solubility, reactivity, and identifying the  $pK_a$  change can aid in making predictions about the compound behavior in different solvents easier to comprehend. Different solvents have different effects on the  $pK_a$  values of analytes. Key solvent properties to consider include hydrogen bond capability, polarity, acidity, and basicity. The stability of charged species in protic solvents can be affected by hydrogen bonding between solvent and analytes, leading to a change in the  $pK_a$  values for acidic or basic compounds<sup>30,33,35</sup>. Organic solvents can act as hydrogen bond donors or acceptors, which can cause the  $pK_a$  to shift. This shift occurs due to the interaction between the organic solvent and analyte, which alters the stability of charged species that form through the ionization reaction, making the analyte less acidic or basic. The type of organic solvent used will influence the magnitude of the shift in  $pK_a$ , with polar solvents shifting  $pK_a$  more than non-polar solvents. Likewise, the degree of solubility of the compound in the organic solvent will also affect the  $pK_a$  shift. This knowledge can be used to improve appropriate synthetic approaches, enhance reaction environments, or even design new compounds with the required properties.

Diverse solvent effects result from the different intermolecular attractions accessible to solvent molecules. Some solvents form hydrogen bonds through either donation or

acceptance. Water is a frequent example, as are alcohols such as methanol. Others can accept hydrogen bonds but not donate them. Acetone and acetonitrile are two examples. Solvent molecules can have polar hydrogen atoms or not, and the related solvents are named protic or aprotic, respectively. Water, which contains just polar hydrogens, is one of the most common protic solvents. Acetonitrile (MeCN) is a common aprotic solvent.

### 1.4.1. Organic solvents and organic-water solvents in capillary electrophoresis

Organic solvents have been used as buffer modifiers in CE to enhance selectivity-resolution, increase the solubility of hydrophobic analytes, or modify analyte electroosmotic flow (EOF) and electrophoretic mobility<sup>37,74,75</sup>. A number of studies have been performed to describe the physical chemistry involved in electrophoretic separations in the presence of background electrolyte (BGE) in the presence of organic solvents<sup>28,76-78</sup>. The dielectric constant ( $\epsilon$ ) of the solvent is the main factor governing the ionic interactions. Solvents with  $\epsilon < 10$  are useless since very small or no ionic dissociation takes place. For  $10 < \epsilon < 30$ , in which ionic dissociation happens, ion pair formation is the main impact. Solvent viscosity ( $\eta$ ) directly influences ion mobility and thus electroosmosis<sup>79</sup>. Nevertheless, viscosity cannot be studied in isolation since variations in the solvent content also have an impact on the permittivity and zeta potential of the medium<sup>57,75,80</sup>.

The fact that the analyte ionization constants in organic media differ from those in aqueous solutions is another significant problem in non-aqueous solutions in capillary electrophoresis studies. Analyte mobility is dependent on the degree of ionization and the real mobility of the fully charged species, both of which are effects of the dissociation equilibrium. The thermodynamic stability of the reactants and products affects the dissociation equilibrium<sup>79</sup>. The solvent capacity to stabilize charged species plays a major role in the equilibrium when switching from an aqueous to an organic medium.

Analyte mobility is controlled by the separation medium BGE viscosity ( $\eta$ ) and dielectric constant ( $\epsilon$ ), and both are influenced by the usage of organic solvent. As a result, if all other parameters remain constant, greater electrolyte  $\epsilon$ :  $\eta$  ratios result in quicker electrophoretic migration and EOF. In addition, organic solvents can have complex effects on capillary wall contacts. Currents are often lower in non-aqueous media than in aqueous buffers of the same ionic strength<sup>79,81</sup>. Moreover, good separations are often obtained even in non-aqueous solutions of moderate ionic strength. Many important analytes are sparingly soluble in water

but are much more soluble in certain organic solvents. The addition of organic solvent led to an increase in the  $pK_a$  of the acid compared to the aqueous medium<sup>57,80,82</sup>.

Furthermore, the form of organic solvent can also affect the resolution of the separation, as it can affect the interactions between the drug molecules and the buffer molecules. Finally, the organic solvent can also affect the migration time of the drug, which can affect the overall resolution of the separation. Therefore, it is important to consider the effects of the organic solvent on the  $pK_a$  of an insoluble drug when using capillary electrophoresis.

The addition of methanol and acetonitrile solvents to the aqueous buffer used in capillary electrophoresis (CE) can have an effect on the  $pK_a$  of the analyte. The effect is dependent on the concentration of the additives.

### **1.4.2. Exploring the effect of organic solvents on the $pK_a$ of very insoluble drugs**

Modern drug development frequently produces compounds that are highly lipophilic and sparingly soluble in water, making it difficult to evaluate their physiochemical properties. One such property. The acidity constant, which measures the compound ability to donate a proton in solution, is one such feature. The determination of the acidity constant of the drug can be difficult when the drug is not sufficiently soluble in water because many assays require the drug to be fully dissolved in water in the measurements. Hence, the determination of the acidity constant of this kind of drugs can be a serious problem<sup>5,30,31</sup>. Many analytical methods like, potentiometry and spectrophotometry, are usually used to determine the  $pK_a$  of very insoluble drug<sup>30,36,43,83</sup>. The  $pK_a$  in water then is extrapolated to 0% organic solvent using Yasuda-Shedlovsky extrapolation method.

The Yasuda-Shedlovsky extrapolation procedure is a popular method for calculating approximately the  $pK_a$  of an analyte in a solvent if the experimental  $pK_a$  values in this solvent are not available. The idea of this method is based on the extrapolation of the  $pK_a$  from data collected in solvents for which the  $pK_a$  is known. The Yasuda-Shedlovsky extrapolation predicts compound acidity or basicity in different solvents, supporting researchers in chemistry and pharmaceuticals by employing solvent properties and  $pK_a$  values. Herein, the  $pK_a$  of the target analyte was determined at different organic compositions, such as (methanol and acetonitrile), from 0 to 90%, and the aqueous  $pK_a$  was obtained by extrapolation to 0% organic solvent through the Yasuda-Shedlovsky method. Understanding how analyte acidity and basicity respond to differences in solvent environment requires determining the  $pK_a$  of the target analyte at different organic mixture

ranging from 0 to 90 % methanol and acetonitrile. This method depends on the linear relationship between the  $pK_a$  of the analyte and the reverse of the solvent dielectric constant. The dielectric constant, which changes with the polarity of the solvent, is a measure of the solvent capacity to separate opposing charges. The Yasuda-Shedlovsky equation links the  $pK_a$  of the analyte in a solvent to the  $pK_a$  of the same analyte in water and the solvent dielectric constant.

$$pK_a + \log [H_2O] = a \frac{100}{\epsilon} + b \quad (40)$$

In this equation,  $\log [H_2O]$  is the logarithm of the water molar concentration in a given solvent mixture, and  $\epsilon$  is the dielectric constant of the solvent mixture. From the plot of the  $pK_a$  vs.  $100/\epsilon$  a linear relationship should be obtained, and extrapolation to pure water would provide the aqueous  $pK_a$  of the compound. Thus, this equation permits the determination of the  $pK_a$  of the analyte in a varied range of solvents, depending on the experimental measurements in just one solvent<sup>30,31,36,43,83</sup>. Extrapolating the behavior of the analyte ionization equilibrium throughout a different solvent condition by performing an experiment to measure the equilibrium constants ( $K_a$ ) of the analyte in a particular solvent and then using the same equation to calculate the  $pK_a$  in a different solvent.

### **1.4.3. Exploring the effect of organic-water solvents on the analyte $pK_a$ and buffer pH in common HPLC mobile phase.**

HPLC separation depends on the degree of ionization of acid-base compounds, which in turn depends on the analyte  $pK_a$  and buffer pH. The effect of the organic-water solvent mixture on the  $pK_a$  of the analyte and pH of the buffer is a critical concern in the common HPLC mobile phase. The addition of organic solvents to water can modify the ionization state of analytes, resulting in variations in their  $pK_a$  values and the pH of the buffer. The pH difference caused by adding an organic solvent to an aqueous buffer depends not only on the organic proportion of the mixture, buffer concentration, and aqueous pH, but also on the type of buffering system<sup>37,73,84,85</sup>. These factors can have an influence on the efficiency of analytes and retention behavior, making it critical to carefully choose and adjust solvent conditions to achieve the desired separation performance<sup>86</sup>.

The addition of methanol and acetonitrile to the aqueous buffer may change the buffer pH and the  $pK_a$  of the analyte mainly due to the differences in the dielectric constant. The dielectric constant is a measure of solvent ability to shield electrical charge. The change in the dielectric constant affects both the buffer pH and the  $pK_a$  of acid-base analyte. The

ionization equilibrium of acidic and basic buffer component affects the pH of an aqueous buffer system. The addition of organic solvent with lower dielectric constant may disturb the ionization equilibrium, lead to decreased ion solvation, resulting in change acid-base equilibrium and changing in the buffer pH <sup>73,85,86</sup>.

In addition, the  $pK_a$  of acidic analytes influences their protonation and deprotonation behavior, and solvent dielectric constants impact the strength of intermolecular interaction and ion solvation. So, understanding how these factors work together is important for foreseeing and controlling the chemical behavior of molecules in different solvents. The addition of methanol and acetonitrile decreases the solvation of acidic analytes, affecting their protonation equilibrium and changing the  $pK_a$  value. These  $pK_a$  alterations might have an impact on their chromatographic behavior and elution profile <sup>37,72,73,84</sup>. important to understanding how these factors work together is essential for predicting and controlling the chemical behavior of molecules in various solvent environments.

The addition of methanol and acetonitrile to the aqueous buffer changes the pH and the  $pK_a$  of the analyte because they have a lower dielectric constant than water, are less polar, and are less efficient at solvating ions.

As a result, the addition of methanol and acetonitrile can affect the solubility of the analyte's and modify its ionization behavior. This can result in a change in the acidic analyte's  $pK_a$ , which is the pH at which the analyte exists in the same proportion of ionized and non-ionized forms. Moreover, the addition of methanol and acetonitrile may cause a shift in the pH of the buffer due to the fact that the buffering capacity of the aqueous buffer is decreased in the presence of organic solvents. This impact is stronger when the buffer concentration is low or the concentration of organic solvent is higher <sup>72,86</sup>.

The addition of methanol and acetonitrile to the aqueous buffer led to a decrease in the analyte solvation and effective charge density for neutral and anionic acidic analytes. As the methanol and acetonitrile concentrations increased in the mobile phase, the solvent environment become less polar and less ability of forming strong hydrogen bond. The electrostatic interaction that contributes to the  $pK_a$  value decreased, resulting in an increase in the  $pK_a$  value. On the other hand, cationic acid has different behavior due to the addition of methanol and acetonitrile because there is no change in the number of charges on both sides of the equilibria Equation (5). Thus, variation of the dielectric constant has no effect on the acid-base equilibria <sup>37,72,73,85,86</sup>.



## 1.5. Relevant physico-chemical properties: octanol-water partition coefficient ( $\log P_{o/w}$ )

As stated at the beginning, drug innovation and development are critical components that depend mostly on in vitro testing. There are numerous in vitro studies available to establish key parameters of absorption, distribution, metabolism, and excretion, such as solubility, lipophilicity, and plasma stability. These methods are valuable in defining how compounds may work and can be applied as alternatives before conducting in vitro experiments and clinical trials. Drug discovery is essentially divided into two types; the first is pharmacodynamics, which studies the effects of drugs on the body and their mechanism of action, such as a receptor or enzyme, to produce a biological response. The second is pharmacokinetics, which examines the behavior of drugs on the body and concerned with how the body affects the drug<sup>87,88</sup>. The key methods of pharmacokinetics are absorption, distribution, metabolism, and excretion ADME, followed by toxicity ADMET<sup>6,9</sup>. Although ADME aims to increase the pharmacological performance of small molecules and decrease all kinds of side effects. So, the estimation of the ADME is very valuable for progressing the compound's development in drug discovery<sup>89</sup>.

Lipophilicity defines a compound tendency to dissolve or associate with lipid-like compound. It defines the degree of hydrophobicity or attraction for lipid environments and impacts the compound's interaction with biological membranes and distribution in the body. The most general approach to stating the lipophilicity of the compound of commercial, medicinal, or environmental importance is the partition constant of a compound between n-octanol and water (or an aqueous solution). Comparing octanol/water to other systems with organic phases, such as alkanes, cycloalkanes, haloalkanes, aromatic solvents, or even other octanols with lower or higher carbon atom counts, octanol/water provides a variation of pertinent advantages<sup>90</sup>. First of all, it is a possible model of the lipid components of biological membranes due to its relatively long alkyl chain and the polar hydroxyl group. This synthetic reference model really consists of two binary phases: one aqueous phase that is saturated with n-octanol and one that is n-octanol saturated with water. In the former, the concentration of water is high, about 2 mol/L. In other words, there are approximately four alcohol molecules for every one water molecule. In addition, these polar groups do not need to be completely dehydrated throughout the transfer method from the aqueous to the octanol phase, indicating that the partition of polar compounds into the octanol phase does not significantly alter the structure or properties of the organic solvent under these

circumstances. The amount of organic solvent in the n-octanol-saturated aqueous phase is in the mmol/L range and has little bearing on the process. The hydroxyl moiety of n-octanol also possesses hydrogen-bond donor (acidity) and acceptor (basicity) capabilities, enabling the stabilization of interactions with a wide range of polar groups and promoting their solubility in the organic phase. Finally, n-octanol has a suitable viscosity, a low vapor pressure, and is compatible with UV detection for quantification purposes from an experimental point of view<sup>91</sup>.

Lipophilicity can be evaluated extensively by the octanol- water partition coefficient<sup>16,89,92</sup>. The partition coefficient of a chemical compound is a physico-chemical parameter and indicative of how pharmacologically active compounds split throughout the aqueous and fatty parts of the human body and is usually used in forming quantitative structure-activity relationships (QSARs). The QSARs models are significant for a variety purposes and have attracted wide scientific interest, particularly in the pharmaceutical industry for drug discovery and in toxicology and environmental science for risk evaluation, also, it based on the assessment of octanol–water as a general solute descriptor for the lipophilicity of organic compounds<sup>89,93-97</sup>. The abbreviation  $\log P_{o/w}$  is used to identify the octanol-water partition coefficient of neutral compounds, and  $\log D_{o/w}$  the distribution coefficient of ionisable compounds. At this point, the ratio of a solute concentration in a single definite form (C) in the water-saturated octanol phase (O) to its concentration in the same form in the aqueous phase (W) at equilibrium, expressed in its decimal logarithmic form, is defined by the octanol-water partition coefficient for an ionizable substance in its neutral form or in neutral substance as follows:

$$\log P_{o/w} = \log \frac{[C]_o}{[C]_w} \quad (41)$$

The IUPAC recommends expressing  $\log P_{o/w}$  as the partition ratio. However, the word partition coefficient, or better yet, partition constant, is commonly used in scientific considerations and publications<sup>91,97</sup>. Nevertheless, it should be stated that  $\log P_{o/w}$  only applies to a single species, which is a principal reason to consider when working with ionizable acidic or basic compounds. To promise that a compound is in its neutral form since  $\log P_{o/w}$  is often specified for the neutral (unionized) form of a compound, the lipophilicity must be measured at the suitable pH, which is characteristically at least two units below the solute  $pK_a$  for acids or two units above for bases<sup>89,91</sup>. The more lipophilic the solute, the higher the  $\log P_{o/w}$  value. A distribution ratio or constant ( $\log D_{o/w}$ ) is established taking into consideration the different species that may be present in either phase at equilibrium, where

the impact of ionization should be considered when measuring lipophilicity, which is extremely frequent for pharmacological compounds. The definition of ( $\log D_{o/w}$ ) for a monoprotic acid (HA/A) or base (BH<sup>+</sup>/B) is in the next equation:

$$\log D_{o/w}(\text{acid}) = \log \frac{[\text{HA}]_o + [\text{A}^-]_o}{[\text{HA}]_w + [\text{A}^-]_w} \quad (42)$$

$$\log D_{o/w}(\text{base}) = \log \frac{[\text{BH}^+]_o + [\text{B}]_o}{[\text{BH}^+]_w + [\text{B}]_w} \quad (43)$$

In the case of the ionic species that do not partition into the octanol phase, the use of the acidity constant of the solute and equations (42) and (43) lead to the following expression:

$$\log D_{o/w}(\text{acid}) = \log \frac{P_{o/w}(\text{HA})}{1 + 10^{\text{pH} - \text{p}K_a}} \quad (44)$$

$$\log D_{o/w}(\text{base}) = \log \frac{P_{o/w}(\text{B})}{1 + 10^{\text{p}K_a - \text{pH}}} \quad (45)$$

Where acidic and basic species are referred to as  $P_{o/w}(\text{HA})$  and  $P_{o/w}(\text{B})$ , respectively. With the use of these equations, a lipophilicity-pH profile may be defined for neutral species and for pH ranges near the  $\text{p}K_a$  value. In the other sections ( $\text{pH} \ll \text{p}K_a$  for bases and  $\text{pH} \gg \text{p}K_a$  for acids), the  $\log D_{o/w}$  drop is infinite. It has been shown experimentally that ionic substances do, in fact, partition into the organic phase, but most frequently as ion pairs. The type and concentration of the counterion as well as the ionic species lipophilicity have an impact on the partition ratio for the ionic species<sup>91,97</sup>. Therefore, based on  $\log P_{o/w}$  and  $\text{p}K_a$  values found in the literature, more accurate formulae may be applied to determine the  $\log D_{o/w}$  profiles of an acid and a base<sup>10</sup> as show in equations (46) and (47):

$$\log D_{o/w}(\text{acid}) = \log \frac{P_{o/w}(\text{HA}) + P_{O/w}(\text{A}^-) \cdot 10^{\text{pH} - \text{p}K_a}}{1 + 10^{\text{pH} - \text{p}K_a}} \quad (46)$$

$$\log D_{o/w}(\text{base}) = \log \frac{P_{o/w}(\text{B}) + P_{O/w}(\text{BH}^+) \cdot 10^{\text{p}K_a - \text{pH}}}{1 + 10^{\text{p}K_a - \text{pH}}} \quad (47)$$

### **1.5.1.Methods used to determine the octanol-water partition coefficient**

The lipophilicity  $\log P_{o/w}$  feature may be estimated using a selection of computational and experimental methods. There are numerous software programs (such as ClogP, AlogPs, and ACDLabs) that can approximate  $\log P_{o/w}$  computationally. Nevertheless, the results typically lack consistency since multiple methods are used in the calculation. In this regard, substantial research on the reliability of  $\log P_{o/w}$  values derived by various software methodologies has been published<sup>91,98-100</sup>.

Either direct or indirect approaches can be used to acquire the experimental  $\log P_{o/w}$  values. The Organization for Economic Co-operation and Development (OECD)<sup>101</sup>, recommends the traditional shake-flask method as a standard method, and potentiometric approaches are also included in the direct methods<sup>91,102</sup>. The most popular indirect method for determining octanol-water partition constants is reversed-phase liquid chromatography (RPLC), which is also recommended as a standard procedure by the OECD due to its high throughput, insensitivity to impurities or degradation products, broad dynamic range, online detection, and sample size requirements.

#### **1.5.1.1.Shake flask method.**

The conventional shake-flask way is the most commonly used technique for establishing the octanol-water partition constants<sup>101</sup>. The partitioning solvents (water and n-octanol-saturated water) are both put in a flask, and a compound is introduced to each of them. In order to find out the  $\log P_{o/w}$  value, the phases are separated, the flask is shaken to accelerate the partition equilibrium, and the amount of compound in each phase is measured Figure (4). For ionizable compounds, the  $\log D_{o/w}$  may be assessed using a similar method as long as the pH is properly regulated.

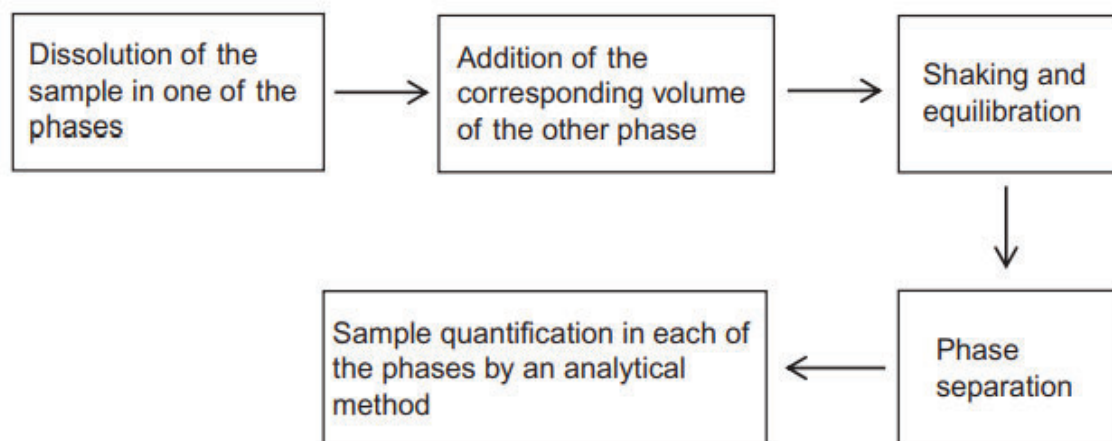


**Figure 4.** Flowchart of the shake-flask method steps <sup>91</sup>.

Although this is a very direct way, a substantial number of parameters must be regulated to guarantee an accurate result <sup>91</sup>:

- I. Temperature: one of the most key variables to control is temperature. Temperature control is necessary throughout the whole process, starting with the saturation of both solvents at the correct temperature.
- II. Volume ratio between phases: Since most lipophilic compounds would require high aqueous volumes and vice versa, it is necessary to estimate the compound  $\log P_{o/w}$  or  $\log D_{o/w}$  value in order to enhance the ratio <sup>102,103</sup>. According to recommendations <sup>91,102</sup>, at least three different volume ratios should be tested: the ratio that fits the predicted  $\log P_{o/w}$  the reliable, the ratio directly above it, and the ratio directly below it. Moreover, duplicate tests for each ratio should be performed.
- III. In order to produce the correct  $\log D_{o/w}$  or  $\log P_{o/w}$  values for ionizable compounds, the pH of the aqueous phase must be modified. The ionized form of the compounds can form ion pairs with specified buffer components when buffer solutions are used to adjust the pH of the aqueous phase. In such a situation, this secondary chemical equilibrium will change the  $\log D_{o/w}$  value, and the buffer concentration will absolutely change the final  $\log D_{o/w}$  value.
- IV. Shaking and equilibration procedure: the rate at which the two phases equilibrate adjusts depending on the containers used (glass tubes, chromatography vials, 96-well plates, etc.) and the intensity of the agitation, but in most cases, equilibrium is achieved rapidly. On average, 1 hour of shaking is sufficient to achieve balance. To

decrease the production of emulsions, which inhibit the final phase separation, vigorous agitation is not recommended. Centrifugation is regularly preventable when agitation is performed using rotatory rollers or orbital baths. But it is a required step when phases are not clearly defined.

- V. Phase separation: how each phase is taken for analysis and the method of phase separation are both fundamental. One of the drawbacks of this technique involves cross contamination, which is important when the volume of the aqueous phase is tested, as the syringe needle must pass through the octanol phase in order to reach the aqueous phase.
- VI. Quantification: numerous analytical approaches, involving UV spectroscopy and liquid chromatography with either UV or MS detection, can be applied to evaluate the concentration of each compound in each phase.

The greatest advantage of the shake-flask methodology is that it doesn't require any specific equipment. Its lack of automation, nevertheless, is its essential flaw. In this context, a number of modifications to the method have been made in recent years with the objective of reaching a high-throughput technique for regular analysis. An important adjustment that has an influence on essentially all parts of the method to achieve valuable results was made it <sup>104</sup>:

- I. The primary progress was the use of chromatographic sample vials as containers to perform both phases equilibration and sample analysis in a single reservoir.
- II. The second improvement was to absolutely establish the volume of the component in the aqueous phase. A stock solution of the compound in aqueous phase was made for this principle. Different partition vials were prepared using this stock solution, which was also employed to establish the initial compound concentration. Then, four vials were prepared for the analysis: one had the standard stock solution, and the other three had stock solution in three different n-octanol/stock solution ratios. The area of the compound in each partition was compared to the area of the compound in the stock solution to determine the concentration in the aqueous phase using Equation (48), which derives from Eq (41):

$$\log D_{o/w} (P_{o/w}) = \log \left( \left( \frac{A_{st}}{A_w} - 1 \right) \frac{V_w}{V_o} \right) \quad (48)$$

In this equation, the peak areas of the compound for the standard stock solution and the aqueous phase of the partition, respectively, are expressed by  $A_{st}$  and  $A_w$ , while the volumes of water and octanol in the partition vials are denoted by  $V_w$  and  $V_o$ .

- III. The use of a vial roller for 90 minutes during the equilibration process was the third enhancement, which ensured appropriate mixing and prevented emulsion formation.
- IV. The HPLC system was directly injected from the vial without first undergoing separation as the fourth enhancement.
- V. The last enhancement involved the examination of the material using a quick generic gradient approach. Including the equilibration stage, the procedure took 7.5 minutes.

The technique proposed was employed to log  $D_{o/w}$  estimations that including a range from 1.5 to 3.5. Nonetheless, a limitation of the approach is that the compound must have a good aqueous solubility.

With a concentration on different steps of the method, other writers have also worked on automating the shake-flask approach. For instance, Hitzel *et al*<sup>105</sup>, proposed a fully automated approach for adding the organic and aqueous phases into a 96-well plate utilizing an automated pipetting machine. Each phase was then directly injected into an HPLC system, where a fast gradient was employed for analysis after the samples had been equilibrated for 30 min. The only problem of this method is the solubility problem, which makes it only useful for log  $D_{o/w}$  values between 2 and 4. Routine analysis now frequently uses 96-well plates rather than chromatographic vials<sup>105-108</sup>.

Andres *et al*<sup>103</sup>, presented three different methods to develop the applicability of the technique to molecules with greater lipophilicity based on the methodology. According to the predicted lipophilicity of the compounds, they were classified into three groups: low, high, and regular. These procedures enhance variables like the sample solvent, the partition ratios, and the phase that will be assessed. The methods were developed to require a small number of samples, and they were established on compounds with log  $D_{o/w}$  values between 2 and 4.5<sup>91</sup>.

Other authors assessed the probability of using compounds initially dissolved in DMSO, since this is the solvent used for most compound libraries<sup>91</sup>. Modifications in log  $D_{o/w}$  were demonstrated to be substantial for DMSO contents as low as 0.5%<sup>108</sup>. Moreover, the increase in the concentration of DMSO in the samples correlated the decrease in the log  $D_{o/w}$  value

<sup>91,103,108</sup>. Other authors recommended a drying stage in which DMOS was removed at 40°C under vacuum <sup>107</sup>, in order to overcome this problem. After that, the dried sample is dissolved in either the aqueous phase or octanol.

The quantification step has also acknowledged numerous innovation recommendations. As HPLC is so simple and only requires a small volume of material, it is typically the technique of choice. Additionally, as impurities are isolated from the primary component during analysis, they do not interfere. Most of the time, a UV detector is sufficient for detection, nonetheless, several methods using MS detection have been established because LC-MS is normally the method of choice for measuring small compounds in industry <sup>91,107,108</sup>. Other methods based on miniaturization have been applied in recent years for the calculation of  $\log D_{o/w}$ . Microchip capillary electrophoresis with contactless conductivity detection (MCE-CCD), which was utilized to calculate the  $\log D_{o/w}$  for a number of drugs with an analysis time of under 40 seconds <sup>109</sup>, is one example. Other approaches rely on microfluidic liquid-liquid extraction (MLLE) devices, which enable high automation and quickly determine  $\log D_{o/w}$  and  $\log P_{o/w}$  <sup>87,110</sup>. MLLE offers a significant change compared to conventional instrumental-based analytical approaches. The main advantage of this approach is the miniaturization of the system. As a consequence, MLLE reduces sample volume, waste, and extraction time, is environmentally friendly and cost-effective, and makes it particularly well-suited for high-throughput purposes. Moreover, it provides precise control over liquids and mixing, resulting in high reproducibility of the liquid-liquid extraction.

#### **1.5.1.1.1. Fundamental of the procedure**

The classic shake-flask technique is appropriate for determining the compound concentration in the octanol and water phases in accordance with Eq (41), after the equilibration of both phases. Eq (49) can be expressed as follows:

$$\log D_{o/w} = \log \left( \frac{m_o}{m_w} \cdot \frac{V_w}{V_o} \right) = \log \left( \frac{A_o}{A_w} \right) \quad (49)$$

where  $m_o$  and  $m_w$  represent compound mass in the organic phase (octanol) and water, respectively, and  $V_o$  and  $V_w$  refer to the volume of octanol and water in the partition flask, and  $A_o$  and  $A_w$  refer to the peak area of octanol and water, respectively.

When drug volumes in both phases are equivalent, the most precise determination is achieved. This fact depends fully on both the exact  $\log D_{o/w}$  of the drug and the particular  $V_w/V_o$  ratio employed in the shake-flask method, as:

$$\log \frac{m_o}{m_w} = \log D - \log \frac{V_w}{V_o} \quad (50)$$

It is vital to analyze the  $\log D_{o/w}$  values of the compounds in issue in order to establish and suggest ( $V_o/V_w$ ) ratios for establishing the  $\log D_{o/w}$  of drugs with distinct solubility properties. For compounds with  $\log D_{o/w}$  values close to 0, similar volumes of the aqueous and organic phases can be equilibrated to achieve precise results. Nonetheless, for compounds with  $\log D_{o/w}$  values that are notably different from 0, it may be mandatory to adjust the volume ratio of the organic and aqueous phases to obtain a precise result. To make sure that the majority of the compound remains in the aqueous phase after equilibration, very low volume ratios of water to octanol may be needed for very hydrophilic compounds with  $\log D_{o/w}$  values that are significantly lower than 0. On the other hand, it may be required to use a very high-volume ratio of water to octanol for very hydrophobic compounds with  $\log D_{o/w}$  values significantly greater than 0 to make sure that the rest of the compound remained in the organic phase after equilibration. It is significant to note that working with either low or extremely high-volume ratios of water to octanol can be difficult and may require specific tools and knowledge. To guarantee accurate and exact measurements of  $\log D_{o/w}$ , it is crucial to carefully evaluate the solubility properties of the compounds being researched and to utilize the proper quantities and volume ratios <sup>103</sup>.

The indicated method is fundamental for calculating the drug concentration in the octanol and water phases using HPLC. Measurement in octanolic phases is challenging, though. Octanol has a high viscosity, making it difficult and time-consuming to clean the column after using it in a typical HPLC column. Moreover, because of its limited solubility due to its high viscosity (Sangster, 1997), it is an inappropriate solvent for mass spectrometer detection (MS), a typical detection method used in analytical drug development laboratory and for determining physico-chemical parameter values <sup>103</sup>.

**I. Regular lipophilic compound (procedure 1):** If different volumes of the two observed solutions are injected, Eq (42), which can be easily advanced to Eq (51) to estimate the  $\log D_{o/w}$  value, may be used to determine the HPLC peak areas of the standard ( $A_{st}$ ) and aqueous ( $A_w$ ) phase solutions:

$$\log D_{o/w} = \log \left( \left( \frac{A_{st}}{A_w} \cdot \frac{v_{inj(w)}}{v_{inj(o)}} r - 1 \right) \frac{V_w}{V_o} \right) \quad (51)$$

where  $v_{inj(st)}$  and  $v_{inj(w)}$  are the injection volumes of the standard solution and the aqueous phase of the partition, respectively, and  $r$  is the proper standard solution dilution factor.

Although Eq (51) has the same applicability range as Eq (46), the process does not include evaluating octanol phases. The most particular results should be found for phase ratios close to  $D_{o/w}$  values since when  $\log V_w/V_o = \log D_{o/w}$ , then  $m_o = m_w = m_{st}$  for Eq (49).

Since the  $\log D_{o/w}$  value is unidentified, it is difficult to determine the proper  $V_w/V_o$  ratio. Nonetheless, it is typically possible to predict the test compound approximate lipophilicity and calculate an approximate  $V_w/V_o$  value. Three shake-flask determinations are suggested; the first one uses the  $V_w/V_o$  ratio obtained from the predicted  $\log D_{o/w}$  value, and the second and third ones use volume ratios that are much lower and higher, respectively. Usually, at least one of these conclusions is accurate enough. In theory, drugs with very low or very high  $\log D_{o/w}$  values that require for very low or very high  $V_w/V_o$  ratios might provide a challenge for the operation.

**II. Poorly lipophilic compounds (procedure 2):** The lowest possible  $V_w/V_o$  ratios may not be enough to produce an appreciable partition into the octanol phase for very low  $\log D_{o/w}$  values, making it impossible to accurately determine  $A_w / v_{inj(w)} \sim A_w \cdot r / v_{inj(st)}$ , and  $\log D_{o/w}$  from Eq (51). If the detector is intelligent enough to measure  $A_o$  and calculate  $\log D_{o/w}$  using Eq (52), which would replace Eq, then detecting the octanoic phase is the only reliable alternative in this situation:

$$\log D_{o/w} = \log \frac{1}{\frac{A_{st}}{A_w} \cdot \frac{v_{inj(w)}}{v_{inj(o)}} - \frac{V_w}{V_o}} r \quad (52)$$

**III. highly lipophilic compounds (procedure 3):** The challenge of measuring the properties of highly lipophilic compounds is that they may have low aqueous solubility, which can make it difficult to prepare a standard solution for use in measurements. To address this issue, two possible procedures are proposed: using a cosolvent such as DMSO to enhance solubility and dissolving the compound in octanol instead of water, Eq (51) can be used to measure the properties of the compound as in (procedure 1). An alternative method is to dissolve the sample in octanol rather than water if DMSO improvement of solubility is insufficient as will explain in (Procedure 3). This stock solution is directly equilibrated with the aqueous phase without any dilution in order to enhance the amount of the drug in the aqueous phase. After measurements of the equilibrated aqueous phase and the stock solution that has been diluted by a  $r$  factor,  $\log D_{o/w}$  may be computed using Eq (53).

$$\log D_{o/w} = \log \left( \frac{A_{st(o)}}{A_w} \cdot \frac{v_{inj(w)}}{v_{inj(st)}} r - \frac{V_w}{V_o} \right) \quad (53)$$

### 1.5.1.2. Potentiometric method

The  $\log P_{o/w}$  of ionizable compounds can be determined via the potentiometric method, especially for those with inadequate chromophores. This technique allows for simultaneous estimation of  $pK_a$  and  $\log P_{o/w}$ , which permits the calculation of the  $\log D_{o/w}$  value at any desired pH.

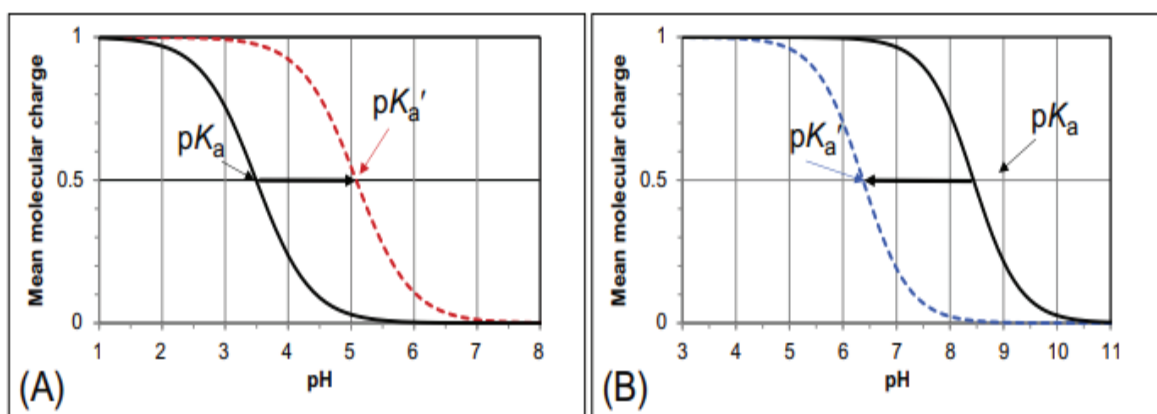


**Figure 5.** Bjerrum plot curves for (A) a monoprotic weak acid (HA) and (B) a monoprotic weak base (B). Solid lines correspond to a titration in water and dashed lines to a titration in the n-octanol-water mixture <sup>91</sup>.

The approach requires estimating how the  $pK_a$  changes when a titration is performed in a two-phase octanol-water system as opposed to water. Two titrations of the chemical are performed through a pH range that encompasses its  $pK_a$ . The acidity constant ( $pK_a$ ) is found from the first titration, which is performed in the aqueous phase. The apparent acidity constant ( $pK'_a$ ), which is displaced from the aqueous  $pK_a$  value, may be determined by the second titration, which is carried out in an octanol-water combination. A monoprotic weak acid (HA) and a monoprotic weak base (B) exhibit a  $pK_a$  shift when the neutral form dissolves in n-octanol, as shown in Figure 5. The ( $pK'_a$ ) value for a monoprotic weak acid is higher than the value in aqueous solution.

The different inflection points of the curve  $pK'_a$ , and  $pK_a$  values for a monoprotic weak acid is higher than the value in aqueous solution. This occurs because, when the acid partitions to n-octanol, the concentration of the neutral form of the acid drops in the aqueous phase. As a result, the equilibrium moves away from hydrogen ion production, giving the material a more basic appearance ( $pK'_a > pK_a$ ). In contrast, a monoprotic weak base (B) experiences

a reduction in pH due to the loss of neutral form in the aqueous phase, which makes the compound look more acidic and shifts the  $pK_a$  to lower values ( $pK'_a < pK_a$ )<sup>36,111,112</sup>.

The size of the shift in both situations is determined by how the species are divided. A high value of  $\log P_{o/w}$  is indicated by a big  $pK_a$  and  $pK'_a$  differential. Equations (54) and (55) enable determination of the partition constant for HA and B, respectively, even if only the neutral form partitions:

$$P_{o/w}(\text{HA}) = \frac{10^{(pK'_a - pK_a)} - 1}{r} \quad (54)$$

$$P_{o/w}(\text{B}) = \frac{10^{(pK_a - pK'_a)} - 1}{r} \quad (55)$$

where  $V_o$  is the volume of octanol and  $V_w$  is the volume of the aqueous phase, and  $r$  is the phase ratio ( $V_o/V_w$ ). The hydrophobicity of the compounds determines the volume ratio that is desired.

Equation (56) describes the relationship between the partition constant and ionization constant and the shift in  $pK'_a$  with respect to  $pK_a$  that occurs when the ionic species partitions into the octanol phase:

$$|pK'_a - pK_a| = \log \frac{1 + rP_n}{1 + rP_i} \quad (56)$$

where  $P_i$  and  $P_n$  are the compound neutral and ionic forms' respective partition constants. Since acids are pushed to higher values and bases are shifted to lower values, the  $|pK'_a - pK_a|$  reveals the absolute size of the differences between the apparent and aqueous  $pK_a$ . Three titrations must be carried out since there is a third parameter ( $P_i$ ) that has to be estimated: one without n-octanol and two in octanol-water mixture with different phase ratios. It is typical for monoprotic weak acids and bases to have an ionized species partition into the octanol phase that is 3–4 orders of magnitude lower than that of the neutral form. Therefore, the third titration n-octanol volume must be higher than the second titration's. The three constants  $pK_a$ ,  $\log P_n$ , and  $\log P_i$  may be computed from the two  $pK_a$  shifts, the volume ratios  $r_1$  and  $r_2$ , and the two  $pK_a$  shifts<sup>36,91,111,113</sup>.

As long as the compound can be dissolved in water or n-octanol, the potentiometric  $\log P_{o/w}$  method may be used to analyze compounds that go through dimerization and/or ion pair partitioning in the organic phase. Since the pH is determined in the dual-phase system without complete phase separation, the approach may be applied to a wide variety of

octanol-to-water volume ratios. However, if values move to  $pK_a$  further than the detectable range, this approach cannot be employed for hydrophobic weak acids and bases with high or low  $pK_a$  values, respectively (2 -12). The volume ratio ultimately determines the measurement range, which approximately ranges from  $\log P_{o/w}$  of 2 to 6 in 0.15 M KCl <sup>114</sup>.

### 1.5.1.3. Liquid chromatographic methods

The typical shake-flask method to calculating  $\log P_{o/w}$  can be labor- and time-intensive, but the titrimetric approach might not be applicable for non-ionizable compounds. As a result, liquid chromatography, in particular RPLC, has emerged as a well-liked and effective technique for calculating  $\log P_{o/w}$  <sup>91</sup>.

RPLC is the best approach for drug discovery in the field of drugs because it allows high-throughput, rapid investigation of several candidate drugs. Furthermore, the versatility of RPLC permits it to be employed to calculate a selection of compounds, involving both ionizable and non-ionizable compounds. The approach the target analyte is divided between the stationary and mobile phases determines how RPLC will separate it. The mobile phase is often a mixture of water and an organic solvent, while the stationary phase is typically a hydrophobic substance, such as C18. The  $\log P_{o/w}$  of the analyte may be estimated by modifying the mobile phase composition. Some studies have focused on the selection of appropriate mobile and stationary phases that can replace the actual octanol-water partitioning system <sup>115</sup>. N-octanol and water should preferably make up the stationary and mobile phases, respectively. Nevertheless, there aren't many n-octanol stationary phases on the market that can be employed for this. Using n-octanol-saturated water as the mobile phase, several attempts have been made to immobilize n-octanol on the stationary phase surface. A commercially available device was also established <sup>91</sup>. A set of reference compounds with determined  $\log P_{o/w}$  values are treated to calibrate the chromatographic system by determining the retention factor ( $\log k$ ). The vital challenge with this process is keeping the amount of n-octanol immobilized on the stationary phase constant while adjusting the octanol/water volume ratio to allow a wide variety of partition constants (i.e.,  $-1 < \log P_{o/w} > 5$ ) <sup>91</sup>.

The retention factor of the measured standards ( $\log k$ ) is associated with  $\log P_{o/w}$  values of standards in various systems to get the connection shown in the following equation:

$$\log P_{o/w} = n + m \log k \quad (57)$$

Different concentrations of the organic solvent in the mobile phase must be employed for the correlation in order to cover a wide range of  $\log P_{o/w}$  values. Because of this, a lot of authors use the retention factor ( $k_w$ ) that was linearly extrapolated to pure water using  $\log k$  studies at different mobile-phase compositions ( $\varphi$ ) as in Eq (58):

$$\log k = S\varphi + m \log k_w \quad (58)$$

However, other writers have discovered better connections between  $\log P_{o/w}$  and  $\log k$  for specific mobile-phase compositions. It is generally accepted that extrapolation to pure water yields retention/partition values in an environment closer to octanol/water partition <sup>116</sup>. The relationship between  $\log k$  and ( $\varphi$ ) is typically not linear, although it can approximate it reasonably for  $\log k$  values between  $0.5 \pm 1.0$ . This should also be considered. However, when they are produced from other sets of mobile-phase compositions or organic modifiers, multiple  $\log k_w$  values can be achieved for the same chemical, column, and apparatus (acetonitrile or methanol, usually) <sup>115</sup>.

The OECD used the results of multiple interlaboratory comparison tests to confirm the isocratic technique for determining  $\log P_{o/w}$  and to create guidelines that should be followed to get accurate  $\log P_{o/w}$  values by RPLC <sup>117</sup>. The following are the guideline principal recommendations <sup>89,91</sup>:

- I. Columns packed with commercially available solid phases that have silica and long hydrocarbon chains (such C8 and C18) chemically connected together are used to perform the procedure.
- II. The eluent pH is valuable for ionizable compounds. It is recommended to use a proper buffer with a pH that is either adequately above the  $pK_a$  for a neutral base or below the  $pK_a$  for neutral acid. The pH of the eluent must be within the column operational pH range (2–8 usually).
- III. It is suggested to use at least six reference compounds in the association line.
- IV. The  $\log P_{o/w}$  range of the target compounds should be covered by the  $\log P_{o/w}$  values of the reference compounds. It is only recommended to extrapolate above the calibration range for highly lipophilic compounds ( $\log P_{o/w} > 6$ ).
- V. It is required to make extra measurements in order to increase the precision of the determinations.

The usual RPLC isocratic techniques, while faster than the shake-flask method, take some time as they require determinations at various mobile-phase compositions, specifically for

collections containing compounds with a large range of lipophilicity. As a result, gradient techniques have been created to speed up the determination of  $\log P_{o/w}$ <sup>118-120</sup>.

The congeneric effect, needed to get a good correlation line and precise  $\log P_{o/w}$  values, is obtained when the target compounds and calibration compounds belong to the same chemical family. This is an important restriction of the RPLC method for the determination of  $\log P_{o/w}$ . On the contrary, the correlation line for compounds with different functionalities usually has poor statistical properties and has low predictive ability. To prevent this impact, the OECD recommends employing reference compounds that are structurally comparable to the target compounds.

The problems of the n-octanol and C18 phases forming hydrogen bonds one with another appear to be the cause of the lack of congeneric effect. While C18 and other directly linked phases do not readily have hydrogen bonds, the water-saturated n-octanol phase does. As a result, in comparison to octanol/water partition, the solute hydrogen-bond donor groups decrease chromatographic retention and partition. The relationship model between  $\log P_{o/w}$  and  $\log k$  has been corrected<sup>115</sup>, with the inclusion of a hydrogen-bond acidity solute descriptor to address the congeneric impact. The correspondence may be extended to include neutral molecules of all functions with the inclusion of this descriptor, producing a standard deviation of 0.2–0.4 log units.

While the  $\log D_{o/w}$  values of partially ionized compounds, that is, at fixed pH values (for example, pH 7.4), cannot be estimated via the RPLC method, it is a consistent method for estimating  $\log P_{o/w}$  for neutral compounds or the neutral forms of ionizable compounds<sup>118</sup>. The dissociation of ionizable compounds in the water-organic solvent mobile phase used in RPLC is essentially difficult to replicate. Depending on the particular buffering agent and co-solvent content, the pH of an aqueous buffer changes when organic co-solvent (such as methanol) is added during the preparation of the mobile phase<sup>36,72,121</sup>. With the addition of co-solvent, ionizable compound  $pK_a$  also changes<sup>85,122</sup>, but not to the same degree as the buffer pH. Therefore, unless one is aware of the precise  $pK_a$  of the target compound in the RPLC mobile phase, measures the pH of the buffer in the mobile phase, and tunes it to the required pH (i.e., the same  $pH-pK_a$  difference as in water), the degree of dissociation at a specific aqueous pH cannot be replicated in the mobile phase. Therefore, it is highly improbable that the  $\log P_{o/w}$  against  $\log k$  correlation established for neutral compounds holds true for compounds that are partially or completely ionized. The  $pK_a$  in water,  $\log P_{o/w}$

of the compound's ionized form, which is considered to be 3.15 log  $P_{o/w}$  units smaller than the log  $P_{o/w}$  of the neutral form, and the log  $D_{o/w}$  values of ionizable compounds have all been calculated using this approach<sup>91,118</sup>. The methods for p*K*<sub>a</sub> determination (II): Sparingly soluble compounds and high-throughput approaches.

RPLC is not the only chromatographic method treated to determine log  $P_{o/w}$ , despite its widespread use. As suitable alternatives to the direct measurement of log  $P_{o/w}$ , micellar electrokinetic chromatography (MEKC) and micro-emulsion electrokinetic chromatography (MEEKC) were proposed<sup>123,124</sup>. The partition between an aqueous mobile phase and a cationic or anionic surfactant-based pseudo-stationary phase or microemulsion is determined by both methods via capillary electrophoresis device. In particular, a micro-emulsion of sodium dodecyl sulfate (0.05 M or 1.44%, w/w), heptane (0.82%, w/w), and 1-butanol (6.5%, w/w) in water was identified as an appropriate replacement model for octanol/water partition for log  $P_{o/w}$  values in the range 0.5 to 4.5 with an uncertainty < 0.2 log units and avoiding the congeneric effect<sup>89,91,97,125,126</sup>.

To determine log  $P_{o/w}$  and log  $D_{o/w}$ , centrifugal partition chromatography and high-speed countercurrent chromatography have been employed<sup>97,127</sup>. Both approaches devote the same principal idea but distinct types of instruments. Both techniques handle a liquid stationary phase with an immiscible liquid mobile phase and no solid support. When centrifugal partition chromatography is employed, a centrifugal field keeps the liquid stationary phase in a collection of cartridges and pumps the mobile phase through the stationary phase. Only the partition method controls the retention mechanism. N-octanol and water are examples of two immiscible phases, and the log  $P_{o/w}$  or log  $D_{o/w}$  at a given pH of the buffered water phase is immediately derived from the observed retention parameter (typically retention volume).

#### **1.5.1.4. Microchip capillary electrophoresis with contactless conductivity detection (MCE-CCD)**

In recent years, the partition coefficient determination method identified as Microchip Capillary Electrophoresis with Contactless Conductivity Detection (MCE-CCD) has advanced and become quite popular<sup>109</sup>. As a substitute of HPLC, the MCE apparatus was used in pharmaceutical analysis due to its quick analysis time of 40 seconds, enormous adaptability, and high efficiency. A particular kind of conductivity-based detector identified as contactless conductivity detection (CCD) isolates the electrodes from the solution with a

thin coating to prevent corrosion. In theory, all charged analytes in CE analysis might be detected with a CCD detector, which is often done. The CCD detector was used with CE and gathered a lot of attention before it was used to detect pharmaceuticals and inorganic ions<sup>109,128-131</sup>.

The development of analytical instruments and their miniaturization for the microchip CE (MCE) in recent years has generated considerable interest in terms of biochemical analysis, microscale analytical instruments, and a variety of chemical applications. Using extremely small volumes of samples, such as picolitres or nanolitres, MCE-CCD has a worthy responsibility in biomedical and pharmaceutical studies, as well as purposes in clinical diagnostics and environmental analysis<sup>110,128</sup>. It has a good approach and fast electrophoretic separations in a matter of seconds. As a result, UV is the detector that was used the most in calculating  $\log P_{o/w}$ , although it has limitations because the analytes of interest needed to have good UV absorbance.

In MCE-CCD, molecules are separated on a microfluidic chip based on their charge-to-size ratio. A small capillary (narrow channel) on the chip is supplied with an electrolyte solution and has a diameter of a few micrometers. The molecules flow toward the electrode with the opposite charge as a result of an electric field being applied through the channel. A contactless conductivity detector (CCD) study the shift in the electrical conductivity of the electrolyte solution generated by the presence of the separated molecules, keeps track of the separation of molecules in the capillary<sup>128</sup>. The CCD works without direct contact with the sample or the separation buffer, eliminating the requirement for electrodes in the separation channel and lowering the possibility of sample contamination<sup>109,129,132</sup>.

A molecule is in the beginning dissolved in a mixture of two immiscible solvents to obtain the  $\log P_{o/w}$  of the compound via MCE-CCD (e.g., octanol and water). A buffer solution is applied to perform the separation once the sample is initiated into the capillary. The  $\log P_{o/w}$  is derived using the ratio of the sample concentrations in the two solvents and the migration time as shown in Eq (59). The migration time of the sample in the capillary is verified through the CCD.

$$P_{o/w} = \frac{C_o \cdot V_w - C_w \cdot V_o}{C_w \cdot V_w} \quad (59)$$

The abbreviation  $C_o$  refers to initial sample concentration in aqueous phase,  $\mu\text{g/mL}$ ;  $C_w$  is the sample concentration in aqueous phase after partition equilibrium,  $\mu\text{g/mL}$ ;  $V_w$  is the volume of aqueous phase, mL;  $V_o$  is the volume of 1-octanol phase, mL.

The same pretreatment technique as defined in Eq (59) was employed to evaluate the distribution coefficient  $\log D_{o/w}$  for 1-octanol/buffer. The distribution coefficient  $\log D_{o/w}$  was determined via the 1-octanol/buffer system with a physiological pH of 7.4 for each analyte, where each has a single  $\log P_{o/w}$  and  $\log D_{o/w}$  value. The results of the two systems (1-octanol/buffer or octanol/water) reveal a pH-dependent partition behavior, with pH having a key influence on the analyte's degree of ionization and hydrophobicity. At pH 7.4, charged properties are partly ionized and dispersed among the aqueous phase and the 1-octanol phase, with the connected form existing in the aqueous phase<sup>84,109</sup>. The analyte in the octanol/water mixture is fully ionized, dispersing into the aqueous phase in substantial amounts, which is why the apparent partition coefficient  $\log P_{app}$  value is lower than the value of  $\log D_{o/w}$ . The  $P_{app}$  value is calculated by measuring the distribution of the analyte between octanol and water in the presence of an excess amount of buffer to maintain a constant pH. This results in the analyte being fully ionized, and the  $P_{app}$  value reflects the ratio of the ionized analyte that remains in the octanol phase to the amount of ionized analyte in the mixture<sup>109,133</sup>. Higher  $\log D_{o/w}$  and  $\log P_{o/w}$  values are produced by analytes whose  $pK_a$  values are near their pH values than by those whose  $pK_a$  and pH values diverge. With the exception of the analyte that lacks a characteristic chromophore, the accuracy of the utilized analytes has been validated and compared using shake-flask HPLC-UV. Evidently, the solubility in the two phases and existence form are what determine the values of  $\log D_{o/w}$ ,  $\log P_{o/w}$ , and the determined  $P_{Calc}$ . The following factors may impact the MCE-CCD  $P_{o/w}$  measurement accuracy<sup>109,128,129</sup>:

- I. pH of the buffer: The determination of  $\log P_{o/w}$  can be influenced by the pH of the buffer used in MCE-CCD. The ionization state of the compound can be modified based on the pH of the buffer, which can alter how the compound partitions.
- II. Electroosmotic flow: The electroosmotic flow is what pushes the analyte inside the capillary in the MCE-CCD approach. The retention time and peak shape of the analyte can be influenced by the strength and direction of the electroosmotic flow, which can reduce the measurement precision.
- III. Temperature: The accuracy of the  $\log P_{o/w}$  measurement might be impacted by the measuring temperature. Higher temperatures may enhance the solubility of the molecule in the solvent, resulting in a higher  $\log P_{o/w}$  value. The partition coefficient is temperature dependent.

- IV. Ionic strength of the buffer: the ionic strength of the buffer in MCE-CCD can also influence the  $\log P_{o/w}$  measurement. Adjustments in ionic strength can have an influence on the partitioning performance of the compound as the partition coefficient is based on the concentration of ions in the solution.
- V. Impurities: the measurement of  $\log P_{o/w}$  can be influenced by the presence of impurities in the sample or buffer. Measurements may be erroneous as a result of impurities interfering with conductivity detection or the separation of the analyte.
- VI. Precision of the detection method: the measurement's accuracy may also be impacted by the contactless conductivity detection tools used in MCE-CCD. The detection approach must be very sensitive and accurate in order to correctly evaluate analyte conductivity.
- VII. Data analysis: using the appropriate software, the partition coefficient should be estimated using the analyte retention time as a starting point. It is important to test the measurement accuracy by comparing the results to approve the literature review or repeat the experiment.
- VIII. Validation: proper statistical procedures should be applied to validate the method accuracy and precision.

Overall, careful control and optimization of each of these variables, together with precise buffer preparation, suitable temperature control, and sensitive detection techniques, are necessary for reliable measurement of  $\log P_{o/w}$  by MCE-CCD.

#### **1.5.1.5. Determination of $\log D_{o/w}$ via Automated Microfluidic Liquid-Liquid Extraction**

New advances in microfluidic technology have made it possible to generate automated microfluidic liquid-liquid extraction (MLLE) systems, which provide a rapid, effective, and accurate replacement for conventional methods. With the use of microfluidic chips, flow rates, mixing, and droplet formation LLE can be precisely controlled, leading to extremely repeatable results <sup>87</sup>.

In 2006, J.G. Kralj *et al.* <sup>134</sup> published a new microfluidic device for continuous MLLE (Figure 6-A). They achieved the formation of solvent-water droplets using flow focusing and removed the non-aqueous solvents by using a porous fluoropolymer membrane. They applied the technique to the extraction of DMF, dichloromethane, isopropanol, and diethyl

ether. Two years later, M. Alimuddin *et al.*<sup>87</sup> published a similar microfluidic system (Figure 6-B), applying it, however, to the determination of the log  $D_{o/w}$  values of several drugs and other compounds of interest. With their proven reliability compared to literature values, microfluidics became a potential tool for the high-throughput determination of log  $D_{o/w}$  values in drug discovery and development.

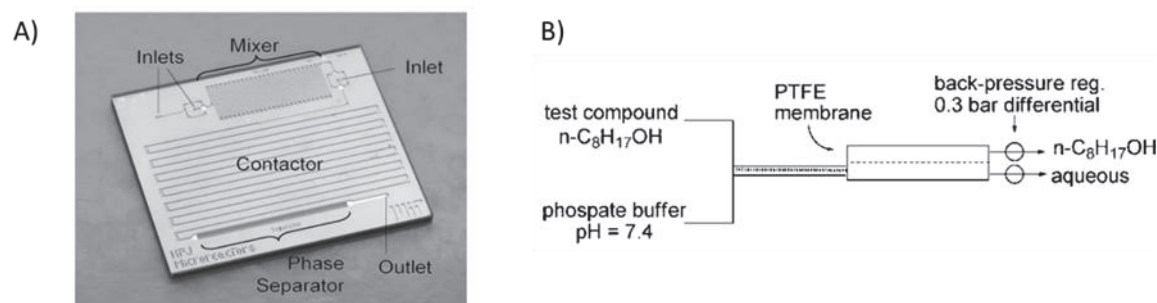


**Figure 6.** Microfluidic liquid-liquid extraction using porous membranes prior to analysis with HPLC. A) Formation of solvent-water droplets using flow focusing and a thin porous fluoropolymer membrane to selectively remove non-aqueous solvents<sup>134</sup>. B) Creation of octanol-water droplets using a T-shape connector and a poly(tetrafluoroethylene) (PTFE) membrane to remove organic solvent. The back pressure regulators are used to control the cross-membrane pressure and ensure the migration of all the organic phases through the membrane<sup>87</sup>.

Compared to conventional extraction methods, continuous flow liquid-liquid extraction using microfluidic devices has a number of advantages<sup>87,134</sup>. First, volume within the range of nanolitres can be precisely controlled over the channel. Second, because the microfluidic channels are so narrow, there is a larger area at the interface between the two phases, which speeds up mass transfer rates and increases extraction efficiency. To finish, the use of membranes decreases the requirement for problematic emulsification processes by enabling the selective partitioning of the two phases<sup>87</sup>.

Using MLLE, the distribution coefficient log  $D_{o/w}$  of a solute between two immiscible phases may be quickly and precisely determined using Eq (60)<sup>87</sup>:

$$\log D_{o/w} = \frac{\text{Peak area of compound in } n\text{-octanol}}{\text{Peak area of compound in buffer (7.4)}} \quad (60)$$

On the basis of the MLLE principles and the requirements for precise and repeatable measurements, some fundamental recommendations may be made<sup>87</sup>:

- I. Choose the right materials for the microfluidic chip: the molecules or the solvent can be absorbed and/or adsorbed due to the high volume-to-surface ratio. Therefore, use always solvent resistance materials with no porosity.
- II. The target compound should reach equilibrium between the two phases in an appropriate and reasonable length of time by improving the extraction factors, which involve flow rates, pressure, and temperature. This may be achieved by doing preliminary experiments to adjust the settings.
- III. Validate the technique: precision and reproducibility of the MLLE technique should be proven by comparing the results with those taken via established methods, such as shake-flask or HPLC-based methods.
- IV. Ensure precise control over the system: The MLLE system should be constructed to guarantee accurate control over the flow rates, pressure, and temperature of the solvents. This can be accomplished by via microfluidic pumps, back pressure regulators, and temperature controllers.
- V. Use applicable detection methods: the target compound can be detected utilizing different methods, such as UV-vis spectroscopy or mass spectrometry after injection in HPLC. The detection method should be carefully chosen based on the specific properties of the target molecule.

Overall, the microfluidic liquid-liquid extraction system is a prospective method to estimate the partition values using small amounts of solvents and compounds, achieving a rapid equilibration with accurate control.

#### **1.5.1.6. Continuous Flow Partition Coefficient Measurements Using a Microfluidics Devices**

Microfluidics can also estimate the partition coefficient via small amounts of the sample as low as picolitre volumes. A good example of one of these systems is the droplet microfluidic device, which delivers a stable interface for partitioning by alternating droplets of two immiscible phases, for instance octanol and water. The immiscible phases are injected into this device, and one of the phases forms a continuous string of droplets going from a range of different sizes. The size of the droplet is strongly related to the cross section of the microfluidic channel. Volumes can range from nanolitre to picolitre depending on the speed of the octanol and water solutions.

A stable interface for partitioning is formed between the droplets by a thin layer of the other phase. Once equilibrium has been reached, the droplets pass through the system, and the partitioning coefficient is determined by assessing the compound's concentration in each phase. The approach features involve the smallest volume of compound required, the high throughput, and the capability for various measurements to be achieved at once. The method does have some disadvantages, containing the possibility of droplet coalescence and the challenge of detecting low levels of the molecule<sup>110,135-137</sup>. The following figure presents the strategies to do droplets in microfluidic channels.

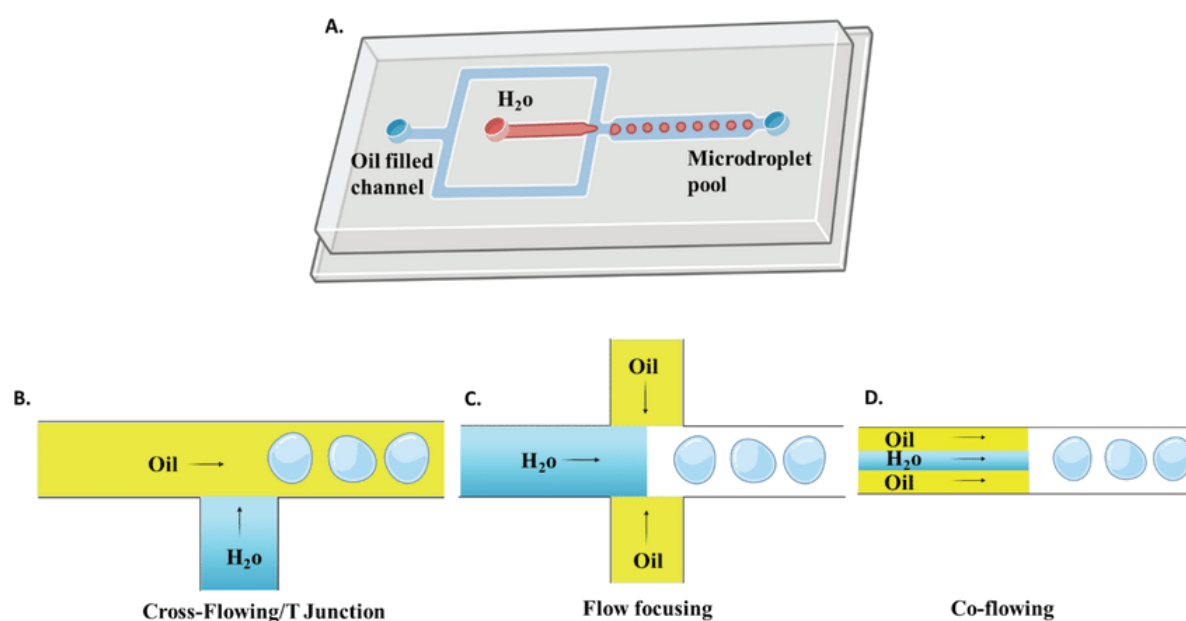


**Figure 7.** Schematic illustration of a droplet-based microfluidics system. A) basic design and passive methods of droplet formation, B) cross-flowing, C) flow focusing, D) co-flowing.

Occasionally, fluorescence is used as a detection system to facilitate the measurement of partition coefficients in microfluidic T-junction<sup>110</sup>, as shown in Figure (8-A). These compounds were utilized as external tests to evaluate compound partition in different phases, allowing for accurate detection and quantification. They facilitate distribution and intensity monitoring, therefore being effective in partition coefficient fields and studies using microfluidic devices and chromatographic methods. Fluorescein partition coefficient may be calculated using the equation  $P_{o/w} = I_o / I_w$ . Unfortunately, it is challenging to test directly since octanol fluorescence is weak and red-shifted by 70 nm. Hence, based on the concentration in the water sample, the sample concentration in octanol may be determined. The formula for calculating the number of moles in the octanol phase is  $n_o = n_{w, initial} - n_w$ ,

final. where  $n_w$ , final is the amount of fluorescein in the initial state and  $n_w$ , initial is the amount of fluorescein in a water drop at equilibrium. Calculations for the molar concentration of water and octanol are as follows:  $C_w = n_w/V_w$ ,  $C_o = n_o/V_o$ , where  $V_w$  and  $V_o$  are the volumes of water and octanol, respectively. The concentration of a dilute sample in water can be measured as:  $C_w = \beta I_w$ , where the abbreviation  $\beta$  constant. where  $I_w$ , octanol is the level of water fluorescence when octanol is present. This equation relates the fluorescence intensities determined in octanol and water to the fluorescein partition coefficient. Rewriting the following equation  $P_{o/w} = I_o / I_w$  in terms of intensity of the water drop <sup>110</sup>:

$$P_{o/w} = \left[ \frac{I_{w, \text{Initial}}}{I_{w, \text{Final}}} - 1 \right] \frac{V_w}{V_o} \quad (61)$$

As the channel depth is constant throughout the whole channel, the volume ratio of the water to octanol droplets is approximated in this equation as the length ratio of the drops. As a result, we have:  $L_w/L_o = V_w/V_o$ , where  $L_w$  and  $L_o$  are, respectively, the lengths of the water and octanol drops. The intensity-time plots may be used to estimate the duration ratio of the drops. When the fluorescence intensities are separated from the background signal, the partition coefficient may be stated using the measured variables as follows:

$$P_{o/w} = \left[ \frac{I_{w, \text{Initial}} - I_{\text{dark}}}{I_{w, \text{Final}} - I_{\text{dark}}} - 1 \right] \frac{V_w}{V_o} \quad (62)$$

where  $I_{\text{dark}}$ , is the background fluorescence intensity and  $I_w$ , initial and  $I_w$ , final are the water initial and equilibrium fluorescence intensities, respectively. After correcting for background signal, this equation correlates the fluoresce partition coefficient to the length ratio of the drops and the fluorescence intensities recorded in water and octanol <sup>110</sup>. To detect the fluoresce of the droplets, these can be photographed for the final intensities at the end of the microfluidic channel, after partition has been complete. This time can take around 15 minutes.

The detection using UV absorbance is also a good and more universal alternative to fluorescence. This technique was used to determine the  $\log P_{o/w}$  from a cross-flowed microfluidic junction of octanol and water using perfluorodecalin (PFD) as pinching solution, as presented in Figure (8-B). The system combines an autosampler with a microfluidic device, avoiding the need for the intervention of an operator, and providing fast extraction. The determination of  $\log P_{o/w}$  values for a group of compounds was achieved

using small amounts of solvent. 5 nL plugs of the extraction phase and an aqueous sample were inserted in the tube. Each plug was connected to an adjacent octanol plug, and these pairs were separated by immiscible PFD carrier fluid. During flow, fast extraction happens at each octanol-water interface. With an online UV detector, the absorbance was quantified and used to calculate the  $\log P_{o/w}$ <sup>136</sup>. The partition coefficient  $\log P_{o/w}$  can be determined via Eq (41).

In this example, the device was prepared using soft lithography on master molds made from standard photolithography processes on silicon wafers. Briefly, the PDMS plastic was prepared with a 1:10 activator on monomer ratio, degassed, and then poured over the master mold with the microfluidic layout. The PDMS with fluidic channels were connected to glass slides utilizing oxygen plasma activation to assemble the devices. Finally, the microfluidic devices were surface treated with a 2% tridecafluoro-1,1,2,2-tetrahydrooctyl trichlorosilane solution in PFD for surface treatment<sup>136</sup>. The

The limitation of this microfluidic approach is mainly related to the UV detection technique used. While applicable for in-line application and small amounts of solvent, capillary UV detection has low sensitivity, limiting its use for compounds with chromophores. To address this problem, prospective solutions involve using larger droplets and thicker channels to raise the absorption. Other detectors, like mass spectrometry, could be investigated for greater sensitivity in these experiments.

Another example of fluorescence detection was published using a microfluidic chip with a Y-junction where octanol and water co-flowed as biphasic parallel partition. This is illustrated in Figure 8-C). The technique involves using microfluidic chip with a double Y serpentine channel shape and hydrophilic microchannel walls produced via oxygen plasma treatment. The article describes a microfluidic device that determined the  $\log P_{o/w}$  of fluorescein disodium salt by separating two immiscible phases of octanol and water on a chip<sup>135</sup>.

When the flow rates of octanol and water are equal, the interface between the two phases showed a laminar behavior and was parallel to the microchannel walls<sup>135</sup>. The intensity of fluorescence molecules in the channel was determined by epifluorescence microscopy. The partition coefficient  $\log P_{o/w}$  involving the two phases can be determined via Eq (41).

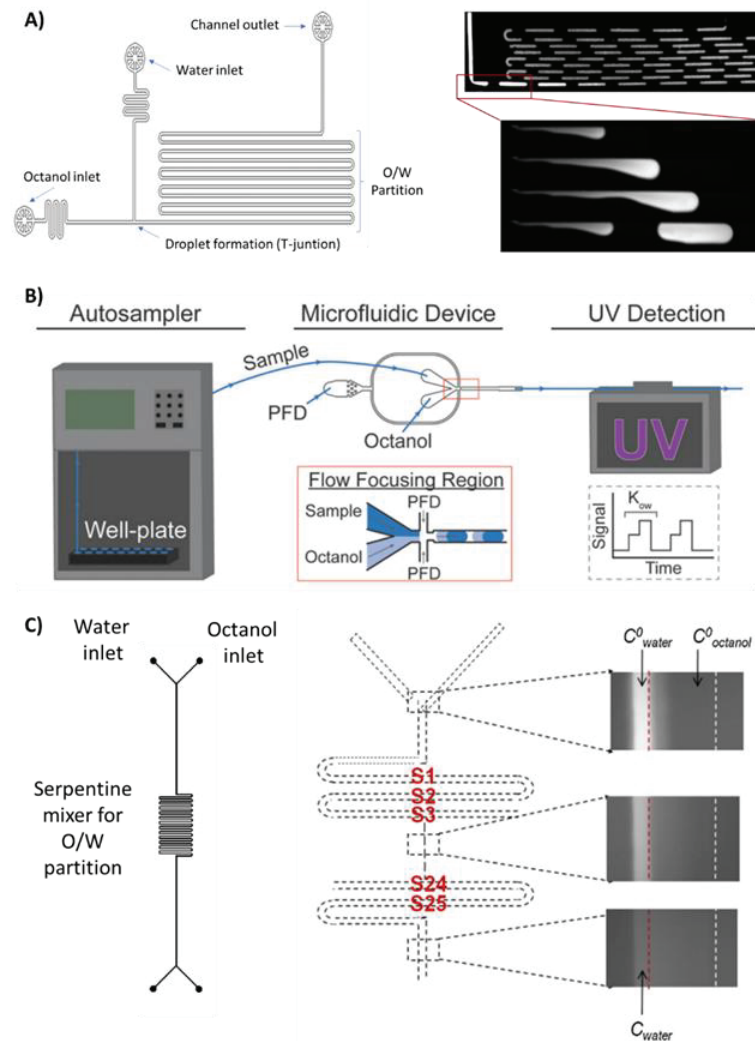


**Figure 8.** Methods of microfluidic continuous flow to determine partition coefficient. A) Microfluidic T-junction to create water droplets (bright) into continuous octanol phase (dark) using fluorescence micrograph <sup>110</sup>. B) Channels of octanol and water are connected using a Y-junction and cross-flowed using perfluorodecalin (PFD) to create the droplet. The detection system they used is based on UV detection <sup>136</sup>. C) Representation of the microfluidic channel with a Y-junction for the determination of the partition coefficient between octanol and water. Fluorescence photos illustrate the parallel flow and occupancy of the two phases in microchannel <sup>135</sup>.

### 1.5.2. Comparison between experimental methods

Many comparisons of numerous experimental methods for analyzing partition coefficients have been conducted. The conclusions are reviewed as follows <sup>91</sup>:

- I. The shake-flask method is a time-tested and widespread way to determine partition coefficients. It involves measuring the concentration in each phase after equilibrating a compound between two immiscible phases, usually water and octanol. This method

is basic and effective with a selection of compounds. Unfortunately, it can take a long time and requires a big volume of samples.

- II. A current technique for figuring out the partition coefficient ( $\log P_{o/w}$ ) and distribution coefficient ( $\log D_{o/w}$ ) of compounds in different solvents or phases is the shake-flask method with LC-UV, LC-MS, or NMR detection. It presents reliable  $\log P_{o/w}$  evaluations for ionizable compounds and is appropriate for both neutral and ionizable compounds. Likewise, it allows the partial ionization of the compound in the buffer to assist the measurement of  $\log D_{pH}$  at a selected pH. This method can be used in the range of -2 to 4, and occasionally up to 5. Nevertheless, sensitive quantification methods are needed for compounds that are particularly lipophilic or sparingly soluble. This method, despite its adaptability, has certain limitations, including time-consuming and delicate quantification procedures. That is still a beneficial and valuable approach, though <sup>101,103,138</sup>.
- III. The potentiometric method: uses a pH meter or an ion-selective electrode to determine the distribution of an ionizable compound between two phases. For establishing the partition coefficients of weak acids and bases, this method is specifically helpful. It may also be automated and is relatively simple. However, the precision can be impacted by modifications in ionic strength, and the pH meter or electrode must be calibrated. For substances that can be ionizable, the potentiometric approach is appropriate <sup>124</sup>, but its application to substances with  $\log P_{o/w}$  values outside of the 1.8 to 6 range is limited <sup>91,139,140</sup>.
- IV. Liquid chromatographic techniques: Reversed-phase, normal-phase, and micellar chromatography are some of the LC methods utilized to determine partition coefficients. These processes involve employing a chromatographic column to separate a compound into two phases and determining the retention time or capacity factor. High-throughput investigations regularly require the use of LC tools as they are able to handle a large collection of compounds. Yet, they could take a while and call for specialist tools <sup>91,139</sup>.
- V. The assessment of  $\log P_{o/w}$  via chromatographic retention on C18 columns is a popular method for reviewing compound lipophilicity. However, as this method heavily depends on the solute hydrogen-bond acidity, simply assessing retention is frequently insufficient. Merging chromatographic data with a hydrogen-Bond donor description is required to properly estimate  $\log P_{o/w}$ . This method is remarkably valuable for extremely lipophilic compounds that fall outside the scope of the shake-flask and

potentiometric methods and is efficient at calculating  $\log P_{o/w}$  values from -1 to 7. For time-consuming determinations containing solutes with stability struggles, it is also useful<sup>101,141</sup>.

- VI. Microchip capillary electrophoresis with contactless conductivity detection (MCE-CCD): this method encompasses using a microchip-based capillary electrophoresis device to separate a compound based on its electrophoretic mobility and a contactless conductivity detector to detect it. A small sample amount may be handled by MCE-CCD, which also provide fast and accurate analyses. This method can accurately determine  $\log P_{o/w}$  values for a selection of compounds, containing both hydrophilic and lipophilic compounds, in the range of -3 to 5<sup>124,138</sup>. Unfortunately, it requires specific equipment and might not be applicable for all chemicals.
- VII. The automated microfluidic liquid-liquid extraction for  $\log D_{o/w}$  measurement uses a microfluidic device to separate a compound into two immiscible phases, and UV or fluorescence detection to find the concentration in each phase. Small sample amount may be handled by this method, which also provides rapid and precise readings. This method can precisely determine  $\log P_{o/w}$  values for a selection of compounds, containing both hydrophilic and lipophilic compounds, in the range of -2 to 5<sup>87,124</sup>. Unfortunately, it necessitates specialized tools and might not be appropriate for all chemicals.
- VIII. Using a droplet microfluidic system, measurements are made in picolitre or nanolitre drops; In this procedure, a compound is divided into picolitre-sized droplets using a microfluidic apparatus, and the concentration in each droplet is estimated using fluorescence or UV detection. Little sample volumes may be handled by this approach, which also offers quick and precise readings. This technique can measure  $\log P_{o/w}$  values in the large range of -3 to 6. Unfortunately, it necessitates specialized tools and might not be appropriate for all chemicals<sup>110</sup>.

Overall, the method of choice will be established by the particulars of the experiment, such as the nature of the compound, the volume of the sample, and the desired throughput and precision. To determine reliable and precise measurements of the partition coefficient, it could be required to use a number of different techniques or to compare the outcomes of several techniques.



## **2. EXPERIMENTAL WORK**

## 2.1. Experimental part and Methodology ( $pK_a$ )

### 2.1.1. Potentiometric titrations - analyte solution

#### 2.1.1.1. Apparatus

Potentiometric  $pK_a$  determinations were carried out in an 888 Titrand potentiometer from Metrohm (Herisau, Switzerland), equipped with a combined pH electrode and a burette also from Metrohm, a glass tempering beaker, stirring, and a temperature-controlled water bath (J. P. Selecta, Abrera, Spain).

#### 2.1.1.2. Chemicals and solvents

0.5 mol/L sodium hydroxide, 1 mol/L potassium hydroxide, and 1 mol/L hydrochloric acid >99% in water, solid potassium hydroxide with a purity of 99% and solid p-Toluenesulfonic acid with a purity of 99% were from Merck (Darmstadt, Germany). Tris >99% was from sigma Aldrich. Potassium hydrogen phthalate standard for volumetric analysis, ACS, ISO 99.95–100.05% was from Panreac (Castellar del Vallès, Spain). Water was purified by a Milli-Q plus system from Millipore (Bedford, MA, USA), with a resistivity of 18.2 M $\Omega$ cm. The compounds used as a referencing drug were reagent grade or purer. The acid drugs were sourced as a follow: 2-chlorbenzoic acid >99.50% was obtained from Scharlau, benzoic acid >99.99% was purchased from Merck, and vanillin was purchased from Panreac. While the bases were sourced as follow: quinoline >97% was purchased from Flucka, 4-*tert*-butylpyridine >99% was purchased from Aldrich, and 2,4-lutidine >99% was purchased from Aldrich.

#### 2.1.1.3. Work procedure

A total of 25 mL of an approximately 0.008 mol/L solution of the compound in the suitable methanol-water or acetonitrile-water mixture were placed in the thermostated beaker for the titration. Once the solution had reached 25 °C, titration was carried out for acids with 0.1 mol/L sodium hydroxide up to 80% methanol or acetonitrile. Then, the titration was carried out using 0.1 mol/L potassium hydroxide up to 90% methanol or acetonitrile. Finally, the titration was performed with 0.1 mol/L potassium hydroxide that had been prepared directly in pure methanol or acetonitrile up to 100% to ensure that there is no water in the titration. For bases compounds, the titration was performed with 0.1 mol/L hydrochloric acid up to 90% methanol or acetonitrile, and then 0.1 mol/L p-Toluenesulfonic acid that had been prepared in pure methanol or acetonitrile was used for the titration at 100% methanol or

acetonitrile to guarantee that there is no water in the titration. The titration was done depending on the nature of the acid-base compound and the desired solvent composition (v/v), from pH 2 to pH 12, or vice versa. The titrand was solved in the same methanol-water or acetonitrile-water mixture media as the titrant. An inert gas (N<sub>2</sub>) was continuously passed through the titrant solution to eliminate CO<sub>2</sub>. All solutions (titrands and titrants) were prepared with pure methanol or acetonitrile and boiled water based on the used organic solvent. 0.1 mol/L sodium hydroxide solution was previously standardized with potassium hydrogen phthalate. 0.1 mol/L hydrochloric acid solution was standardized using Tris as primary standard. The potentiometric system was calibrated with the aqueous standard reference solutions at pH 2, 4, 7, and 9 at 25 °C. The combined glass electrode was conditioned for each methanol-water composition or acetonitrile-water mixture, storing it at least for 24 h in the solvent mixture. In the potentiometric measurements, a minimum of 20 s and a maximum of 60 s were established as equilibration times between consecutive additions. Solvent evaporation was avoided by closing the reservoir in which the determination was done and shortening as much as possible the total analysis time (around 5–10 min per determination).

Potentiometric titration was used in this method for determining the  $pK_a$  value of acid-base compounds at different % of organic-water mixture (0-100) using 888 Titrand as shown in Figure (9). In this process, a known volume of a strong base or acid solution of known concentration (titrant) is added to a solution of the analyte (analyte) while the pH of the solution is continuously measured. As the titrant is added, the pH of the solution increases until it reaches a certain point where a dramatic shift in pH happens. The pH of the solution is normally high (for acid titration) or low (for base titration) at the beginning of the titration. The thermodynamic point at which all of the analyte has interacted with the titrant is known as the equivalent point, or EP as shown on Figure (10). The volume and concentration of the titrant (NaOH and HCl) was used to calculate the concentration of the titrated compound at the equivalent point, where all of the analyte interacted with the titrant. The Henderson-Hasselbalch equation, which connects the pH,  $pK_a$ , and the ratio of the concentrations of the acidic and basic forms of the analyte, can be used to determine the  $pK_a$  value of the analyte from the pH at the EP.

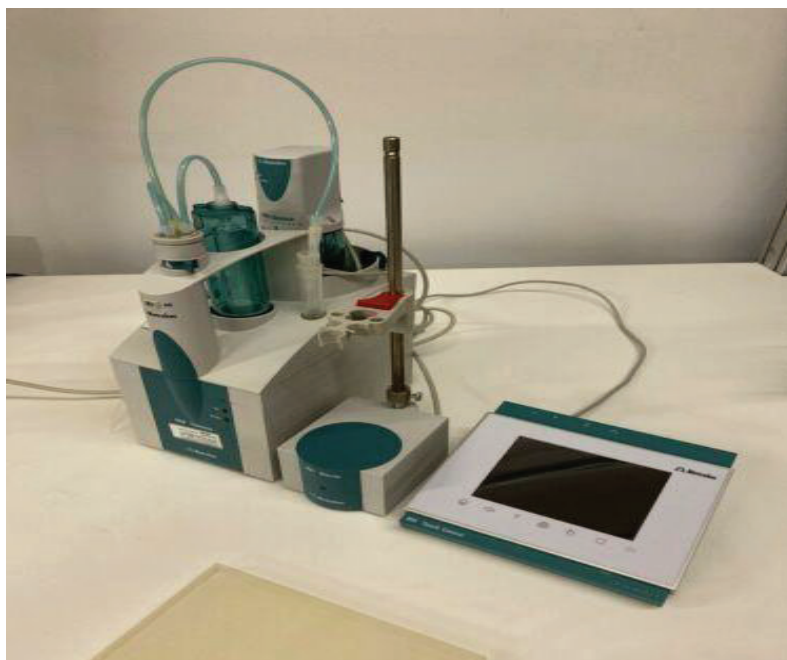


**Figure 9.** Metrohm 888 Titrando

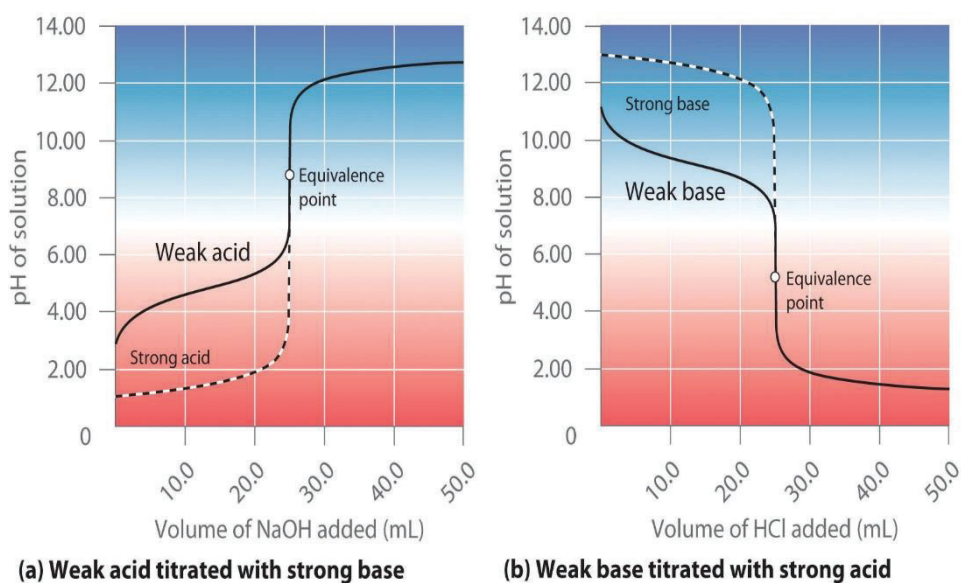


**Figure 10.** The titration curves of strong acid titrated with strong base and strong base titrated with strong acid are inverse of each other, referred to the thermodynamic point which is known as the (equivalent point).

## 2.1.2. Capillary electrophoresis

### 2.1.2.1. Apparatus

Capillary electrophoresis experiments were done with an Agilent 7100 Capillary Electrophoresis (Agilent Technologies, Santa Clara, California, USA), equipped with a diode array spectrophotometric detector. The capillary was made of fused silica and was obtained from Polymicro Technologies (Phoenix, Arizona, USA). The dimensions of the capillary are 50  $\mu\text{m}$  I.D., 375  $\mu\text{m}$  O.D., and 48.5 cm length, (40 cm length to the detector). The temperature of the capillary was set to  $25.0 \pm 0.1$  °C. Test compounds and internal standards were injected sequentially at a hydrodynamic pressure of 50 mbar psi for 5 s, and the applied voltage during separation was 20 kV for (0-40%) and 25 kV for (50-90) in the case of MeOH and 20 kV to percentage of acetonitrile. To speed up analysis, an additional hydrodynamic pressure of 50 mbar was applied during separation. The detection was carried out at 210, 214, 230, 254, and 260 nm.

### 2.1.2.2. Chemicals and solvents

Dimethyl sulfoxide >99.9% (DMSO), methanol HPLC grade, 0.5 mol/L sodium hydroxide, 1 mol/L potassium hydroxide, 1 mol/L hydrochloric acid, and sodium dihydrogenphosphate monohydrate >99% were from Merck (Darmstadt, Germany). Anhydrous sodium acetate >99.6%, 2-(cyclohexylamino)ethanesulfonic acid >99% (CHES), and 3-(cyclohexylamino)-1-propanesulfonic acid >98% (CAPS) were from Sigma (St. Louis, MO, USA). 2,2-bis(hydroxymethyl)-2,2',2''-nitrilotriethanol >99.9% (BisTris) and sodium formate were from Fluka (Buchs, Switzerland). Tris(hydroxymethyl) aminomethane >99.9% (Tris) was purchased from Aldrich (Milwaukee, WI, USA). Potassium hydrogen phthalate standard for volumetric analysis, ACS, ISO 99.95–100.05% was from Panreac (Castellar del Vallès, Spain). Water was purified by a Milli-Q plus system from Millipore (Bedford, MA, USA), with a resistivity of 18.2 M $\Omega$ cm. All studied drugs and internal standards were reagent grade or purer, and were purchased from Sigma Aldrich, Fluka, Merck, Baker, Panreac, or Carlo Erba as explain in Tables (1) ,(2) and (3).

**Table 1. Acidic and basic internal standards used in the experiments.**

<b>Acidic Compounds</b>	<b>Manufacturer</b>	<b>Purity</b>	<b>Bases Compounds</b>	<b>Manufacturer</b>	<b>Purity</b>
2-Chlorobenzoic acid	Scharlau	99.50%	Aniline	Baker	99%
2,6-dibromo-4-nitrophenol	Aldrich	98%	Quinoline	Baker	98.5%
4-Nitrobenzoic acid	Scharlau	99.50%	4-Tert-butylanilin	Fluka	99 %
2,6-dinitrophenol	Fluka	Pure	N,N-dimethylaniline	Fluka	Pure
3-Bromobenzoic acid	Merck	98%	Pyridine	Merck	98%
2,4-dinitrophenol	Aldrich	99%	Acridine	Aldrich	99%
Benzoic acid	Baker	99%	4-Tert-butylpyridine	Baker	99%
Ibuprofen	Merck	98%	Papaverine	Panreac	p.a.
Warfarin	Sigma	> 98%	2,4-lutidine	Sigma	> 99%
2,5-dinitrophenol	Aldrich	99%	Trazodone	Sigma	99%
Sulfacetamide	Sigma	98%	Pilocarpine	Sigma	98%
2,4,6-tribromophenol	Carlo Erba	>99 %	2,4,6-trimethylpyridine	Merck	> 99 %
4-nitrophenol	Fluka	>99%	Lidocaine	Sigma	99%
Vanillin	Fluka	Pure	Bupivacaine	Sigma	99%
4-hydroxybenzaldehyde	Aldrich	98%	1-phenylpiperazine	Fisher	98%
Phenobarbital	Aldrich	> 97%	Benzyl-dimethylamine	Merck	>98%
3,5 dichlorophenol	Aldrich	98%	Diphenhydramine	Aldrich	> 98%
Methylparaben	Aldrich	98%	Imipramine	Sigma	99%
2-Chlorophenol	Aldrich	≥ 98%	Procainamide	Sigma	≥ 99%
3-Chlorophenol	Synthesis	≥ 98%	Propranolol	Sigma	99%
4-bromophenol	Carlo Erba	99%	1-aminoethylbenzene	Sigma	< 99%
Paracetamol	Sigma	99%	Ephedrine	Sigma	99%
Phenol	Carlo Erba	99%	Nortriptyline	Sigma	99%

**Table 2. Insoluble drugs used in the experiments.**

<b>Acidic Compounds</b>	<b>Manufacturer</b>	<b>Purity</b>
Mefenamic acid	Sigma	≥ 98%
Meclofenamic acid	Sigma	≥ 99%
Sertaconazole	API	99%
Glyburide	Merck	≥ 98%
Loperamide	Fluka	≥ 99%
Terfenadine	API	> 99%
Amiodarone	Sigma	98%

**Table 3. Bases used in the test of HPLC column.**

<b>Acidic Compounds</b>	<b>Manufacturer</b>	<b>Purity</b>
Codeine	Sigma	99%
Quinine	Fluka	> 99%
Amitriptyline	Sigma	99%
Benzylamine	Fluka	> 99%
Procainamide	Sigma	≥ 99%
Diphenhydramine	Aldrich	> 98%
Nortriptyline	Sigma	99%
Protriptyline	Sigma	≥ 98%

### **2.1.2.3. Capillary conditioning**

New capillaries were conditioned with NaOH 1.0 M (10 min), NaOH 0.1 M (10 min), and H<sub>2</sub>O (10 min) at the beginning of the session (2.0 min). To be used, preconditioning was done with NaOH 1.0 M (2 min), H<sub>2</sub>O (3 min), and buffer (5 min), and capillaries were flushed with NaOH 0.1 M (2.0 min) and H<sub>2</sub>O at the end of the session. Between each run, the capillary was rinsed for (5 min) with the same background electrolyte.

### **2.1.2.4. Preparation of sample**

The stock solutions of the test compounds and internal standards at a concentration of 1 mg/mL in water, methanol/water, or acetonitrile/water are prepared. Then, 4% DMSO must

be added as an EOF marker. A 1/10 dilution of the stock solution is prepared in water to prepare the sample solutions, which have a concentration of 100 mg/L For CE analysis.

#### **2.1.2.5. Buffer solution preparation**

The preparation of the background electrolyte (BGE) for capillary electrophoresis includes preparing stock solutions of sodium dihydrogenphosphate, sodium formate, sodium acetate, Bis-TrisH<sup>+</sup>, TrisH<sup>+</sup>, CHES<sup>-</sup>, CAPS, or sodium hydroxide in aqueous media at a concentration of 0.1 mol/L.

To obtain hydro-organic BGE solutions at the desired pH and ionic strength, an appropriate amount of 1 mol/L HCl, 1 mol/L KOH or 0.5 mol/L NaOH is added to 5 mL of the corresponding stock solution. The amount added depends on the desired pH of the BGE solution. Pure methanol or acetonitrile is then added to achieve the desired solvent composition (v/v). Afterward, the contents of the volumetric flask are diluted with the methanol-water mixture or the acetonitrile-water mixture in the same v/v proportion up to 25 mL to achieve the final concentration of the BGE solution. The final ionic strength is kept constant at 0.05 mol/L.

Buffer solutions covering practically all the useful pH range (from 2 to 11.5) separated within intervals of 0.5 pH units, as explained in Table (1) are then prepared at different methanol-water or acetonitrile/water mixtures of 10%, 20%, 30%, 40%, 50%, 60%, 70%, 80%, and 90% (v/v) of organic solvent.

The buffer preparation procedure is as follows: Stock solutions were prepared at a concentration of 0.1 mol/L. These solutions were adjusted to different pH levels while maintaining a constant ionic strength of 0.05 mol/L.

In the instance of sodium dihydrogenphosphate, sodium formate, sodium acetate, the preparation involves accurately weighing the required amount of each compound and then adding Milli-Q water to fill the volumetric flask up to the mark. Then, to prepare the buffer, a constant volume of the stock solution was taken. Next, the required volume of 1 mol/L HCl was added. Afterwards, the desired concentration of pure methanol or acetonitrile was added to achieve the desired solvent composition (v/v), followed by diluting the content of the volumetric flask with the methanol-water mixture or the acetonitrile-water mixture in the same v/v proportion up to 25 mL to achieve the final concentration of the BGE solution.

In the case of Bis-Tris and Tris, to prepare Bis-Tris<sup>+</sup> or Tris<sup>+</sup>, required volume of Bis-Tris or Tris is weighted and neutralized with exact amount of 1 mol/L HCl before adding the Milli-Q water up to the mark of volumetric flask to get fully protonated form. Then, to prepare the buffer, a constant volume of the stock solution was taken. Next, the required volume of 0.5 mol/L NaOH was added. Afterwards, the desired concentration of pure methanol or acetonitrile was added to achieve the desired solvent composition (v/v), followed by diluting the content of the volumetric flask with the methanol-water mixture or the acetonitrile-water mixture in the same v/v proportion up to 25 mL to achieve the final concentration of the BGE solution.

In the case of CHES and CAPS buffer, to prepare CHES<sup>-</sup> or CAPS<sup>-</sup>, required amount of CHES or CAPS<sup>-</sup> is weighted and neutralized with exact amount of 0.5 mol/L NaOH before adding the Milli-Q water up to the mark of volumetric flask to get fully deprotonated form. Then, to prepare the buffer, a constant volume of the stock solution was taken. Next, the required volume of 1 mol/L HCl was added. Afterwards, the desired concentration of pure methanol or acetonitrile was added to achieve the desired solvent composition (v/v), followed by diluting the content of the volumetric flask with the methanol-water mixture or the acetonitrile-water mixture in the same v/v proportion up to 25 mL to achieve the final concentration of the BGE solution.

**Table 4.** Buffers solutions, and their usable pH range were used as background electrolyte for p*K*<sub>a</sub> determination.

Buffer	range	p <i>K</i> <sub>a</sub>
PHOSPHORIC ACID/ SODIUM DIHYDROGENPHOSPHATE BUFFER (H <sub>3</sub> PO <sub>4</sub> -NaH <sub>2</sub> PO <sub>4</sub> )	2.0-2.5	2.15
FORMIC ACID / FORMATE BUFFER (HCOOH/HCOONa)	3.0-4.0	3.74
ACETIC ACID / ACETATE BUFFER (CH <sub>3</sub> COO/CH <sub>3</sub> COONa)	4.5-5.5	4.75
Bis-TrisH <sup>+</sup>	6.0-7.0	6.48
TrisH <sup>+</sup>	7.5-8.5	8.08
CHES <sup>-</sup>	9.0-9.5	9.50
CAPS <sup>-</sup>	10-11.5	10.4

All the buffers and samples were stored at 4 °C. Before usage, all samples and buffers were filtered through a nylon mesh 0.45µm porous size (Whatman, Maidstone, UK).

### **2.1.2.6. Data Analysis**

Data calculations were performed on Excel version 2010 from Microsoft (Redmond, WA, USA).

### **2.1.2.7. Determination of $pK_a$ values by IS-CE**

The effective mobilities were measured in appropriate buffers where both internal standards and test compounds were partially ionized. The limiting mobilities were determined in proper buffers where both the internal standard and analyte are totally ionized, for acids (pH 12, CAPS was used) and for bases (pH=2, phosphoric acid was used). The  $pK_a$  of the analytes was calculated from the  $pK_a$  value of the internal standards and the measured effective and limiting mobilities of the internal standards and test compounds through equations (32) and (39).

### **2.1.2.8. Establishment of the $pK_a$ scales of the internal standards.**

The  $pK_a$  values of the internal standards in the different methanol-water and acetonitrile-water mixtures were established using the same experimental and calculation procedures as for the test compounds explained in point 1.2.7.

All compounds were considered internal standards and test compounds simultaneously. An initial approximate  $pK_a$  value was supposed for each test compound (i.e. the  $pK_a$  value of the compound in water or in organic solvent mixture previously established) and used to calculate the  $pK_a$  of other compounds partially ionized in the same measuring buffer (approximately of  $\pm 1$   $pK_a$  units). These new calculated  $pK_a$  values were used to establish the  $pK_a$  of the other close compounds. The mean  $pK_a$  value obtained for each compound from other compounds of close  $pK_a$  values was used for a new  $pK_a$  recalculation. This method was iterated several times until the mean value of each compound for successive iterations reaches the same value ( $\pm 0.02$   $pK_a$  units).

The iteration method produces a relative scale of coherent  $pK_a$  values for each internal standards set (one for neutral acids and one for neutral bases).

To get the absolute  $pK_a$  values for each internal standard set and solvent medium, the  $pK_a$  values were anchored to the potentiometrically measured  $pK_a$  values of benzoic acid (for the acid internal standards) and 2,4-lutidine (for the base internal standards). The relative  $pK_a$  values were shifted until the relative  $pK_a$  values of the anchored compound matched the potentiometric one.



## 2.2. Experimental part and methodology (log $P_{o/w}$ )

### 2.2.1. Determining octanol-water partition coefficient log $P_{o/w}$

#### 2.2.1.1. Chemicals and solvents

Methanol was 99.9% for HPLC, gradient grade, and has been obtained from Prolabo (West Chester, PA, USA). Double deionized water has been obtained with a Milli-Q system from Millipore (Bedford, MA, USA), with a resistivity of 18.2 M $\Omega$ cm. N-octanol >99% from Merck (Darmstadt, Germany) have been also used in this work. Two types of fluorescent dyes were used in the experiment; Fluorescein >99.9% was purchased from Scharlab, and rhodamine >97% was purchased from sigma Aldrich. A set of 6 neutral compounds (propranolol, hydrocortisone, acetophenone, prednisolone, griseofulvin and butyrophenone) were used and purchased from Sigma Aldrich, Fluka, Merck, or Carlo Erba, and involving log  $P_{o/w}$  values from -0.06 to 2.8, has been chosen in order to carry out this study.

#### 2.2.1.2. Microfluidic design and fabrication

Microfluidic devices were designed with SolidWorks 2021 (Dassault Systems SE, France) and 3 main microfabrication strategies were utilized depending on the design and the material utilized. All microfluidic devices have been designed, fabricated, and assembled in collaboration with Leitat Technological Center (Terrassa, Spain). Techniques for the fabrication are described below:

**I. Soft lithography:** a polydimethylsiloxane (PDMS) mixture (10:1 mixture of PDMS and its crosslinking agent, SYLGARD 184, DOWSIL) was cast on the 3D printed multilevel molds following the same protocol described below (section 2.1.2.II). Subsequently, the polymer mixture was degassed and cured in an oven at 60 °C overnight. After peeling, the PDMS chip was plasma bonded (Plasma treat Steinhagen FG3001 + RD1004, Germany) on a glass substrate covered. Having a hydrophilic base attached to the hydrophobic microfluidic device permitted the octanol and water phases to function correctly. Figure (11-A) depicts the steps for the fabrication and bonding of the PDMS chip. Figure (11-B) presented soft lithography preparation procedure.

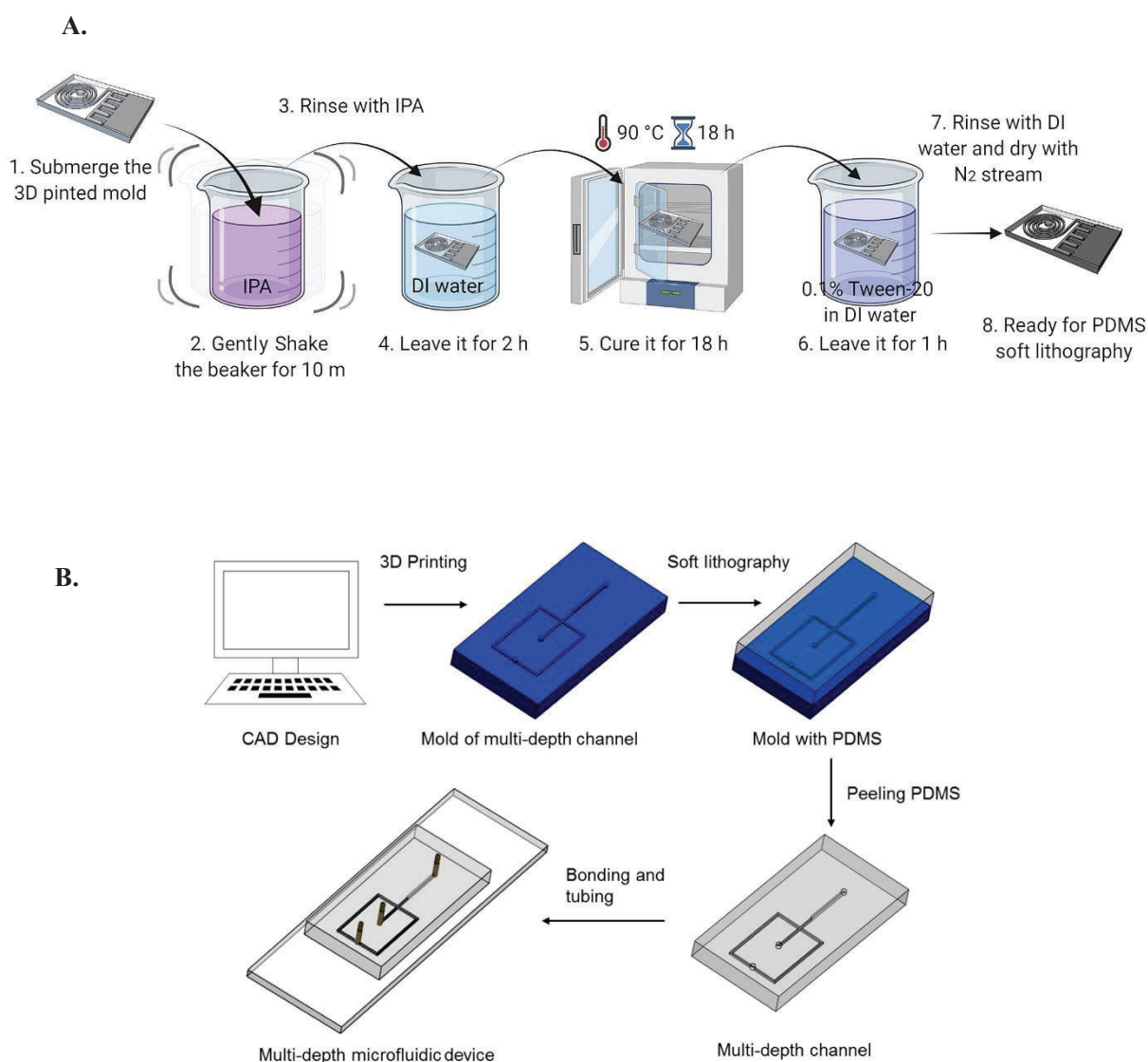


**Figure 11.** A) Washing and post-curing steps of the 3D printed mold for PDMS soft lithography<sup>142</sup>. B) Shows the diagram of soft lithography and preparation procedure<sup>143</sup>.

**II. 3D printing:** the CAD designs were converted into a standard triangulation language (STL), sliced into 50  $\mu\text{m}$  thickness layers (PreForm, Formlabs, USA), and printed using the stereolithography (SLA) 3D printer Form3 (Formlabs, USA). Clear V4 Resin was used in all cases. Postprocessing involved cleaning (rinsing with isopropanol, using Formwash, Formlabs, USA) to wash away uncured resin, drying (under a stream of pressurized nitrogen gas), curing (10 min under a UV lamp at 60 °C Formcure, Formlabs, USA). The microchannels were 3DP with one open side to avoid trapping resin and reduce over-polymerization. The base of the 3D printed microfluidic chip was sealed with a hydrophilic polyethylene terephthalate (hPET) using an optically clear double-

side pressure sensitive adhesive (PSA, ARclear, Adhesives Research, Ireland). Similar to the PDMS chip, the base was hydrophilic (water contact angle of  $20^\circ$  approximately), whereas the microfluidic chip was slightly hydrophobic (water contact angle of  $75^\circ$  approximately). Figure (12) shows the assembly.

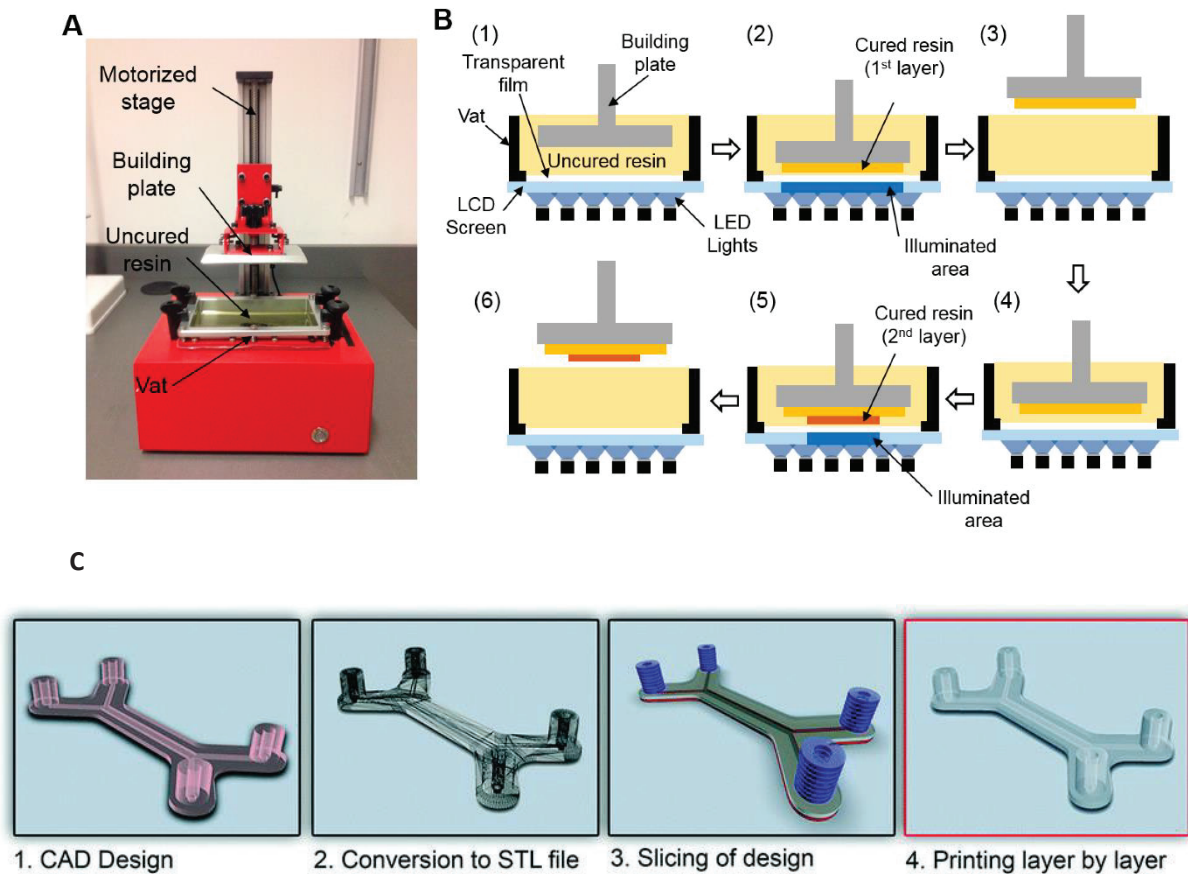


**Figure 12.** A) Photograph of a custom-built LCD SLA 3D printer. B) Step-by-step workflow of the SLA 3D printer for the fabrication of 3D printed microfluidic devices <sup>143</sup>. C) Workflow to manufacture a 3D printed microfluidic chips. The CAD file is converted into a STL file and later digitally sliced into individual layers that are sequentially printed to build an object in a layer-by-layer manner <sup>144</sup>.

**III. Micromilling:** the solid block or rectangular piece of Teflon or PMMA was attached on the stage of the engraving Computer Numerical Control (CNC) machine with accuracy of  $< 25 \mu\text{m}$ . Engraving depth and dimensions of the milling was set-up in the instrument. The 3D design was then uploaded in the system and CNC machined over the solid structure to engrave the microfluidic channels and reservoirs. Like the other techniques, the base of the milled microfluidic chip was sealed with a hydrophilic polyethylene terephthalate (hPET) using an optically clear double-side pressure sensitive adhesive (PSA, ARclear, Adhesives Research, Ireland). The base of the milled microfluidic chip was sealed using an optically clear double-side pressure sensitive adhesive silicone

adhesive was used to seal the microchannels (PSA, ARclear, Adhesives Research, Ireland). Similar to the PDMS chip, the hPET base was hydrophilic (water contact angle of 20° approximately), whereas the microfluidic chip was hydrophobic (water contact angle of 70° for PMMA or 100° for Teflon, approximately). Figure (13) shows the assembly.

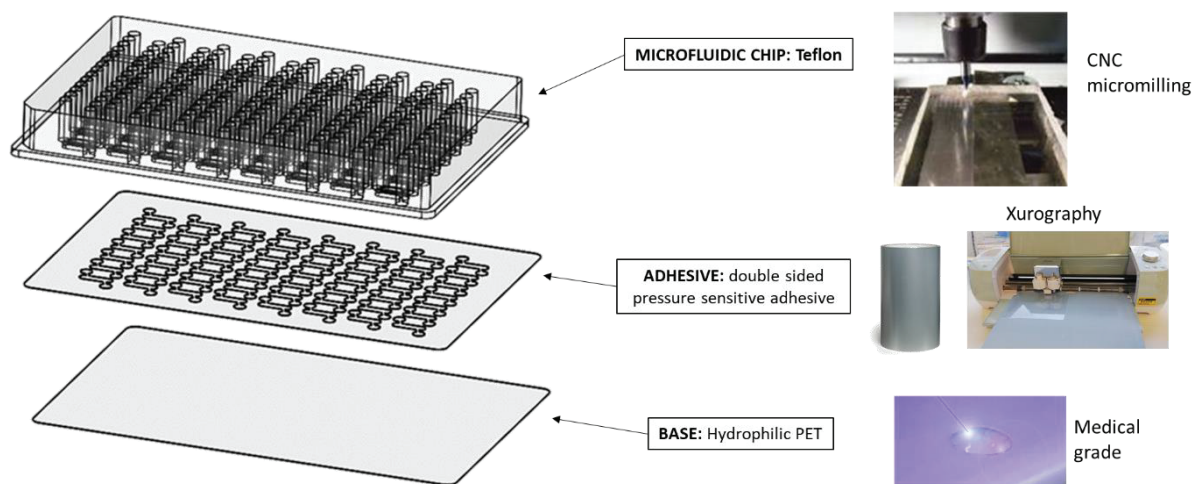


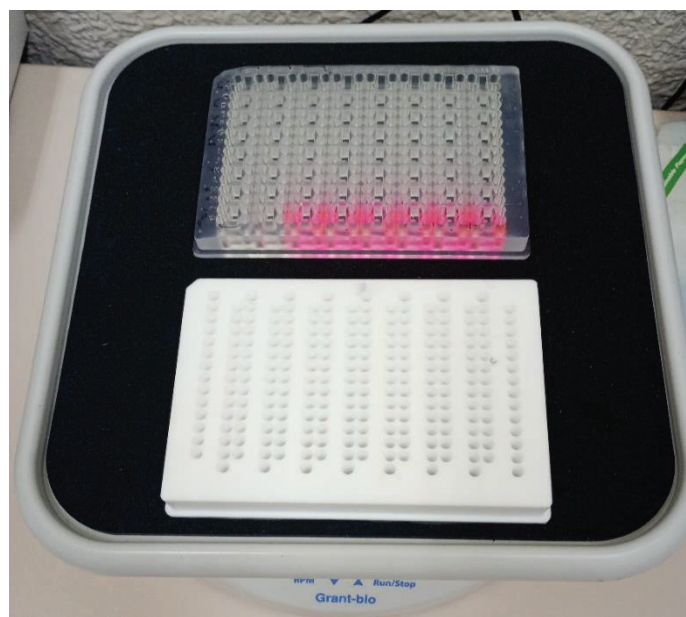
**Figure 13.** Draw of the microfluidic chip assembly. The microfluidic chip was either 3D printed or Computer Numerical Control (CNC) machined from a solid masterpiece (typically PMMA or Teflon). The hydrophilic PET (hPET) base was attached underneath of the chip using a double side adhesive previously cut using a dye cutting machine (xerography).

### 2.2.1.3. Apparatus

To increase partition and reduce equilibration time, microfluidic devices were placed in a rocker shaker (Grant-Bio, PMR-30 Platform 2D Rocker – Fixed Tilt) to induce perfusion and agitation, as shown in Figure (14-A). The rocker has a fixed inclination of 7° with a variable speed from 5 to 30 rpm range. For inspection, a digital fluorescent microscope (AM4115TFUW-EDGE Dino-Lite) as shown in Figure (14-B) was used to record videos and take pictures. ImageJ (National Institutes of Health, <http://rsb.info.nih.gov/ij/>) was used to analyze the region of interest (ROI) and monitor the mean intensity value of the ROI versus time. Images were processed to split into color channels in which the black background was set at an intensity value of 0. The fluorescence intensity value (in arbitrary intensity, A.I.) obtained in ImageJ depends on the calibration of the camera and other settings used during image acquisition. To compare fluorescence intensity values between different images and experiments, it is important to use consistent imaging and analysis conditions.

For HPLC measurements, a Shimadzu UHPLC system has been employed; the system consisted of two LC-10ADVP pumps, a SIL-20ACHT auto-injector, an SPD-M10AVP diode array detector (DAD), a CTO-10ASVP oven and an SCL-10AVP controller. The columns utilized were a KINETEX® 2.6  $\mu\text{m}$  EVO C18 100 Å, size LC Column 100  $\times$  4.6 mm from Phenomenex (Torrance, CA, USA). The mobile phase used for the UHPLC separation was 80% methanol with a flow rate of 0.5 mbar. The DAD was set to detect at wavelengths 214 and 254nm to allow for detection of compounds with different absorption spectra.

A.



B.



**Figure 14.** A) Rocking shaker. B) Dino-Lite, AM4115TFUW-EDGE digital microscope to inspect microfluidic flow and fluorescence underneath the device.

#### 2.2.1.4. Work procedure

The experimental method involved several steps to determine  $\log P_{o/w}$  of the drug. First, the plate was positioned on a flat surface, and the lower channel was filled with water, followed by the upper channel with octanol. To speed up the equilibrium between the phases, hydrodynamic flow to both octanol and water microfluidic channels was produced by tilting the device to a certain degree ( $-7^\circ$ ). When tilted, a gravitational force is created from the difference in the level between the inlet and outlet reservoirs. To complete 1 cycle, the microfluidic device is subsequently tilted to the other side ( $+7^\circ$ ) to create again the hydrodynamic flow but this time, to the other side (from outlet to inlet). Successive rotation of the microfluidic device was used to enhance the transfer of the analyte between the two phases at different speeds (5, 10, and 20 cycles/minute). To measure the flow and partition dynamics, a digital fluorescence microscope was used to observe the transfer of the analyte from the octanol phase to the water phase. Under static and horizontal conditions, the analyte transfer could be observed, but the process was slow. However, when the chip was inclined, the fluorescence in the water phase increased rapidly, indicating a faster transfer of the analyte, as explained in the flow working principal part. The fluorescence intensity value (arbitrary intensity, A.I.) was established via ImageJ and choosing the ROI (region of interest). Finally, to calculate the octanol-water partition coefficient, three different partitions were injected into the parallel design device at different volume ratios (5/100  $\mu\text{L}$ , 20/100  $\mu\text{L}$  and 100/100  $\mu\text{L}$ ). Similarly, three different partitions were injected into the perpendicular design device at different volume ratios (5/70  $\mu\text{L}$ , 20/70  $\mu\text{L}$  and 50/70  $\mu\text{L}$ ). To avoid solubility problems in water, each analyte stock solution was prepared at 10 mM in DMSO and diluted to 1 mM in the aqueous phase (water saturated octanol). The injection process was started by injecting octanol into the top phase, and water into the bottom phase, followed by shaking the plate using a rocker at (10 cycles/minute for 1 hour). After shaking, 50  $\mu\text{L}$  of water phase was added to the UHPLC vial. During the UHPLC analysis, the separation was achieved using a mobile Phase of 80% methanol at flow rate of (0.5 mL/min), and a temperature of  $25^\circ\text{C}$  was maintained throughout the analysis. The  $\log P_{o/w}$  value of the analyte was determined by analyzing the area determined by the UHPLC analysis for standard ( $A_{st}$ ) and aqueous ( $A_w$ ) phase solutions. In this calculation, the injection volumes of the standard solution ( $v_{inj(st)}$ ), aqueous phase of the partition ( $v_{inj(w)}$ ), the volumes of the octanolic phase ( $V_o$ ), the volumes of the aqueous phase ( $V_w$ ) and the proper standard solution dilution factor ( $r$ ) were considered, as shown in Eq (51). This equation divides the

calculation of  $\log P_{o/w}$  into four parts: the ratio of peak area ( $A_{st}/ A_w$ ), the ratio of injected volume ( $v_{inj(w)}/ v_{inj(st)}$ ), the ratio of injected volume of octanolic and aqueous phase into the chip ( $V_w/ V_o$ ), and the proper standard solution dilution factor ( $r$ )<sup>103</sup>.

### **3. RESULTS AND DISCUSSIONS**

## 3.1. Potentiometric determination of the $pK_a$ of the anchoring acid-base compounds

### 3.1.1. Determination of $pK_a$ by potentiometric titration at different % of Methanol - water mixture

One neutral acid (benzoic acid) and one neutral base (2,4-lutidine) of different acid-base strength were selected as anchor compounds for the two sub-sets of internal standards (the 23 neutral acids and the 23 neutral bases). In addition, for the effectiveness of anchoring, one more neutral acid (2-chlorobenzoic acid) and two additional neutral bases (quinoline and 4-*tert*-butylpyridine) were selected. These compounds provide a method to assess the accuracy and reliability of anchoring process. The potentiometrically determined  $pK_a$  values of these acid-base compounds in the different methanol-water mixtures (0 – 100 %, v/v) are presented in Table (5). The results are the mean of three independent titrations and the standard deviation is given too. The standard deviations for the different data points are 0.01–0.05. Thus, we estimate the standard deviation of the determined  $pK_a$  values to be less than 0.05.

The trend of the  $pK_a$  variation is as expected<sup>34</sup>. The  $pK_a$  of neutral acids / conjugated anionic bases (HA/A<sup>-</sup> pairs) increases with the increase in methanol proportion; however, the  $pK_a$  of neutral bases / conjugated cationic acids (A/HA<sup>+</sup> pairs) decreases with the increase in methanol proportion up to 80% and then starts to increase up to 90% methanol. This occurs because the addition of methanol influences the ionization of the acidic or basic compound. Three different factors interact to justify the alteration in  $pK_a$  values as the proportion of methanol increases<sup>30,34,37,42,43,78,145</sup>.

- i. The increase in methanol fraction results in a decrease in the solvent dielectric permittivity. Due to this disadvantage for ionic dissociation, acidic compounds (HA) may be less likely to dissociate when there are more ions involved in the right-hand side than left side process ( $HA + S \rightleftharpoons HS^+ + A^-$ ), where S is the methanol-water solvent. The electrostatic interaction between  $HS^+$  and  $A^-$  may increase because of the decrease in dielectric permittivity, shifting the equilibrium to the left and increasing the  $pK_a$  value. The decrease in dielectric permittivity has no effect on the dissociation of

protonated acid of the bases ( $\text{HA}^+ + \text{S} \rightleftharpoons \text{HS}^+ + \text{A}$ ) because there is no variation in the number of ions at both sides of the equilibria.

- ii. The difference in the intrinsic basicity of the solvent, or (the ability of the particular methanol-water mixture to receive dissociated hydrogen ions). Methanol-water mixtures are more basic than water and thus increase the dissociation of acids and decrease the  $\text{p}K_{\text{a}}$  value.
- iii. The specific solvation effects of the different acid-base species in methanol and water: by varying the solvation shell around the compound and adjusting the stability of the different procedures, this phenomenon may impact the equilibrium between the compound's protonated and deprotonated forms.

However, a decrease of dielectric permittivity reasonably does not impact the dissociation of cationic acids due to the fact that there is no difference in the number of ions ( $\text{HA}^+ + \text{S} \rightleftharpoons \text{HS}^+ + \text{A}$ ). Therefore,  $\text{p}K_{\text{a}}$  values decrease with the methanol content because of the combination of the increase in the basicity of the methanol-water media and possible specific solvation effects. From 80 to 100% methanol, the  $\text{p}K_{\text{a}}$  of neutral acid and cationic acid always increases, implying that pure methanol is more basic than methanol-water mixtures. In the case of neutral acids, the effect of dielectric permittivity overcomes the consequence of solvent basicity and results in a moderate increase in the values. Overall, a difference of the  $\text{p}K_{\text{a}}$  values for the reference acid-base compounds in the studied range of solvent compositions (0 – 100% methanol) is an increase of 3.69 – 4.57  $\text{p}K_{\text{a}}$  units for neutral acids and a decrease of 1.35 – 1.93  $\text{p}K_{\text{a}}$  units for cationic acids.

**Table 5.** Potentiometric  $pK_a$  values (standard deviations) of the neutral acids and conjugated cationic acids of the neutral bases selected for anchoring and testing IS-CE relative  $pK_a$  scales at different concentrations of MeOH-water mixture.

% MeOH (v/v)	0		10		20		30		40		50		60		70		80		90		100	
<b>2-chlorobenzoic Acid</b>	2.84	(0.02)	2.96	(0.01)	3.14	(0.02)	3.35	(0.01)	3.58	(0.01)	3.78	(0.03)	4.05	(0.02)	4.29	(0.01)	4.87	(0.01)	5.85	(0.01)	7.44	(0.02)
<b>Benzoic Acid</b>	4.17	(0.01)	4.27	(0.01)	4.39	(0.01)	4.59	(0.02)	4.80	(0.01)	4.96	(0.01)	5.12	(0.00)	5.40	(0.02)	5.98	(0.02)	7.04	(0.02)	8.72	(0.03)
<b>Vanillin</b>	7.37	(0.02)	7.45	(0.01)	7.60	(0.01)	7.70	(0.01)	7.87	(0.02)	7.99	(0.01)	8.2	(0.00)	8.38	(0.01)	8.78	(0.01)	9.36	(0.01)	11.06	(0.01)
<b>Quinoline</b>	4.92	(0.02)	4.80	(0.03)	4.66	(0.03)	4.43	(0.03)	4.23	(0.01)	3.86	(0.02)	3.56	(0.01)	3.43	(0.01)	3.56	(0.02)	3.78	(0.02)		
<b>4-tert-butylpyridine</b>	6.09	(0.02)	5.91	(0.03)	5.68	(0.02)	5.50	(0.02)	5.20	(0.02)	4.86	(0.02)	4.41	(0.02)	4.20	(0.02)	4.16	(0.02)	4.62	(0.02)	5.15	(0.03)
<b>2,4-lutidine</b>	6.80	(0.01)	6.61	(0.01)	6.42	(0.01)	6.24	(0.00)	5.98	(0.02)	5.67	(0.01)	5.31	(0.01)	5.07	(0.01)	5.01	(0.02)	5.45	(0.03)	6.30	(0.02)

**Table 6.** Potentiometric  $pK_a$  values (standard deviations) of the neutral acids and conjugated cationic acids of the neutral bases selected for anchoring and testing IS-CE relative  $pK_a$  scales at different concentrations of ACN-water mixture.

% ACN (v/v)	0		10		20		30		40		50		60		70		80		90		100	
<b>2-Chlorobenzoic acid</b>	2.84	(0.02)	3.17	(0.07)	3.51	(0.05)	3.85	(0.01)	4.18	(0.03)	4.50	(0.09)	4.94	(0.02)	5.37	(0.05)	5.91	(0.02)	6.21	(0.02)	6.97	(0.01)
<b>Benzoic Acid</b>	4.17	(0.02)	4.36	(0.05)	4.66	(0.05)	5.05	(0.03)	5.31	(0.04)	5.59	(0.07)	6.00	(0.03)	6.39	(0.03)	6.97	(0.06)	7.24	(0.03)	7.99	(0.02)
<b>Vanillin</b>	7.37	(0.02)	7.58	(0.02)	7.90	(0.04)	8.11	(0.02)	8.39	(0.01)	8.63	(0.02)	8.85	(0.05)	9.12	(0.03)	9.69	(0.06)	9.76	(0.04)	10.96	(0.03)
<b>Quinoline</b>	4.92	(0.02)	4.58	(0.01)	4.38	(0.04)	4.09	(0.03)	3.96	(0.04)	3.75	(0.04)	3.69	(0.01)	3.62	(0.04)	3.64	(0.02)	3.77	(0.08)		
<b>4-tert-butylpyridine</b>	6.09	(0.06)	5.67	(0.03)	5.41	(0.11)	5.14	(0.10)	4.95	(0.03)	4.75	(0.11)	4.69	(0.03)	4.62	(0.03)	4.68	(0.04)	5.00	(0.04)	8.07	(0.02)
<b>2,4-lutidine</b>	6.80	(0.02)	6.44	(0.04)	6.19	(0.03)	5.94	(0.08)	5.78	(0.04)	5.60	(0.02)	5.54	(0.02)	5.48	(0.01)	5.49	(0.01)	5.81	(0.01)	6.98	(0.04)

### 3.1.2. Determination $pK_a$ by potentiometric titration at different % of Acetonitrile- water mixture

Similarly to methanol-water, in the case of acetonitrile-water, one neutral acid (benzoic acid) and one neutral base (2,4-lutidine) were chosen as anchor compounds for the two sub-sets of internal standards (the 23 neutral acids and the 23 neutral bases). Additionally, to evaluate the effectiveness of the anchoring process, one more neutral acid (2-chlorobenzoic acid) and two additional neutral bases (quinoline and 4-*tert*-butylpyridine) were chosen. These compounds provide a method to evaluate the accuracy and reliability of anchoring process. These compounds  $pK_a$  values were determined potentiometrically in acetonitrile-water mixtures with concentrations ranging from 0 to 100% acetonitrile (v/v). Table 6 presents the results together with the standard deviation. The results are the mean of three separate titrations. The determined  $pK_a$  values have a standard deviation that is less than 0.06. Similar to the methanol-water mixtures, three different reasons interact to explain the variation in  $pK_a$  values as the percentage of acetonitrile increases, namely the dielectric constant, the basicity of the solvent and specific solvation effects.

The  $pK_a$  variation with the proportion of acetonitrile (v/v) is shown in Table 6. Similarly to methanol-water and for the same reasons, the  $pK_a$  of neutral acids/conjugated anionic bases (HA/A<sup>-</sup> pairs) increases with the increase in acetonitrile proportion, whereas the  $pK_a$  of neutral bases/conjugated cationic acids (A/HS<sup>+</sup> pairs) decreases with the increase in acetonitrile proportion up to 80% and then starts to increase because of the lower basicity of acetonitrile at high concentration. In the end, the range of solvent composition studied (0 – 100% acetonitrile) results in an increase of 4.13  $pK_a$  units of neutral acid and a decrease 1.32 – 1.41  $pK_a$  units of neutral bases for the reference acid-base compounds.

## 3.2. Joule heating and ohm's law verification

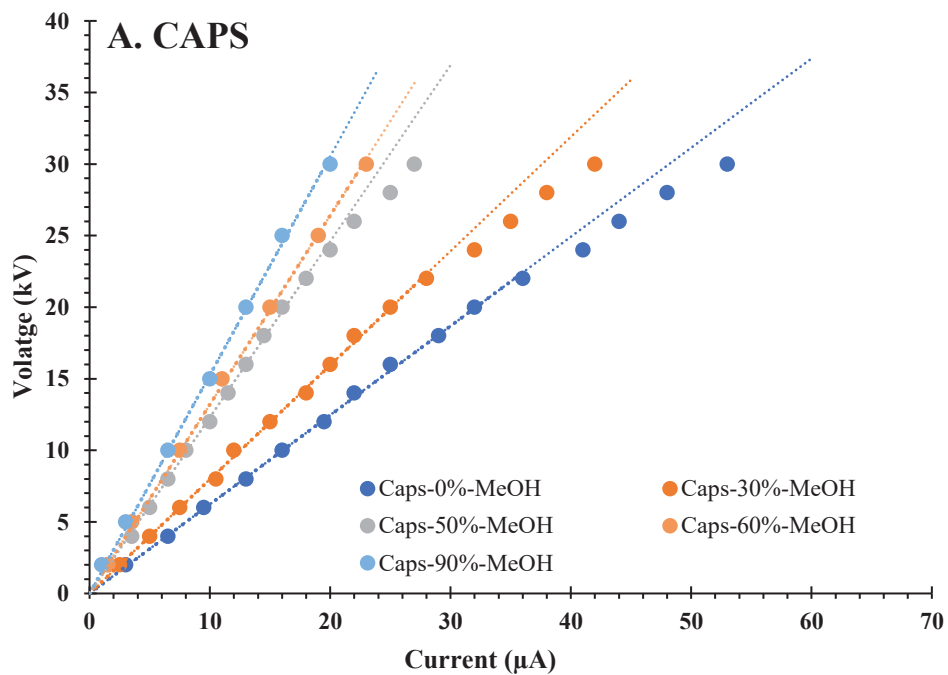
Testing the joule heating effect provides valuable information about changes in the electrical properties of buffers specially at high pH <sup>146-148</sup>, which can affect the reproducibility and accuracy of experimental results. It is important to understand that the particular heat produced by joule heating is based on several factors, such as the solution, applied voltage, current conductivity, and resistance <sup>56,60-66</sup>. Measurements were performed by applying incremental voltages increasing from 1 to 30 kV at different methanol concentrations (v/v) and maintaining the desired temperature for the CAPS and KOH buffer. According to Ohm's law verification we checked out Ohm's law for the buffer of interest and made the plot to see the effect of Joule heating. The plot presents the relationships between the voltage and current intensity in a buffer.

As shown in Figure (15-A), we conduct joule heating tests on CAPS buffer at different concentrations of methanol to verify Ohm's law. The plot is shown through interesting observation. At concentrations between 0 and 50%, it shown that there is a straight-line relationship between the voltage and current intensity up 20 kV. This shows that Ohm's law is being followed within this concentration range. Likewise, for concentrations between 60% and 90%, it displayed that there is a straight-line relationship between the voltage and current intensity up 30kV. Notably, the desired voltage between up 25 kV because the current is low that indicates the joule heating effect is relatively low, implying that Ohm's law is valid under these conditions <sup>56,60-66</sup>. At concentrations ranging from 60% to 90%, the current observed is low. This is the reason why the voltage needs to be increased from 20 kV, which is enough for concentrations 0% to 50% methanol, to 25 kV at higher methanol concentration. The decrease in the current results in slower migration times for analytes, not enough separation, and reduced peak quality. Peaks may overlap, lose resolution, and border, making it difficult to analyze the analytes.

On the other hand, to achieve the limiting mobility of some acidic compounds, we had to look for another basic buffer with a high pH, and KOH was selected. Before starting with the analysis by capillary electrophoresis, testing the joule effect is important to avoid dissipating heat. As shown in Figure (15-B), we conduct joule heating tests on KOH buffer at different concentrations of methanol to verify Ohm's law. At concentrations between 0 and 50%, it

shown that there is a straight-line relationship between the voltage and current intensity from 0 to 9 kV only. This shows that Ohm's law is not being followed within this concentration range. Likewise, for concentrations between 60 and 90%, it displayed that there is a straight-line relationship between the voltage and current intensity from 0 to 15 kV. Notably, the desired voltage between 20 and 25 kV that implies the joule heating effect is relatively high, implying that Ohm's law is not valid under these conditions. Thus, the results explained that the relationship between voltage and current intensity in the KOH buffer deviates from linearity, indicating that under the studied concentration range, Ohms law is not fulfilled and using low voltage will affect the mobility and the separation.

This approach allows the electrical properties of the buffer to be determined under specific conditions. Voltage-current diagrams are useful for visualizing the relationship between electrical properties and buffer performance.



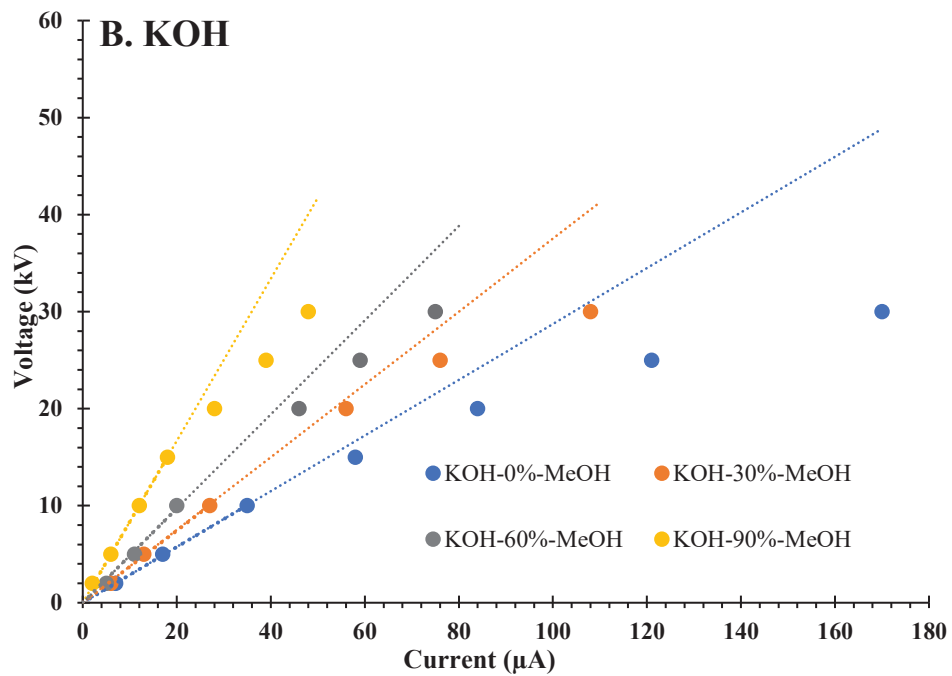


**Figure 15.** joule heating test for the buffers; **A)** CAPS and **B)** KOH at different % of MeOH.

### **3.3. Determination of the $pK_a$ of acid-base analytes by IS-CE at different % of methanol - water mixture and different % of acetonitrile- water mixture.**

The  $pK_a$  of neutral acid and neutral base was determined in a methanol-water mixture or acetonitrile-water mixture up to 90% because it was difficult to prepare buffer without water for 100% due to the solubility problem. The IS-CE method has to accurately measure the limiting mobility of acids and bases. In this method, the limiting mobility of the analyte and internal standard must be measured in a buffer where they are fully or almost fully ionized. We shall consider that they exhibit at least 98% ionization, as per the criteria we decided with a maximum 2% error. The neutral acid must be in the cationic form (buffer of high pH), while the base must be protonated in the cationic form (buffer of low pH)<sup>35</sup>. The pH value of these buffers was measured to ensure full ionization; the buffer selected for the acid compounds is CAPS, while the buffer chosen for the base compounds is mixture of sodium dihydrogen phosphate and phosphoric acid. In terms of the used criteria, this means that the  $pK_a$  value of the acid and base compounds has to be 1.7 units lower or higher than the pH of limiting mobility, depending on the nature of the compounds, whether they are neutral acid or neutral base. Once the limiting pH of the buffers is known, it has to be compared to the determined  $pK_a$  value in order to fulfill the 1.7 criteria. The  $pK_a$  values determined at different concentrations of the methanol-water mixture with the measured limiting pH of buffer and the limiting mobility for the neutral acids and neutral bases are shown in Tables (7) and (8) for acid, respectively, while bases are presented in Tables (9) and (10).

The internal standards are the same ones that were used in earlier studies on water<sup>39,68,149</sup>, except of vanillin, and phenol. Vanillin was removed because it has a side reaction in the aldehyde group, which can oxidize at high pH to create vanillin acid<sup>150-155</sup>. Likewise, phenol was excluded because it doesn't fulfill 98% ionization in the limiting mobility buffer and has a  $pK_a$  value that is not 1.7 units lower than the limiting pH. Thus, small errors in the measurement of the internal standard can have a significant impact on the calculated  $pK_a$  value of other acidic compounds.

Benzoic acid was used as an anchoring compound for the acidic internal standard compounds, and 2-chlorobenzoic acid was compared only to the one obtained electrophoretically to check the accuracy of the calculation. These compounds  $pK_a$  values were established using potentiometric titration, and they were used as standards for acidic compounds  $pK_a$  values determined through the IS-CE method. Thus, there is a good agreement between the  $pK_a$  that were determined by the potentiometric method and by capillary electrophoresis, with a maximum different between the potentiometric and capillary electrophoresis values less than 0.07  $pK_a$  units, as shown in Figure (17) and Tables (5) and (7).

To ensure consistency, all internal standards were determined using the same methodology and evaluation criteria at all methanol concentrations (ranging from 0 to 90 %), with a standard deviation ranging from 0.00 to 0.12, as shown in Table (7). This approach could have made it possible to determine the  $pK_a$  values of all the tested acids more effectively. For example, the  $pK_a$  of 4-hydroxybenzaldehyde was determined using 4 different ISs (4-nitrophenol, phenobarbital, 3,5-dichlorophenol and methylparaben) using  $\text{TrisH}^+$  buffers ((at 50% MeOH v/v), and the following results were obtained: 7.87, 7.98, 8.02, and 8.04 respectively. So, the final  $pK_a$  value after anchoring obtained for 4-hydroxybenzaldehyde at 50% MeOH v/v buffers was  $7.97 \pm 0.08$ , which shows a high degree of precision.

The  $pK_a$  value of paracetamol could be calculated at 0%, 10%, and 20% MeOH because paracetamol has a  $pK_a$  of 9.67 with a variation between the limiting pH and the  $pK_a$  at 20% methanol of 1.7  $pK_a$  units, whereas at higher methanol concentration it doesn't fulfill the applied criteria of 1.7 difference. For the same reason, the calculations were possible for 4-bromophenol only up to 40%, 3-chlorophenol only up to 50%, 2-chlorophenol and methylparaben only up to 70%, 3,5-dichlorophenol only up to 80%, and the  $pK_a$  value for the rest of the acids could be calculated up to 90% MeOH. All the  $pK_a$  values of acids are shown in Table (7).

**Table 7.** The  $pK_a$  values with (standard deviations) of the acids internal standards at studied methanol-water compositions (v/v), at 25 °C and 0 ionic strength.

% MeOH (v/v)	0	10 %	20 %	30 %	40 %	50 %	60 %	70 %	80 %	90 %
<b>2,6-Dibromo-4-nitrophenol</b>	3.27 (0.02)	3.30 (0.01)	3.34 (0.01)	3.36 (0.02)	3.39 (0.01)	3.56 (0.04)	3.77 (0.06)	4.28 (0.03)	4.77 (0.05)	5.75 (0.06)
<b>2-Chlorobenzoic acid</b>	2.80 (0.03)	2.90 (0.02)	3.20 (0.02)	3.28 (0.01)	3.54 (0.01)	3.77 (0.05)	4.00 (0.02)	4.28 (0.04)	4.81 (0.04)	5.91 (0.03)
<b>4-Nitrobenzoic acid</b>	3.33 (0.01)	3.34 (0.01)	3.45 (0.01)	3.62 (0.03)	3.78 (0.03)	3.96 (0.09)	4.16 (0.08)	4.36 (0.07)	5.02 (0.10)	5.82 (0.07)
<b>2,6-Dinitrophenol</b>	3.65 (0.01)	3.66 (0.01)	3.68 (0.01)	3.77 (0.01)	3.81 (0.01)	3.98 (0.06)	4.18 (0.06)	4.57 (0.04)	5.03 (0.07)	5.82 (0.09)
<b>2,4-Dinitrophenol</b>	4.03 (0.02)	4.04 (0.04)	4.04 (0.04)	4.06 (0.01)	4.08 (0.02)	4.11 (0.06)	4.37 (0.02)	4.54 (0.07)	4.99 (0.06)	6.17 (0.09)
<b>3-Bromobenzoic acid</b>	3.75 (0.03)	3.82 (0.02)	3.88 (0.02)	4.13 (0.02)	4.31 (0.02)	4.47 (0.05)	4.67 (0.05)	4.92 (0.07)	5.47 (0.12)	6.45 (0.09)
<b>Benzoic acid</b>	4.17 (0.02)	4.27 (0.02)	4.39 (0.02)	4.59 (0.03)	4.80 (0.02)	4.96 (0.07)	5.12 (0.03)	5.40 (0.03)	5.98 (0.05)	7.04 (0.04)
<b>Ibuprofen</b>	4.43 (0.03)	4.56 (0.06)	4.73 (0.06)	5.01 (0.02)	5.19 (0.01)	5.29 (0.07)	5.47 (0.08)	5.74 (0.05)	6.30 (0.08)	7.38 (0.11)
<b>2,5-Dinitrophenol</b>	5.16 (0.05)	5.20 (0.03)	5.24 (0.03)	5.31 (0.03)	5.32 (0.03)	5.36 (0.06)	5.55 (0.08)	5.81 (0.06)	6.48 (0.06)	7.40 (0.11)
<b>Warfarin</b>	5.09 (0.05)	5.17 (0.04)	5.22 (0.04)	5.37 (0.05)	5.43 (0.03)	5.53 (0.06)	5.71 (0.08)	5.86 (0.06)	6.51 (0.03)	7.49 (0.11)
<b>Sulfacetamide</b>	5.31 (0.02)	5.53 (0.01)	5.63 (0.01)	5.91 (0.01)	6.04 (0.03)	6.09 (0.02)	6.32 (0.06)	6.45 (0.02)	7.09 (0.03)	8.09 (0.09)
<b>2,4,6-Tribromophenol</b>	5.90 (0.10)	6.03 (0.10)	6.27 (0.02)	6.38 (0.02)	6.48 (0.03)	6.74 (0.05)	7.02 (0.04)	7.21 (0.04)	7.45 (0.02)	8.30 (0.05)
<b>4-Nitrophenol</b>	6.90 (0.02)	7.01 (0.03)	7.12 (0.03)	7.17 (0.03)	7.26 (0.01)	7.57 (0.03)	7.92 (0.05)	8.14 (0.06)	8.46 (0.07)	9.09 (0.02)
<b>4-Hydroxybenzaldehyde</b>	7.50 (0.04)	7.51 (0.03)	7.64 (0.02)	7.73 (0.03)	7.83 (0.01)	7.97 (0.08)	8.20 (0.01)	8.41 (0.04)	8.90 (0.12)	9.30 (0.00)
<b>Phenobarbital</b>	7.43 (0.08)	7.43 (0.02)	7.67 (0.03)	7.77 (0.02)	7.92 (0.02)	8.07 (0.11)	8.30 (0.03)	8.51 (0.02)	9.03 (0.04)	9.39 (0.01)
<b>3,5-Dichlorophenol</b>	8.08 (0.03)	8.16 (0.03)	8.20 (0.08)	8.33 (0.02)	8.41 (0.01)	8.63 (0.08)	8.83 (0.05)	8.98 (0.05)	9.36 (0.05)	
<b>Methylparaben</b>	8.26 (0.04)	8.35 (0.02)	8.41 (0.03)	8.54 (0.01)	8.63 (0.02)	8.83 (0.00)	8.99 (0.03)	9.20 (0.06)		
<b>2-Chlorophenol</b>	8.41 (0.01)	8.51 (0.02)	8.59 (0.03)	8.79 (0.01)	8.97 (0.03)	9.21 (0.02)	9.39 (0.05)	9.49 (0.07)		
<b>3-Chlorophenol</b>	8.95 (0.02)	8.99 (0.01)	9.09 (0.01)	9.21 (0.04)	9.33 (0.03)	9.54 (0.02)				
<b>4-Bromophenol</b>	9.19 (0.02)	9.22 (0.02)	9.28 (0.02)	9.43 (0.02)	9.56 (0.01)					
<b>Paracetamol</b>	9.52 (0.02)	9.53 (0.03)	9.67 (0.02)							
<b>pH of Limiting mobility</b>	11.43	11.39	11.36	11.34	11.29	11.25	11.25	11.27	11.30	11.34

**Table 8.** Limiting mobility ( $\text{m}^2 \text{V}^{-1} \text{s}^{-1}$ ) of the acids internal standards at studied methanol-water compositions (v/v), at 25 °C and 0 ionic strength.

% MeOH (v/v)	0	10 %	20 %	30 %	40 %	50 %	60 %	70 %	80 %	90 %
<b>2,6-Dibromo-4-nitrophenol</b>	143.58	124.80	110.55	101.20	93.86	92.84	91.91	90.21	89.94	93.58
<b>2-Chlorobenzoic acid</b>	148.40	131.78	118.01	107.05	99.88	97.12	95.57	93.47	93.15	94.13
<b>4-Nitrobenzoic acid</b>	152.79	132.96	120.13	108.78	100.44	97.37	95.87	93.17	92.86	94.64
<b>2,6-Dinitrophenol</b>	166.62	145.40	131.04	119.31	110.54	106.24	105.43	102.82	99.92	103.32
<b>2,4-Dinitrophenol</b>	163.83	137.24	125.78	112.38	104.15	100.26	99.76	96.55	96.19	98.47
<b>3-Bromobenzoic acid</b>	152.14	131.75	118.66	104.23	98.69	96.03	93.85	91.30	90.22	93.67
<b>Benzoic acid</b>	164.51	142.59	127.01	114.28	106.43	100.79	100.20	97.33	96.09	99.40
<b>Ibuprofen</b>	113.49	98.90	89.32	80.39	75.27	74.02	72.56	70.52	69.57	71.20
<b>2,5-Dinitrophenol</b>	161.65	138.75	124.07	114.81	104.33	99.31	98.82	93.37	92.30	98.75
<b>Warfarin</b>	107.41	89.90	80.25	72.21	67.29	64.54	63.76	63.42	62.32	63.45
<b>Sulfacetamide</b>	130.86	111.64	98.85	87.44	80.49	78.00	76.46	73.68	72.06	74.31
<b>2,4,6-Tribromophenol</b>	136.25	116.38	105.76	94.02	89.34	86.25	84.18	82.46	81.45	83.66
<b>4-Nitrophenol</b>	161.28	144.09	127.28	114.01	103.93	98.45	97.36	96.23	93.11	96.60
<b>4-Hydroxybenzaldehyde</b>	156.80	134.69	117.93	106.99	96.48	92.29	91.39	89.17	86.73	89.71
<b>Phenobarbital</b>	129.19	108.87	96.35	86.68	80.28	77.88	75.80	73.02	72.45	73.10
<b>3,5-Dichlorophenol</b>	148.61	128.20	115.59	103.81	96.36	93.89	90.66	89.18	88.35	
<b>Methylparaben</b>	138.32	114.90	104.74	93.68	86.19	83.53	81.47	79.98		
<b>2-Chlorophenol</b>	161.01	138.05	123.16	111.91	101.68	98.65	96.18	94.93		
<b>3-Chlorophenol</b>	162.23	137.56	122.55	111.06	101.36	98.92				
<b>4-Bromophenol</b>	148.17	124.36	110.64	99.43	90.51					
<b>Paracetamol</b>	119.90	96.32	85.49							

**Table 9.** The  $pK_a$  values with (standard deviations) of the bases internal standards at studied methanol-water compositions (v/v), at 25 °C and 0 ionic strength.

% MeOH (v/v)	0	10 %	20 %	30 %	40 %	50 %	60 %	70 %	80 %	90 %
<b>pH of Limiting mobility</b>	1.94	1.98	2.02	2.09	2.12	2.19	2.21	2.3	2.38	2.41
<b>Aniline</b>	4.67 (0.03)	4.63 (0.02)	4.57 (0.05)	4.46 (0.02)	4.29 (0.07)					
<b>Quinoline</b>	4.96 (0.01)	4.83 (0.05)	4.71 (0.04)	4.49 (0.02)	4.24 (0.06)					
<b>4- tert-Butylaniline</b>	4.96 (0.01)	4.95 (0.04)	4.90 (0.05)	4.79 (0.02)	4.61 (0.08)	4.29 (0.03)	4.13 (0.01)			
<b>N,N-Dimethylaniline</b>	5.22 (0.04)	5.18 (0.02)	5.10 (0.02)	4.92 (0.03)	4.70 (0.08)	4.35 (0.04)	4.07 (0.06)			
<b>Pyridine</b>	5.31 (0.03)	5.28 (0.04)	5.11 (0.05)	4.87 (0.02)	4.52 (0.08)	4.21 (0.03)	4.03 (0.02)			
<b>Acridine</b>	5.58 (0.05)	5.43 (0.09)	5.29 (0.02)	5.06 (0.02)	4.73 (0.08)	4.43 (0.05)	4.23 (0.03)			4.14 (0.03)
<b>4-tert-Butylpyridine</b>	6.06 (0.04)	5.95 (0.06)	5.71 (0.02)	5.54 (0.03)	5.17 (0.08)	4.89 (0.08)	4.49 (0.04)	4.16 (0.04)	4.24 (0.05)	4.63 (0.04)
<b>Papaverine</b>	6.42 (0.04)	6.36 (0.06)	6.07 (0.02)	5.90 (0.02)	5.64 (0.05)	5.44 (0.05)	5.05 (0.05)	4.62 (0.03)	4.54 (0.07)	5.02 (0.03)
<b>2,4-Lutidine</b>	6.80 (0.03)	6.61 (0.09)	6.42 (0.02)	6.24 (0.03)	5.98 (0.05)	5.67 (0.05)	5.31 (0.06)	5.07 (0.06)	5.01 (0.04)	5.45 (0.03)
<b>Trazodone</b>	6.82 (0.02)	6.75 (0.03)	6.61 (0.03)	6.34 (0.03)	6.22 (0.07)	5.77 (0.04)	5.47 (0.04)	5.11 (0.05)	5.20 (0.03)	5.57 (0.03)
<b>Pilocarpine</b>	7.06 (0.03)	6.93 (0.10)	6.71 (0.05)	6.46 (0.03)	6.29 (0.05)	5.92 (0.03)	5.57 (0.04)	5.31 (0.06)	5.34 (0.06)	5.54 (0.04)
<b>2,4,6-Trimethylpyridine</b>	7.48 (0.02)	7.38 (0.07)	7.24 (0.07)	6.81 (0.05)	6.59 (0.07)	6.25 (0.07)	5.83 (0.03)	5.41 (0.09)	5.56 (0.05)	5.87 (0.09)
<b>lidocaine</b>	7.90 (0.05)	7.83 (0.04)	7.76 (0.03)	7.57 (0.03)	7.32 (0.04)	7.05 (0.03)	6.64 (0.07)	6.12 (0.10)	5.70 (0.04)	6.63 (0.07)
<b>Bupivacaine</b>	8.15 (0.02)	8.11 (0.03)	8.06 (0.05)	7.92 (0.02)	7.52 (0.07)	7.20 (0.04)	6.73 (0.06)	6.23 (0.06)	5.76 (0.06)	6.88 (0.03)
<b>1-Phenylpiperazine</b>	8.67 (0.02)	8.62 (0.05)	8.52 (0.02)	8.41 (0.05)	8.19 (0.08)	7.80 (0.04)	7.38 (0.04)	6.56 (0.07)	6.40 (0.03)	7.54 (0.04)
<b>Benzyl dimethylamine</b>	8.95 (0.04)	8.91 (0.06)	8.81 (0.05)	8.60 (0.04)	8.33 (0.09)	8.03 (0.09)	7.52 (0.04)	6.63 (0.04)	6.40 (0.02)	7.65 (0.04)
<b>Diphenhydramine</b>	9.03 (0.03)	9.02 (0.05)	8.97 (0.04)	8.71 (0.03)	8.43 (0.06)	8.06 (0.05)	7.63 (0.07)	6.77 (0.05)	6.46 (0.04)	7.65 (0.05)
<b>Procainamide</b>	9.25 (0.01)	9.16 (0.06)	9.00 (0.03)	8.74 (0.03)	8.52 (0.06)	8.15 (0.03)	7.68 (0.05)	6.83 (0.05)	6.46 (0.03)	7.60 (0.03)
<b>Imipramine</b>	9.30 (0.01)	9.26 (0.06)	9.15 (0.03)	8.92 (0.03)	8.60 (0.05)	8.44 (0.04)	7.85 (0.06)	6.91 (0.04)	6.68 (0.03)	7.97 (0.04)
<b>Propranolol</b>	9.46 (0.01)	9.40 (0.04)	9.18 (0.04)	8.99 (0.07)	8.81 (0.05)	8.60 (0.05)	7.91 (0.06)	6.95 (0.04)	6.90 (0.03)	8.07 (0.04)
<b>1-Aminoethylbenzene</b>	9.50 (0.01)	9.40 (0.04)	9.20 (0.02)	9.05 (0.04)	8.82 (0.04)	8.62 (0.05)	8.10 (0.04)	7.17 (0.05)	7.05 (0.03)	8.30 (0.04)
<b>Ephedrine</b>	9.71 (0.02)	9.60 (0.03)	9.36 (0.03)	9.30 (0.06)	9.08 (0.07)	8.71 (0.05)	8.30 (0.03)	7.36 (0.05)	7.18 (0.03)	8.34 (0.04)
<b>Nortriptyline</b>	10.06 (0.01)	9.87 (0.08)	9.66 (0.02)	9.47 (0.04)	9.26 (0.06)	8.88 (0.04)	8.38 (0.04)	7.51 (0.06)	7.16 (0.03)	8.36 (0.04)

**Table 10.** Limiting mobility ( $\text{m}^2 \text{V}^{-1} \text{s}^{-1}$ ) of the bases internal standards at studied methanol-water compositions (v/v), at 25 °C and 0 ionic strength.

% MeOH (v/v)	0	10 %	20 %	30 %	40 %	50 %	60 %	70 %	80 %	90 %
Aniline	-184.0	-152.1	-136.8	-113.8	-113.1					
Quinoline	-183.2	-151.9	-135.1	-113.6	-106.0					
4- <i>tert</i> -Butylaniline	-136.5	-111.5	-98.6	-83.1	-77.2	-98.11	-92.68			
<i>N,N</i> -Dimethylaniline	-170.2	-142.1	-127.1	-106.2	-99.9	-125.18	-120.02			
Pyridine	-238.9	-203.4	-181.5	-154.9	-145.4	-179.58	-169.98			
Acridine	-148.6	-123.9	-109.3	-94.0	-88.3	-108.40	-105.28			-101.42
4- <i>tert</i> -Butylpyridine	-158.6	-136.9	-120.9	-104.7	-92.5	-124.47	-123.23	-116.26	-116.46	-115.42
Papaverine	-90.4	-77.7	-65.7	-54.4	-50.8	-65.88	-63.01	-63.01	-72.94	-69.50
2,4-Lutidine	-178.3	-157.5	-138.4	-118.4	-113.9	-134.79	-130.94	-117.52	-117.19	-121.42
Trazodone	-88.4	-75.2	-62.9	-52.3	-48.4	-63.05	-59.50	-59.50	-57.83	-58.71
Pilocarpine	-127.2	-112.2	-91.9	-81.2	-76.0	-94.27	-91.84	-88.23	-87.75	-85.85
2,4,6-Trimethylpyridine	-152.3	-136.6	-116.0	-104.5	-100.4	-124.40	-118.07	-117.25	-116.66	-107.15
lidocaine	-98.3	-80.2	-73.3	-64.4	-60.6	-77.17	-73.18	-72.43	-70.73	-71.68
Bupivacaine	-86.1	-71.5	-64.5	-58.4	-54.1	-68.29	-66.13	-68.62	-66.83	-66.15
1-Phenylpiperazine	-132.0	-110.9	-102.1	-86.3	-80.3	-105.66	-100.32	-98.57	-97.29	-95.70
Benzylidimethylamine	-144.5	-123.4	-120.0	-100.5	-90.0	-120.72	-114.15	-112.21	-111.17	-111.06
Diphenhydramine	-100.3	-83.8	-81.1	-69.5	-65.6	-82.55	-76.92	-78.14	-77.83	-78.10
Procainamide	-97.0	-82.0	-80.3	-72.7	-64.2	-94.31	-83.52	-82.67	-78.94	-79.09
Imipramine	-94.0	-79.8	-78.2	-65.6	-61.2	-74.86	-72.60	-69.82	-71.67	-71.24
Propranolol	-90.4	-77.2	-73.7	-62.0	-56.9	-72.73	-67.11	-66.22	-67.43	-67.65
1-Aminoethylbenzene	-132.8	-115.1	-113.8	-95.8	-89.5	-120.88	-113.09	-110.04	-111.97	-108.87
Ephedrine	-113.0	-96.7	-93.7	-77.4	-72.8	-95.25	-86.76	-70.61	-73.65	-72.65
Nortriptyline	-93.1	-79.8	-77.8	-65.9	-61.0	-81.03	-73.26	-72.79	-75.09	-72.86

In the case of the bases, the potentiometric  $pK_a$  value of 2,4-lutidine was used as an anchoring point for the bases internal standard compounds, while quinoline and 4-*tert*-butylpyridine were compared only to the one obtained electrophoretically to check the accuracy of the calculation. Therefore, there is a good agreement between the  $pK_a$  that were determined by potentiometric method and by capillary electrophoresis, with a maximum different between the potentiometric and capillary electrophoresis values less than 0.08  $pK_a$  units, as shown in Figure (19) Tables (5) and (9).

To achieve a better degree of precision in the determination of  $pK_a$  values, the same criteria method was applied to all bases internal standards at all methanol concentrations (from 0 to 90%), with a standard deviation ranging from 0.01 to 0.1, as shown in Table (9). The established method proved a high degree of precision. For example, the  $pK_a$  of Trazodone was determined using 5 different ISs (4-*tert*-butylpyridine, papaverine, 2,4-lutidine, pilocarpine, and 2,4,6-trimethylpyridine) using acetate buffer (at 50% MeOH v/v), and the following results were obtained: 5.71, 5.79, 5.77, 5.75, and 5.71 respectively. So, the final  $pK_a$  value obtained for Trazodone at 50% MeOH v/v buffers was  $5.77 \pm 0.04$ , which shows a high degree of precision.

The  $pK_a$  values of quinoline and aniline could be calculated only up to 40% MeOH because the difference between the  $pK_a$  of the analyte and the pH of limiting mobility was higher than 1.7 units, but it wasn't higher after 40% methanol. Similarly, the  $pK_a$  values of 4-*tert*-butylaniline, pyridine, acridine, and *N,N*-dimethylaniline can't be calculated for more than 60% MeOH since the difference between their  $pK_a$  and the limiting pH was less than 1.7-unit. The  $pK_a$  of neutral bases decreases with increasing the concentration of methanol up to 80%, and then starts to increase again up to 90% methanol. It is interesting to note that despite the challenges observed when calculating the  $pK_a$  values of compounds in MeOH-water solvent mixtures, the acridine  $pK_a$  value was effectively determined at 90% MeOH as there is a 1.73-unit difference between acridine  $pK_a$  and the limiting pH, as the chosen criteria can be used. Because of specific solvation effects on the compound in the MeOH-water mixture, the  $pK_a$  value of acridine was successfully determined at high concentrations of MeOH. All the  $pK_a$  values of bases are displayed in Table (9).

Similar to what was discussed in the methanol part, same criteria were applied to the determination of the  $pK_a$  of acid-base compound at different concentrations of acetonitrile, from 0 to 90%.

To validate the accuracy of the calculation, benzoic acid was used as an anchoring compound for the acidic internal standard compounds, and 2-chlorobenzoic acid was compared only to the one obtained electrophoretically. These compounds  $pK_a$  values were established using potentiometric titration, and they were used as standards for acidic compounds  $pK_a$  values determined through the IS-CE method. Hence, there is a good agreement between the  $pK_a$  that were determined by the potentiometric method and by capillary electrophoresis at different acetonitrile concentration from 0 to 90%, with a maximum different between the potentiometric and capillary electrophoresis values less than 0.06  $pK_a$  units, as shown in Figure (21) Tables (6) and (11).

It was practicable to observe and determine the  $pK_a$  values of all established acids more successfully by determining all internal standards using the same technique and evaluation criteria at all acetonitrile concentrations from (0 to 90%), with a standard deviation ranging from 0.01 to 0.13, as presented in Table (11). With this method,  $pK_a$  values may be determined across many compounds and solvent conditions with better precision and reliability. For example, the  $pK_a$  of 2,4,6-tribromophenol was determined using 4 different ISs (warfarin, 2,5 dinitrophenol, sulfacetamide and 4-nitrophenol) using Bis-TrisH<sup>+</sup> buffers (at 20% ACN v/v), and the following results were obtained: 6.35, 6.38, 6.37, and 6.40, respectively. So, the final  $pK_a$  value after anchoring obtained for 2,4,6-tribromophenol at 20% ACN v/v buffers was  $6.38 \pm 0.04$ , which shows a high degree of precision.

All the acids can be calculated up to 90% acetonitrile, except for 4-bromophenol and paracetamol. The  $pK_a$  of paracetamol can't be calculated for more than 40% acetonitrile, and the  $pK_a$  of 4-bromophenol can't be calculated for more than 50% because the difference between their  $pK_a$  and the limiting pH was less than 1.7 units at higher acetonitrile content, which can lead to unfavorable effects on other results.

As in methanol, the accuracy of the calculation at different acetonitrile concentrations was validated using 2,4-lutidine as an anchoring point for the bases internal standard compounds, while quinoline and 4-*tert*-butylpyridine were compared only to the ones obtained

electrophoretically. Consequently, there is a good agreement between the  $pK_a$  that were determined by the potentiometric method and by capillary electrophoresis at different acetonitrile concentration, with a maximum different between the potentiometric and capillary electrophoresis values less than 0.07  $pK_a$  units, as shown in Figure (23) Table (6) and (13).

To achieve a better degree of precision in the determination of the  $pK_a$  values of the bases, the same approach was applied at all acetonitrile concentrations (from 0 to 90%), with standard deviation ranging from 0.01 to 0.15, as shown in Table (13). The developed method showed a high degree of precision. For example, the  $pK_a$  of acridine was determined using 4 different ISs (*N,N*-dimethylaniline, pyridine, 4-*tert*-butylpyridine, and papaverine) using acetate buffer (at 90% ACN v/v), and the following results were obtained: 4.58, 4.59, 4.55 and 4.53 respectively. So, the final  $pK_a$  value obtained for acridine at 90% ACN v/v buffers were  $4.54 \pm 0.03$  which shows a high degree of precision.

The  $pK_a$  values of all the bases can be calculated up to 90% acetonitrile, except for aniline and quinoline, which have  $pK_a$  values that can only be calculated up to 40%, but not for higher acetonitrile content because they don't fulfill the used criteria. For the same reason, the  $pK_a$  value of 4-*tert*-butylaniline can be determined only up to 70% acetonitrile, but not higher. The  $pK_a$  value determined from 0 to 90% acetonitrile-water mixture with the measured limiting pH and the limiting mobility for the neutral acids and neutral bases are shown in Tables 11 and 12 for acid, respectively, while bases are presented in Tables 13 and 14.

**Table 11.** The  $pK_a$  values with (standard deviations) of the acids internal standards at studied acetonitrile-water compositions (v/v), at 25°C and 0 ionic strength.

% ACN (v/v)	0%		10%		20%		30%		40%		50%		60%		70%		80%		90	
<b>2-Chlorobenzoic acid</b>	2.80	(0.02)	3.12	(0.07)	3.51	(0.05)	3.88	(0.01)	4.20	(0.03)	4.48	(0.09)	4.93	(0.02)	5.32	(0.05)	5.87	(0.02)	6.25	(0.02)
<b>2,6-Dibromo-4-nitrophenol</b>	3.27	(0.03)	3.34	(0.05)	3.65	(0.07)	3.79	(0.06)	3.89	(0.03)	4.41	(0.07)	4.80	(0.03)	5.24	(0.05)	5.82	(0.08)	6.03	(0.09)
<b>4-Nitrobenzoic acid</b>	3.33	(0.01)	3.42	(0.04)	3.73	(0.06)	4.08	(0.07)	4.25	(0.04)	4.69	(0.04)	5.09	(0.06)	5.37	(0.05)	5.95	(0.11)	6.32	(0.07)
<b>2,6-Dinitrophenol</b>	3.65	(0.01)	3.68	(0.05)	3.98	(0.06)	4.13	(0.07)	4.28	(0.04)	4.73	(0.05)	5.12	(0.07)	5.77	(0.05)	5.99	(0.12)	6.33	(0.09)
<b>3-Bromobenzoic acid</b>	3.75	(0.02)	4.00	(0.09)	4.30	(0.07)	4.49	(0.08)	4.83	(0.05)	5.19	(0.10)	5.50	(0.05)	5.85	(0.08)	6.19	(0.05)	6.68	(0.06)
<b>2,4-Dinitrophenol</b>	4.03	(0.03)	4.15	(0.04)	4.37	(0.02)	4.37	(0.08)	4.53	(0.05)	4.95	(0.07)	5.36	(0.08)	5.98	(0.07)	6.51	(0.13)	6.69	(0.09)
<b>Benzoic acid</b>	4.17	(0.02)	4.36	(0.05)	4.66	(0.05)	5.05	(0.03)	5.31	(0.04)	5.59	(0.07)	6.00	(0.03)	6.39	(0.03)	6.97	(0.06)	7.24	(0.03)
<b>Ibuprofen</b>	4.43	(0.03)	4.47	(0.05)	4.76	(0.08)	5.47	(0.10)	5.64	(0.09)	6.05	(0.06)	6.38	(0.06)	6.45	(0.05)	6.88	(0.08)	7.27	(0.09)
<b>Warfarin</b>	5.09	(0.05)	5.18	(0.05)	5.46	(0.05)	5.71	(0.02)	5.88	(0.03)	6.23	(0.05)	6.61	(0.04)	6.84	(0.09)	7.60	(0.12)	7.85	(0.12)
<b>2,5-Dinitrophenol</b>	5.16	(0.05)	5.26	(0.03)	5.55	(0.04)	5.63	(0.02)	5.75	(0.05)	6.17	(0.05)	6.54	(0.05)	7.05	(0.08)	7.56	(0.13)	8.15	(0.12)
<b>Sulfacetamide</b>	5.31	(0.02)	5.45	(0.09)	5.74	(0.08)	6.24	(0.02)	6.39	(0.05)	6.80	(0.04)	7.16	(0.04)	7.24	(0.10)	7.67	(0.07)	8.28	(0.11)
<b>2,4,6-Tribromophenol</b>	5.90	(0.10)	6.13	(0.07)	6.38	(0.04)	6.65	(0.14)	6.74	(0.08)	7.11	(0.05)	7.50	(0.05)	7.79	(0.06)	8.22	(0.14)	8.56	(0.12)
<b>4-Nitrophenol</b>	6.90	(0.02)	7.34	(0.11)	7.45	(0.11)	7.71	(0.11)	7.92	(0.10)	8.22	(0.08)	8.62	(0.08)	9.01	(0.04)	9.35	(0.14)	9.54	(0.12)
<b>4-Hydroxybenzaldehyde</b>	7.50	(0.04)	7.79	(0.08)	7.86	(0.07)	8.13	(0.08)	8.35	(0.08)	8.65	(0.07)	9.05	(0.07)	9.45	(0.09)	9.77	(0.08)	9.91	(0.09)
<b>Phenobarbital</b>	7.43	(0.08)	7.87	(0.06)	7.91	(0.02)	8.20	(0.05)	8.43	(0.05)	8.72	(0.04)	9.13	(0.05)	9.53	(0.05)	9.84	(0.07)	9.97	(0.07)
<b>3,5-Dichlorophenol</b>	8.08	(0.03)	8.19	(0.11)	8.26	(0.11)	8.51	(0.09)	8.73	(0.09)	9.03	(0.08)	9.42	(0.10)	9.83	(0.02)	10.12	(0.01)	10.25	(0.03)
<b>Methylparaben</b>	8.26	(0.04)	8.36	(0.05)	8.42	(0.05)	8.66	(0.04)	8.89	(0.03)	9.16	(0.08)	9.58	(0.03)	10.00	(0.02)	10.29	(0.02)	10.43	(0.06)
<b>2-Chlorophenol</b>	8.41	(0.01)	8.51	(0.08)	8.58	(0.07)	8.82	(0.04)	9.05	(0.04)	9.32	(0.06)	9.73	(0.02)	10.19	(0.04)	10.48	(0.04)	10.64	(0.08)
<b>3-Chlorophenol</b>	8.95	(0.02)	9.11	(0.02)	9.15	(0.02)	9.35	(0.04)	9.58	(0.04)	9.85	(0.04)	10.19	(0.01)	10.35	(0.05)	10.61	(0.09)	10.80	(0.09)
<b>4-Bromophenol</b>	9.19	(0.02)	9.42	(0.05)	9.46	(0.04)	9.63	(0.02)	9.86	(0.02)	10.03	(0.02)								
<b>Paracetamol</b>	9.52	(0.02)	9.65	(0.01)	9.71	(0.01)	9.83	(0.03)	10.06	(0.03)										
<b>pH of Limiting mobility</b>	11.38		11.36		11.36		11.32		11.31		11.29		11.27		11.27		11.28		11.30	

**Table 12.** Limiting mobility ( $\text{m}^2 \text{V}^{-1} \text{s}^{-1}$ ) of the bases internal standards at studied acetonitrile-water compositions (v/v), at 25 °C and 0 ionic strength.

% ACN (v/v)	0	10	20	30	40	50	60	70	80	90
<b>2-Chlorobenzoic acid</b>	148.40	149.58	148.97	147.6	143.94	141.20	139.26	136.74	136.93	137.93
<b>2,6-Dibromo-4-nitrophenol</b>	148.58	144.38	141.47	138.4	134.87	132.37	131.53	130.97	116.31	101.60
<b>4-Nitrobenzoic acid</b>	152.79	149.91	147.79	146.2	142.47	140.91	140.54	141.45	143.41	137.93
<b>2,6-Dinitrophenol</b>	166.62	160.96	159.89	158.9	154.07	150.85	148.35	149.62	146.70	143.78
<b>3-Bromobenzoic acid</b>	152.14	156.38	152.760	145.3	143.23	143.64	143.37	144.81	146.42	124.48
<b>2,4-Dinitrophenol</b>	163.83	156.60	151.10	148.2	144.18	142.20	140.20	142.29	144.46	151.65
<b>Benzoic acid</b>	164.51	154.14	149.07	148.4	146.03	145.39	142.02	142.89	142.27	146.93
<b>Ibuprofen</b>	113.49	112.86	110.07	110.0	108.69	106.97	102.38	102.86	106.19	102.99
<b>Warfarin</b>	107.41	104.86	101.50	97.1	96.44	95.13	94.36	97.13	100.41	107.68
<b>2,5-Dinitrophenol</b>	161.65	156.57	153.07	145.5	144.97	142.74	140.57	144.38	137.90	136.27
<b>Sulfacetamide</b>	130.86	127.70	125.90	120.5	118.60	114.54	113.54	112.45	113.81	113.07
<b>2,4,6-Tribromophenol</b>	136.25	131.42	131.42	128.5	123.42	121.42	121.01	124.42	124.22	128.45
<b>4-Nitrophenol</b>	161.28	162.87	160.87	159.7	156.74	151.45	150.74	151.74	152.87	154.87
<b>4-Hydroxybenzaldehyde</b>	156.80	144.90	142.08	141.7	141.66	140.64	139.45	137.66	139.43	141.66
<b>Phenobarbital</b>	129.19	121.96	117.05	114.1	113.05	110.23	107.93	107.05	104.45	108.45
<b>3,5-Dichlorophenol</b>	148.61	140.70	139.91	137.6	136.23	133.45	131.71	130.45	123.10	118.96
<b>Methylparaben</b>	138.32	129.61	126.96	126.0	123.10	122.34	120.10	123.10	122.52	121.71
<b>2-Chlorophenol</b>	161.01	152.01	150.90	149.2	148.90	146.90	145.55	147.90	149.01	150.13
<b>3-Chlorophenol</b>	162.23	148.49	147.51	145.6	145.12	147.51	147.01	150.01	152.13	151.44
<b>4-Bromophenol</b>	148.17	140.84	140.09	137.2	137.18	137.00				
<b>Paracetamol</b>	119.90	111.84	110.09	107.2	104.00					

**Table 13.** The  $pK_a$  values with (standard deviations) of the bases internal standards at studied acetonitrile-water compositions (v/v), at 25 °C and 0 ionic strength.

% ACN (v/v)	0 %		10 %		20%		30%		40%		50%		60%		70%		80%		90%	
pH of Limiting mobility	1.94		1.94		2.09		2.11		2.18		2.25		2.32		2.38		2.41		2.50	
Aniline	4.67	(0.02)	4.46	(0.03)	4.27	(0.05)	4.08	(0.02)	3.98	(0.03)										
Quinoline	4.96	(0.05)	4.56	(0.04)	4.42	(0.02)	4.11	(0.05)	4.03	(0.04)										
4- tert -Butylaniline	4.96	(0.04)	4.76	(0.03)	4.49	(0.05)	4.34	(0.02)	4.25	(0.03)	4.20	(0.06)	4.18	(0.07)	4.13	(0.07)				
N,N-Dimethylaniline	5.22	(0.02)	4.88	(0.05)	4.65	(0.10)	4.46	(0.06)	4.40	(0.05)	4.27	(0.04)	4.20	(0.03)	4.15	(0.06)	4.11	(0.04)	4.43	(0.04)
Pyridine	5.31	(0.04)	4.93	(0.05)	4.69	(0.06)	4.52	(0.05)	4.41	(0.05)	4.32	(0.06)	4.31	(0.04)	4.26	(0.07)	4.21	(0.07)	4.53	(0.07)
Acridine	5.58	(0.09)	5.04	(0.05)	4.78	(0.11)	4.47	(0.10)	4.47	(0.05)	4.41	(0.09)	4.30	(0.09)	4.26	(0.07)	4.22	(0.03)	4.54	(0.03)
4-tert-Butylpyridine	6.06	(0.06)	5.60	(0.03)	5.41	(0.11)	5.17	(0.10)	5.01	(0.03)	4.74	(0.11)	4.73	(0.03)	4.67	(0.03)	4.68	(0.04)	5.00	(0.04)
Papaverine	6.42	(0.06)	6.05	(0.02)	5.78	(0.08)	5.54	(0.07)	5.40	(0.02)	5.18	(0.11)	5.16	(0.06)	5.10	(0.05)	5.11	(0.04)	5.43	(0.04)
2,4-Lutidine	6.80	(0.02)	6.44	(0.04)	6.19	(0.03)	5.94	(0.08)	5.78	(0.04)	5.60	(0.02)	5.54	(0.02)	5.48	(0.01)	5.49	(0.01)	5.81	(0.01)
Trazodone	6.82	(0.03)	6.72	(0.06)	6.43	(0.07)	6.23	(0.08)	6.11	(0.06)	5.88	(0.11)	5.80	(0.03)	5.74	(0.07)	5.75	(0.07)	6.07	(0.07)
Pilocarpine	7.06	(0.10)	6.73	(0.06)	6.47	(0.03)	6.16	(0.07)	6.05	(0.06)	5.87	(0.10)	5.78	(0.10)	5.72	(0.07)	5.73	(0.08)	6.05	(0.08)
2,4,6-Trimethylpyridine	7.48	(0.07)	7.11	(0.09)	6.74	(0.05)	6.43	(0.07)	6.28	(0.09)	6.07	(0.10)	6.09	(0.10)	6.06	(0.08)	6.07	(0.08)	6.39	(0.08)
Lidocaine	7.90	(0.04)	7.53	(0.07)	7.24	(0.06)	6.88	(0.05)	6.76	(0.07)	6.37	(0.10)	6.33	(0.10)	6.31	(0.08)	6.32	(0.08)	6.64	(0.08)
Bupivacaine	8.15	(0.03)	7.75	(0.03)	7.40	(0.05)	7.08	(0.06)	6.81	(0.03)	6.39	(0.03)	6.34	(0.03)	6.47	(0.09)	6.48	(0.09)	6.80	(0.09)
1-Phenylpiperazine	8.67	(0.05)	8.56	(0.07)	8.07	(0.06)	7.60	(0.08)	7.38	(0.07)	7.12	(0.11)	6.67	(0.11)	6.64	(0.08)	6.64	(0.15)	6.96	(0.08)
Benzyl dimethylamine	8.95	(0.06)	8.39	(0.08)	8.07	(0.08)	7.61	(0.08)	7.10	(0.08)	6.99	(0.10)	6.82	(0.06)	6.78	(0.08)	6.78	(0.08)	7.10	(0.08)
Diphenhydramine	9.03	(0.05)	8.46	(0.09)	8.34	(0.10)	7.79	(0.06)	7.22	(0.09)	6.98	(0.09)	6.92	(0.06)	6.87	(0.08)	6.88	(0.05)	7.20	(0.08)
Imipramine	9.25	(0.06)	8.92	(0.11)	8.44	(0.06)	8.05	(0.03)	7.64	(0.11)	7.35	(0.11)	7.35	(0.06)	7.29	(0.05)	7.30	(0.09)	7.62	(0.05)
Procainamide	9.30	(0.06)	8.60	(0.07)	8.19	(0.05)	7.81	(0.07)	7.33	(0.07)	7.08	(0.07)	7.04	(0.07)	6.98	(0.09)	6.98	(0.09)	7.30	(0.07)
Propranolol	9.46	(0.04)	8.99	(0.06)	8.48	(0.07)	8.23	(0.06)	7.72	(0.06)	7.51	(0.07)	7.43	(0.09)	7.37	(0.09)	7.37	(0.08)	7.69	(0.09)
1-Aminoethylbenzene	9.50	(0.04)	9.27	(0.06)	8.53	(0.08)	8.41	(0.06)	8.10	(0.06)	7.81	(0.09)	7.75	(0.15)	7.74	(0.04)	7.74	(0.04)	8.06	(0.08)
Ephedrine	9.71	(0.03)	9.20	(0.03)	8.71	(0.06)	8.48	(0.03)	7.95	(0.03)	7.67	(0.03)	7.63	(0.03)	7.58	(0.03)	7.58	(0.03)	7.90	(0.04)
Nortriptyline	10.06	(0.08)	9.35	(0.02)	8.81	(0.08)	8.49	(0.02)	8.11	(0.02)	7.87	(0.05)	7.76	(0.03)	7.76	(0.03)	7.76	(0.08)	8.08	(0.03)

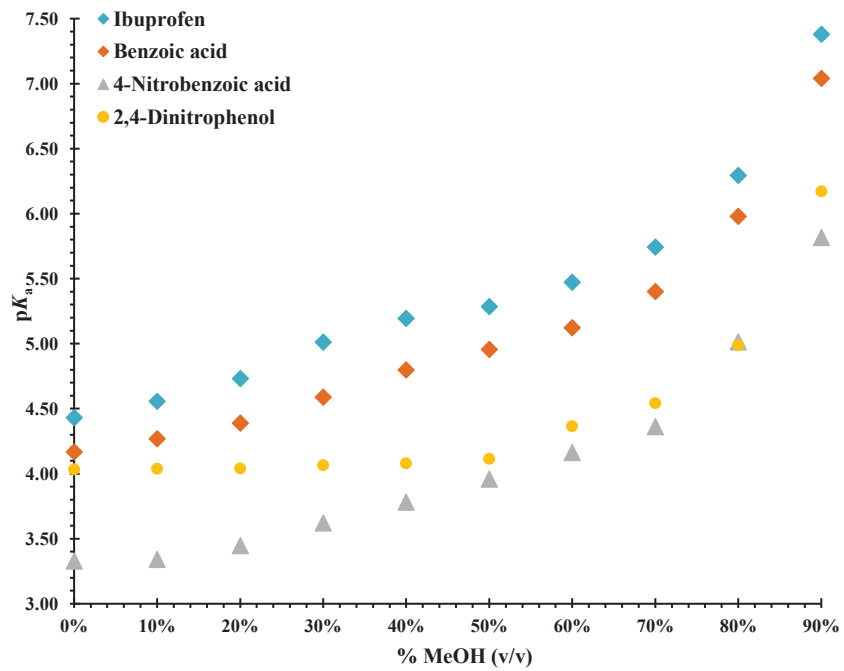
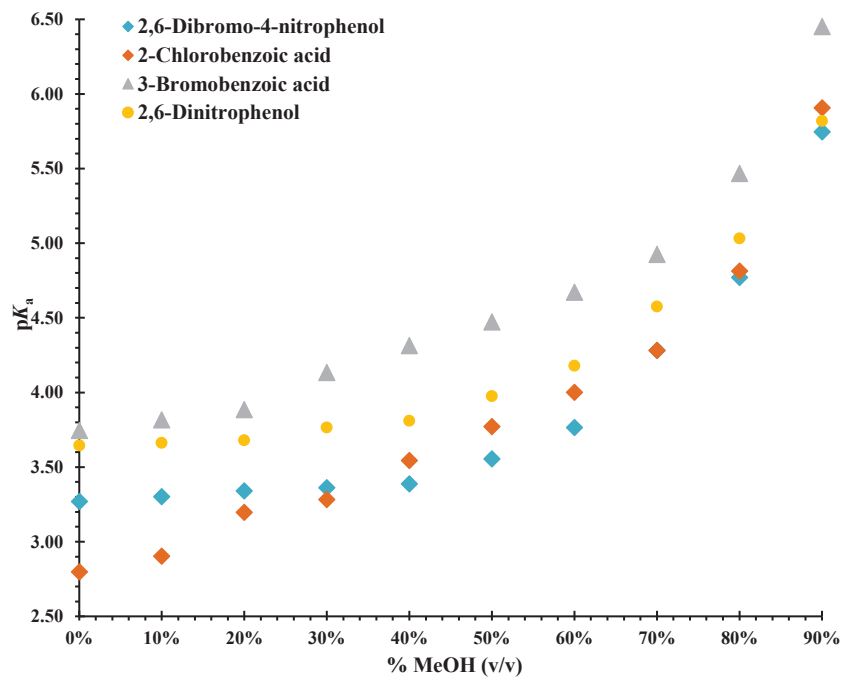
**Table 14.** Limiting mobility ( $\text{m}^2 \text{V}^{-1} \text{s}^{-1}$ ) of the bases internal standards at studied acetonitrile-water compositions (v/v), at 25 °C and 0 ionic strength.

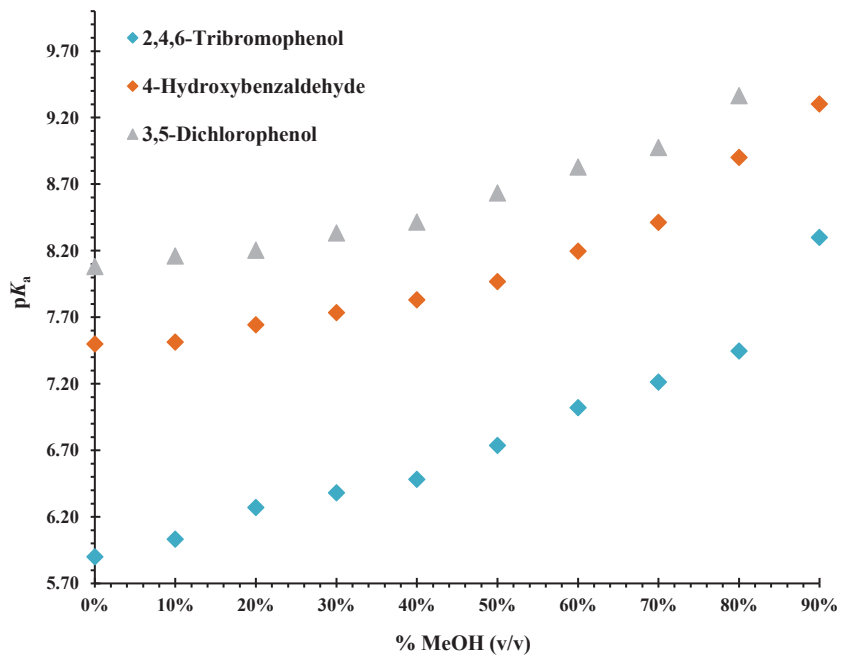
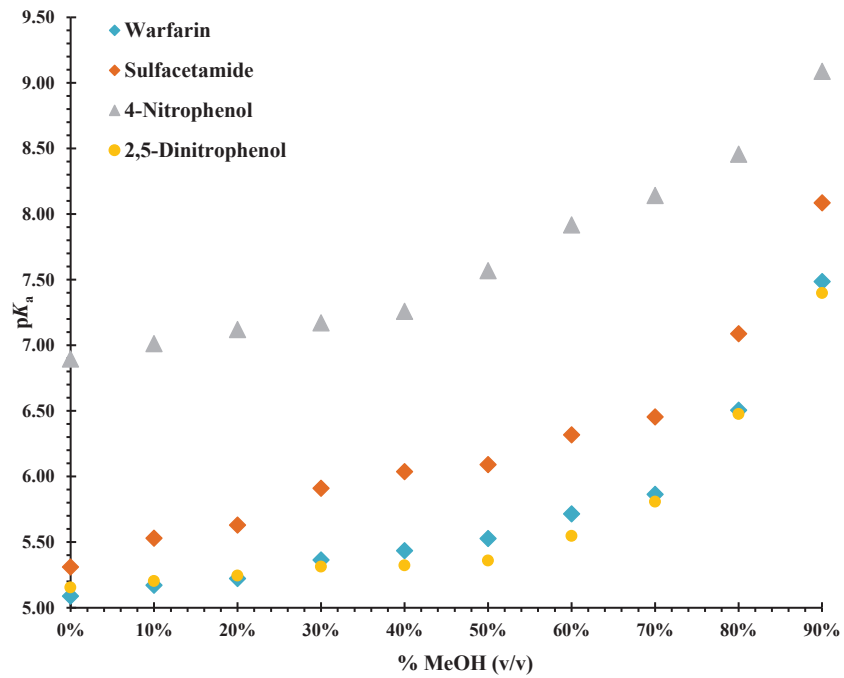
<b>% ACN (v/v)</b>	<b>0%</b>	<b>10%</b>	<b>20%</b>	<b>30%</b>	<b>40%</b>	<b>50%</b>	<b>60%</b>	<b>70%</b>	<b>80%</b>	<b>90%</b>
<b>Aniline</b>	-184.0	-181.57	-190.58	-189.76	-181.57					
<b>Quinoline</b>	-183.2	-186.82	-190.26	-194.25	-191.28					
<b>4-tert-Butylanilin</b>	-136.5	-133.64	-138.21	-139.57	-133.64	-132.04	-133.64	-140.90		
<b>N,N-Dimethylanilin</b>	-170.2	-179.34	-175.71	-175.71	-179.34	-179.34	-173.78	-169.90	-157.44	-159.54
<b>Pyridine</b>	-238.9	-244.09	-248.50	-253.53	-247.05	-244.09	-241.21	-247.37	-232.12	-240.82
<b>Acridine</b>	-148.6	-152.41	-154.60	-162.46	-163.14	-152.41	-151.11	-148.85	-132.98	-132.30
<b>4-tert-Butylpyridine</b>	-158.6	-173.84	-173.97	-182.99	-186.08	-173.84	-172.54	-173.18	-171.83	-175.88
<b>Papaverine</b>	-90.4	-94.24	-97.60	-100.64	-103.40	-98.74	-94.26	-94.46	-94.24	-96.30
<b>2,4-Lutidine</b>	-178.3	-193.10	-196.32	-204.27	-202.14	-193.10	-192.01	-191.01	-193.10	-195.14
<b>Trazodone</b>	-88.4	-90.62	-93.02	-95.80	-96.97	-93.62	-92.55	-90.82	-91.60	-93.34
<b>Pilocarpine</b>	-127.2	-134.62	-140.75	-142.72	-147.16	-134.62	-131.32	-134.50	-134.56	-136.50
<b>2,4,6-Trimethylpyridine</b>	-152.3	-173.79	-170.94	-180.28	-178.15	-173.79	-171.43	-173.20	-171.74	-173.04
<b>Lidocaine</b>	-98.3	-113.61	-114.31	-120.56	-121.80	-118.87	-113.61	-113.43	-113.30	-115.43
<b>Bupivacaine</b>	-86.1	-105.25	-102.58	-108.46	-105.25	-104.30	-104.24	-105.70	-105.25	-106.80
<b>1-Phenylpiperazine</b>	-132.0	-147.75	-133.75	-158.38	-150.76	-148.88	-147.75	-144.08	-147.78	-148.79
<b>Benzyl dimethylamine</b>	-144.5	-168.00	-171.34	-178.63	-169.87	-168.00	-167.22	-166.16	-164.96	-166.62
<b>Diphenhydramine</b>	-100.3	-117.17	-120.51	-123.94	-121.66	-117.17	-115.32	-117.27	-114.27	-119.27
<b>Imipramine</b>	-97.0	-111.05	-112.95	-119.46	-121.73	-118.92	-111.05	-110.19	-110.64	-113.86
<b>Procainamide</b>	-94.0	-145.39	-163.75	-162.18	-150.97	-145.39	-144.84	-143.34	-142.39	-145.84
<b>Propranolol</b>	-90.4	-103.51	-107.62	-106.17	-103.51	-106.10	-104.10	-103.35	-102.55	-104.39
<b>1-Aminoethylbenzene</b>	-132.8	-168.11	-174.39	-173.70	-168.11	-166.54	-165.12	-161.67	-164.55	-168.95
<b>Ephedrine</b>	-113.0	-135.25	-137.01	-136.84	-135.25	-133.16	-132.92	-131.33	-135.25	-136.82
<b>Nortriptyline</b>	-93.1	-110.83	-114.97	-115.06	-110.83	-112.91	-110.83	-108.86	-104.29	-110.53

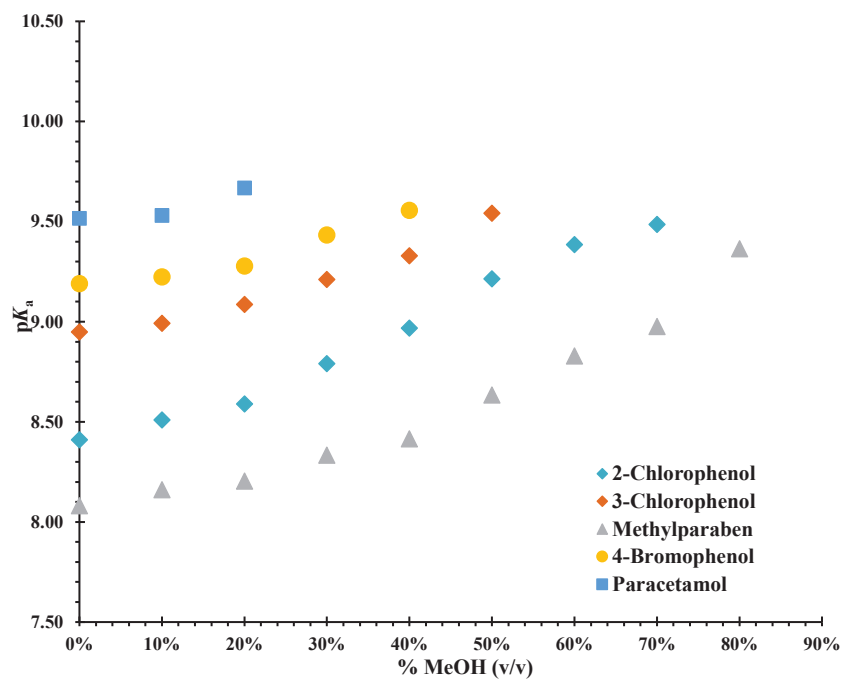
### 3.3.1. Trends in variation of $pK_a$ values of acid ISs with different percentages of methanol

The trend in the  $pK_a$  variation of acids with a change in the concentration of methanol in the solvent is presented in Figure (16). As explained previously, there are three different reasons related to the variation in  $pK_a$  values as the percentage of methanol or acetonitrile increases, namely the dielectric constant, the basicity of the solvent, and specific solvation effects. The addition of methanol or acetonitrile leads to an increase in the basicity of the solvents in the medium up to 80%, and then the basicity starts to decrease due to the lower basicity of the organic solvent in the medium. Also, the addition of methanol or acetonitrile results in a decrease in the dielectric constant, which can affect acid dissociation ( $HA^z$ ) due to the increase in the number of ions in the dissociation process. Thus, the effect of dielectric constant surpasses solvent basicity, resulting in an increase in the  $pK_a$  value of neutral acids.

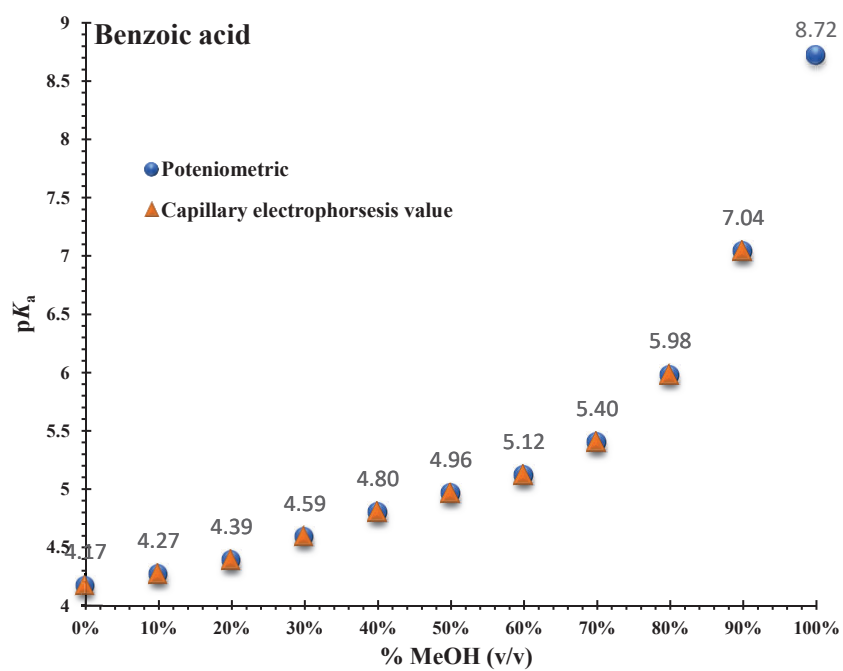
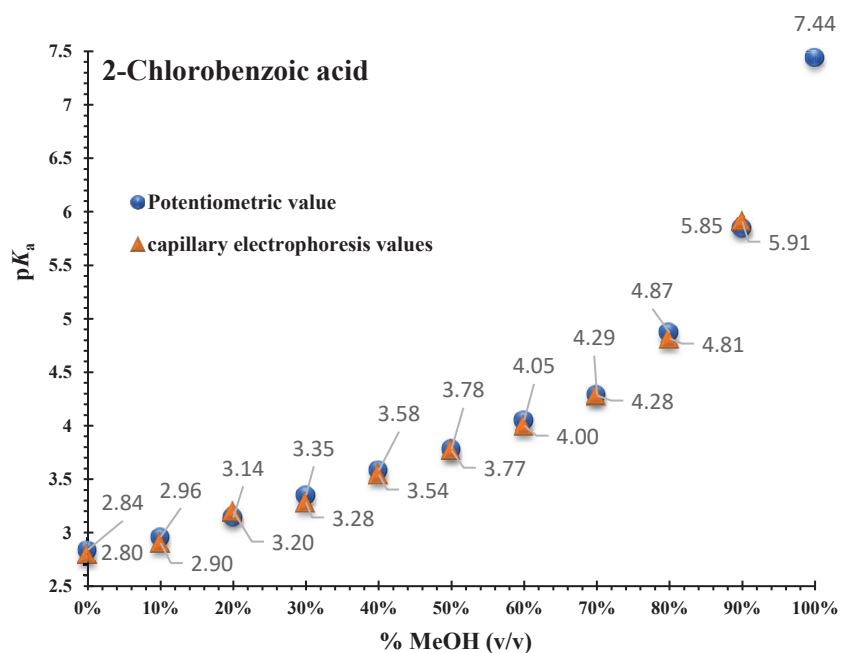
The  $pK_a$  values of neutral acids are significantly affected by increasing methanol concentrations in the methanol-water mixture, with such compounds showing a marked increase in  $pK_a$  value. For 2-chlorobenzoic acid and ibuprofen showed the largest increases in  $pK_a$  value, with increases of 3.11 and 2.95  $pK_a$  units between 0 and 90% MeOH, respectively. The minimum increase was stated for 4-hydroxybenzaldehyde, with a 1.8  $pK_a$  unit increase between 0 and 90% MeOH. The  $pK_a$  value of phenobarbital was 9.39 at 90% MeOH and increased by 1.97  $pK_a$  units between 0 and 90% MeOH, whereas the  $pK_a$  value of 3,5-dichlorophenol was 9.36 at 80% MeOH and increased by 1.28  $pK_a$  units between 0 and 80% MeOH. Methylparaben and 2-chlorophenol could be determined up to 70% MeOH with  $pK_a$  values of 9.20 and 9.49 and a 0.94 and 1.08  $pK_a$  unit increase between 0 and 70% MeOH, respectively. 3-Chlorophenol could be calculated up to 60% MeOH with a  $pK_a$  value of 9.54 and a 0.59  $pK_a$  unit increase between 0 and 60% MeOH. 4-bromophenol could be determined only up to 50% MeOH with a  $pK_a$  value of 9.56 and a 0.37  $pK_a$  unit increase between 0 and 50% MeOH. Paracetamol could be calculated up to 20% MeOH with a  $pK_a$  value of 9.67 and a 0.15  $pK_a$  units increase between 0 and 20% MeOH. The highest methanol percentage at which the  $pK_a$  value could be calculated for other acidic compounds varied according to the particular properties of the compound.







**Figure 16.** Trends in variation of  $pK_a$  values of neutral acids from 0-90 % methanol.



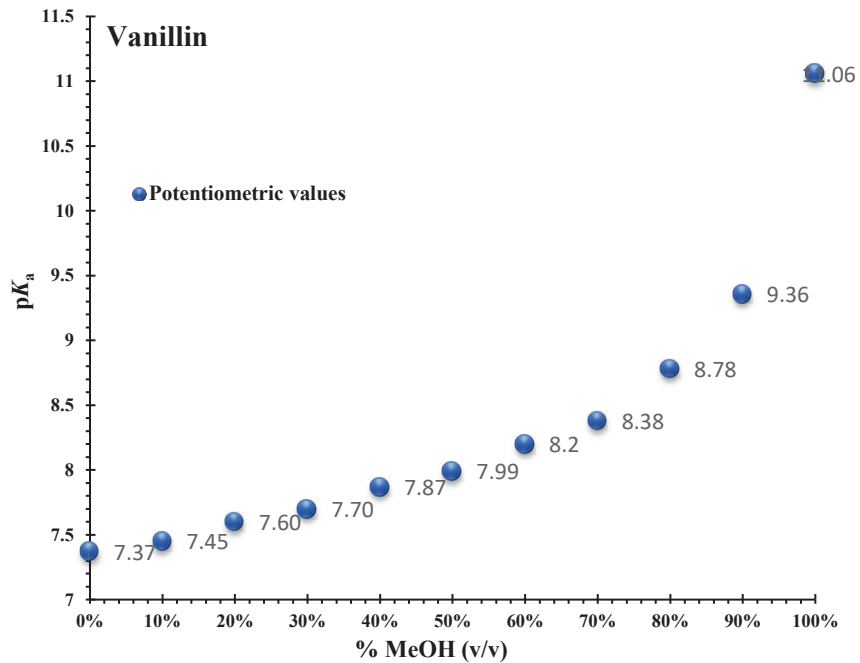


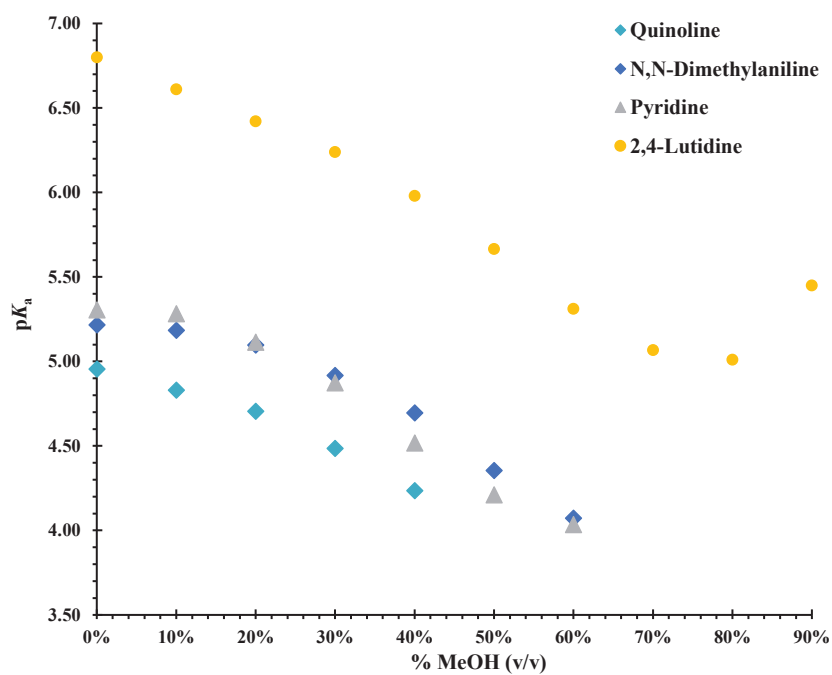
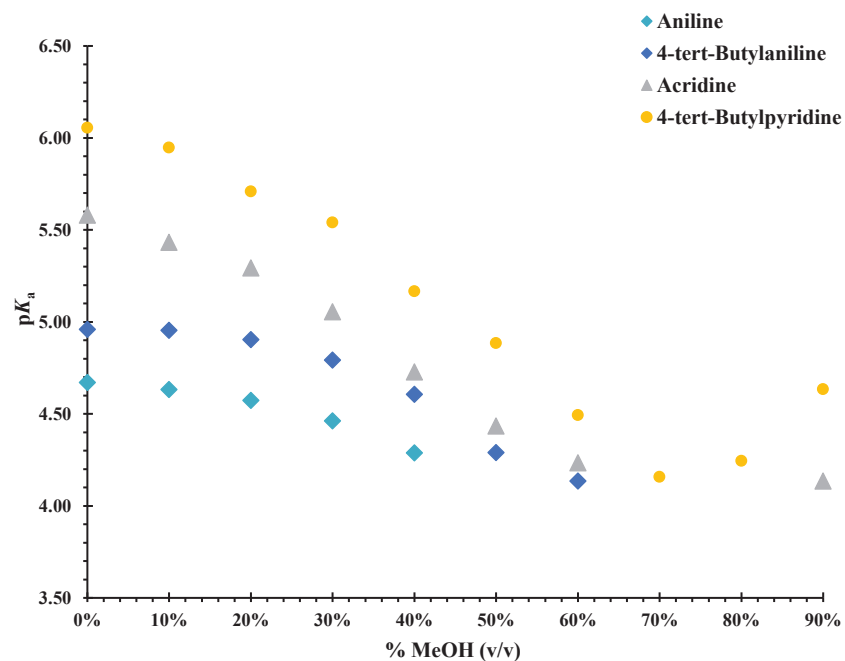
**Figure 17.** Variation of the pK<sub>a</sub> values of the reference neutral acids at different methanol percentages. ● potentiometric values, ▲ capillary electrophoresis values at different methanol-water mixture (0 -90 %).

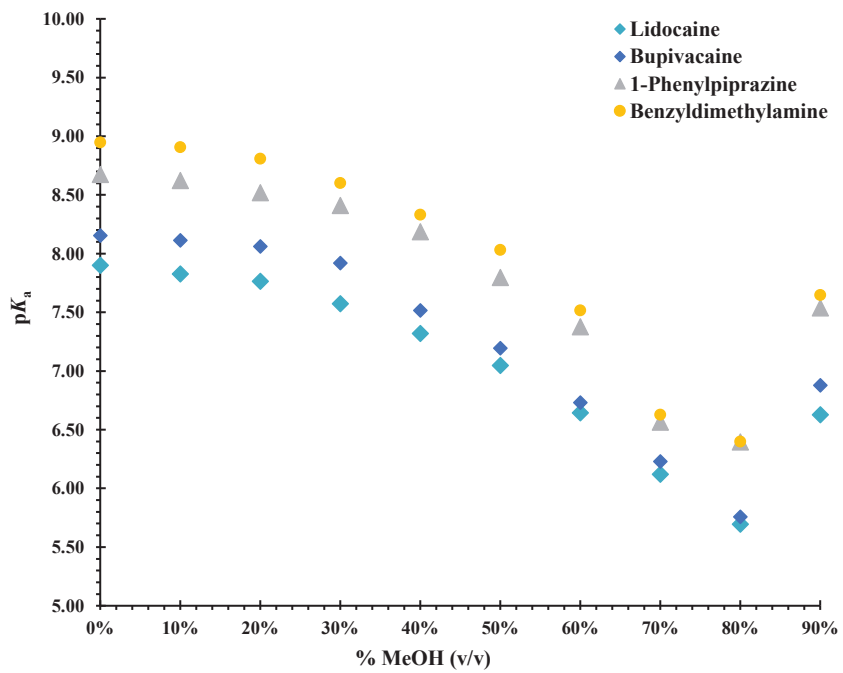
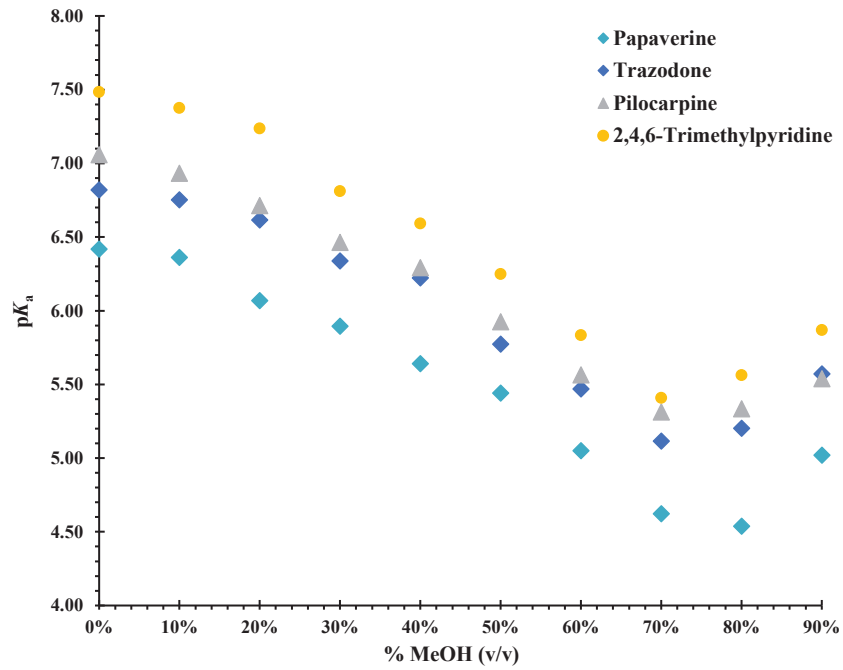
### 3.3.2. Trends in variation of $pK_a$ values of bases ISs with different percentages of methanol

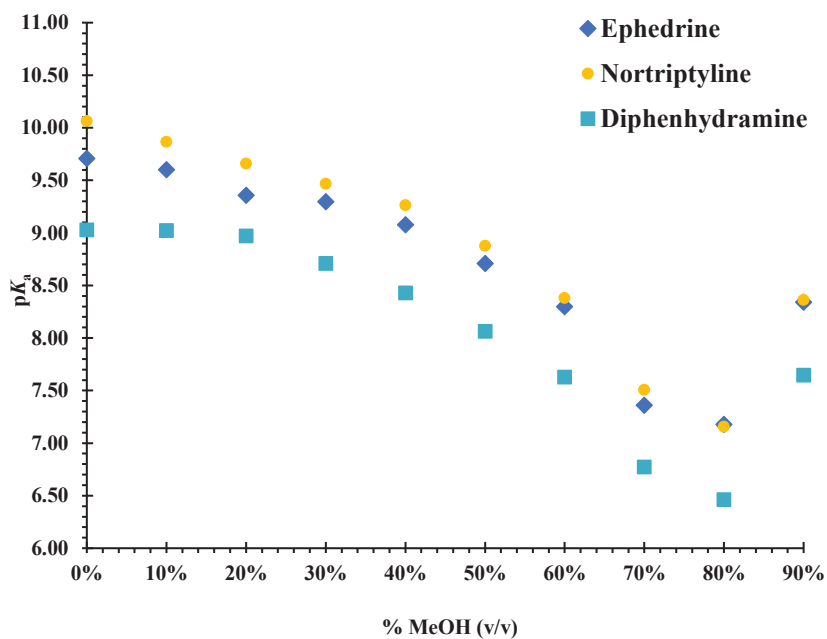
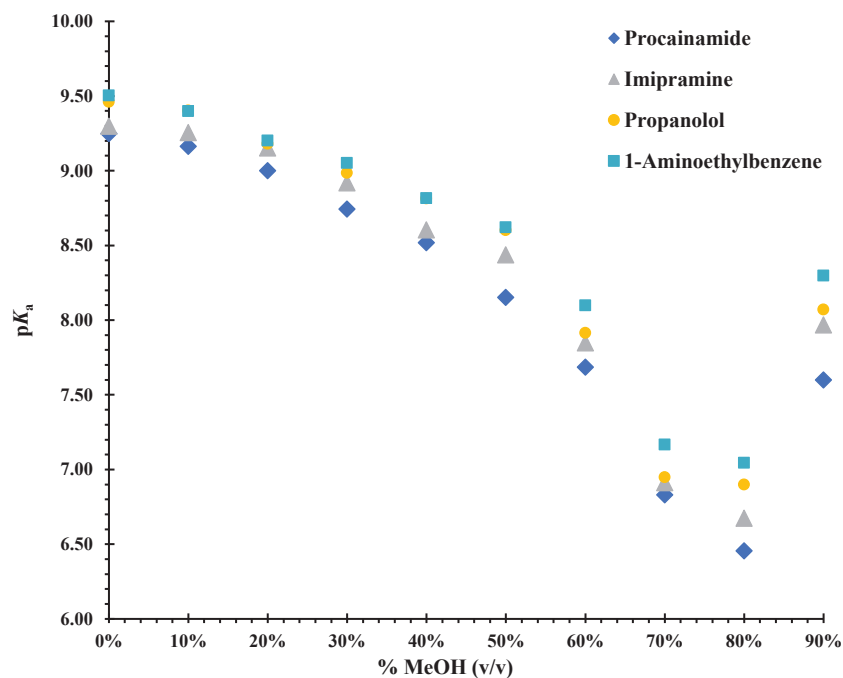
Neutral bases decrease the  $pK_a$  of their conjugated acids with the increase in the methanol percentage up to 80% because of the effect of the increase in the basicity of the solvent, which then causes the  $pK_a$  to increase up to 90% due to the less basicity of the methanol in the medium or the possible specific solvation effect. While the decrease in the dielectric constant has no effect on the dissociation of the bases because there is no variation in the number of ion<sup>30,33-35</sup>.

The decrease for aniline and quinoline from 0.38 to 0.72  $pK_a$  units, between 0 and 40% MeOH, for 4-*tert*-butylanilin, *N,N*-dimethylaniline, pyridine, and acridine decreased from 0.83 to 1.44  $pK_a$  units difference between 0 and 60% MeOH. Acridine has 1.44  $pK_a$  units difference between 0 and 90% MeOH because the difference between the  $pK_a$  of acridine and pH of the buffer is more than 1.7 units. The  $pK_a$  values for the remaining basic compounds dropped from 1.62 to 2.79  $pK_a$  units difference between 0 and 80 % MeOH and they give 1.14 to 1.62  $pK_a$  units difference between 0 and 90% showing a more significant impact of the MeOH-water solvent mixture on the ionization of these compounds. The trend in the  $pK_a$  of the bases with a variation in the proportion of methanol is shown in Figure (18).

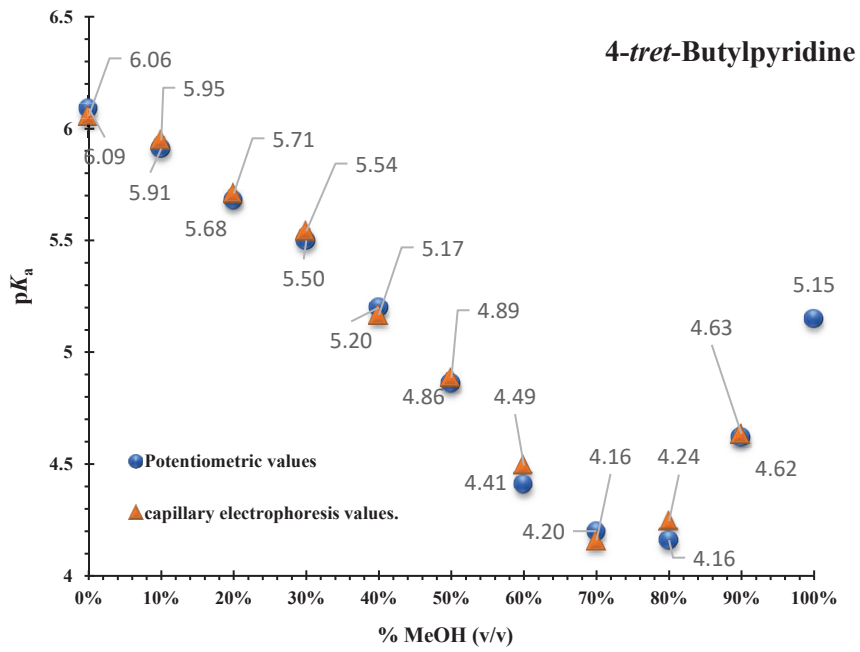
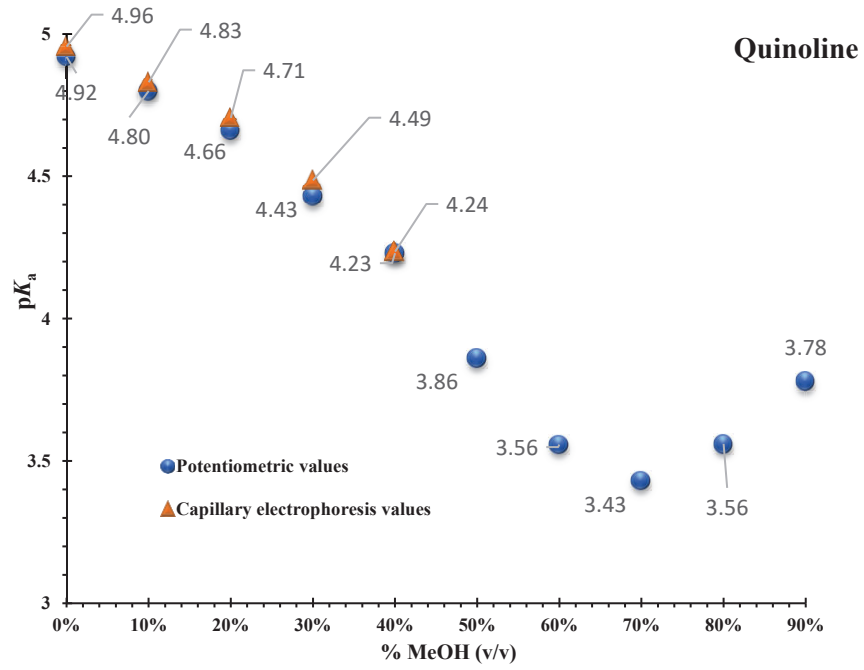
According to the data I presented, the influence of the MeOH-water solvent mixture on the ionization of the basic compounds of study is relatively negligible up to 40% MeOH but becomes more significant at higher MeOH concentrations. When the amount of MeOH in the solvent mixture rises, up to 80% MeOH, the  $pK_a$  values of base compounds decrease. Nevertheless, the  $pK_a$  values start increasing once more at 90% MeOH. As a results of the increased basicity of the methanol-water mixture in comparison with water, the  $pK_a$  values of protonated bases decreased with an increase in methanol concentration and the subsequent formation of the methanol-water mixture (at a low mole fraction of methanol). For the higher methanol concentration, the protonated bases are mostly solvated by the less basic methanol, and the  $pK_a$  value increases with methanol concentration up to values slightly higher than the  $pK_a$  in water<sup>34</sup>.

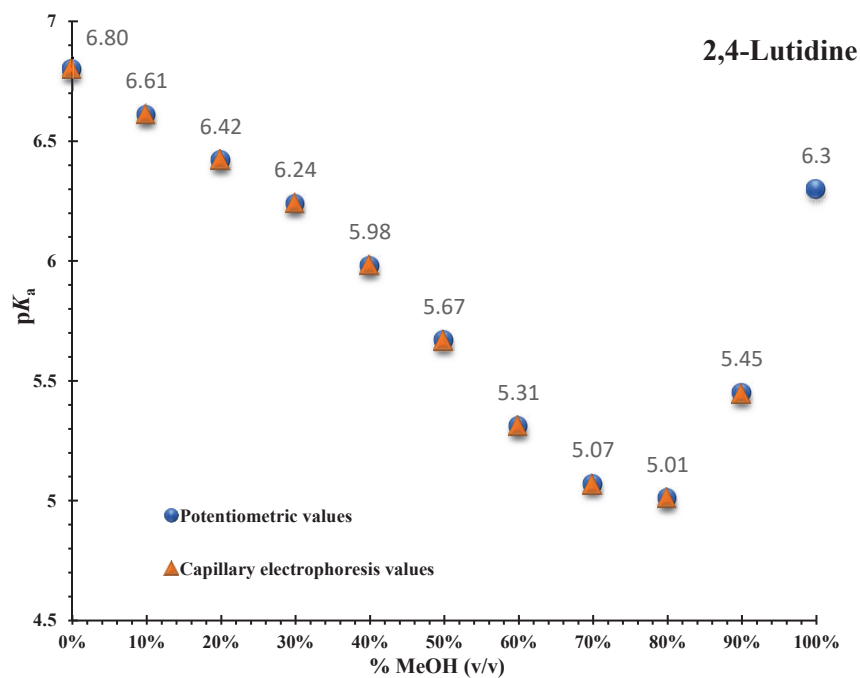






**Figure 18.** Trends in variation of  $pK_a$  values of neutral bases from 0-90 % methanol.

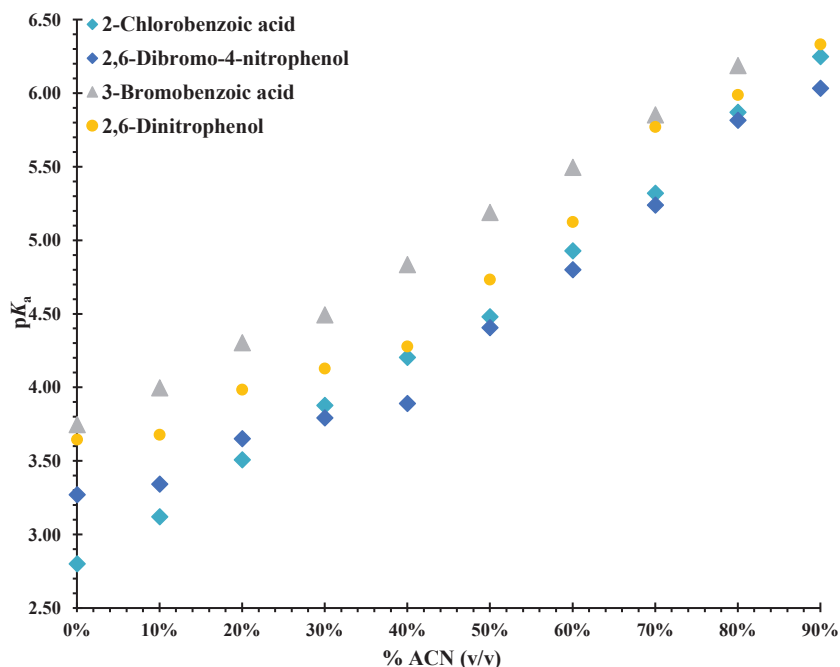


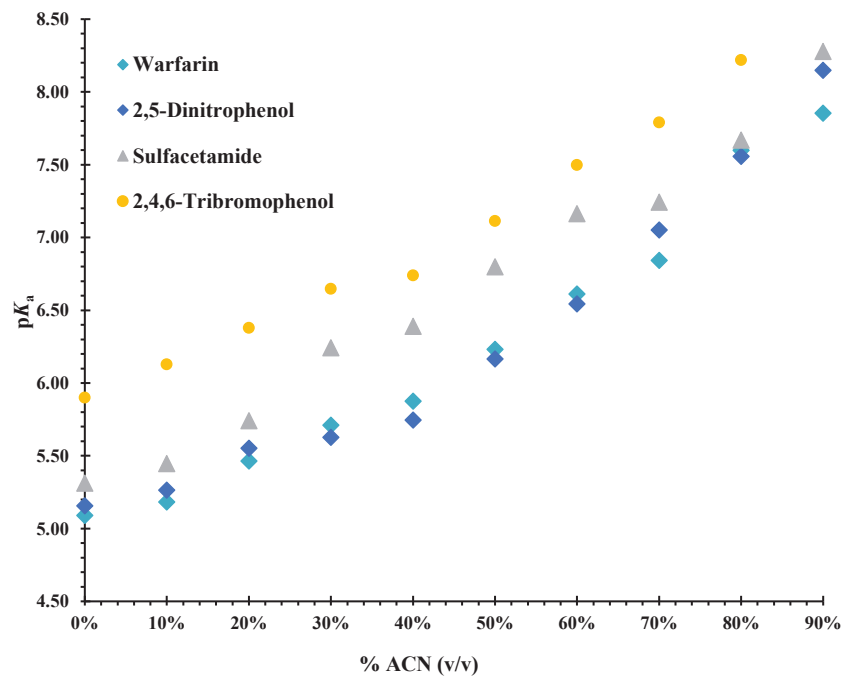
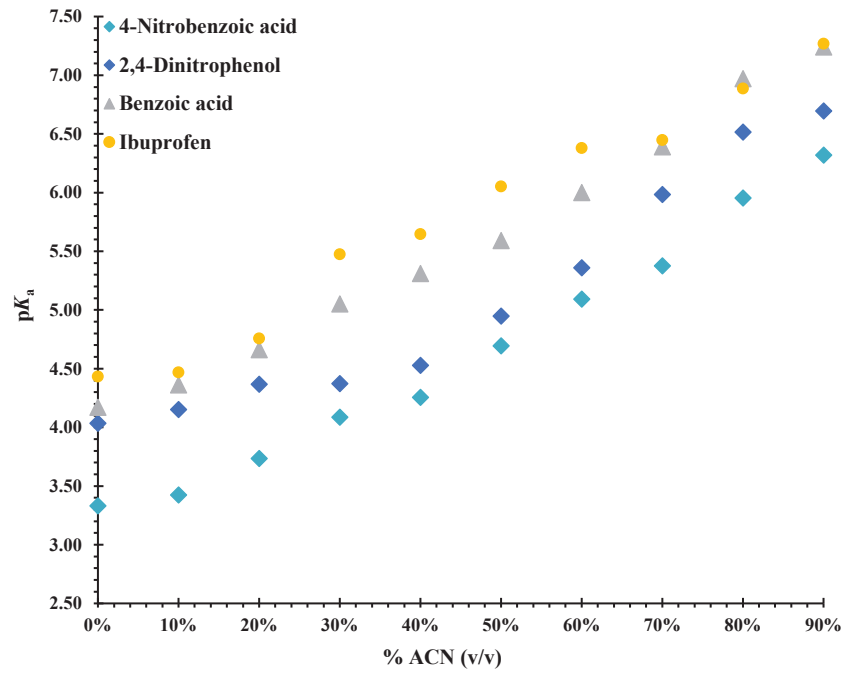


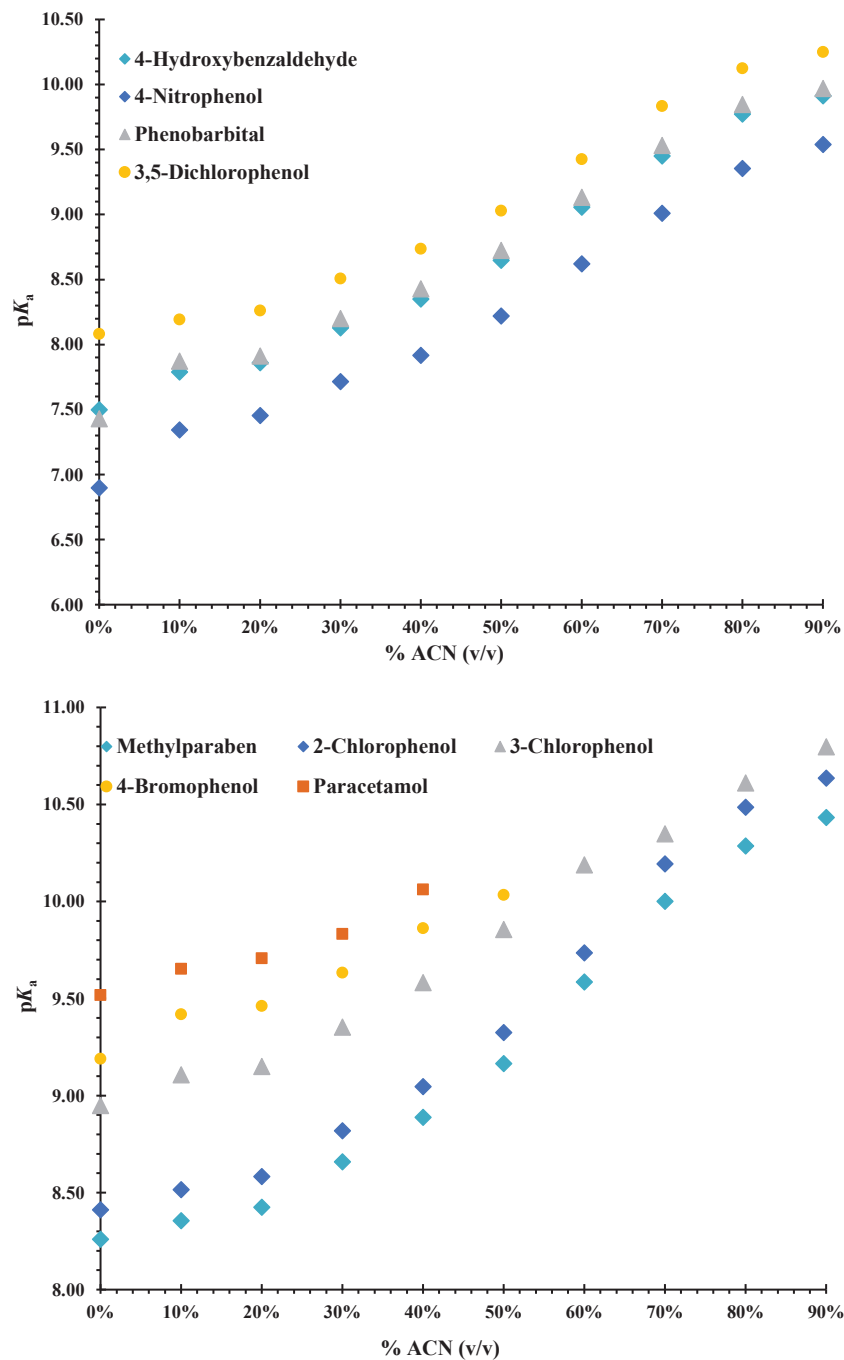
**Figure 19.** Variation of the pK<sub>a</sub> values of the conjugated cationic acids of the neutral bases at different methanol percentages. ● potentiometric values, ▲ capillary electrophoresis values at different methanol-water mixture (0 -90 %).

### 3.3.3. Trends in variation of $pK_a$ values of acids ISs with different percentages of acetonitrile

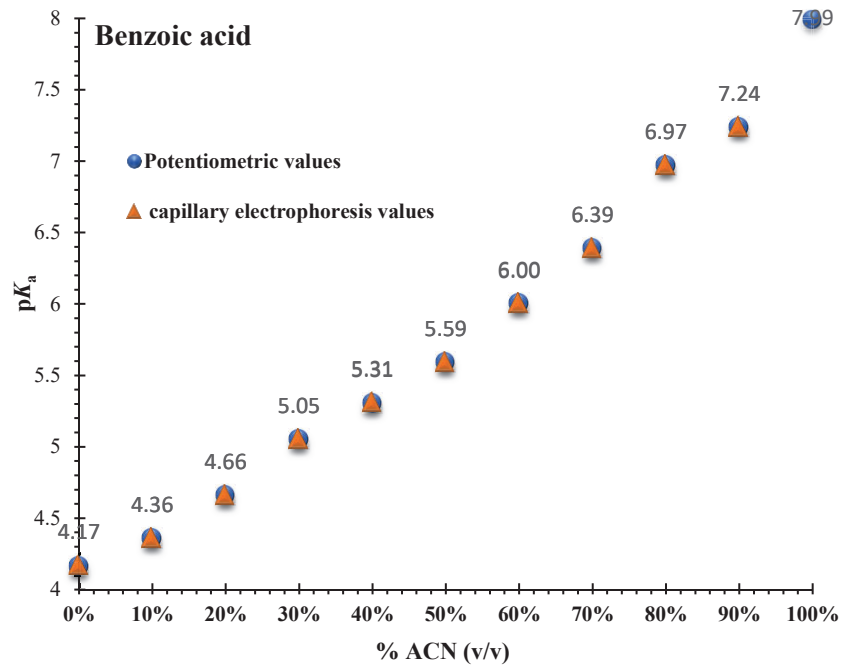
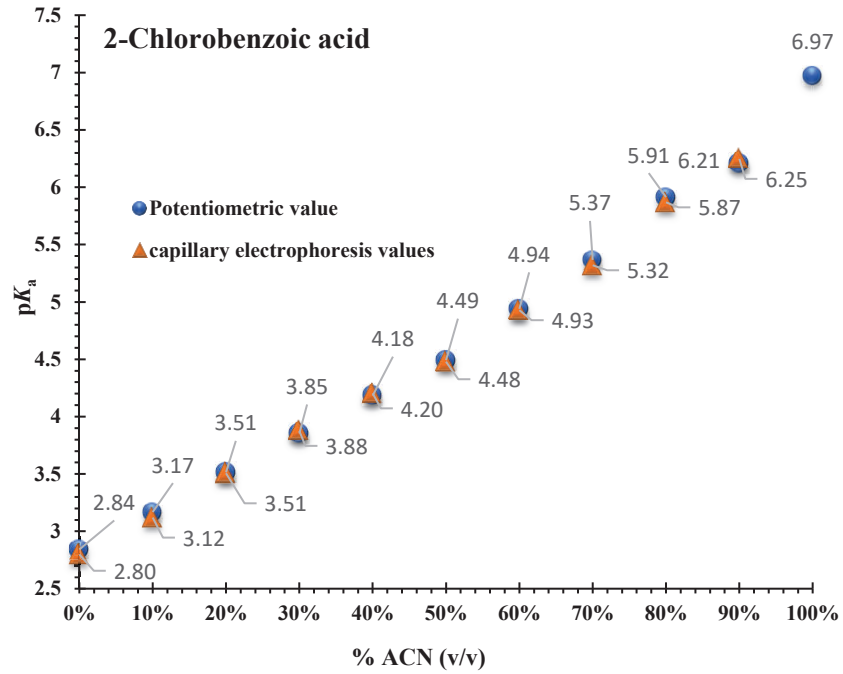
Similar criteria that were used for methanol must be used for acetonitrile, and the same reasons for increasing the  $pK_a$  of acids at the different acetonitrile concentration were explained previously. The trend in the  $pK_a$  variation of acids with a change in the concentration of acetonitrile in the mixture is presented in Figure (20). The  $pK_a$  values of neutral acids are changed by increasing acetonitrile concentrations in the acetonitrile-water mixture, with such compounds indicating an observed increase in  $pK_a$  value. The internal standards 2-chlorobenzoic acid and benzoic acid displayed the largest increases in  $pK_a$  values, with increases of 3.45 and 3.07  $pK_a$  units different between 0 and 90% ACN. The minimum increase was stated for 3-chlorophenol, with a 1.85  $pK_a$  unit difference increases between 0 and 90% ACN. The remaining  $pK_a$  acids can be calculated up to 90% ACN with a 2.17 to 2.99  $pK_a$  units difference between 0 and 90 % ACN, except 4-bromophenol, which can be calculated to 50% with a  $pK_a$  value of 10.03, 0.85  $pK_a$  units between 0 and 50% ACN. Another compound is paracetamol, which can be calculated up to 40% ACN with a  $pK_a$  value of 10.06, 0.55  $pK_a$  units between 0 and 40% ACN.

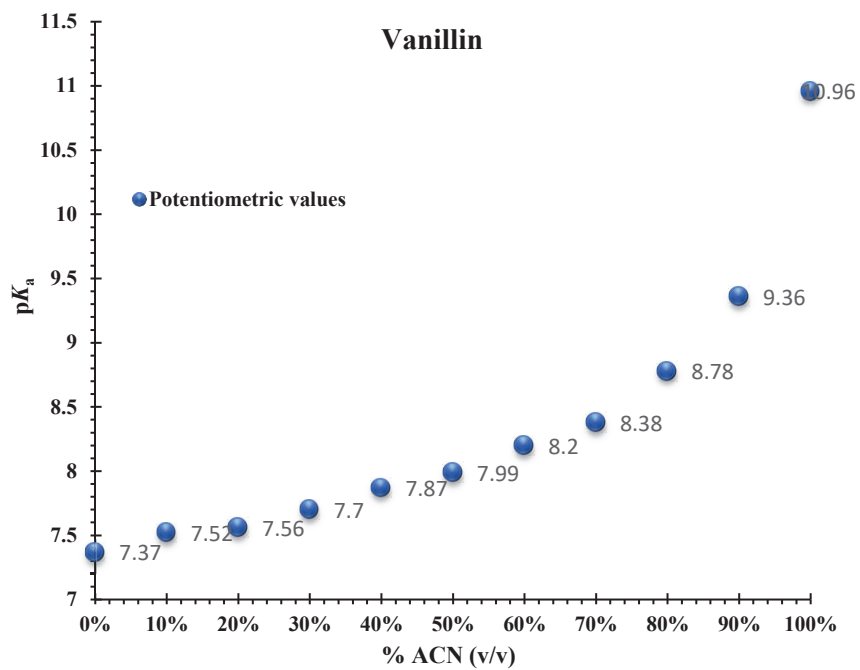






**Figure 20.** Trends in variation of  $pK_a$  values of neutral acids from 0-90 % acetonitrile.

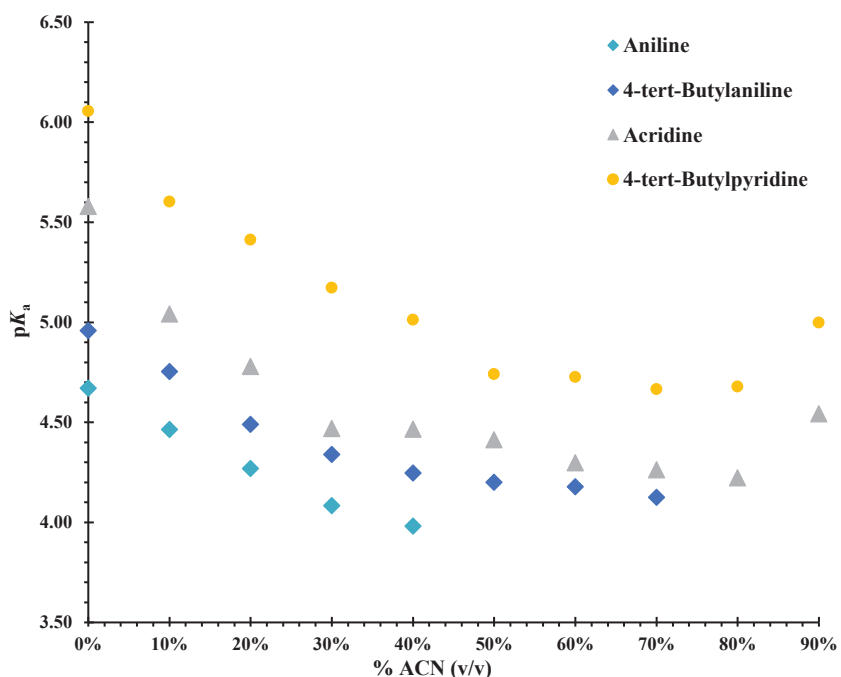


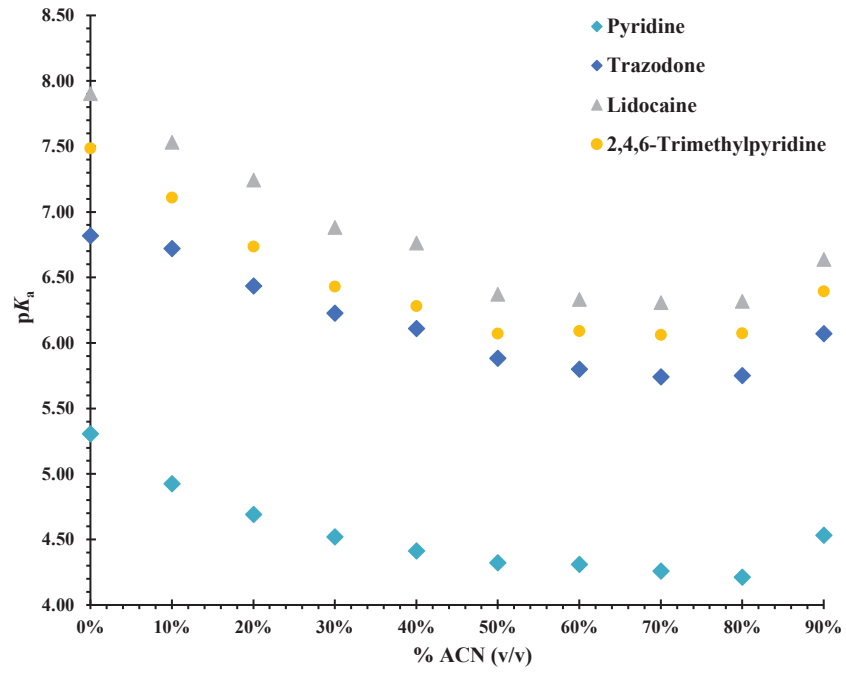
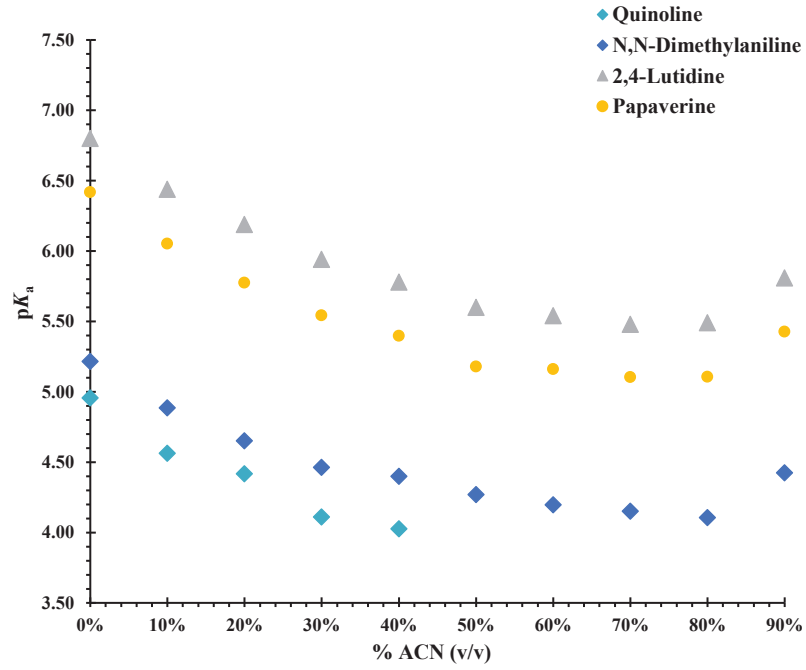


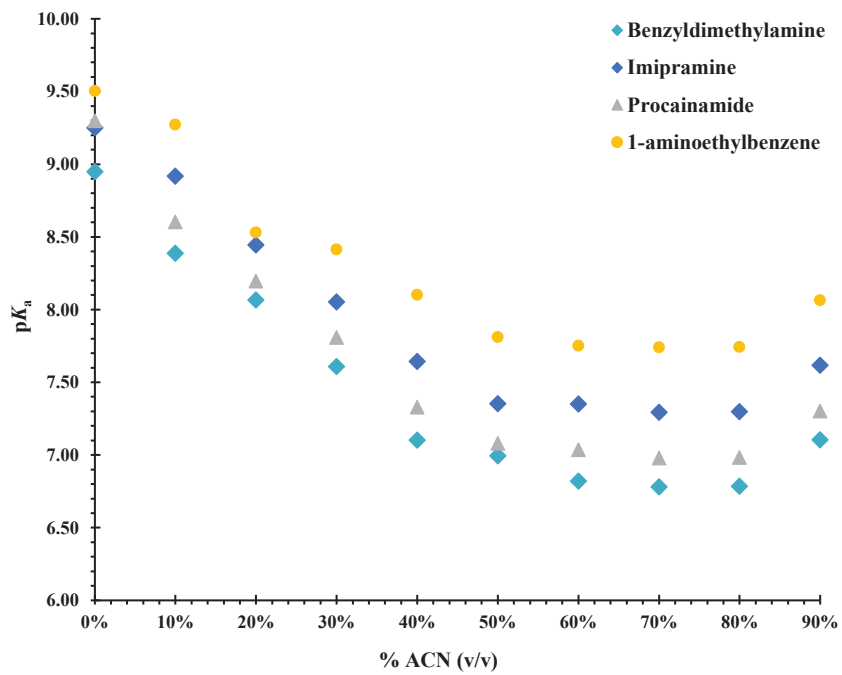
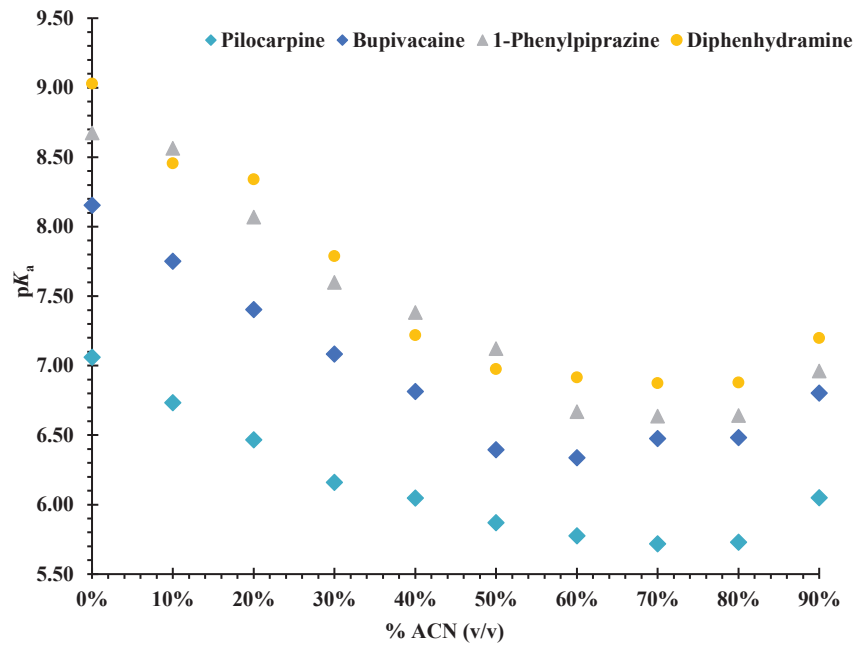
**Figure 21.** Variation of the  $pK_a$  values of the reference neutral acids at different acetonitrile percentages. ● potentiometric values, ▲ capillary electrophoresis values at different methanol-water mixture (0 -90 %).

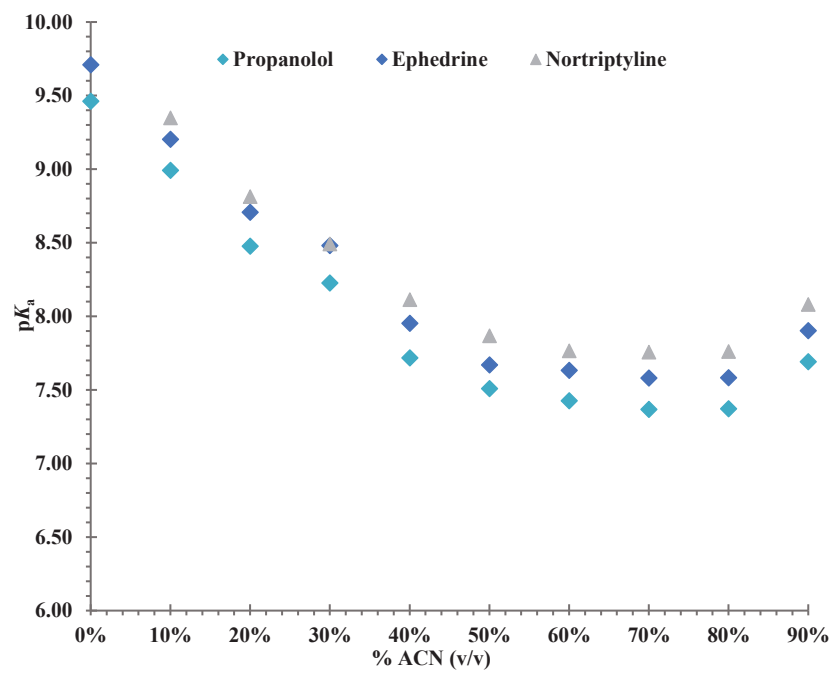
### 3.3.4. Trends in variation of $pK_a$ values of bases ISs with different percentages of acetonitrile

As in methanol, the same criteria and reasons were applied for decreasing the  $pK_a$  of the bases. The trend in the  $pK_a$  variation of bases with a change in the concentration of acetonitrile in the mixture is presented in Figure (22). Neutral bases decrease the  $pK_a$  of their conjugated acids with the increase in the acetonitrile percentage because of the effect of the increase in the basicity of the solvent up to 80 % acetonitrile and then started to increase up to 90% acetonitrile due to the lower basicity of the solvent. The decrease for aniline and quinoline from 0.69 to 0.93  $pK_a$  units difference between 0 and 40% ACN, and for 4-tert-butylanilin decreased from 0.83  $pK_a$  units difference between 0 and 70% ACN. The  $pK_a$  values for the remaining basic compounds dropped from 1.11 to 2.30  $pK_a$  units difference between 0 and 80% ACN and started to increase to give 0.79 to 1.98  $pK_a$  units difference between 0 and 90%, showing a more significant impact of the ACN-water solvent mixture on the ionization of these compounds.

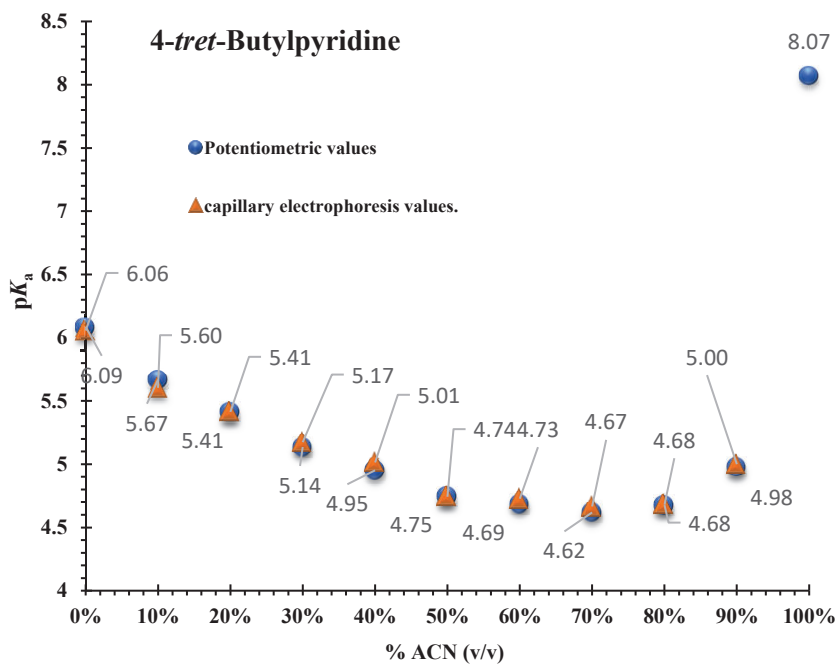
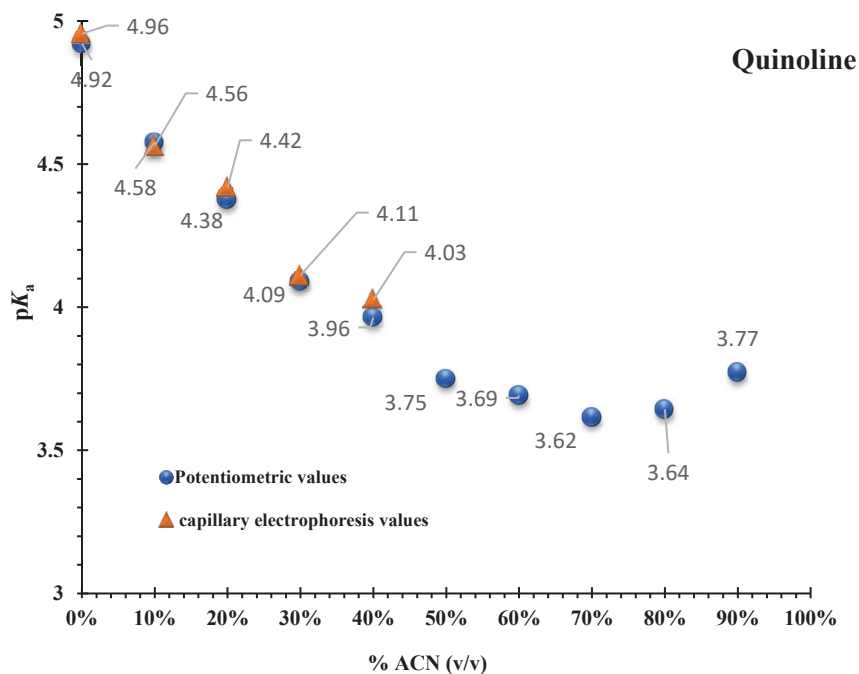








**Figure 22.** Trends in variation of  $pK_a$  values of neutral bases from 0-90 % acetonitrile.



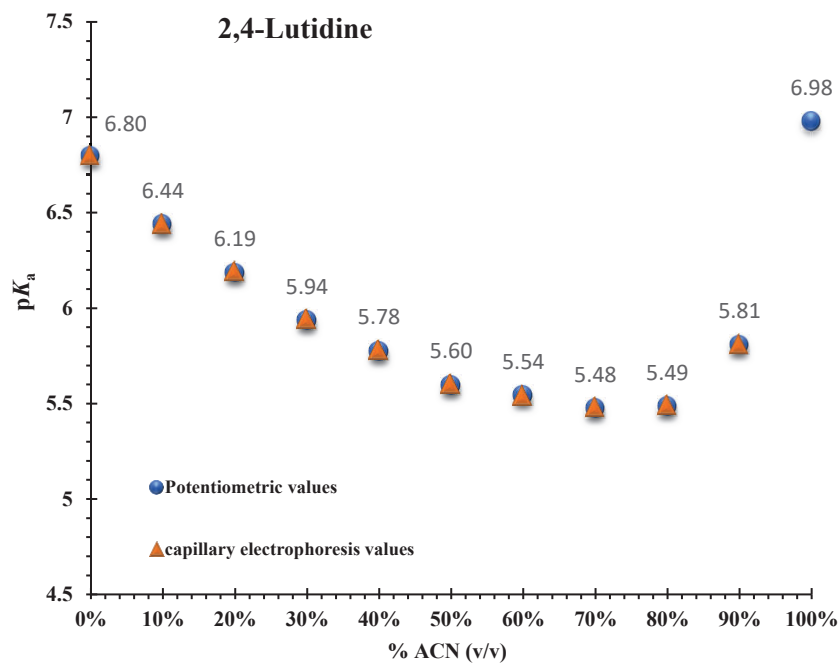


**Figure 23.** Variation of the  $pK_a$  values of the reference conjugated cationic acids of the neutral bases at different acetonitrile percentage. ● potentiometric values, ▲ capillary electrophoresis values at different methanol-water mixture (0 -90 %).

### 3.4. Determination of the aqueous $pK_a$ of very insoluble drugs by capillary electrophoresis: Internal standards for methanol-water extrapolation

Recent drug development frequently results in very lipophilic and sparsely soluble compounds, making it challenging to determine their acidity constant. Analytical methods as potentiometry and spectrophotometry can be used to determine the  $pK_a$  of these insoluble compounds, which can then be extrapolated to 0% organic solvent using the  $pK_a$  values obtained in mixed solvents, where they are soluble<sup>30,34,149,156</sup>.

In this study, the set of internal standards that have been described in the previous section have been used to determine the aqueous  $pK_a$  of these insoluble drugs. The effectiveness of the method to determine the acidity constant of very low soluble drugs (solubility below  $10^{-6}$  mol  $L^{-1}$ ) was evaluated in reference to the results from the literature obtained by other methods. The test compounds desired for the estimation of the effectiveness of the IS-CE technique in hydro-organic mixtures involve 7 compounds, most of them commercially existing drugs, as shown in Figure (24). These drugs (3 acids and 4 bases) were chosen because their insolubility in water makes it impossible to implement an aqueous IS-CE determination<sup>26,157-159</sup>. The test compounds as well as the logarithmic form of their intrinsic solubility ( $\log S_{(lit)}$ ,  $S$  in mol  $L^{-1}$ ) were presented in Table (16). These solubility values were collected from several sources or predicted through ACD/Percepta software when experimental data was not available in literature<sup>26,157-159</sup>. The compounds are listed in decreasing order of solubility, from mefenamic acid with  $\log S$  of  $-6.34$  to amiodarone with  $\log S$  of  $-8.17$ . The  $pK_a$  values of the drugs were established at different proportions of methanol (10, 20, 30, and 40% v/v) as shown in Table (16). The limiting mobilities ( $m^2 V^{-1} s^{-1}$ ) of insoluble drugs were presented in Table (17). As an instance, the two electropherograms at 20% MeOH at pH 5.0 (partially ionized) and pH 9.5 (totally ionized) are shown in Figure (25). Calculating the mobilities for TC (glyburide) and IS (2,5-dinitrophenol) at these 2 pH values, the  $pK_a$  at 20% MeOH of glyburide was determined by means of Eq (28). The  $pK_a$  value at 0% MeOH was determined by extrapolation. Table (18) also shows the extrapolation to 0% obtained by using the Yasuda-Shedlovsky equation, and the

fitting parameters of the regression curve.  $\epsilon$  values were calculated as specified in bibliography<sup>30,37</sup>. The equation of Yasud-Sheldovsky was selected for two reasons: it is a linear equation that involves less input data, and it is a universal equation for any experimental method used for aqueous  $pK_a$  extrapolation. Figure (26) presented Yasuda-Shedlovsky plots for the studied insoluble drugs as well as the values of Debye-Hückel parameters,  $\delta$  values, and some other relevant macroscopic parameters at different methanol-water mixtures are stated in Table(15). The aqueous  $pK_a$  values determined by the IS-CE method were compared to those gotten from the other approaches except for sertaconazole, which was not found in any reliable source, so comparison is not possible. As explained previously, increasing methanol concentrations in the medium results in an increase in the  $pK_a$  values of the acid and a decrease in the  $pK_a$  values for the bases.

In conclusion, the literature analysis shows that potentiometry, spectrophotometry, and the classic CE method require co-solvent and extrapolation methods in water for drug  $pK_a$  estimation on at solubility levels, except CE-MS due to its high sensitivity, which allows direct determination in aqueous buffers at very low concentration levels, but CE-MS is a less common and more expensive and complex technique. The IS-CE method provides good agreement with literature results, although there is an important difference in the percentage of methanol required to complete the determinations. The IS-CE method used methanol in the range of 10-40% in buffers, while potentiometric titrations, spectrophotometric titrations, and the classic CE method used methanol in the range of 40-70% for the same compounds. One of the reasons why the IS-CE allows the use of lower methanol content compared to other methods is because low concentration of sample is needed (5–100 mg L<sup>-1</sup> is enough). At these concentrations, detection using diode-array spectrophotometric detector can be performed correctly. The use of DMSO, appropriate MeOH/H<sub>2</sub>O mixtures, and reported strategies to increase solubility is enough to solubilize the TCs at concentration of 100 mg L<sup>-1</sup>. In summary, solubility can be enhanced by previous ionization using a suitable amount of HCl or NaOH, allowing for effective mobility measurement to be carried out at a new pH closer to the ionic form of the compound that predominates. This adjustment results in a higher ionization of the drugs. Since only a small amount of the analyte is injected into the capillary, it tends to be able to prevent precipitation by pre-ionizing and solubilizing the analyte, even when the pH and surrounding medium inside the capillary change.

The IS-CE method is fast, accurate, and low-cost in solvent mixtures; likewise, the pH of the buffer solution can be directly calculated inside the capillary in each determination by means of the IS, obtaining the pH of the solution immediately. Unlike other methods like potentiometry, spectrophotometry, and the classical CE, which require calibrations or corrections. The IS-CE method avoids approximations and tedious pH-meter calibrations, resulting in faster and more accurate  $pK_a$  values.

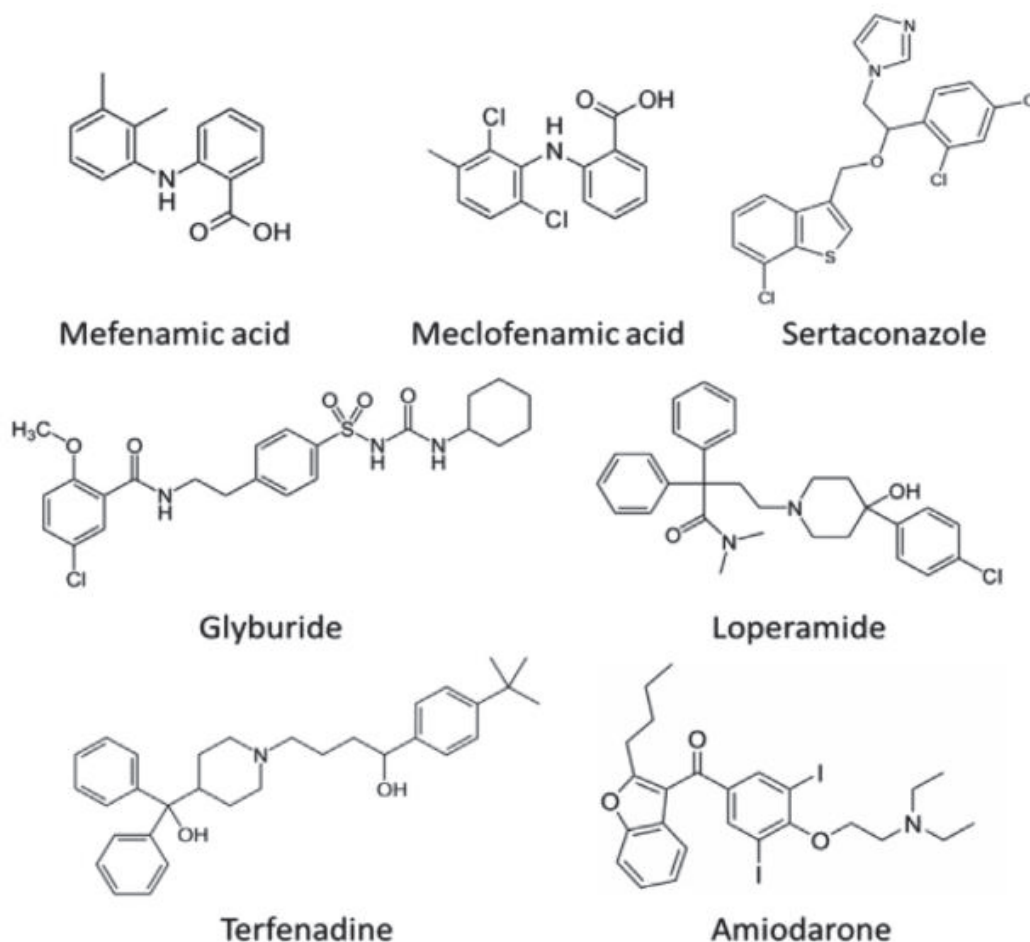


**Figure 24.** chemical structure of the set of highly insoluble drugs.

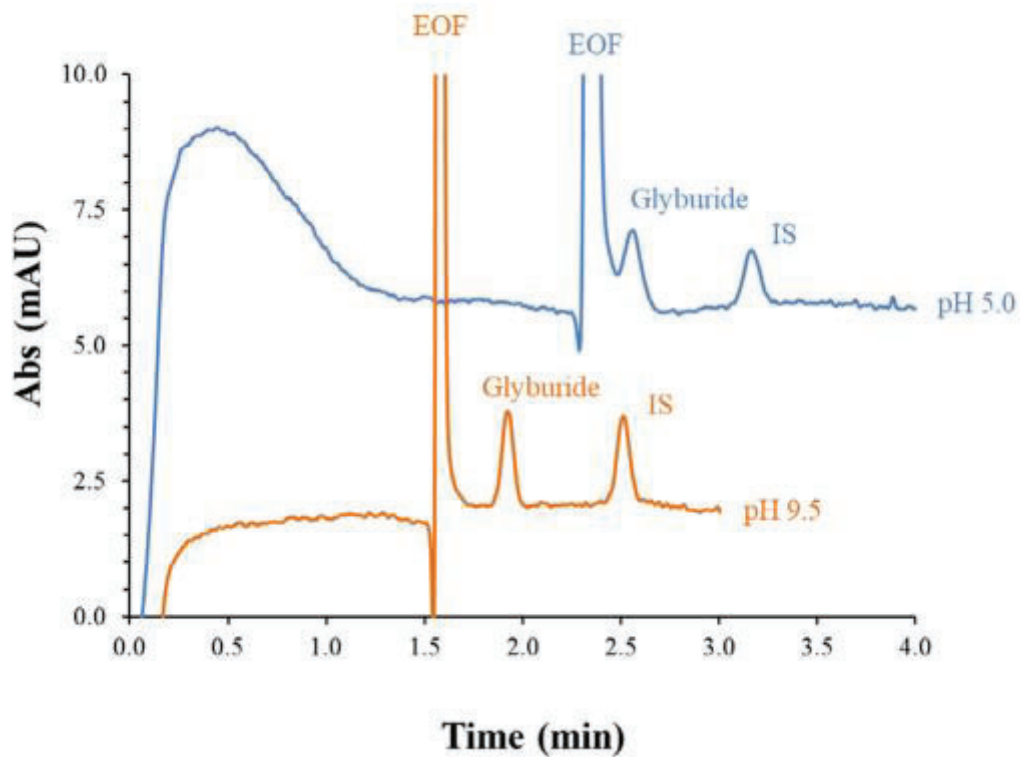


**Figure 25.** Electropherograms at 20% MeOH for glyburide (TC) and 2,5-dinitrophenol (IS) at pH 5.0 (in blue) for the determination of the effective mobilities and at pH 9.5 for the mobilities of the ionized species. EOF: Electroosmotic flow.

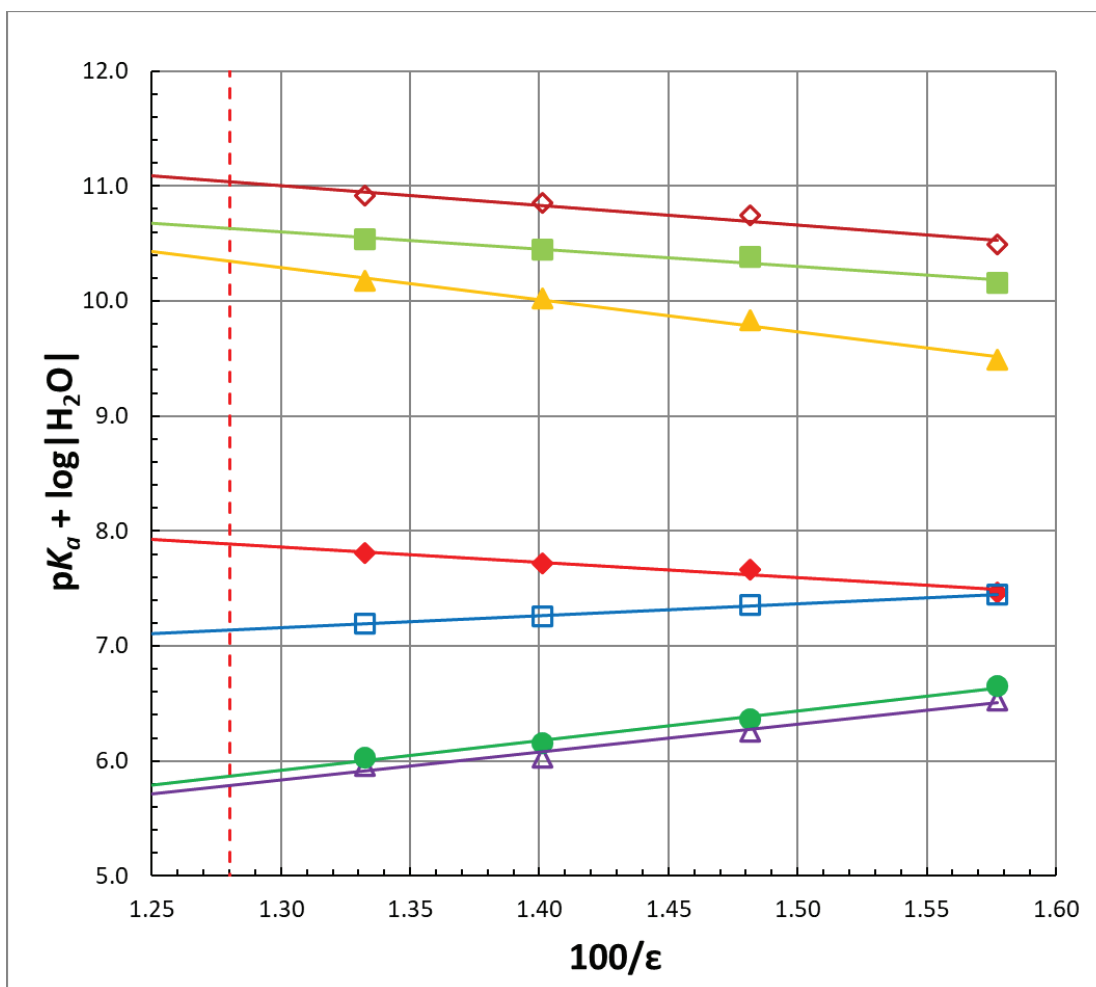


**Figure 26.** Yasuda-Shedlovsky plots for the water insoluble drugs studied by the IS-CE method in methanol-water mixtures. Symbols:  $\Delta$  Meclofenamic acid,  $\bullet$  Mefenamic acid,  $\square$  Glyburide,  $\blacklozenge$  Sertaconazole,  $\blacktriangle$  Amiodarone,  $\blacksquare$  Loperamide,  $\blacklozenge$  Terfenadine. Dashed red line: cutting point for the dielectric permittivity of pure water.

**Table 15.** Macroscopic properties of relevant interest for the studied methanol-water mixtures at 25 °C.

% MeOH (v/v)	$X_{\text{MeOH}}$	$\log [\text{H}_2\text{O}]$	$\rho$ (kg dm <sup>-3</sup> )	$\epsilon$	A	$a_0B$	$\delta$	$pK_{ap}$
0	0.000	1.74	0.995	78.30	0.53	1.50	0.00	14.00
10	0.047	1.70	0.983	75.05	0.56	1.53	0.01	14.08
20	0.100	1.65	0.969	71.37	0.59	1.56	0.03	14.08
30	0.160	1.59	0.955	67.49	0.64	1.61	0.05	14.07
40	0.229	1.52	0.939	63.39	0.70	1.66	0.09	14.09

**Table 16.** Intrinsic solubility (mol L<sup>-1</sup>) as logS, pK<sub>a</sub> values obtained in methanol-water media, parameters of the Yasuda-Shedlovsky Eq (40) (pK<sub>a</sub> + log[H<sub>2</sub>O] = a · 100/ε + b) and extrapolated aqueous pK<sub>a</sub> values (standard deviations) for the set of test compounds, at 25 °C and 0 ionic strength. ε were calculated as specified in bibliography <sup>26,157-159</sup>.

	LogS <sub>(lit)</sub>	pK <sub>a</sub>				a	b	r <sup>2</sup>	Aqueous
		10%	20%	30%	40%				pK <sub>a</sub>
<b>Methanol (v/v)</b>								<b>0.00</b>	
<b>100/ε</b>		<b>1.333</b>	<b>1.401</b>	<b>1.482</b>	<b>1.578</b>			<b>1.277</b>	
<b>Mefenamic acid</b>	-6.34	4.33	4.51	4.78	5.14	2.580	2.565	0.9895	4.12 (0.04)
<b>Meclofenamic acid</b>	-6.86	4.26	4.38	4.67	5.01	2.422	2.684	0.9737	4.04 (0.04)
<b>Sertaconazole</b>	-6.99	6.11	6.07	6.08	5.95	-1.327	9.588	0.9533	6.15 (0.05)
<b>Glyburide</b>	-7.05	5.50	5.71	5.77	5.92	1.038	5.810	0.9937	5.39 (0.01)
<b>Loperamide</b>	-7.13	8.84	8.80	8.80	8.64	-1.496	12.549	0.9463	8.90 (0.04)
<b>Terfenadine</b>	-7.74	9.22	9.20	9.16	8.97	-1.712	13.232	0.9451	9.30 (0.05)
<b>Amiodarone</b>	-8.17	4.33	4.51	4.78	5.14	-2.795	13.926	0.9858	8.61 (0.02)

**Table 17.** Limiting mobility ( $\text{m}^2 \text{V}^{-1} \text{s}^{-1}$ ) of the insoluble drugs at studied methanol-water compositions (v/v), at 25 °C and 0 ionic strength.

<b>% MeOH (v/v)</b>	<b>10%</b>	<b>20%</b>	<b>30%</b>	<b>40%</b>
<b>Mefenamic acid</b>	85.66	74.41	68.165	64.22
<b>Meclofenamic acid</b>	83.55	71.64	64.88	61.33
<b>Glyburide</b>	58.22	50.32	45.88	42.70
<b>Sertaconazole</b>	-73.46	-63.77	-58.39	-55.04
<b>Loperamide</b>	-54.92	-47.29	-44.10	-39.93
<b>Terfenadine</b>	-49.47	-43.44	-38.94	-37.09
<b>Amiodarone</b>	-52.99	-48.69	-45.30	-42.65

**Table 18.** Comparison of aqueous  $pK_a$  determined by the IS-CE method to the values determined by other methods<sup>26,157-159</sup>.  $pK_{a(IS-CE)}$  were determined by Yasuda-Shedlovsky extrapolation using methanol as a co-solvent within the range 10–40% v/v. All acidity constants are given at 25 °C and 0 ionic strength. Known standard deviations are in brackets.

<b>Methanol (v/v)</b>	<b><math>pK_{a(IS-CE)}</math> (0%)</b>	<b><math>pK_{a(lit)}</math></b>	<b>Method</b>	<b>Cosolvent</b>	<b>(%v/v) range</b>
<b>Mefenamic acid</b>	4.12 (0.04)	4.22	GLp $K_a$ spectrophotometry	MeOH	n.s
<b>Meclofenamic acid</b>	4.04 (0.04)	4.10	GLp $K_a$ n.s	n.s	n.s
<b>Sertaconazole</b>	6.15 (0.05)	-	-	-	-
<b>Glyburide</b>	5.39 (0.01)	5.22	CE-MS	None	-
<b>Loperamide</b>	8.90 (0.04)	8.90	GLp $K_a$ spectrophotometry	MeOH	n.s
<b>Terfenadine</b>	9.30 (0.05)	9.25	GLp $K_a$ potentiometry 35	MeOH	MeOH 50–70
		9.74	potentiometry 55	n.s	n.s
		9.31	Multiplexed CE	MeOH	40–60%
		9.21	CE-MS	None	-
<b>Amiodarone</b>	8.61 (0.02)	8.76	GLp $K_a$ spectrophotometry	MeOH	46–60%
		8.80	potentiometry	MDM*	36–53%
		8.73	potentiometry	MeOH	n.s
		10.12 (0.05)	potentiometry	MeOH	n.s
		8.73	GLp $K_a$ spectrophotometry	MeOH	40–50%
		8.85	Classic CE	MeOH	50%
		8.62	Multiplexed CE	MeOH	50–60%

### 3.5. Application of the Capillary Electrophoresis Internal Standards method to determine the $pK_a$ of HPLC columns test bases.

In the field of HPLC, accurately determining the  $pK_a$  of acid-base constant compounds is important for enhancing separation and analysis process. The retention of acid-base compounds is strongly dependent on the degree of ionization of the solute, which in turn depends on the pH of the mobile phase and the  $pK_a$  of the acid-base compound in this mobile phase. The main purpose of the study was to determine the  $pK_a$  values for a set of drugs that are frequently used as tests in high-performance liquid chromatography (RP-HPLC) <sup>160,161</sup>. The determination of the  $pK_a$  values can help in a better understanding of retention and peak shape in RP-HPLC analysis. The study targeted to determining the  $pK_a$  values of these drugs in methanol-water, and acetonitrile-water mobile phase using IS-CE method. Understanding the chemical properties and behavior of organic bases in varied settings might advance from knowing their  $pK_a$  values. The organic bases were codeine, quinine, diphenhydramine, procainamide, amitriptyline, benzylamine, nortriptyline, and protriptyline <sup>162,163</sup>.

McCalley and co-workers used the classical capillary electrophoresis method to determine the  $pK_a$  values of these organic bases from 0 to 70% methanol and 0 to 60% acetonitrile <sup>162,163</sup>. The classic CE method for  $pK_a$  measurement is based on the relationship between the electrophoretic mobility of an ionizable compound and the pH of the background electrolyte solution. To obtain reliable  $pK_a$  values, the mobility measurements must be done in several buffers of adequate and constant ionic strength, and well-known pH. Starting with methanol, the  $pK_a$  values were determined at different percentages of methanol (0-70% v/v) by plotting the mobility of the base against the (pH of the buffer) and identifying the inflection point of the sigmoidal curve. The same procedure was then applied to the determination of the  $pK_a$  at different percentages of acetonitrile (0-60% v/v). The inflection point gives the apparent  $pK_a$  values, which were then converted to the thermodynamic  $pK_a$  values using the Debye-Hückel equation. The capillary electrophoresis  $pK_a$  values were compared to those reported by NMR spectroscopy, but only for pure water <sup>162,163</sup>.

However, the authors calibrated the pH electrode with water buffers ( ${}^s_w\text{pH}$  scale), which means that the  $\text{p}K_a$  values obtained were referred to water as standard state for hydrogen ion activity ( ${}^s_w\text{p}K_a$  scale). Thus, degrees of the ionization of the studied bases cannot be calculated from these  $\text{p}K_a$  values unless pH values are measured with the same electrode system than  $\text{p}K_a$  values were determined or the  $\delta$  value is known. Since  $\delta$  term includes the medium effect for transfer of  $\text{H}^+$  from solvent  $w$  to  $s$  and the difference between the liquid junction potentials of the electrode system in  $s$  and  $w$  it depends on the particular mobile phase, but it may also depend on the particular electrode system used.

The IS-CE method and the  ${}^s_s\text{p}K_a$  values of the internal standards set we have established can overcome these problems because the method does not require potentiometric measurements with any electrode system. The  ${}^s_s\text{p}K_a$  value of the test acid-base compound can be directly determined from the electrophoretic mobilities of test and internal standards and the  ${}^s_s\text{p}K_a$  of the internal standards. The degree of dissociation of the test acid-base compound can be obtained from the  ${}^s_s\text{p}K_a$  value of the compound and the pH of the buffer measured in the same way, i.e. by the internal standards of the CE-IS method.

In this work, we sought to compare the IS-CE application we used to determine the  $\text{p}K_a$  values for the set of drugs frequently used in RP-HPLC studied by McCalley<sup>162,163</sup>. However, we found that the  $\text{p}K_a$  values obtained by McCalley cannot be directly compared to our  $\text{p}K_a$  values because of the reasons explained earlier. To begin, we used each methanol-water mixture or acetonitrile-water mixture as our standard state for the measurements, while McCalley used water as standard state. This fundamental variation in the standard state influences the comparison of the  $\text{p}K_a$  values. In addition, we lack information on the residual liquid junction potential for the electrode system that the author used, which contributes to the correction of delta values together with the medium effect. As a result, comparing  $\text{p}K_a$  values becomes challenging without knowing of these decisive parameters. Only  $\text{p}K_a$  values for pure water can be compared because there is no  $\delta$  correction and  ${}^s_s\text{p}K_a$ ,  ${}^s_w\text{p}K_a$ , and  ${}^w_w\text{p}K_a$  are the same ( $s = w$ ). It is worth remembering that the  $\text{p}K_a$  values reported by the author in the literature are only applicable when pH is measured using the same standard state (calibration in water) and electrode system<sup>162,163</sup>. Our IS-CE System allows measurement of pH for the methanol-water or acetonitrile-water mixture standard state with the internal standards, and using both values

we can calculate dissociation degrees of compounds and relate them to HPLC retention, which the author's system can't do.

The IS-CE method simplifies the experimental method in that it does not need an accurate measure of the pH of the electrophoretic buffers, few measurements are needed for a single  $pK_a$  determination (just two, at two different pH values). In addition, the use of appropriate internal standards decreases experimental errors resulting from assumed interactions between the test compounds, buffers, and other systematic errors, like temperature or buffer pH variations due to electrolysis processes during run analysis. We have developed an application to determine the  $pK_a$  values of these organic bases that were used in the RP-HPLC column test using the internal standard capillary electrophoresis technique in hydro-organic solvent from 0 to 90% methanol and acetonitrile. The  $pK_a$  value of each base was determined using the IS-CE method and calculated using at least three separate internal standards with a standard variation of less than 0.2. The trend in the  $pK_a$  variation with the amount of methanol in the solvent is shown in Figure (27). The  $pK_a$  values of the organic bases are presented in Table (19).

What was explained in the determination of the  $pK_a$  values of the organic bases using the IS-CE at different percentages of methanol also applied to acetonitrile. The trend in the  $pK_a$  variation demonstrated a higher deviation with increasing acetonitrile fraction, as shown in Figure (28). The  $pK_a$  values of the organic bases are presented in Table (20). The study I conducted determined the  $pK_a$  of two more bases, namely amitriptyline and protriptyline, in acetonitrile, where they were not studied by McCalley.

A set of internal standards bases were used to achieve the determination of the  $pK_a$  of a set of drugs that are frequently used as tests in (RP-HPLC). The used drugs are lidocaine, bupivacaine, 1-phenylpiperazine, benzyldimethylamine, diphenhydramine, procainamide, imipramine, propranolol, 1-aminoethylbenzene, ephedrine, and nortriptyline. The limiting mobilities of the drugs that are frequently used as tests in (RP-HPLC) were measured in Phosphoric acid/Sodium dihydrogenphosphate buffer at pH 2, except those of quinine, which were measured in a formate buffer at pH 4 (in water), and the effective mobilities of all bases and internal standards were measured in the particular buffers Tris and Ches in the pH range of 8–9.5. The  $pK_a$  values of diphenhydramine, procainamide, and nortriptyline are from the internal standards that we were used, which determined when I determined the  $pK_a$  of internal standards at different

concentrations of methanol and acetonitrile. I compared the  $pK_a$  values obtained from the McCalley method with the  $pK_a$  values determined using IS-CE method, focusing on measurements performed in pure water since both methods used water as the standard state. After reviewing the literature, I found that McCalley gave more literature for the  $pK_a$  (or  $pK_a$  range) for pure water, which I included in the comparison<sup>162,163</sup>. We obtained a  ${}^w pK_a$  value of codeine 8.32, while McCalley reported values of 8.20 and 8.25. In the literature review the  ${}^w pK_a$  range for codeine was reported as 7.82 – 8.21. We gotten a  ${}^w pK_a$  value of quinine 8.41, while McCalley reported values of 8.48 and 8.56. The  ${}^w pK_a$  value of quinine was reported as 8.39 – 8.52 in the literature review. The  ${}^w pK_a$  value of diphenhydramine obtained using our IS-CE method was 9.03, whereas McCalley stated values of 9.16 and 9.25. The  ${}^w pK_a$  value of diphenhydramine was stated as 9.00 – 9.40 in the literature review. We obtained a  ${}^w pK_a$  value of procainamide 9.30, while McCalley reported values of 9.32 and 9.42. In the literature review the  ${}^w pK_a$  range for procainamide was reported as 9.20 – 9.40. We obtained a  ${}^w pK_a$  value of amitriptyline 9.42, but McCalley stated values of 9.32. The  ${}^w pK_a$  value of amitriptyline was reported as 9.40 – 9.45 in the literature review. We obtained a  ${}^w pK_a$  value of benzylamine 9.53, but McCalley stated values of 9.45 and 9.55. The  ${}^w pK_a$  value of benzylamine was reported as 9.33 – 9.73 in the literature review. The  $pK_a$  value of benzylamine at 50% methanol determined by our method IS-CE was found to be comparable to the value indicated by Rived *et al*<sup>34</sup>. According to their results, benzylamine at 50% methanol has a  $pK_a$  range of 8.81 to 9.03 in the literature<sup>34,164</sup>, which is quite close to our IS-CE value of 9.08. This agreement shows that our method and the literature have a good agreement in determining the  $pK_a$  value for benzylamine under similar conditions. We obtained a  ${}^w pK_a$  value of nortriptyline 10.06, while McCalley reported values of 10.19 and 10.33. In the literature review the  ${}^w pK_a$  range for nortriptyline was reported as 10.00 – 10.11. Finally, the  ${}^w pK_a$  value of protriptyline obtained using our IS-CE method was 10.65, whereas McCalley stated value of 10.71. The  ${}^w pK_a$  value of protriptyline was stated as 10.70 in the literature review. The differences in the  $pK_a$  values can be shown in Tables (19) and (20) and the limiting mobilities ( $m^2 V^{-1} s^{-1}$ ) of the bases were depicted in Tables (21) and (22).

Thus, the studies I conducted achieved higher percentages of methanol and acetonitrile, permitting further thorough research into their impacts. Moreover, the study included more

intermediate points, which allowed for more detailed information about the behavior, properties, and effects of these solvents.

**Table 19.** The  $s_pK_a$  values of the eight organic bases determined using the IS-CE method from 0-90% MeOH compositions (v/v), and the available literature values<sup>34,162,164</sup>, at 25 °C and 0 ionic strength.

% MeOH (v/v)	0%			10%	20%	30%	40%	50%		60%	70%	80%	90%
	Det	Lit <sub>McCalley</sub>	Lit	Det	Det	Det	Det	Det	Lit	Det	Det	Det	Det
Codeine	8.32 (0.07)	8.20	7.83-8.21	8.24 (0.16)	8.19 (0.07)	8.12 (0.13)	7.98 (0.08)	7.72 (0.15)	-	7.49 (0.10)	7.15 (0.06)	6.84 (0.15)	7.84 (0.07)
Quinine	8.41 (0.05)	8.48	8.39-8.52	8.30 (0.17)	8.28 (0.05)	8.26 (0.14)	8.21 (0.10)	8.12 (0.08)	-	8.00 (0.10)	7.74 (0.02)	7.37 (0.10)	8.13 (0.09)
Diphenhydramine	9.03 (0.03)	9.16	9.00-9.40	9.02 (0.05)	8.97 (0.04)	8.71 (0.03)	8.43 (0.06)	8.06 (0.05)	--	7.63 (0.07)	6.77 (0.05)	6.46 (0.04)	7.65 (0.05)
Procainamide	9.30 (0.01)	9.32	9.20-9.40	9.16 (0.06)	9.00 (0.03)	8.74 (0.03)	8.52 (0.06)	8.15 (0.03)	-	7.68 (0.05)	6.83 (0.05)	6.46 (0.03)	7.60 (0.03)
Amitriptyline	9.42 (0.23)	9.32	9.40-9.45	9.23 (0.21)	9.14 (0.15)	9.00 (0.13)	8.95 (0.19)	8.72 (0.19)	-	8.42 (0.05)	8.06 (0.07)	7.62 (0.10)	8.42 (0.05)
Benzylamine	9.53 (0.23)	9.45	9.33-9.73	9.44 (0.14)	9.30 (0.18)	9.27 (0.13)	9.17 (0.18)	9.08 (0.10)	8.81 - 9.03	8.82 (0.05)	8.46 (0.08)	8.21 (0.07)	9.01 (0.06)
Nortriptyline	10.06 (0.01)	10.19	10.00-10.11	9.87 (0.08)	9.66 (0.02)	9.47 (0.04)	9.26 (0.06)	8.88 (0.04)	-	8.38 (0.04)	7.51 (0.06)	7.16 (0.03)	8.36 (0.04)
Protriptyline	10.65 (0.14)	10.43	10.70	10.37 (0.03)	10.25 (0.10)	10.10 (0.02)	9.91 (0.02)	9.71 (0.10)	-	9.35 (0.01)	8.60 (0.10)	8.29 (0.07)	9.37 (0.09)

**Table 20.** The  $s_pK_a$  values of the eight organic bases determined using the IS-CE method from 0-90% ACN compositions (v/v) and the available literature values<sup>163</sup>, at 25 °C and 0 ionic strength.

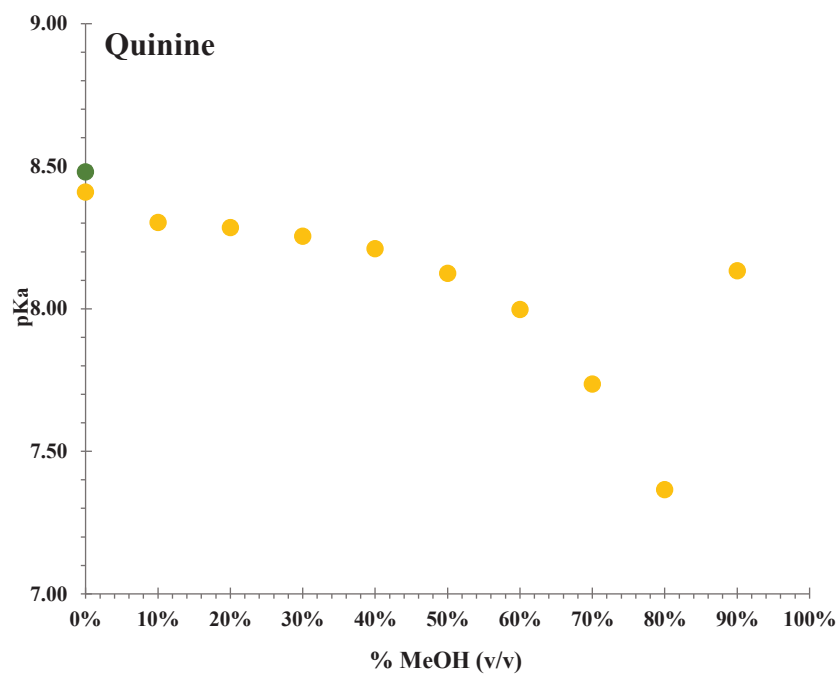
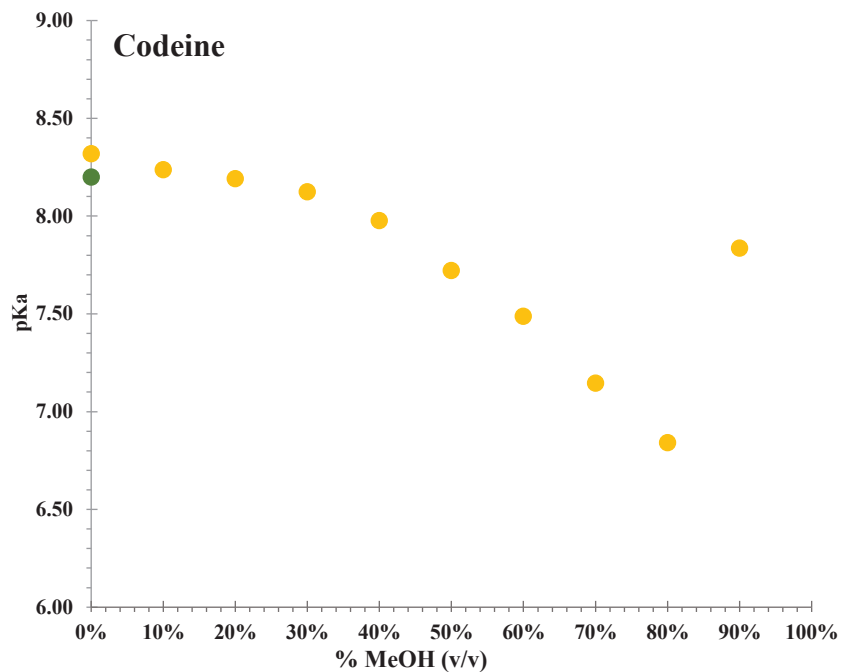
% ACN (v/v)	0%			10%	20%	30%	40%	50%	60%	70%	80%	90%
	Det	Lit <sub>McCalley</sub>	Lit	Det	Det	Det	Det	Det	Det	Det	Det	Det
Codeine	8.32 (0.07)	8.25	7.83-8.21	8.10 (0.04)	7.95 (0.11)	7.68 (0.08)	7.49 (0.02)	7.44 (0.12)	7.35 (0.12)	7.30 (0.11)	7.25 (0.15)	7.65 (0.13)
Quinine	8.41 (0.05)	8.56	8.39-8.52	8.16 (0.03)	8.12 (0.13)	7.85 (0.08)	7.68 (0.03)	7.53 (0.12)	7.49 (0.13)	7.36 (0.11)	7.36 (0.14)	7.69 (0.05)
Diphenhydramine	9.03 (0.03)	9.25	9.00-9.40	8.46 (0.09)	8.34 (0.10)	7.79 (0.06)	7.22 (0.09)	6.98 (0.09)	6.92 (0.06)	6.87 (0.08)	6.88 (0.05)	7.20 (0.07)
Procainamide	9.30 (0.01)	9.42	9.20-9.40	8.60 (0.07)	8.19 (0.05)	7.81 (0.07)	7.33 (0.07)	7.08 (0.07)	7.04 (0.07)	6.98 (0.09)	6.98 (0.08)	7.30 (0.08)
Amitriptyline	9.42 (0.23)	-	9.40-9.45	9.25 (0.04)	9.13 (0.10)	8.92 (0.18)	8.74 (0.06)	8.62 (0.18)	8.50 (0.11)	8.44 (0.19)	8.39 (0.15)	8.76 (0.12)
Benzylamine	9.53 (0.23)	9.55	9.33-9.73	9.25(0.14)	9.01 (0.06)	8.87 (0.18)	8.65 (0.13)	8.54 (0.08)	8.46 (0.06)	8.43 (0.06)	8.36 (0.11)	8.66 (0.18)
Nortriptyline	10.06 (0.01)	10.33	10.00-10.11	9.35 (0.02)	8.81 (0.08)	8.49 (0.02)	8.11(0.02)	7.87 (0.05)	7.76 (0.03)	7.76 (0.03)	7.76(0.08)	8.08 (0.03)
Protriptyline	10.65 (0.14)	-	10.70	10.05 (0.09)	9.53 (0.04)	9.49 (0.01)	9.10 (0.09)	8.95 (0.09)	8.83 (0.05)	8.54 (0.08)	8.49 (0.06)	8.97 (0.08)

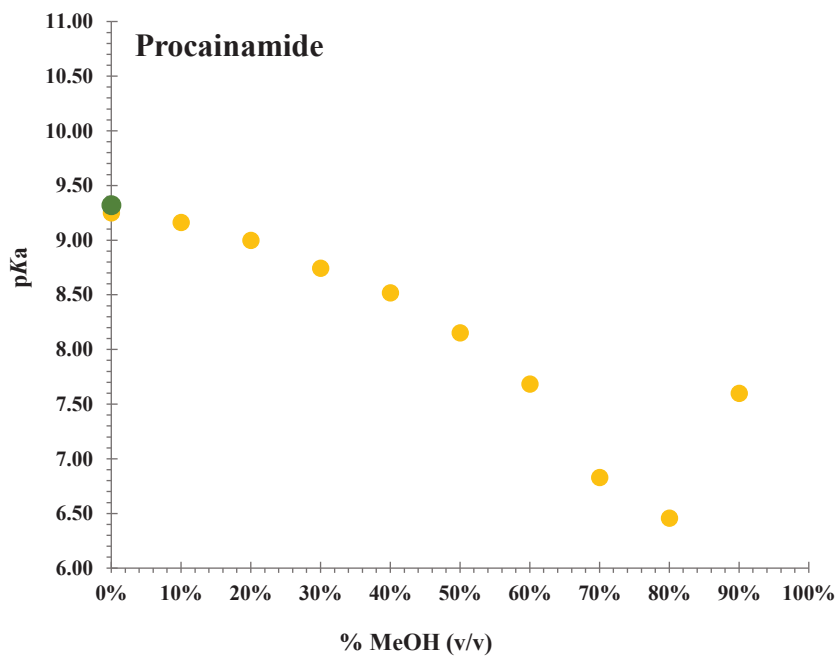
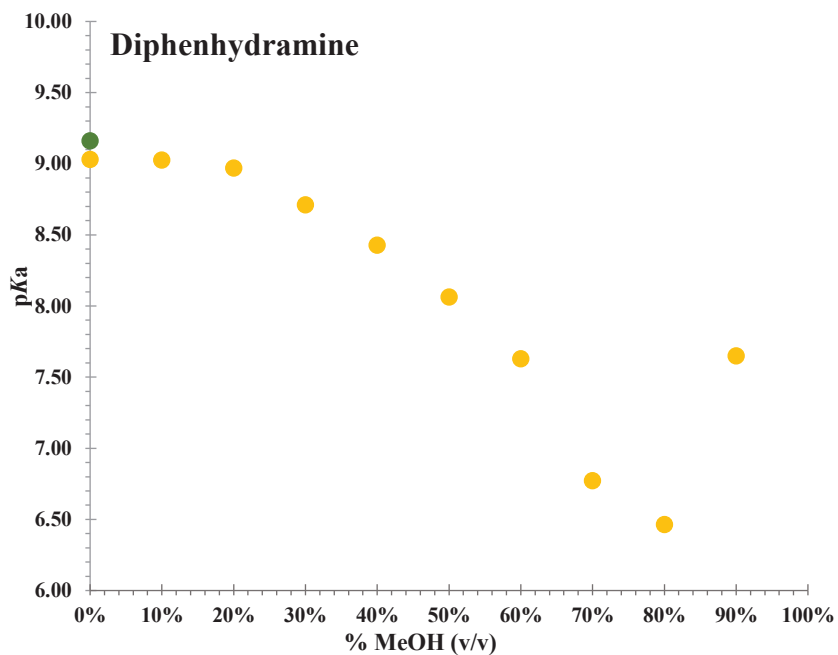
**Table 21.** Limiting mobility ( $\text{m}^2 \text{V}^{-1} \text{s}^{-1}$ ) of the bases at studied methanol-water compositions (v/v), at 25 °C and 50 ionic strength.

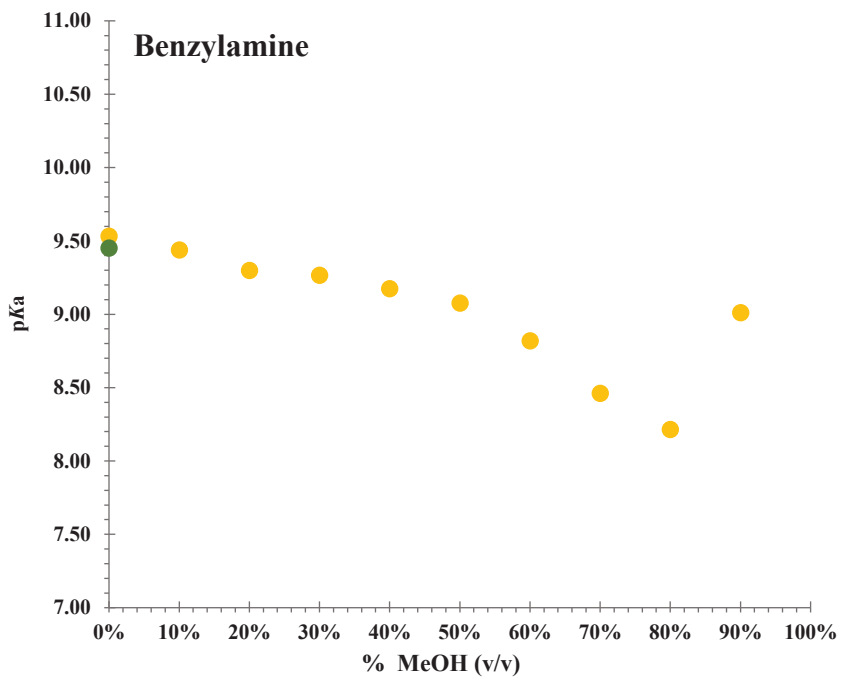
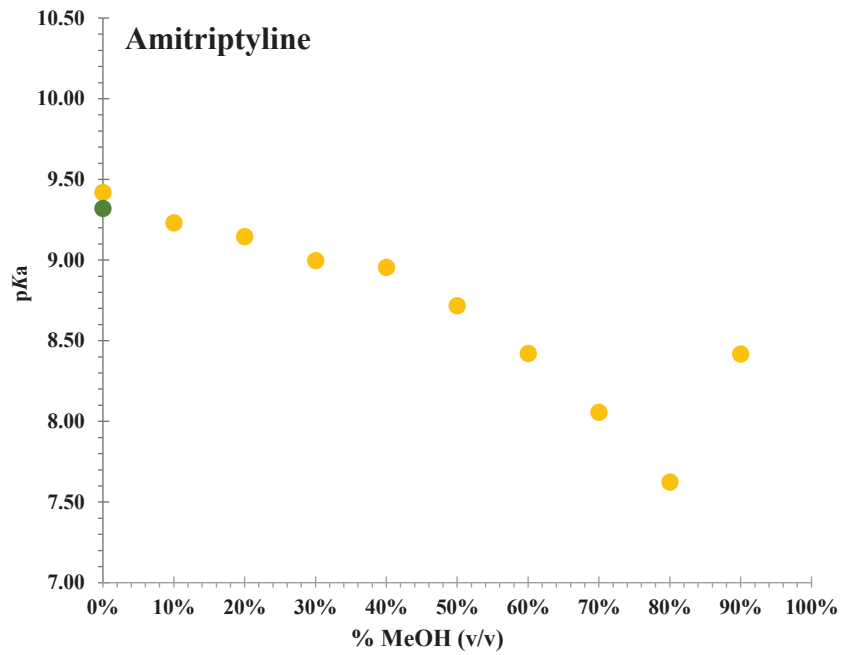
% MeOH (v/v)	0%	10%	20%	30%	40%	50%	60%	70%	80%	90%
<b>Codeine</b>	-119.05	-91.88	-86.10	-72.90	-68.85	-67.74	-64.90	-58.01	-58.00	-61.08
<b>Quinine</b>	-168.05	-160.49	-132.35	-123.89	-114.33	-99.42	-97.59	-80.90	-82.73	-87.33
<b>Diphenhydramine</b>	-100.30	-83.80	-81.10	-69.50	-65.60	-82.55	-76.92	-78.14	-77.83	-78.10
<b>Procainamide</b>	-97.00	-82.00	-80.30	-72.70	-64.20	-94.31	-83.52	-82.67	-78.94	-79.09
<b>Amitriptyline</b>	-113.41	-98.85	-88.04	-84.25	-80.67	-77.31	-71.41	-67.15	-68.52	-71.24
<b>Benzylamine</b>	-196.00	-178.98	-164.00	-151.39	-143.04	-136.46	-119.19	-109.85	-111.00	-111.51
<b>Nortriptyline</b>	-93.10	-79.80	-77.80	-65.90	-61.00	-81.03	-73.26	-72.79	-75.09	-72.86
<b>Protriptyline</b>	-136.77	-123.29	-96.66	-82.18	-77.07	-75.14	-72.033	-71.92	-71.58	-71.95

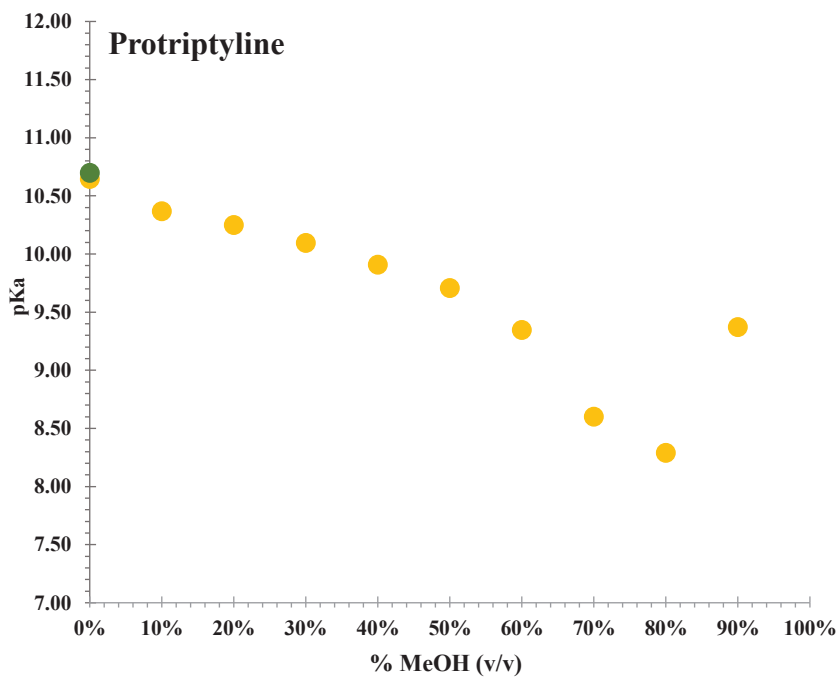
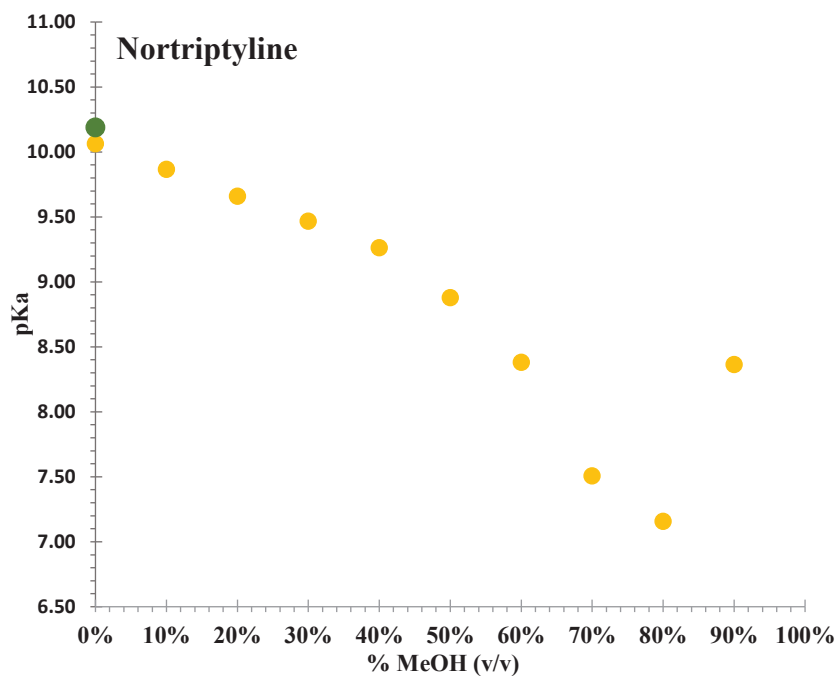
**Table 22.** Limiting mobility ( $\text{m}^2 \text{V}^{-1} \text{s}^{-1}$ ) of the bases at studied acetonitrile-water compositions (v/v), at 25 °C and 50 ionic strength.

% ACN (v/v)	0%	10%	20%	30%	40%	50%	60%	70%	80%	90%
<b>Codeine</b>	-119.05	-104.06	-92.61	-86.70	-83.56	-73.44	-71.17	-70.83	-75.88	-76.65
<b>Quinine</b>	-168.05	-158.27	-134.73	-128.46	-125.30	-118.86	-117.57	-113.25	-114.91	-115.08
<b>Diphenhydramine</b>	-100.30	-117.17	-120.51	-123.94	-121.66	-117.17	-115.32	-117.27	-114.27	-119.27
<b>Procainamide</b>	-94.00	-145.39	-163.75	-162.18	-150.97	-145.39	-144.84	-143.34	-142.39	-145.84
<b>Amitriptyline</b>	-113.41	-105.10	-86.54	-84.65	-83.37	-78.70	-74.11	-71.10	-72.01	-71.68
<b>Benzylamine</b>	-196.00	-173.39	-145.96	-137.70	-133.28	-125.51	-121.86	-112.63	-109.33	-109.17
<b>Nortriptyline</b>	-93.10	-110.83	-114.97	-115.06	-110.83	-112.91	-110.83	-108.86	-104.29	-110.53
<b>Protriptyline</b>	-136.77	-110.32	-107.23	-102.46	-103.93	-96.73	-96.93	-94.90	-94.05	-97.21

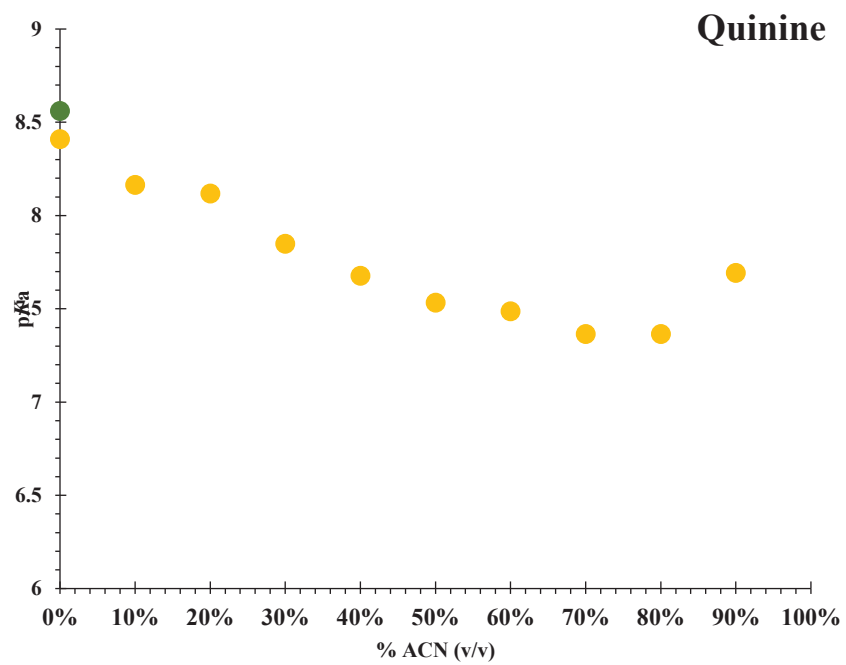
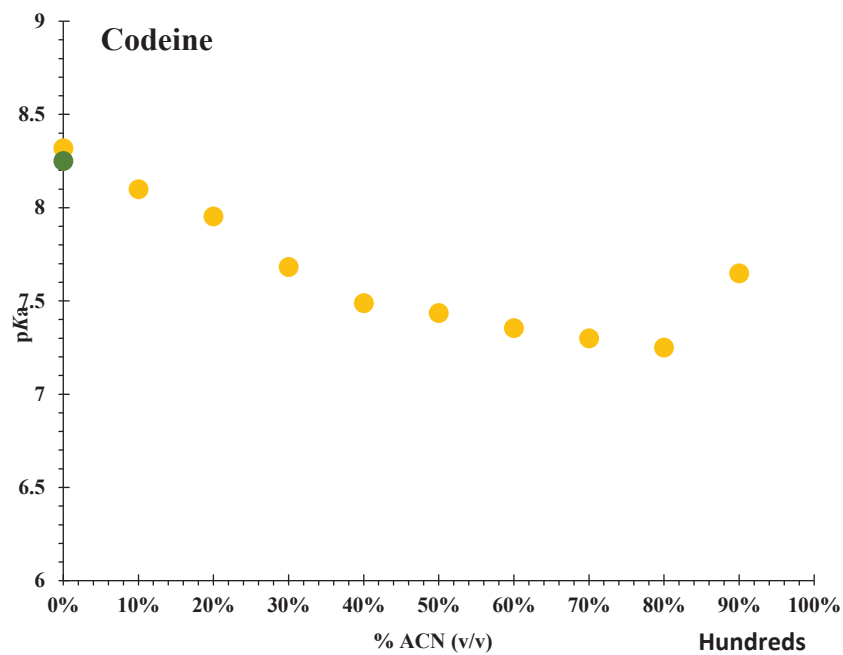


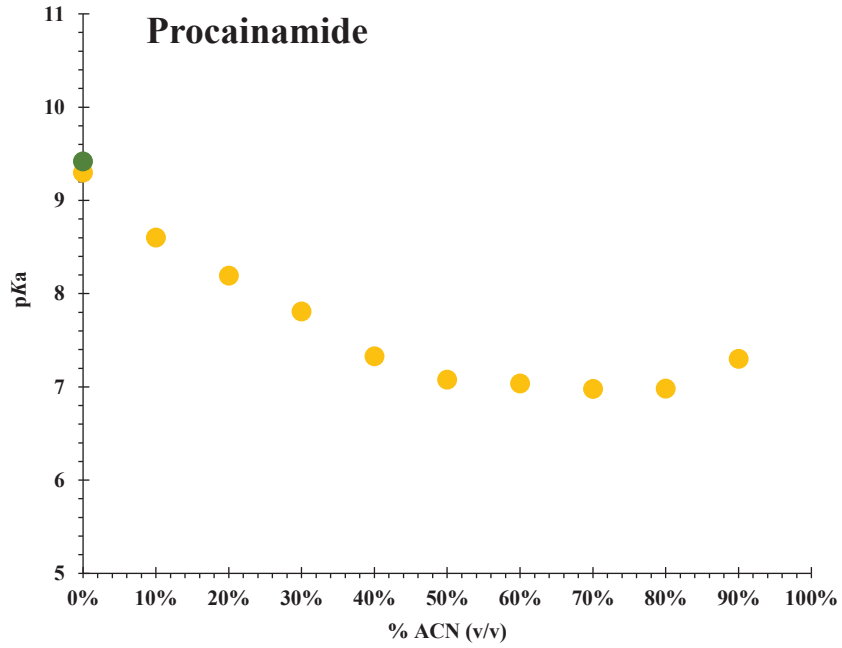
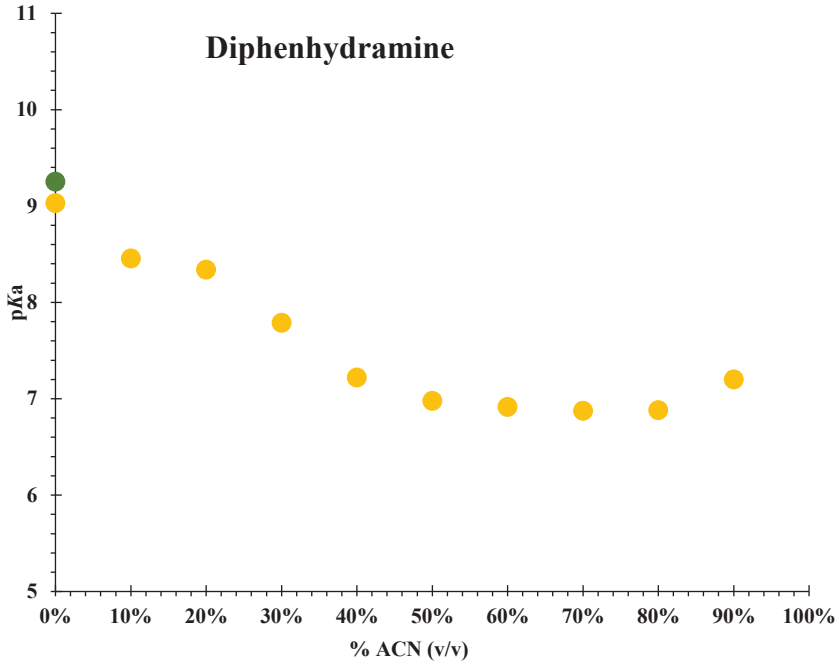


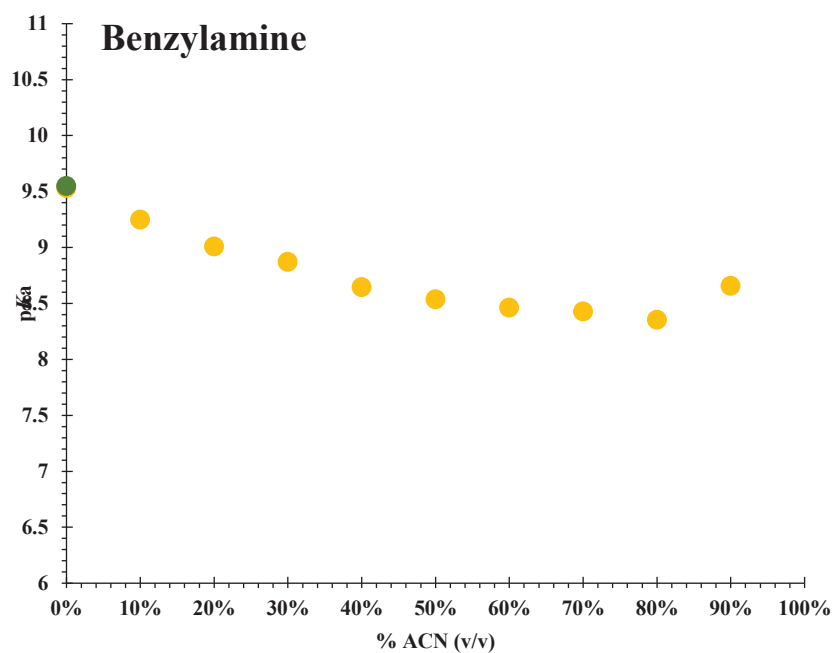
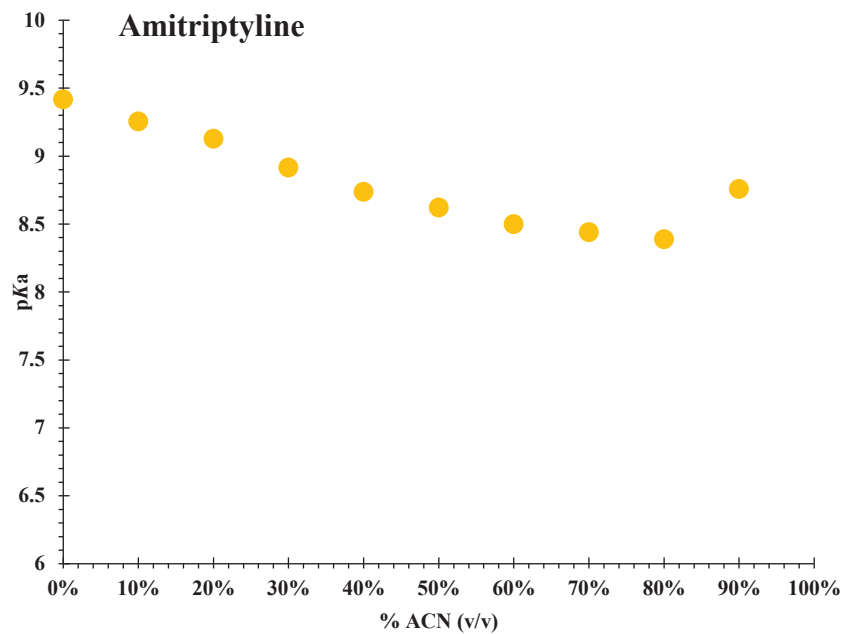




**Figure 27.** The trends in variations of pKa values of the eight organic bases that were determined using the IS\_CE method from 0-90% methanol is shown in the 8<sup>th</sup> figure above. (●) display determined value (●) display McCalley literature value.







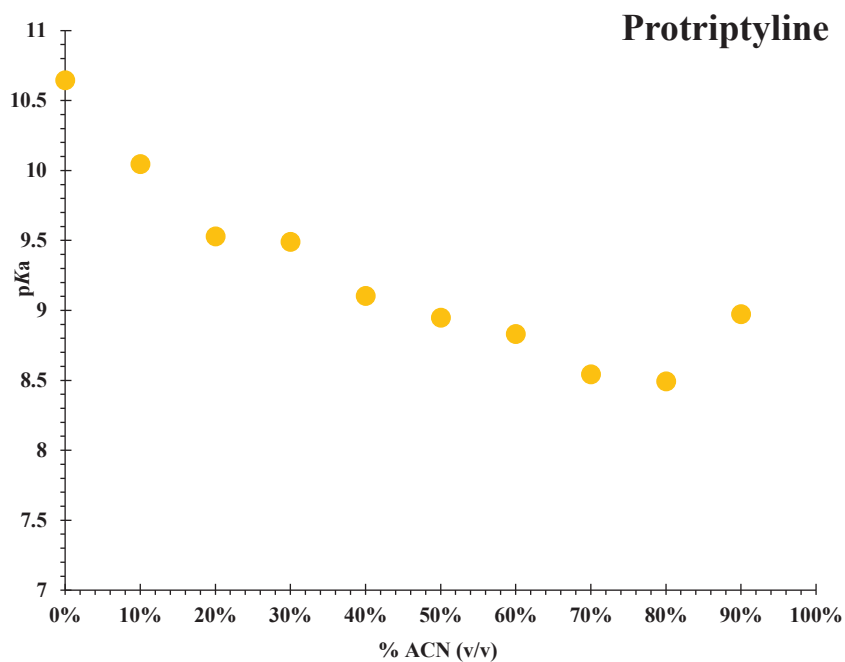
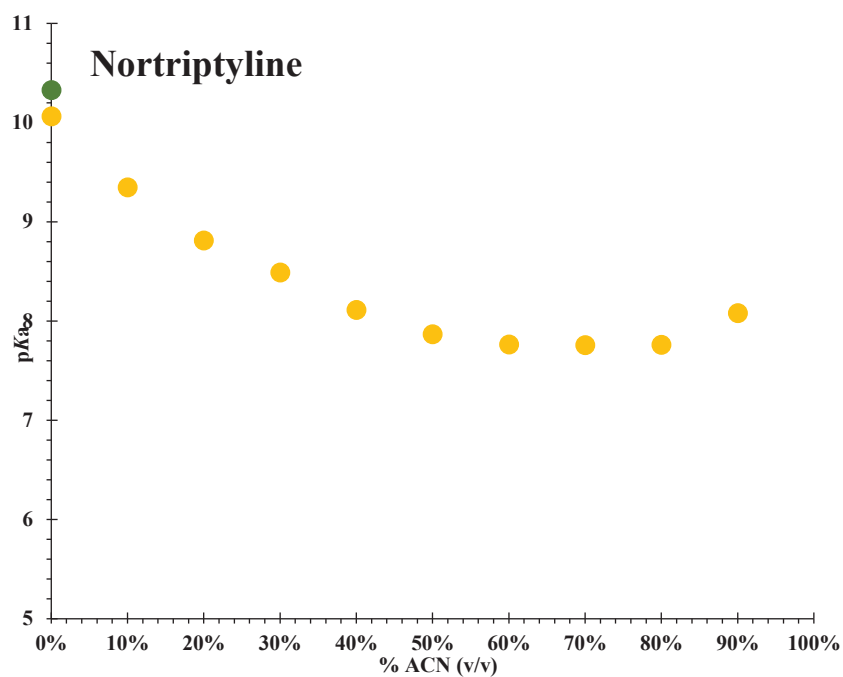


**Figure 28.** The trends in variations of pKa values of the eight organic bases that were determined using the IS\_CE method from 0-90% acetonitrile is shown in the 8<sup>th</sup> figure above. (●) display determined value (●) display McCalley literature value.



## 3.6. Determination of partition coefficient using Microfluidic chip

Similar to  $pK_a$ , the partition coefficient octanol/water ( $\log P_{o/w}$ ) is another physico-chemical parameter that also plays an important role in drug discovery and development. The value of  $\log P_{o/w}$  is addressed by the compound hydrophilicity and hydrophobicity, and it may be determined experimentally using a variety of procedures, as mentioned in the introduction. The most popular is the traditional "shake-flask" technique. However, this method is static, time-consuming, and require important volumes of solvents and reagents. For this reason, in this thesis, novel microfluidic techniques were studied and developed to elaborate more high-throughput and miniaturized alternative.

The octanol-water partition in microfluidics was evaluated by designing and implementing microscale systems that allowed precise fluid control for assessing octanol and water partition. Techniques such as capillary-driven microfluidics and gravitational flow were employed to create large volume to surface interfaces between the two phases. Subsequently, analytical methods like fluorescence imaging and chromatography were utilized to measure the partition efficiency and the partition coefficient of specific compounds, providing insights into their distribution between octanol and water in a miniaturized setting. The microfluidic design was also parallelized and configured to be compatible with HPLC sampling microplates. Finally, the performance of the designed microfluidic chips was tested by measurement of the  $\log P_{o/w}$  of some well-known pharmaceutical drugs. Overall, this technique allowed faster equilibration times, lower consumption of reagents and high automation, making it appropriate for standard laboratory use.

### 3.6.1. Design and development of the dynamic microfluidic device

In collaboration with LEITAT, a dynamic microfluidic architecture was designed, fabricated, and tested to study its feasibility for the determination of  $\log P_{o/w}$ . A fit-to-purpose design was developed based on the needs for a cost-effective, low reagent consumption, and reliable technique. The microfluidic device was designed based on 3D structure with two independent and interconnected microfluidic channels, where the octanol (O) channel flows above the water (W) channel. The reason of this disposition is due to density of the solvents (octanol density =

0.827 g/ml, while water density = 0.998 g/ml)<sup>165</sup>. The O phase, less dense, remains on the top section, whereas the W is at the bottom. This disposition avoids undesired flow of water droplet to the octanol phase, and vice versa. The design of the chip is stated in Figure (29) and consists of two parts; (i) the microfluidic chip, which includes the channels and reservoirs, and (ii) the base, which includes a hydrophilic polyethylene terephthalate (hPET) film allowing the correct assembly and tightness of the device.

The fabrication process and the assembly were explained in Chapter 2. Briefly, 3D printing was selected as one of the prototyping techniques because it has the ability to fabricate a complete microfluidic device in a single step from a computer model. Precisely, the computer model was converted into a standard triangulation language (STL) where was digitally sliced into individual layers. These slices were then sequentially realized to build an object in a layer-by-layer manner. The chip was 3DP with one open side to avoid trapping resin and reduce over-polymerization. The base of the 3DP microfluidic chip was sealed with hPET using an optically clear double-side pressure sensitive adhesive for a tight seal. The base is required to prevent fluid leakage and preserve the fluidic performance of the device. Transparent material was used for both microfluidic chip and base to ease the inspection fluorescent compounds during the partition and equilibrium.

Each of the channels is connected to one inlet and one outlet. Position B1 is the water inlet and it is connected to A3 through the water microfluidic channel. This W channel is in contact with the hPET, which wicks the water solution from B1 to A3 and is located at the lowest point of the plate. Position A1 is the octanol inlet and it is connected through the octanol microfluidic channel to octanol outlet position, B3. This channel flow over the water channel and it does not get in contact with the hPET base. Water and octanol are connected only in the observation window area. As can be seen, the O channel flows above and perpendicularly through the water (W) channel. This design was developed to maximize the partition of molecules between the W/O phases. Perpendicular intersection increases shear stress between the phases during the perfusion. Also, the bigger width of the water channel increases the contact area and maintains the W/O meniscus at the intersection of the channels.

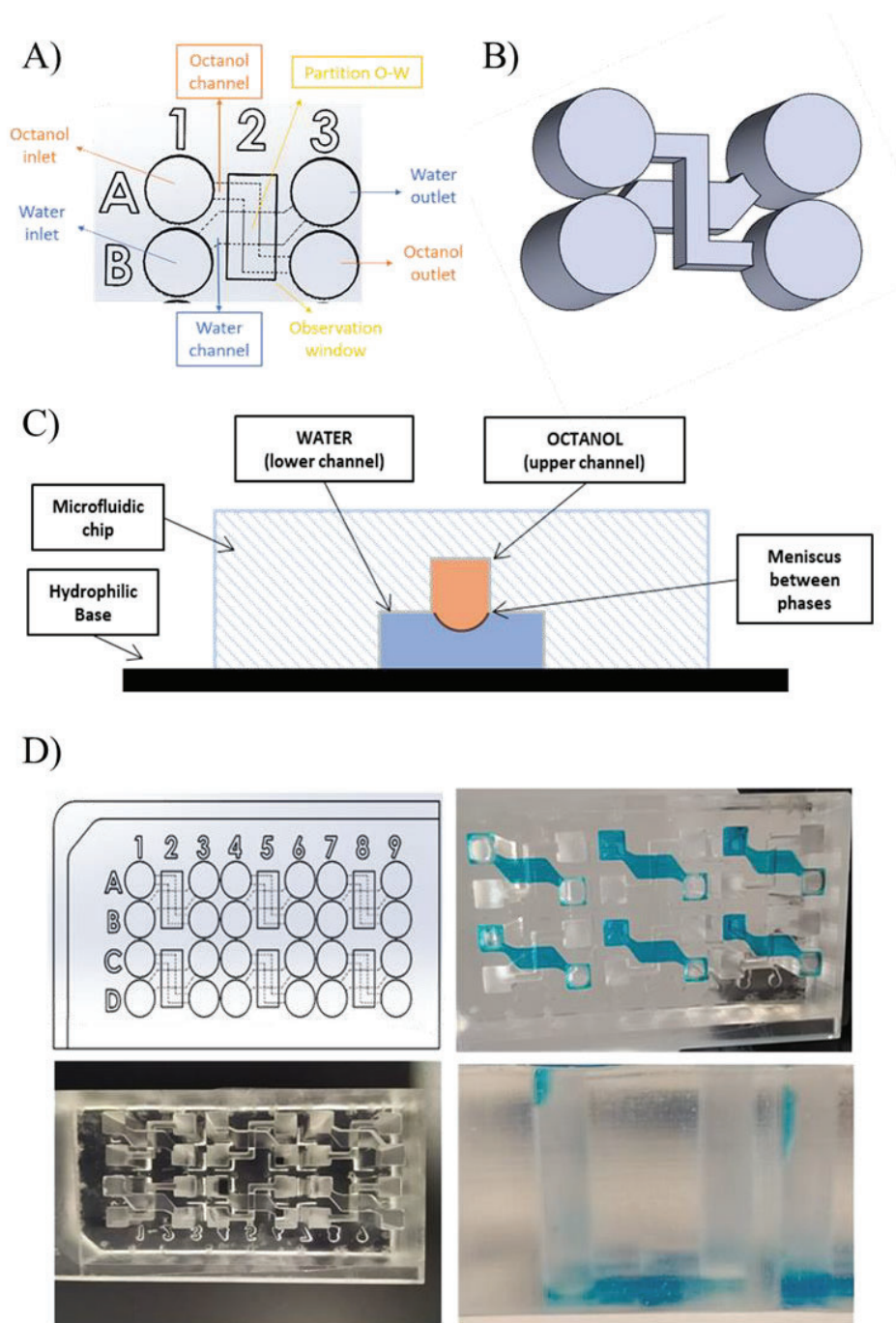


**Figure 29.** Microfluidic device for log  $P_{o/w}$  partition. Top (A) and isometric (B) CAD view of the design of the 3D microfluidic chip. C) Representation of a transversal cut (section) of the device showing the intersection between O/W phases. D) Design (top-left) and picture (bottom-left) from the bottom of the 3D printed microfluidic chip, and pictures of the wicking of the water phase from the bottom (top-right) and from the side (bottom-right) when it is introduced in from the inlet (i.e. B1). The water was colored using a blue food dye.

Utilization of microfluidic devices requires careful consideration of the hydrophobic or hydrophilic properties of these materials as they can have a significant effect on the device's performance and the results of experiments. For this reason, the materials and their combination were selected based on the requirements of the O/W interaction with surface properties. On one side, the base, in contact with the W phase, was hydrophilic (water contact angle of  $20^\circ$  approximately) to foster the flux of water solution over the base, especially when the water is introduced for the first time. On the other side, the microfluidic chip was slightly hydrophobic (water contact angle of  $75^\circ$  approximately) to reduce the water adhesion forces on the microfluidic wall and therefore avoid the movement of water droplets towards the O channel.

When water and octanol phases were introduced, two separate phases with an intersection area were created, as shown in Figure (30). As octanol and water are immiscible, the distribution of a compound between water and octanol at the interphase where both phases are in contact is possible.

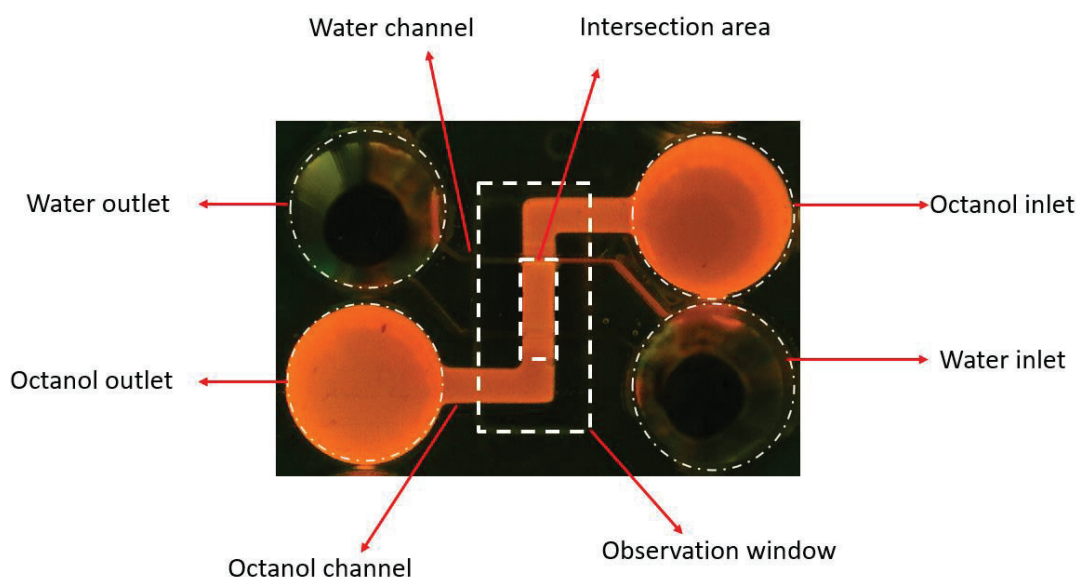


**Figure 30.** Picture of the 3DP microfluidic device taken from underneath using a fluorescent microscope. To ease the contrast between phases, rhodamine B (fluorescent dye) was dissolved in octanol. White dashed line represents the observation window, defining inside the area of contact between O/W phases.

### 3.6.2. Flow working principle and evaluation of hydrodynamic perfusion

The flow is induced by leveling the two reservoirs (inlet and outlet) that are connected by the O or W channel. The difference creates hydrodynamic flow spontaneously in both water and octanol. By placing the plate under an angle on a rocker that inverts the angle at regular intervals, a continuous bi-directional flow through the channel is induced. The flow principle is depicted in Figure (31).

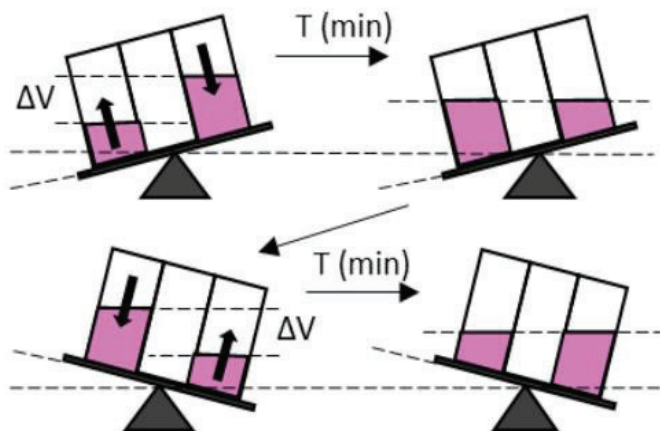


**Figure 31.** Gravitational flow, pumptless.  $\Delta V$  is the difference between the height of the reservoirs and  $T$  is time for each cycle.

A difference in hydrostatic pressure between two reservoirs (either water or octanol) causes fluid to flow from the container with the higher height to the one with lower height. The big advantage of this approach is that there is no need for external pumps since the flow occurs spontaneously and it is controlled by the degree of inclination and the frequency of the rotation. Moreover, this perfusion system also allows the perfusion of parallel devices at the same time without the need for multiple pumps or flow splitters.

To evaluate the perfusion of the channels fluorescein (green) and rhodamine B (orange) fluorescent dyes were used in water and octanol, respectively, in 2 different experiments to evaluate each channel. The first (Figure 32-A) was carried out to monitor the movement of octanol phase. Initially, the bottom channel was filled with a solution of water with fluorescein (green) and the upper channel with pure octanol. Then, a 20  $\mu\text{L}$  drop of octanol with rhodamine B (orange) was introduced in the octanol outlet (B3) to observe how the octanol with the dye moved along the upper (octanol) channel. Initially, it was appreciated a spontaneous movement of the fluorescent dye ( $T = 0$  s). This was due to the increase of height in one of the reservoirs

when the 20  $\mu\text{L}$  of octanol with the dye were introduced. Subsequently, the device was tilted  $+7^\circ$  and a spontaneous flow from the B3 toward the inlet reservoir (A1) was observed until the orange dye reached the outlet (T = 18 s). The second experiment (Figure 32-B) demonstrated the flow of water over the bottom channel. Initially, the bottom channel was filled with pure water and the upper channel with an octanol solution with rhodamine B. Subsequently, a 20  $\mu\text{L}$  drop of water with fluorescein was introduced in reservoir A3 to observe how the dye moves along the bottom (water) channel. When the device was tilted  $+7^\circ$ , a flow from the A3 toward the inlet reservoir (B1) was observed.

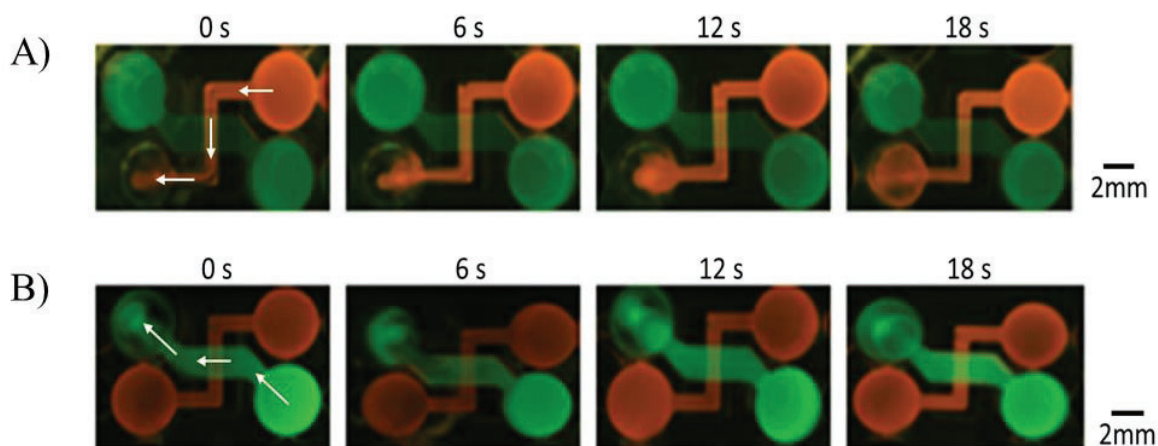


**Figure 32.** Sequence of pictures of the microfluidic design when the device was tilted  $+7^\circ$ . Water was loaded with 50 mg/L of fluorescein (green) and octanol with 50 mg/L of rhodamine B (orange). A) The orange channel shows the hydrodynamic flow in the octanol layer. The octanol reservoir on the bottom right was previously filled with octanol without rhodamine B. B) The channel with green color displays the hydrodynamic flow in the water. The water reservoir on the top right was previously filled with water without fluorescein. Note that the images appear inverted due to the images are taken from underneath the chip with the fluorescent microscope.

### 3.6.3. Partition dynamics between octanol and water phases in the microfluidic device

Microfluidics allow the study of the partition dynamics in a precisely controlled environment. So, partition constant can be monitored by controlling the increase or decrease of the intensity of a molecule in one of the channels. Fluorescence detection was chosen because it can be easily visualized using fluorescence microscopy and thus molecule distribution behavior can be monitored in situ. In that sense, the intensity of a fluorescence dye was used to evaluate the

partition from octanol to water by simply using the fluorescent microscope and the ImageJ software to calculate the change in concentration with the time. Rhodamine B was selected as a target model during the equilibration process. Hence, to monitor the intensity of the dye, a known concentration of the rhodamine B dye was dissolved in octanol and its intensity in water was monitored over time. In this experiment, saturated solutions (water saturated octanol, and the other way round) were used to monitor the partitioning behavior under octanol-water conditions. 10 mM of rhodamine B dye was prepared in octanol saturated water, and its transfer to the water layer was analyzed to determine the time required to attain equilibrium. To test the effectiveness of the microfluidic chip, the increase of fluorescence in water was determined with and without perfusion, as well as the different speed of the rocker.

It is important to remark that the purpose of these tests is to assess the dynamics of the partition using the proposed design and there is no need to determine the partition coefficient. Likewise, the molecule and its initial concentration were the same in all cases, so the equilibrium time can be compared.

### **3.6.3.1. Evaluation of the partition dynamics in static condition**

When working in static conditions the diffusion is the main driving force for the movement of a molecule. The partition of the target molecule is spontaneous and goes from a high-concentration region to a low-concentration region over time. If the solution is left without perfusion, the target compound will ultimately diffuse from the high-concentration phase to the low-concentration phase until equilibrium is well established. For volumes within the range of the "shake-flask" technique, the equilibrium can go from several hours to a few days. In the case of microfluidics, where the volumes are perfectly defined in the range of tens of microliters, this procedure can be much quicker.

The process for the partition with the microfluidic device began by first placing the plate on a level surface and filling the observation window with 100  $\mu$ L of deionized water to increase the material transparency. Subsequently, B1 (the water inlet) was gradually filled with 100  $\mu$ L of water solution ensuring that the water flowed up to A3 (water outlet) and did not reach the octanol channel. Then, 70  $\mu$ L of the octanol solution with 10 mM of rhodamine B was added slowly from A1 (the octanol inlet). After the octanol flowed up to B3 (octanol outlet), a rapid inspection was made to ensure that octanol did not go down to the water channel. Fluorescent

microscopic pictures were taken to analyze the intensity at different intervals of time for up to 120 minutes. The assay was repeated 5 times and analyzed by ImageJ to determine the intensity of rhodamine B in water. The average intensity of fluorescence was plotted versus the time, to see the partition of rhodamine B from octanol to the water. The values of the intensity are summarized in Table (23) and the Figure (33) depicts the results. As can be seen, rhodamine B reached equilibrium in just 120 minutes in static conditions. At first, the transfer of dye was quite rapid, but it slows down as equilibrium is reached. In the scale of microliters, equilibrium can be reached faster than other time-consuming techniques.

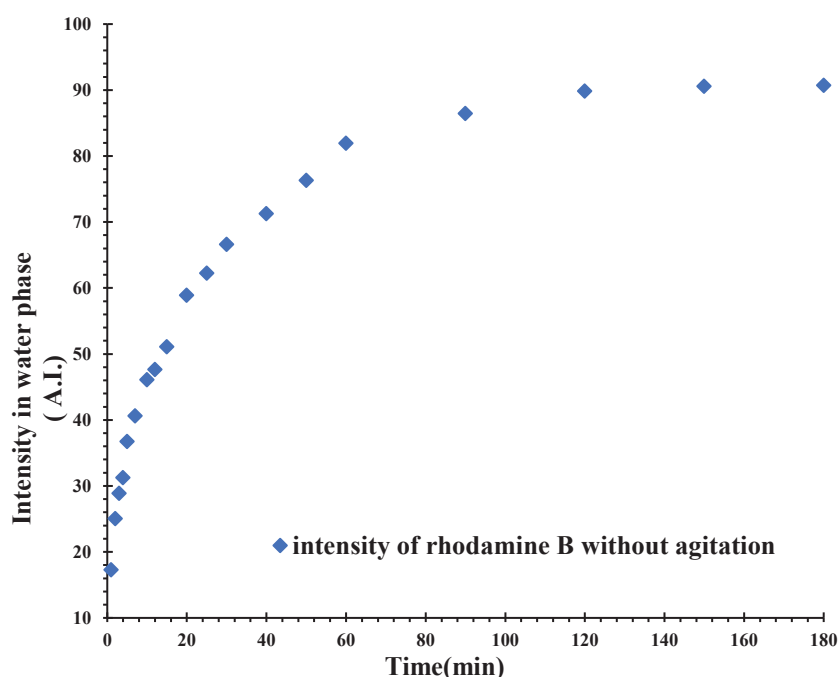


**Figure 33.** Average intensity of rhodamine B in the water phase in static conditions. The concentration of rhodamine B was 10 mM, with volumes of 70  $\mu\text{L}$  and 100  $\mu\text{L}$  for the octanol and water phase, respectively. Results are based on  $n=5$ . Standard deviation is shown in Table 23.

**Table 23.** Shows average values of the intensity of rhodamine B without agitation, the same assay condition was used as shown in Figure (33).

<b>Time (min)</b>	<b>Average Intensity (n=5)</b>
1	17.3 ± 3.9
2	25.0 ± 3.6
3	28.9 ± 5.1
4	31.3 ± 3.6
5	36.7 ± 6.2
7	40.6 ± 8.1
10	46.1 ± 7.5
12	47.7 ± 8.3
15	51.1 ± 7.6
20	58.9 ± 8.5
25	62.3 ± 7.6
30	66.6 ± 4.4
40	71.2 ± 1.4
50	76.3 ± 1.8
60	81.9 ± 2.1
90	86.5 ± 0.6
120	89.9 ± 2.5
150	90.6 ± 5.1
180	90.7 ± 2.2

### **3.6.3.2. Evaluation of the partition dynamics in perfusion conditions**

When the device was tilted, the change in between the leveling of the inlet and outlet reservoirs created a hydrodynamic flow spontaneously in both water and octanol channels. Hence, by placing the plate under an angle on a rocker that inverts the angle at regular intervals, a continuous bi-directional flow should increase the mixing of each individual phase and the shear stress at the junction between them. From previous results in section 6.2, an inclination of  $\pm 7$  degrees was selected as it showed appropriate fluid velocity in the microfluidic channels. However, the rotation frequency can affect the partition efficiency. For this reason, the concentration of rhodamine B in water phase was monitored over time at different cycles per minute. Figure (34) shows the fluorescent images at 5, 10 and 20 cycles/min with a constant inclination of  $\pm 7$  degrees. The results are summarized and depicted in Table (24) and Figure

(35), respectively. The intensity of rhodamine B in water from the microscope images were measured using ImageJ.

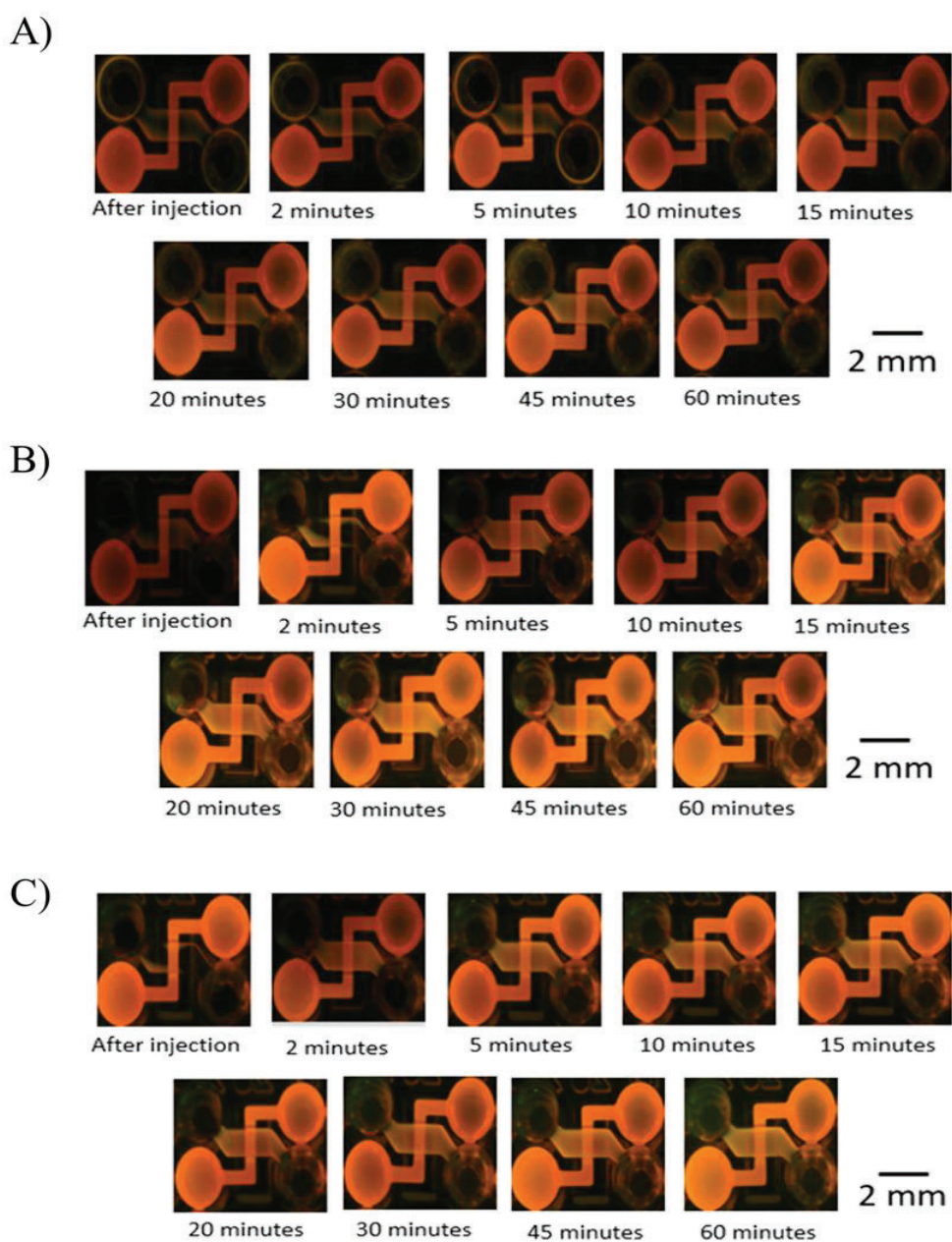


**Figure 34.** Sequence of pictures (from 0 to 60 min) of the microfluidic device. The device was under perfusion rocking at 5 (A), 10 (B), and 20 (C) cycle/min with an inclination of  $\pm 7^\circ$ . The volume was  $70 \mu\text{L}$  and  $100 \mu\text{L}$  for the octanol and water phase, respectively.

**Table 24.** Values of the dye intensity in water phase in under different gravitational flow. The standard deviation is based on 3 separate assays.

Time ( min)	5 cycle/min	SD	10 cycle/min	SD	20 cycle/min	SD
0	28.0	0.8	28.4	0.7	30.3	6.1
2	57.8	1.4	73.1	3.6	79.5	5.7
5	63.9	0.2	79.4	2.3	84.0	8.2
10	69.5	2.5	81.1	1.4	84.8	8.1
15	78.5	0.8	83.5	1.5	85.6	7.8
20	79.7	1.1	84.6	1.3	86.1	7.8
30	84.12	0.4	85.2	0.7	87.0	7.4
45	88.8	2.3	86.5	0.0	91.4	5.4
60	91.4	3.0	87.0	0.8	92.3	6.4

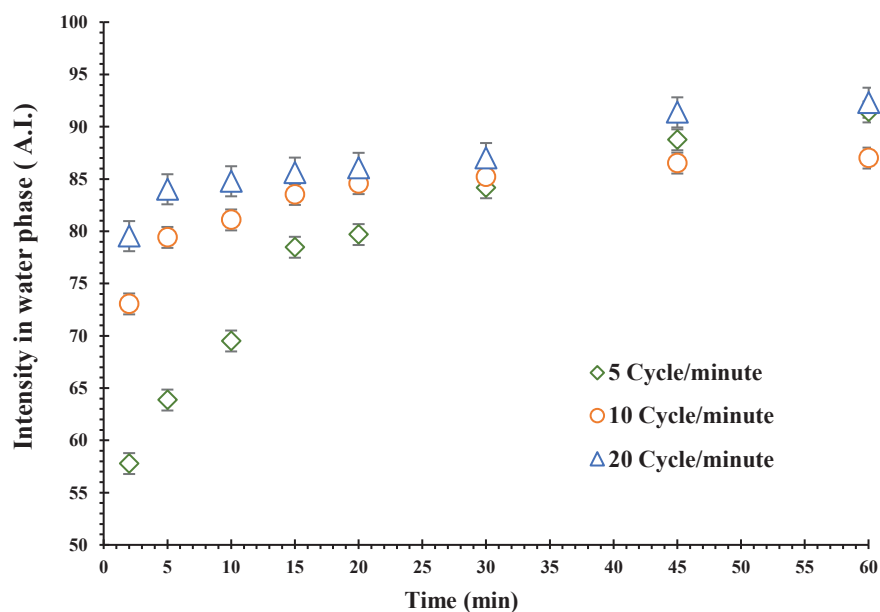


**Figure 35.** Effect of the speed of the rocker on the partition efficiency of rhodamine B in the water phase. The concentration of rhodamine B was 10 mM, with volumes of 70  $\mu$ L and 100  $\mu$ L for the octanol and water phase, respectively. Results are based on n=3.

It can be seen from the figures that in all cases the equilibrium is reached over 2-times faster than in static conditions. In the case of 10 and 20 cycles/min, the time was reduced to approximately 30 and 20 minutes, respectively (up to 6-fold). Clearly, the partition of rhodamine B increases with the speed with the rotation frequency. The higher rotation frequency, the faster partition efficiency. The main reason is that the perfusion enhances the

mixing between inlet and outlet reservoirs and equilibrates the phases faster than in static conditions. Diffusion also plays a role in this process, but equilibration is fastened with the perfusion process.

It can be noted from the images that the fluorescent intensity in octanol is higher than intensity in water due to the quantum yield, which describes the inherent emission of the fluorescence of a molecule in the specific medium. In non-polar solvent like octanol, fluorescent molecules can show higher fluorescence yields because non-polar solvents can offer a more favorable condition for efficient energy transfer and emission of fluorescence. Also, the intensity in the center of the reservoirs appears to be lower than at the edge. This is caused mainly by an optical effect created by the meniscus of liquid present in the reservoir, which results in a higher height at the edge of the reservoir than the center of the reservoir. It is a common phenomenon known as optical diffraction, where the emitted fluorescence that goes to the detectors gets diffuse along the edge indicating that higher intensity.

To conclude, based on the results, 5 cycles/min was considered relatively slow, and equilibrium could be reached at a certain point faster than in the static condition. However, 10 cycle/min was the best option to reach equilibrium relatively quickly, avoiding excessive agitation, and leading to desirable results. Higher cycling rate (20 cycle/min) was discarded due to the rapid agitation can introduce undesired turbulence, resulting in an increase chance of disturbance of the homogeneity of the solvents. Also, it can cause the formation of microdroplets and/or unequal mixing, leading to a decrease in the accuracy and reproducibility of the experiments.

### **3.6.4. Up-scalability and parallelization of the microfluidic device**

#### **3.6.4.1. Redesign of the dynamic microfluidic device**

One drawback of this microfluidic design is that it can only be manufactured using 3D printing techniques. The internal channels and structure of the chip make it impossible to manufacture hundreds or thousands of units using more cost-effective microfabrication techniques (i.e. CNC machining or microinjection molding). Clearly, 3D printing reduced the time for the development of the design and its fabrication during the initial phases of the prototyping of the microfluidic chip. However, 3D printing is not suitable to produce this design in large quantities. The throughput is relatively slow, and the costs get higher compared to traditional fabrication techniques. Besides, undesired defects can be randomly encountered with the

printed chips. Some examples can be the layer separation and splitting, blobs and zits on the surface, curling and rough corners, shrinkage, over-polymerization or bending of the chip due to internal tensions in the structure. Therefore, to scale up the fabrication of the device the design should be tailored to be produced using mass-production manufacturing, such as micromilling, etching (glass and silicon) or embossing and injection molding (thermoplastics). The first consideration contemplated was to expose the internal channels that are not accessible from outside at any axis. This limits the range of possibilities since 3D microfluidic structures should be moved to a 2.5D (structures with varying width but identical depth) where at least one of the sides of the channel is exposed. Microfluidic chips with different depths are possible but each depth can be an increase the complexity of the manufacturing process. Additionally, a final step for closing is required as explained in the experimental section.

After several trials, the design was adapted to a parallel configuration between the octanol and the water channels. This architecture was found to be the best compromise between scalability and functionality of the device. This configuration minimizes the manufacturing cost, especially for inject molding while increasing substantially the contact area at the interphase between the O/W phases, maximizing the partition of the target molecules. Pictures of the new design can be observed in Figure (36-A). The design consists of two overlapped channels with no physical separation where each channel is connected to two cylindric chambers. The lower channel belongs to the water phase with a total volume of 70  $\mu\text{L}$  (including the adjacent small channels and part of the cylindric chamber). The upper is for the octanol phase with a total volume of approximately 11  $\mu\text{L}$ . The area of contact between octanol and water phases is 10.5  $\text{mm}^2$ . The extreme of each channel is independently connected to two cylindric reservoirs. There is a total of 4 chambers for each chip. The microfluidic chip was fabricated using CNC machining on a piece of PMMA. This material was selected due to its transparency to visible light, clear finish after the fabrication and, more importantly, the similar water contact angle of the 3D printed material. The microfluidic chip was finally sealed with a hPET. It is worth mentioning that the same design was also fabricated using replica molding technique. For that, a 3D printed mold was used to cast PDMS. After peeling and assembly via plasma activation, the microfluidic device was fabricated successfully. The complete processes for the fabrication of PMMA and PDMS microfluidic chips are explained in Chapter 2. Herein and unless stated, all the results with this design were carried out using the PDMS substrate. To increase the throughput of the

device, the design was multiplexed in a multiwell plate format. Each unit was then disposed according to the ANSI/SLAS Microplate Standards for 384 well microplates. With this configuration, the microfluidic chip was successfully parallelized up to 56 subunits in a single device. Figure (36-B) shows the configuration and the manufactured plate in PMMA. The developed device is compatible with standard laboratory equipment (HPLC, autoinjectors, microplate readers, spectrophotometers, liquid handling robots, ...) to be applicable as a high-throughput screening tool.

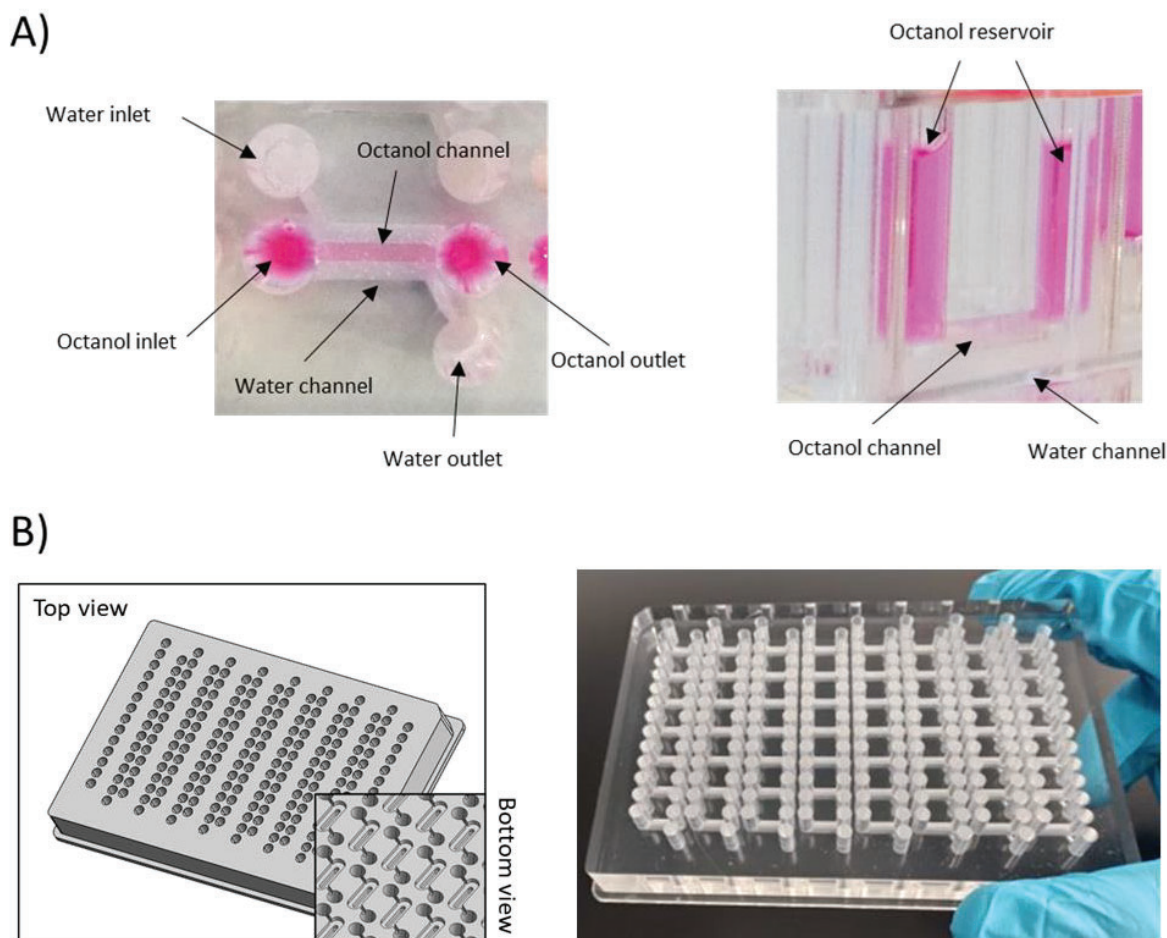


**Figure 36.** Up-scalable version of the microfluidic design. **A)** Picture of the microfluidic design from upper view (left) and front view (right). The white/transparent part represents the water channel. The pink part represents the octanol channel. The inlet and outlet of the channels correspond to the chambers (reservoirs). **B)** Top and bottom view of the microfluidic plate CAD design (left) and picture of the plate (right) with the 56 subunits fabricated with PMMA.

As seen in the picture, this design complies with the microfluidic requirements of the microfluidic technique. The parallel configuration of microfluidic chip showed a correct distribution of the two phases. Specifically, the interface between the O/W channels exhibited a correct interaction without any apparent emulsion from the microscope images. Likewise, any formation of microdroplets was found in either water or octanol reservoirs after the rocking the plate at 10 cycles/min. The evaluation of the distribution of molecules in octanol-water equilibrium using this design is described in the next section.

### 3.6.4.2. Molecule partition and influence of initial concentration of molecules in microscale octanol-water equilibrium systems

To evaluate the partition and also the influence of initial concentration in the new configuration of the microfluidic device, saturated solutions (water saturated octanol and vice versa) and rhodamine B dye were used to monitor the partitioning behavior. Three different concentration of rhodamine B were selected (1, 10 and 100 mM in octanol phase) with a perfusion set at 10 cycle/min with  $\pm 7$  degrees of inclination. Similar to the previous experiments, the fluorescent dyes were chosen because they can be easily visualized using fluorescence microscopy and thus their distribution behavior can be monitored in situ. Initially, the octanol solution contained 10 mM of rhodamine B whereas the aqueous phase was pure water. Results are summarized in Table (25) and Figures (37) and (38).

**Table 25.** Average values of the Intensity of rhodamine B in water over the time at different concentration of analyte in dynamic conditions. Results are based on n=3.

Time (min)	1 mM	SD	10 mM	SD	100 mM	SD
0	40.5	2.5	64.2	3.8	91.1	7.4
5	42.7	2.0	81.6	2.4	107.5	6.8
10	48.0	2.2	91.7	2.2	116.1	4.8
15	51.4	1.4	108.0	2.5	124.1	3.6
20	56.5	0.9	112.5	0.9	124.5	2.9
30	57.7	1.0	115.2	1.1	127.1	2.5
40	59.3	0.8	115.7	1.4	128.6	0.2
50	60.0	0.1	116.9	0.4	128.7	0.2
60	59.9	0.1	118.3	0.1	129.2	0.2

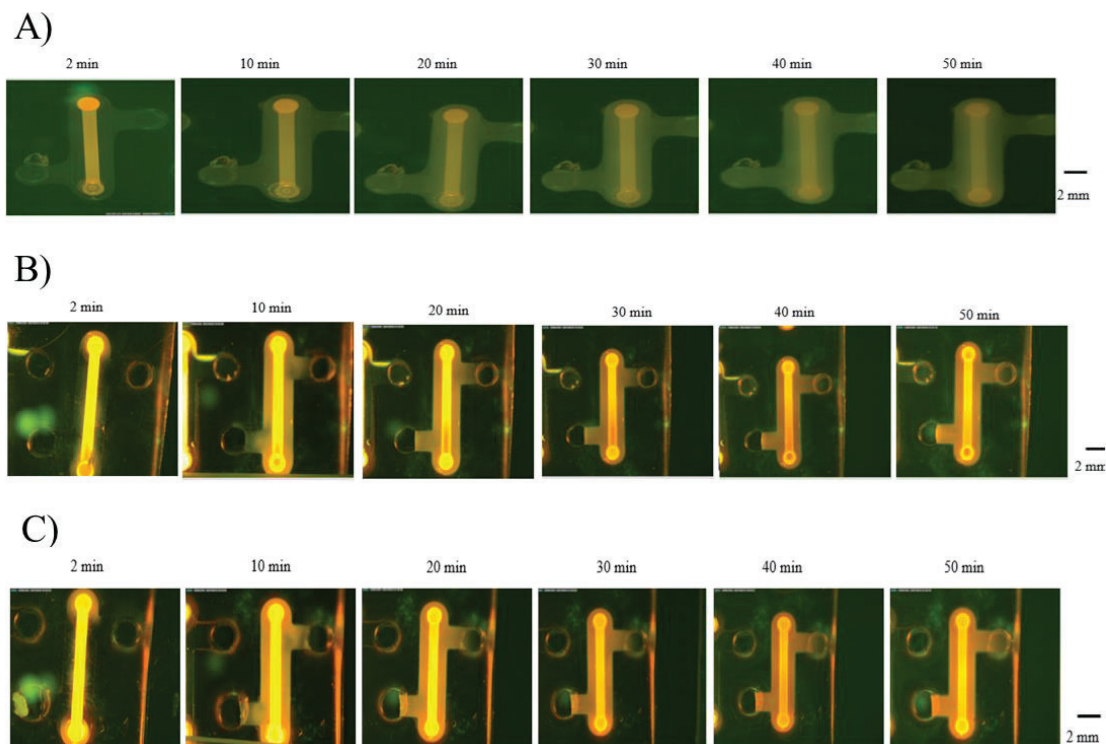


**Figure 37.** Sequence of pictures (from 0 to 60 min) of the microfluidic device at different concentrations of 1 (A), 10 (B) and 100 (C) mM. The device was under perfusion (rotation of 10 cycle/min with an inclination of  $\pm 7^\circ$ ).

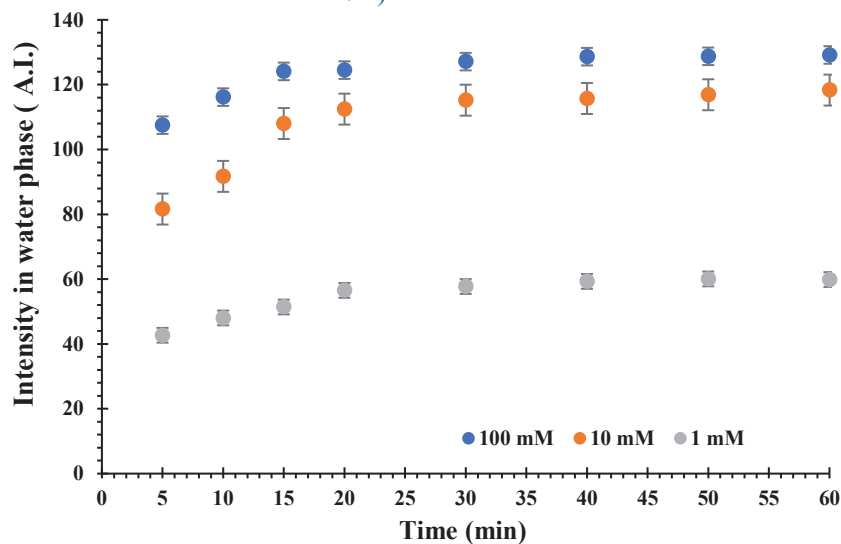


**Figure 38.** Intensity of rhodamine B in the water phase depends on the concentration of analyte in dynamic perfusion. Initially, rhodamine B was only present in the octanol phase. The volumes were 70  $\mu\text{L}$  and 100  $\mu\text{L}$  for the octanol and water phase, respectively. Results are based on  $n=3$ .

According to the results, dye concentration had some influence on the partitioning, with higher concentrations resulting in greater dye mass transfer from the octanol phase to water phase and lower concentrations resulting in less dye mass transfer. The maximum transfer by time occurred at 100 mM concentration, followed by 10 mM and finally 1 mM. It is clear that the change of the initial concentration of rhodamine B influenced their partition in octanol-water equilibriums. A higher initial concentration of a rhodamine B in the system leads to an increased amount of that molecule partitioning. This is governed by the partition coefficient, which represents the ratio of concentrations of a compound in octanol to that in water at equilibrium. In other terms, starting with a higher concentration of rhodamine B leads to higher partition rate or distribution from the octanol to the water phase until equilibrium is reached. This phenomena can be seen from the figure, where the slope for the concentration of 100 mM was highest compared to the others.

Besides, the initial concentration of rhodamine B can also impact the time it takes to reach equilibrium in octanol-water partitioning. Generally, a higher initial concentration often leads to longer time to achieve equilibrium. This is because the process of partitioning involves molecules moving between the two phases until a balance is reached. At higher initial concentrations, there are a greater number of rhodamine B molecules trying to move from the octanol to the water phase, making the system take more time to settle into equilibrium. However, a different behaviour was observed using the microfluidic device. It can be appreciated from the figure that similar equilibration times were obtained regardless the initial concentration of rhodamine B. There can be two reason why this is happening. The first is that octanol and water volumes are in the range of the microscale and the higher volumes to surface ration can increase the speed of the molecule distribution. The second reason can be due to the bi-directional perfusion. The composition of rhodamine B in octanol and water fluids at the interface are influenced by factors such as the diffusion rate, the characteristics of the partitioning system, and the kinetics of the partitioning process. Since the partition is happening only at the intersection, the equilibrium can be reach when the whole solution (including the reservoirs) are at the a constant concentration. For that, both lower and higher initial concentrations may be conditioned to the same mixing at the reservoir region and the same attainment of equilibrium during the partitioning process.

So, the conclusions from these results demonstrates that the proposed design with this microfluidic methodology allows the evaluation of molecule partition of fluorescent compounds, achieving high efficiency in terms of constant flow rate and assessing partition dynamics from the dye intensity. Furthermore, the equilibrium in octanol/water partition can be reached faster, with very limited amount of solvents, and in a more cost-effective and high-throughput way. It is important to note that the partition coefficient itself is a constant characteristic of a specific solute and solvent system, and it does not change with the initial concentration. The initial concentration affects the amount of the molecule partitioned, but the partition coefficient remains constant under given conditions. In the next section, the microfluidic plate was validated for the determination of partition coefficients in drugs using different approaches.

### 3.6.5. Determination of the octanol-water partition coefficient ( $\log P_{o/w}$ ) of pharmaceutical drugs by microfluidics and HPLC.

The lipophilicity can be evaluated from the determination of the octanol-water partition coefficient, commonly known as  $\log P_{o/w}$ . To calculate this parameter using the microfluidic device, the partitioning solvents (water and n-octanol-saturated water) were both introduced from the inlet reservoirs, and the target compound was loaded to only one of solvents. In order to determine the  $\log P_{o/w}$  value, the microfluidic channels were perfused using in the rocker at 10 cycles/min and 7 degrees of inclination to accelerate the partition equilibrium. Finally, the amount of compound in each phase can be measured after equilibration time using a spectrophotometer or HPLC. The  $\log P_{o/w}$  can be calculated from the equations (51) and (53) depending on the analyte, as mentioned in chapter I.

The volume of the phases and/or analyte loss play crucial roles in the determination of octanol-water partition coefficients. If the volumes or the amount of target compound changes unexpectedly during the partition, the determination of the partition coefficient could be inaccurate. Consistent and accurate volume measurements are essential for calculating concentrations and determining the partition coefficients accurately. Deviations in volumes can lead to errors in concentration calculations, affecting the reliability of the partition coefficient determination. The loss of analytes during the experimental process can result in underestimation of concentrations and, consequently, incorrect partition coefficient values. Furthermore, it compromises the reliability of results, as the actual amount of the compound partitioning between octanol and water may be underestimated. This can lead to inaccurate conclusions about the compound's behavior in the system. This consideration is particularly important when working with small-scale systems, such as microfluidic setups, where precise control over volumes and minimizing losses become even more critical.

Therefore, solvents and target analytes must be compatible with the materials commonly used in microfluidic to avoid possible evaporations, absorption, adsorption, or undesired chemical reaction. In the case of 3D printed material, the effects of the octanol or organic molecules are unknown as the composition of the material is a trade secret from the provider. Also, no information can be found in the literature. Previous studies in Leitat laboratories suggested that organic molecules with high lipophilicity or those with strong polar groups could be absorbed

in the 3D printed material. In any case, none of those observations were clearly demonstrated with the 3D printed chips. For this reason, we decided to test them for the determination of the partition coefficient, keeping the perpendicular microfluidic architecture validated in previous sections. Regarding materials such as PMMA or PDMS, octanol exhibits good compatibility and does not give significant chemical interactions or degradation. However, PDMS is known for its high permeability to gases, and this property can be detrimental for some volatile solvents or analytes. Furthermore, PDMS is a silicon-based elastomer with microscopic pores within the structure, which can affect its absorption properties. This material, typically hydrophobic, repels water, but it can absorb non-polar compounds or liquids. Some papers have demonstrated the absorption of drugs in the structure of PDMS<sup>166-169</sup>. In the case of PMMA, is considered resistant to non-polar and weakly polar molecules. However, prolonged exposure to strong polar molecules, such as acetone, chlorinated compounds, or aromatic substances, may induce to irreversible stress cracking and embrittlement<sup>170</sup>. Consequently, another material was selected to carry out the determination of  $\log P_{o/w}$  values for the up-scalable design, namely the parallel design.

Teflon was perfect choice as it complies with all requirements needed for lipophilicity measures (hydrophobic nature, chemical resistance and non-porous). So, a microfluidic plate made from Teflon with 56 independent partition units was manufactured. The device can be seen in Figure (39). The main drawback from this material is its lack of transparency. However, since the determine of the  $\log P_{o/w}$  can be done by HPLC, transparency is not a constraint.

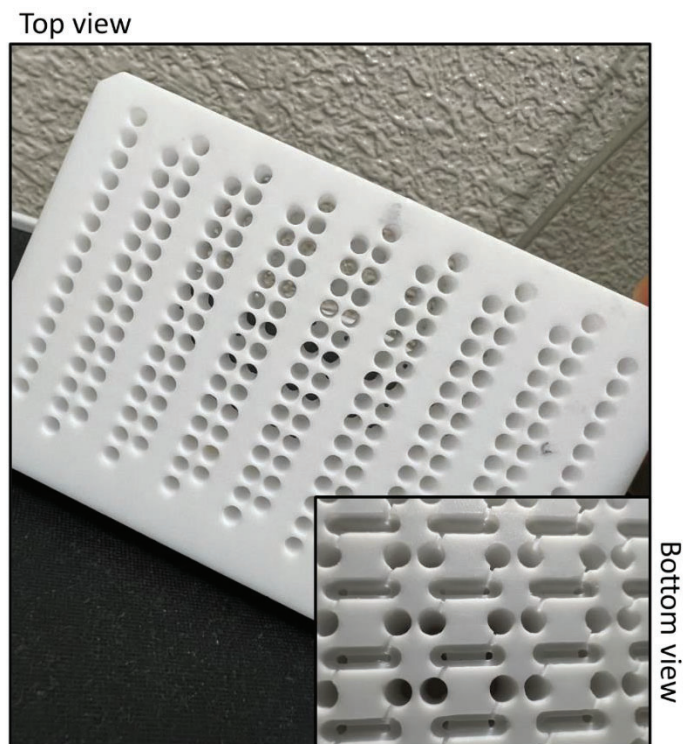


**Figure 39.** Teflon microfluidic plate with parallel design consisting of 56 O/W subunits. The device was fabricated using CNC machining as a manufacturing technique.

In the following section, the microfluidic devices were utilized to measure the partition coefficient ( $\log P_{o/w}$ ) by HPLC of 6 pharmaceutical drugs. The chemical structures of pharmaceutical drugs are presented in Figure (40). Proxyphylline, hydrocortisone, acetophenone, prednisolone, griseofulvin and butyrophenone were chosen because they have a well standardize  $\log P_{o/w}$  value and they cover a wide range lipophilicity, between - 0.07 to 2.8, useful for the microfluidic approach. This range permits proof of concept study of a group of drugs that exhibit moderate to high lipophilicity. This range is frequently preferred for pharmaceutical industries during drug discovery and development processes.

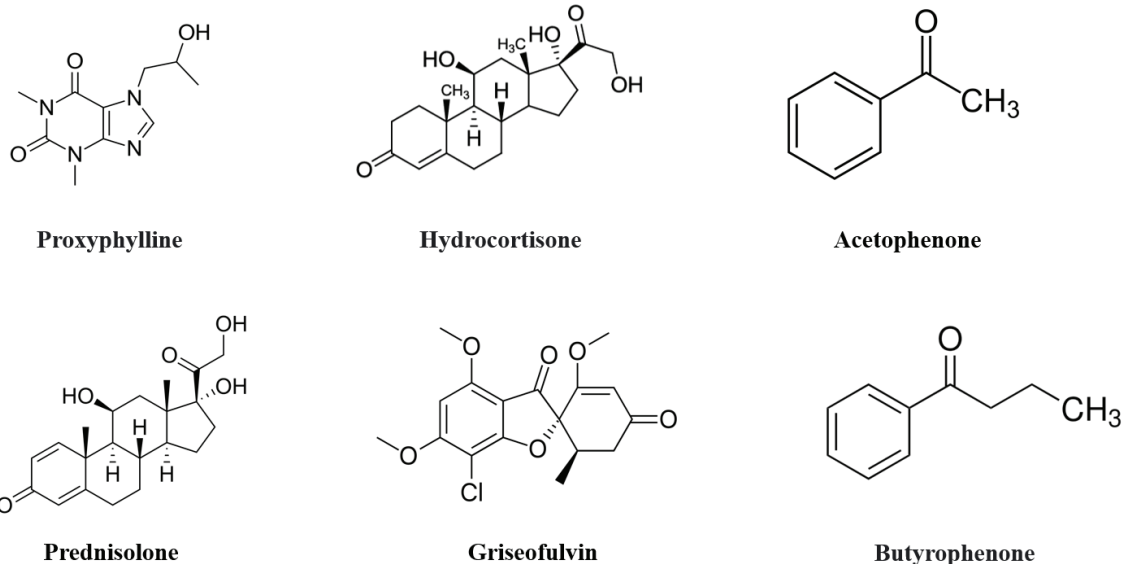


**Figure 40.** The chemical structure of pharmaceutical drugs that were used for the determination of the partition coefficient  $\log P_{o/w}$ .

### 3.6.5.1. Determination of $\log P_{o/w}$ of pharmaceutical drugs

The determination of  $\log P_{o/w}$  gives decisive knowledge on a drug physicochemical nature, which may be applied to develop drug's design and formulation, estimate drug behavior in vivo, and increase drug safety and effectiveness. The process began with injecting each sample partition in triplicate onto the two separate configuration plates, a perpendicular design (using the 3D printed device), and a parallel design (using Teflon as preferred material). The lipophilicity of the pharmaceutical drugs was determined by triplicate and compared to the literature values. More details about the experiments can be found in chapter II.

The  $\log P_{o/w}$  values of the drugs were determined with the perpendicular 3D printing plate, in which the sample was loaded in water saturated octanol at the concentration of 1 mM. The partition was carried out in triplicate for each sample, firstly at 20/70  $\mu\text{L}$  ( $V_o/V_w$ ) volumes. The results are summarized in Table (26). As can be seen, there was good agreement with literature with those substances ranging from  $\log P_{o/w}$  values of 0.0 to 1.6 (proxiphylline, hydrocortisone, and acetophenone). However, for those drugs with higher  $\log P_{o/w}$  values (prednisolone, griseofulvin and butyrophenone) the results obtained were lower than the ones from literature. To identify the possible causes from this disagreement, the partition was also determined by triplicate for prednisolone, griseofulvin and butyrophenone at two other octanolic volumes (50/70 and 5/70  $\mu\text{L}$ ,  $V_o/V_w$ ).

**Table 26.** Results of the log  $P_{o/w}$  using the 3DP microfluidic plate with the perpendicular design determined by HPLC. The log  $P_{o/w}$  were determined at three diverse O/W volumes ( $V_o/V_w$ ). The sample was prepared at the concentration of 1 mM in water saturated octanol and compared to the literature value. The values highlighted in blue correspond to an inaccurate determination of the partition coefficient. Standard deviation is based on n=3.

Compound name	(50/70 $\mu$ L)	SD	(20/70 $\mu$ L)	SD	(5/70 $\mu$ L)	SD	Lit
Proxyphylline			-0.064	0.03			-0.07
Hydrocortisone			1.58	0.09			1.53
Acetophenone			1.49	0.01			1.58
Prednisolone	1.65	0.04	1.65	0.04	1.70	0.03	1.83
Griseofulvin	1.69	0.01	1.69	0.01	2.30	0.02	2.20
Butyrophenone	2.15	0.01	2.15	0.01	2.81	0.05	2.77

In lower octanol volumes (5/70  $\mu$ L,  $V_o/V_w$ ), the log  $P_{o/w}$  results were in good agreement with literature values. Whereas, with higher volumes (50/70  $\mu$ L,  $V_o/V_w$ ), the log  $P_{o/w}$  results did not change from those determined initially. One explanation of this phenomena can be related to the chemical compatibility of microfluidic material. The exposure to chemicals, especially the one with high log  $P_{o/w}$  values, can cause the material to swell or even dissolve, causing the loss of analyte due to the absorption. Consequently, the loss of analyte leads to an underestimated value. Another reason is that the ratio of octanol-water volume change during the assay. A loss of octanol volume can reduce this ration and cause an underestimation of the log  $P_{o/w}$  value. Adjusting the volumes of water and octanol is an important factor to consider in highly lipophilic compounds <sup>91</sup>. Hydrophobic drugs have a strong attraction to nonpolar solvents like octanol, and the increase in water volume and decrease in octanol improve the polarity of the aqueous phase, promoting the solubility and partitioning of lipophilic compounds into the aqueous phase, resulting a more reliable log  $P_{o/w}$  result.

Table (27) shows the log  $P_{o/w}$  values determined with the Teflon microfluidic plate in the parallel configuration. As in the previous section, the drug was loaded in water saturated octanol at the concentration 1 mM. The partition was carried out in triplicate for each sample, firstly at 20/100  $\mu$ L ( $V_o/V_w$ ) volumes. Similar behavior was observed compared to the results found in Table (26). As can be seen, there was good agreement with literature with those substances ranging from log  $P_{o/w}$  values of 0.0 to 1.6 (proxyphylline, hydrocortisone, and acetophenone).

However, for those drugs with higher log  $P_{o/w}$  values (prednisolone, griseofulvin and butyrophenone) the results obtained were also underestimated. To investigate if the octanol volume caused any effect on the determination, the partition was also determined by triplicate for prednisolone, griseofulvin and butyrophenone in two other octanol volumes  $V_o/V_w$  (100/100 and 5/100  $\mu\text{L}$ ).

**Table 27.** Log  $P_{o/w}$  values determined by HPLC using the Teflon microfluidic plate with the parallel design. Three different octanol volumes ( $V_o/V_w$ ) were used and the sample was prepared 1 mM in water saturated octanol. Results were compared to the ones in literature. The values highlighted in blue correspond to an inaccurate determination of the partition coefficient. Standard deviation is based on  $n=3$ .

Compound name	(100/100 $\mu\text{L}$ )	SD	(20/100 $\mu\text{L}$ )	SD	(5/100 $\mu\text{L}$ )	SD	Lit
Proxyphylline			-0.095	0.01			- 0.07
Hydrocortisone			1.45	0.06			1.53
Acetophenone			1.52	0.01			1.58
Prednisolone	1.99	0.029	1.70	0.08	1.89	0.03	1.83
Griseofulvin	0.87	0.129	1.95	0.03	2.15	0.01	2.20
Butyrophenone	1.84	0.020	2.22	0.02	2.89	0.02	2.77

Again, the results with low octanol volume (5/100  $\mu\text{L}$ ,  $V_o/V_w$ ) showed good agreement with the log  $P_{o/w}$  values found in the literature. In the case of Teflon, this phenomenon cannot be explained by the chemical compatibility with the material. Consequently, the most plausible reason is that the hydrophobic drugs have a strong attraction to octanol, promoting the solubility and partitioning of lipophilic compounds into the aqueous phase. To prevent this effect, the analyte can be solubilized in the octanol phase instead of the aqueous one.

Table (28) shows the log  $P_{o/w}$  values determined with the Teflon microfluidic plate using the parallel design. This time, the drugs were prepared in octanol saturated water at the same concentration, 1 mM. The partition was carried out in triplicate for each sample and at the same three volumes (100/100, 20/100, and 5/100  $\mu\text{L}$ ) as Table (27).

**Table 28.** Log  $P_{o/w}$  values determined by HPLC using the Teflon microfluidic plate with the parallel design at three different octanol volumes ( $V_o/V_w$ ). The drug was prepared at the concentration of 1mM in octanol saturated water. Results were compared to the literature value. The values highlighted in blue correspond to an inaccurate determination of the partition coefficient.

Compound name	(100/100 $\mu$ L)	SD	(20/100 $\mu$ L)	SD	(5/100 $\mu$ L)	SD	Lit
Proxyphylline	-0.08	0.004	-0.076	0.01			-0.07
Hydrocortisone	1.50	0.03	1.40	0.06			1.53
Acetophenone	1.58	0.01	1.59	0.04			1.58
Prednisolone	1.82	0.03	1.73	0.06	1.80	0.07	1.83
Griseofulvin	1.81	0.02	2.23	0.07	2.20	0.01	2.20
Butyrophenone	2.31	0.05	2.31	0.02	2.25	0.05	2.77

This time there was good agreement with literature log  $P_{o/w}$  values ranging from 0.0 - 1.8 at any octanol volume. In higher log  $P_{o/w}$  values (only for griseofulvin and butyrophenone), the results showed again inaccurate values. Furthermore, the log  $P_{o/w}$  for butyrophenone at low octanol volume (5/100  $\mu$ L,  $V_o/V_w$ ) showed a difference of 0.5 log  $P_{o/w}$  units with respect to the literature. The differences in the determination of log  $P_{o/w}$  when a drug is dissolved in octanol compared to water can be primarily attributed to the drug's hydrophobicity<sup>91,103</sup>.

The ratio of O/W volume can have a significant impact in the determination of partition coefficients. The organic phase can become more polar as the amount of octanol increases relative to the volume of water. This improved polarity might change the compound's solubility in the organic phase and affect its partition coefficient<sup>91</sup>. For instance, a higher octanol volume will reduce the partition coefficient of a compound. The reason for that is that the compound tends to stay in the aqueous phase because it has a less polar phase. In contrast, if the quantity of water is larger, the aqueous phase will be more polar than the organic phase, affecting compound solubility and partitioning. Absolutely, as the volume of water increases, the partition coefficient of a compound will increase. This is due to the compound movement to partition into the organic phase, which is the less polar phase. Thus, the volume of octanol/water in a partition investigation can have a significant effect on compound partition activity, and the variations in volume of any phase can affect the polarity of the system and the compound solubility and therefore its partition coefficient.

When evaluating hydrophobic compounds, using a lesser volume of octanol and a larger volume of water is preferable since the hydrophobic molecule has a stronger attraction for non-polar solvents such as octanol and a lower attraction for polar solvents such as water. As a result, hydrophobic chemicals are exposed to more water, which improves their solubility and aids in their partitioning into the aqueous phase. Using more water and less octanol can also help to decrease the potential for emulsions or other types of mixing between the two phases, which can interfere with accurate partition coefficient measurements.

As a result, the fabrication method and design employed could have an influence on the overall performance and efficiency of drug transport within the chip. Thus, the partition coefficient may be calculated using a microfluidic chip and an HPLC in the range (-0.07 - 2.89). Likewise, this application is desirable in the calculation of partition coefficients since it saves time, uses less solvents, and is a high throughput method.



## 4. CONCLUSION

The main objective of this thesis was the development of fast and precise analytical methods for the determination of the acidity ( $pK_a$ ) and lipophilicity ( $\log P_{o/w}$ ) of drugs of potential pharmacokinetic interest.

Regarding the determination of acid-base constants the following conclusions have been reached:

- It is demonstrated that IS-CE can be used as a high-throughput technique for  $pK_a$  determination at different concentrations of methanol-water mixtures (0-90% v/v methanol), as well as acetonitrile-water mixtures (0-90% v/v acetonitrile), which are solvents of interest in liquid chromatographic separations. The  $pK_a$  of acid and base internal standards have been successfully anchored to the ones determined potentiometrically in both the methanol-water mixture and the acetonitrile-water mixture. Consequently, the identified set of compounds can be reliably employed as internal standards for precise and routine  $pK_a$  measurements using capillary electrophoresis in methanol-water mixture and acetonitrile-water buffers.
- The IS-CE approach has been proven that it can be used as a high-throughput technique for determining the  $pK_a$  of highly insoluble compounds with water solubility less than  $10^{-6}$  mol L<sup>-1</sup>, determining the  $pK_a$  values in methanol-water mixtures (0-40% of methanol). This method provides accurate relative acid and base scales and is useful for precise measurements of  $pK_a$  in methanol-water media, offering a fast and consistent alternative to other approaches.
- The IS-CE approach has proven that it can be used to determine the  $pK_a$  values of organic bases at different concentrations of methanol-water mixture and acetonitrile-water mixture (0-90% v/v), used to evaluate the resolution, selectivity, and separation capabilities of HPLC columns. The results prove that the IS-CE method guarantees appropriate pH conditions for ionizable compounds, aids in selecting mobile phase compositions, and provides accurate  $pK_a$  values for several analytes due to internal standards and buffer pH identification.

In the case of the determination of lipophilicity, we have arrived at the following conclusions:

- The proposed methodology allows the fabrication of microfluidic devices to determine the  $\log P_{o/w}$  of drugs in a range going from -0.07 to 2.89 using low amounts of solvents ( $\mu\text{L}$  range) and analytes (1 mM) in very short time (20 minutes). Using the microfluidic device is a big step forward in this analytical chemistry field; where the equilibrium in octanol/water partition can be reached faster and more cost-effective with less waste generated.
- The results obtained show good similarity with the literature values, but the phase ratio between octanol and water must be optimized depending on the  $\log P_{o/w}$  value. Future studies may increase the applicability of this method to drugs with extreme  $\log P_{o/w}$  values. For instance, the same methodology can be applied to prepare similar designs with larger capacity that allows higher octanol to water (or vice-versa) volume ratios for assessment of compounds with very low ( $\log P_{o/w} < 0$ ) or very high ( $\log P_{o/w} > 2.5$ ) lipophilicities.
- The prototypes demonstrated a rapid and efficient partition of fluorescent molecules between octanol and water phases, regardless of the materials used. However, careful considerations must be taken with the chemical compatibility with octanol and the analytes determined. The results show that the perfusion produced by the gravitational flow increases the efficiency of the partition in octanol/water phases. Furthermore, analyte concentration has some influence on partitioning dynamics. However, it does not affect the determine the drug  $\log P_{o/w}$ .
- The configuration of the microfluidic design can be parallelized in multiple O/W subunits in the format of a multi-well plate (up to 56), making it compatible with standard laboratory equipment such as HPLC samplers, and therefore applicable as a high-throughput screening tool. Also, the microfluidic device can be couplet with HPLC, enabling the simultaneous determination of  $\log P_{o/w}$  of different drugs in different O/W proportions.



## References

1. Tarbit MH, Berman J. High-throughput approaches for evaluating absorption, distribution, metabolism and excretion properties of lead compounds. *Current opinion in chemical biology*. 1998;2(3):411-416. doi:10.1016/s1367-5931(98)80017-3
2. Smith DA, Jones BC, Walker DK. Design of drugs involving the concepts and theories of drug metabolism and pharmacokinetics. *Medicinal research reviews*. 1996;16(3):243-266. doi:10.1002/(sici)1098-1128(199605)16:3<243:aid-med2>3.3.co;2-r
3. Stenberg P, Norinder U, Luthman K, Artursson P. Experimental and computational screening models for the prediction of intestinal drug absorption. *Journal of medicinal chemistry*. 2001;44(12):1927-1937. doi:10.1021/jm001101a
4. Abdel-Rahman SM, Kauffman RE. The integration of pharmacokinetics and pharmacodynamics: understanding dose-response. *Annu Rev. Pharmacol. Toxicol.* 2004;44(1):111-136. doi:10.1146/annurev.pharmtox.44.101802.121347
5. Alsenz J, Kansy M. High throughput solubility measurement in drug discovery and development. *Advanced drug delivery reviews*. 2007;59(7):546-567. doi:10.1016/j.addr.2007.05.007
6. Avdeef A. Physicochemical profiling (solubility, permeability and charge state). *Current topics in medicinal Chemistry*. 2001;1(4):277-351. doi:10.2174/1568026013395100
7. Lin JH, Lu AY. Role of pharmacokinetics and metabolism in drug discovery and development. *Pharmacological reviews*. 1997;49(4):403-449. doi: 0031-6997/97/4904-0403\$03.00/0

8. Hamilton HW, Steinbaugh BA, Stewart BH, et al. Evaluation of physicochemical parameters important to the oral bioavailability of peptide-like compounds: implications for the synthesis of renin inhibitors. *Journal of medicinal chemistry*. 1995;38(9):1446-1455. doi:10.1021/jm00009a005
9. Cabot JM, Subirats X, Fuguet E, Rosés M. High throughput determination  $\log P_{o/w}/pK_a/\log D_{o/w}$  of drugs by combination of UHPLC and CE methods. *ADMET & DMPK*, 2014, vol.2, num.2, p.98-106. 2014. doi.org/10.5599/admet.2.2.44
10. Avdeev A. Solubility, permeability and charge state. In: *Absorption and drug development*. John Wiley & Sons, Hoboken, New Jersey; 2012. doi:10.1002/9781118286067
11. Deák K, Takács-Novák K, Tihanyi K, Noszál B. Physico-chemical profiling of antidepressive sertraline: solubility, ionization, lipophilicity. *Medicinal chemistry*. 2006;2(4):385-389. doi:10.2174/157340606777723997
12. Kerns EH, Di L. Physicochemical profiling: Overview of the screens. *Drug Discovery Today: Technologies*. 2004;1(4):343-348. doi:10.1016/j.ddtec.2004.08.011
13. Melo Diaz JM. *Suitability of Capillary Electrophoresis for the Determination of  $pK_a$  of Pharmaceuticals at Biorelevant Temperatures*. [Master dissertation]. Barcelona, Spain. University of Barcelona; 2018.
14. Krämer SD. Absorption prediction from physicochemical parameters. *Pharmaceutical science & technology today*. 1999;2(9):373-380. doi:10.1016/s1461-5347(99)00188-1
15. Ferlenghi, F. *An Integrated Approach for Physico-Chemical Profiling in Drug Discovery*. [Doctoral dissertation]. Parma, Italy. University of PARMA; 2019.
16. Sangster JM. Octanol-water partition coefficients: *Fundamentals and physical chemistry*. John Wiley & Sons. 1997;32(11):842. doi.org/10.1016/s0223-5234(97)82764-x

17. Curatolo W. Physical chemical properties of oral drug candidates in the discovery and exploratory development settings. *Pharmaceutical science & technology today*. 1998;1(9):387-393. doi:10.1016/s1461-5347(98)00097-2
18. Shoghi Kalkhoran E. *Physico-Chemical Characterization of Drugs: Acidity and Solubility*. [Doctoral dissertation]. Barcelona, Spain. University of Barcelona; 2013.
19. Takacs-Novak K. Physicochemical profiling in drug research and development. Physico-chemical methods in drug discovery and development. *1st ed. Zagreb: IAPC Publishing*. 2012:1-59. doi.org/10.5599/obp.7.1
20. Wan H, Ulander J. High-throughput pK<sub>a</sub> screening and prediction amenable for ADME profiling. *Expert opinion on drug metabolism & toxicology*. 2006;2(1):139-155. doi.org/10.1517/17425255.2.1.139
21. Kibbey CE, Poole SK, Robinson B, Jackson JD, Durham D. An integrated process for measuring the physicochemical properties of drug candidates in a preclinical discovery environment. *Journal of pharmaceutical sciences*. 2001;90(8):1164-1175. doi:10.1002/jps.1070
22. Wan H, Holmen AG. High throughput screening of physicochemical properties and in vitro ADME profiling in drug discovery. *Combinatorial chemistry & high throughput screening*. 2009;12(3):315-329. doi:10.2174/138620709787581701
23. Manallack DT. The pK<sub>a</sub> distribution of drugs: Application to drug discovery. *Perspectives in medicinal chemistry*. 2007. doi/10.1177/1177391X0700100003
24. Lipinski CA. Drug-like properties and the causes of poor solubility and poor permeability. *Journal of pharmacological and toxicological methods*. 2000;44(1):235-249. doi:10.1016/s1056-8719(00)00107-6
25. De La Nuez A, Rodríguez R. Current methodology for the assessment of ADME-Tox properties on drug candidate molecules. *Biotechnología Aplicada*. 2008;25(2):97-110.

26. Kerns EH. High throughput physicochemical profiling for drug discovery. *Journal of pharmaceutical sciences*. 2001;90(11):1838-1858. doi:10.1002/jps.1134
27. Xu X, Hurtubise RJ. Influence of organic solvents in the capillary zone electrophoresis of polycyclic aromatic hydrocarbon metabolites. *Journal of Chromatography A*. 1998;829(1-2):289-299. doi:10.1016/s0021-9673(98)00794-8
28. Honore S, Tjørnelund J, Bjørnsdottir I. Selectivity enhancement in capillary electrophoresis using non-aqueous media. *TrAC Trends in Analytical Chemistry*. 1996;15(4):175-180. doi.org/10.1016/0165-9936(96)00006-4
29. Sykora D, Tesarová E, Armstrong DW. Practical considerations of the influence of organic modifiers on the ionization of analytes and buffers in reversed-phase LC. *LC GC NORTH AMERICA*. 2002;20(10):974-981.
30. Albishri A, Cabot JM, Fuguet E, Rosés M. Determination of the aqueous  $pK_a$  of very insoluble drugs by capillary electrophoresis: Internal standards for methanol-water extrapolation. *Journal of Chromatography A*. 2022;1665:462795. doi: 10.1016/j.chroma.2021.462795.
31. Babić S, Horvat AJ, Pavlović DM, Kaštelan-Macan M. Determination of  $pK_a$  values of active pharmaceutical ingredients. *TrAC Trends in Analytical Chemistry*. 2007;26(11):1043-1061. doi:10.1016/j.trac.2007.09.004
32. Poole SK, Patel S, Dehring K, Workman H, Poole CF. Determination of acid dissociation constants by capillary electrophoresis. *Journal of Chromatography A*. 2004;1037(1-2):445-454. doi:10.1016/j.chroma.2004.02.087
33. Rosés M, Bosch E. Influence of mobile phase acid–base equilibria on the chromatographic behavior of protolytic compounds. *Journal of Chromatography A*. 2002;982(1):1-30. doi:10.1016/s0021-9673(02)01444-9

34. Rived F, Canals I, Bosch E, Rosés M. Acidity in methanol–water. *Analytica chimica acta*. 2001;439(2):315-333. doi:10.1016/s0003-2670(01)01046-7
35. Rosés M. Determination of the pH of binary mobile phases for reversed-phase liquid chromatography. *Journal of Chromatography A*. 2004;1037(1-2):283-298. doi:10.1016/j.chroma.2003.12.063
36. Avdeef A, Box KJ, Comer J, et al. PH-metric log P 11.  $pK_a$  determination of water-insoluble drugs in organic solvent–water mixtures. *Journal of pharmaceutical and biomedical analysis*. 1999;20(4):631-641. doi:10.1016/s0731-7085(98)00235-0
37. Bosch E, Bou P, Allemann H, Rosés M. Retention of ionizable compounds on HPLC. pH scale in methanol– water and the  $pK_a$  and pH values of buffers. *Analytical Chemistry*. 1996;68(20):3651-3657. doi.org/10.1021/ac960104l
38. Cabot Canyelles JM, Fuguet i Jordà E, Rosés Pascual M, Smejkal P, Breadmore MC. Novel instrument for automated  $pK_a$  determination by internal standard capillary electrophoresis. *Analytical Chemistry*, 2015, vol.87, num.12, p.6165-6172. 2015. doi.org/10.1021/acs.analchem.5b00845
39. Cabot JM, Fuguet E, Roses M. Internal standard capillary electrophoresis as a high-throughput method for  $pK_a$  determination in drug discovery and development. *ACS combinatorial science*. 2014;16(10):518-525. doi.org/10.1021/co500059p
40. Reijenga J, Van Hoof A, Van Loon A, Teunissen B. Development of methods for the determination of  $pK_a$  values. *Analytical chemistry insights*. 2013;8:ACI. S12304. doi:10.4137/ACI.S12304
41. Subirats X, Fuguet E, Rosés M, Bosch E, Ràfols C. Methods for  $pK_a$  determination (I): Potentiometry, spectrophotometry, and capillary electrophoresis. In: *Reference Module in Chemistry, Molecular Sciences and Chemical Engineering*. Elsevier; 2015:1-10. doi.org/10.1016/b978-0-12-409547-2.11559-8

42. Erdemgil FZ, Şanlı S, Şanlı N, et al. Determination of  $pK_a$  values of some hydroxylated benzoic acids in methanol–water binary mixtures by LC methodology and potentiometry. *Talanta*. 2007;72(2):489-496. doi.org/10.1016/j.talanta.2006.11.007
43. Takács-Novák K, Box KJ, Avdeef A. Potentiometric  $pK_a$  determination of water-insoluble compounds: Validation study in methanol/water mixtures. *International journal of pharmaceutics*. 1997;151(2):235-248. doi:10.1016/s0378-5173(97)04907-7
44. Kraft A. The determination of the  $pK_a$  of multiprotic, weak acids by analyzing potentiometric acid-base titration data with difference plots. *Journal of chemical education*. 2003;80(5):554. doi:10.1021/ed080p554
45. Canals I, Oumada FZ, Rosés M, Bosch E. Retention of ionizable compounds on HPLC. 6. pH measurements with the glass electrode in methanol–water mixtures. *Journal of Chromatography A*. 2001;911(2):191-202. doi:10.1016/s0021-9673(00)01271-1
46. Albert A. The determination of ionization constants: A laboratory manual. *Springer Science & Business Media*; 2012. doi.org/10.1007/978-94-009-5548-6
47. Fuguet E, Ràfols C, Bosch E, Rosés M. A fast method for  $pK_a$  determination by capillary electrophoresis. *Chemistry & biodiversity*. 2009;6(11):1822-1827. doi:10.1002/cbdv.200900120
48. Lebanov L, Fuguet E, Melo JM, Rosés M. Determination of acidity constants at 37° C through the internal standard capillary electrophoresis (IS-CE) method: Internal standards and application to polyprotic drugs. *Analyst*. 2020;145(17):5897-5904. doi.org/10.1039/d0an00918k
49. Nowak P, Woźniakiewicz M, Kościelniak P. Application of capillary electrophoresis in determination of acid dissociation constant values. *Journal of chromatography A*. 2015;1377:1-12. doi:10.1016/j.chroma.2014.12.032

50. Nowak PM, Klag M, Kózka G, Gołąb M, Woźniakiewicz M. The first online capillary electrophoresis-microscale thermophoresis (CE-MST) method for the analysis of dynamic Equilibria—The determination of the acidity constant of fluorescein isothiocyanate. *Molecules*. 2022;27(15):5010. doi:10.3390/molecules27155010
51. Tagliaro F, Manetto G, Crivellente F, Smith FP. A brief introduction to capillary electrophoresis. *Forensic science international*. 1998;92(2-3):75-88. doi:10.1016/s0379-0738(98)00010-3
52. Paul D, Grossman JC, eds. Capillary Electrophoresis. *Theory and Practice*. Vol 352. Academic Press; 1992. doi.org/10.1006/abio.1993.1033
53. Štěpánová S, Kašička V. Application of capillary electromigration methods for physicochemical measurements. In: *Capillary electromigration separation methods*. Elsevier; 2018:547-591. doi.org/10.1016/b978-0-12-809375-7.00024-1
54. Lian D, Zhao S. Capillary electrophoresis based on nucleic acid detection for diagnosing human infectious disease. *Clinical Chemistry and Laboratory Medicine (CCLM)*. 2016;54(5):707-738. doi.org/10.1515/cclm-2015-0096
55. Lebanov L. *Set-up of the Capillary Electrophoresis Internal Standard Method for pK<sub>a</sub> Determination of Drugs at Biorelevant Temperatures*. [Master dissertation]. Barcelona, Spain. University of Barcelona; 2016.
56. Xuan X, Li D. Joule heating effects on peak broadening in capillary zone electrophoresis. *Journal of Micromechanics and Microengineering*. 2004;14(8):1171. doi:10.1088/0960-1317/14/8/008
57. N.A. Guzman (Ed.), *Capillary Electrophoresis Technology*, Marcel Dekker, New York, 1993.
58. Kalsoom U. *Analysis of plant analytes using capillary electrophoresis and high-performance liquid chromatography*. [Doctoral dissertation]. Joondalup, Western Australia. Edith Cowan University; 2015.

59. Quirino JP, Terabe S. Approaching a million-fold sensitivity increase in capillary electrophoresis with direct ultraviolet detection: Cation-selective exhaustive injection and sweeping. *Analytical Chemistry*. 2000;72(5):1023-1030. doi:10.1021/ac990344b
60. Evenhuis CJ, Haddad PR. Joule heating effects and the experimental determination of temperature during CE. *Electrophoresis*. 2009;30(5):897-909. doi:10.1002/elps.200800643
61. Evenhuis CJ, Guijt RM, Macka M, Marriott PJ, Haddad PR. Temperature profiles and heat dissipation in capillary electrophoresis. *Analytical Chemistry*. 2006;78(8):2684-2693. doi:10.1021/ac052075x
62. Rogacs A, Santiago JG. Temperature effects on electrophoresis. *Analytical Chemistry*. 2013;85(10):5103-5113. doi:10.1021/ac400447k
63. Evenhuis CJ, Hruska V, Guijt RM, et al. Reliable electrophoretic mobilities free from joule heating effects using CE. *Electrophoresis*. 2007;28(20):3759-3766. doi:10.1002/elps.200700343
64. Burgi DS, Salomon K, Chien R. Methods for calculating the internal temperature of capillary columns during capillary electrophoresis. *Journal of liquid chromatograph*. 1991;14(5):847-867. doi:10.1080/01483919108049291
65. Jones AE, Grushka E. Nature of temperature gradients in capillary zone electrophoresis. *Journal of Chromatography A*. 1989;466:219-225. doi:10.1016/s0021-9673(01)84618-5
66. Knox JH, McCormack KA. Temperature effects in capillary electrophoresis. 1: Internal capillary temperature and effect upon performance. *Chromatographia*. 1994;38:207-214. doi:10.1007/bf02290338
67. Nowak PM, Biel I, Kózka G, Klag M, Woźniakiewicz M. Influence of pH measurement inaccuracy on the values of acidity constant determined on the basis of electrophoretic and thermophoretic data. *Microchemical Journal*. 2022;181:107689. doi: 10.1016/j.microc.2022.107689.

68. Cabot JM, Fuguet E, Ràfols C, Rosés M. Fast high-throughput method for the determination of acidity constants by capillary electrophoresis. II. acidic internal standards. *Journal of Chromatography A*. 2010;1217(52):8340-8345. doi:10.1016/j.chroma.2010.10.060
69. Ishihama Y, Nakamura M, Miwa T, Kajima T, Asakawa N. A rapid method for  $pK_a$  determination of drugs using pressure-assisted capillary electrophoresis with photodiode array detection in drug discovery. *Journal of pharmaceutical sciences*. 2002;91(4):933-942. doi:10.1002/jps.10087
70. Herrero-Martínez JM, Sanmartin M, Rosés M, Bosch E, Ràfols C. Determination of dissociation constants of flavonoids by capillary electrophoresis. *Electrophoresis*. 2005;26(10):1886-1895. doi:10.1002/elps.200410258
71. Rossini E, Bochevarov AD, Knapp EW. Empirical conversion of  $pK_a$  values between different solvents and interpretation of the parameters: Application to water, acetonitrile, dimethyl sulfoxide, and methanol. *ACS omega*. 2018;3(2):1653-1662. doi.org/10.1021/acsomega.7b01895
72. Subirats X, Bosch E, Rosés M. Retention of ionisable compounds on high-performance liquid chromatography XVII: Estimation of the pH variation of aqueous buffers with the change of the methanol fraction of the mobile phase. *Journal of Chromatography A*. 2007;1138(1-2):203-215. doi.org/10.1016/j.chroma.2006.10.087
73. Subirats X, Bosch E, Rosés M. Retention of ionisable compounds on high-performance liquid chromatography: XVI. estimation of retention with acetonitrile/water mobile phases from aqueous buffer pH and analyte  $pK_a$ . *Journal of Chromatography A*. 2006;1121(2):170-177. doi.org/10.1016/j.chroma.2006.03.126
74. Sarmini K, Kennedler E. Influence of organic solvents on the separation selectivity in capillary electrophoresis. *Journal of Chromatography A*. 1997;792(1-2):3-11. doi:10.1016/s0021-9673(97)00720-6

75. Bjørnsdottir I, HonoréHansen S. Comparison of separation selectivity in aqueous and non-aqueous capillary electrophoresis. *Journal of Chromatography A*. 1995;711(2):313-322. doi:10.1016/0021-9673(95)98953-t
76. Scriba GK. Nonaqueous capillary electrophoresis–mass spectrometry. *Journal of Chromatography A*. 2007;1159(1-2):28-41. doi:10.1016/j.chroma.2007.02.005
77. Riekkola M. Recent advances in nonaqueous capillary electrophoresis. *Electrophoresis*. 2002;23(22-23):3865-3883. doi:10.1002/elps.200290007
78. Sarmini K, Kenndler E. Capillary zone electrophoresis in mixed aqueous–organic media: Effect of organic solvents on actual ionic mobilities, acidity constants and separation selectivity of substituted aromatic acids.: I. methanol. *Journal of Chromatography A*. 1998;806(2):325-335. doi.org/10.1016/s0021-9673(98)00060-0
79. Cantu MD, Hillebrand S, Carrilho E. Determination of the dissociation constants ( $pK_a$ ) of secondary and tertiary amines in organic media by capillary electrophoresis and their role in the electrophoretic mobility order inversion. *Journal of Chromatography A*. 2005;1068(1):99-105. doi:10.1016/j.chroma.2004.12.009
80. Grob M, Steiner F. Characteristics of the electroosmotic flow of electrolyte systems for nonaqueous capillary electrophoresis. *Electrophoresis*. 2002;23(12):1853-1861. doi:10.1002/1522-2683(200206)23:12<1853::AID-ELPS1853>3.0.CO;2-D
81. Lister AS, Dorsey JG, Burton DE. Current measurement of nonaqueous solvents: Applications to capillary electrophoresis and electrochromatography. *Journal of High -Resolution Chromatography*. 1997;20(10):523-528. doi:10.1002/jhrc.1240201003
82. Porras SP, Jyske P, Riekkola M, Kenndler E. Mobility and ionization constant of basic drugs in methanol. application of nonaqueous background electrolytes for capillary zone electrophoresis based on a conventional pH scale. *Journal of Microcolumn Separations*. 2001;13(4):149-155. doi:10.1002/mcs.1034

83. Fuguet E, Subirats X, Ràfols C, Bosch E, Rosés M. Methods for  $pK_a$  determination (II): Sparingly soluble compounds and high-throughput approaches. In: *Reference Module in Chemistry, Molecular Sciences and Chemical Engineering*. Elsevier; 2015. doi.org/10.1016/b978-0-12-409547-2.11631-2
84. Han SY, Liang C, Zou K, Qiao JQ, Lian HZ, Ge X. Influence of variation in mobile phase pH and solute  $pK_a$  with the change of organic modifier fraction on QSRRs of hydrophobicity and RP-HPLC retention of weakly acidic compounds. *Talanta*. 2012;101:64-70. doi.org/10.1016/j.talanta.2012.08.051
85. Rosés M, Subirats X, Bosch E. Retention models for ionizable compounds in reversed-phase liquid chromatography: Effect of variation of mobile phase composition and temperature. *Journal of chromatography A*. 2009;1216(10):1756-1775. doi:10.1016/j.chroma.2008.12.042
86. Subirats X, Rosés M, Bosch E. On the effect of organic solvent composition on the pH of buffered HPLC mobile phases and the  $pK_a$  of Analytes—A review. *Separation & Purification Reviews*. 2007;36(3):231-255. doi.org/10.1080/15422110701539129
87. Alimuddin M, Grant D, Bulloch D, Lee N, Peacock M, Dahl R. Determination of log  $D$  via automated microfluidic liquid– liquid extraction. *Journal of medicinal chemistry*. 2008;51(16):5140-5142. doi.org/10.1021/jm8005228
88. Koziolk M, Alcaro S, Augustijns P, et al. The mechanisms of pharmacokinetic food-drug interactions—A perspective from the UNGAP group. *European Journal of Pharmaceutical Sciences*. 2019;134:31-59. doi.org/10.1016/j.ejps.2019.04.003
89. Poole SK, Poole CF. Separation methods for estimating octanol-water partition coefficients. *Journal of Chromatography B*. 2003;797(1-2):3-19. doi:10.1016/j.jchromb.2003.08.032
90. Smith RN, Hansch C, Ames MM. Selection of a reference partitioning system for drug design work. *Journal of Pharmaceutical Science*. 1975;64(4):599-606. doi:10.1002/jps.260064040

91. Amézqueta S, Subirats X, Fuguet E, Rosés M, Ràfols C. Octanol-water partition constant. *Liquid-phase extraction*. 2020;183-208. doi.org/10.1016/b978-0-12-816911-7.00006-2
92. Lambert WJ. Modeling oil—water partitioning and membrane permeation using reversed-phase chromatography. *Journal of Chromatography A*. 1993;656(1-2):469-484. doi.org/10.1016/0021-9673(93)80814-o
93. Hansch C, Leo AJ, Hoekman D. Exploring QSAR: Fundamentals and Applications in Chemistry and Biology. *American Chemical Society*; 1995. doi.org/10.1021/jm950902o
94. Bradbury SP. Quantitative structure-activity relationships and ecological risk assessment: An overview of predictive aquatic toxicology research. *Toxicology letters*. 1995;79(1-3):229-237. doi:10.1016/0378-4274(95)03374-t
95. Perkins R, Fang H, Tong W, Welsh WJ. Quantitative structure-activity relationship methods: Perspectives on drug discovery and toxicology. *Environmental Toxicology and Chemistry: An International Journal*. 2003;22(8):1666-1679. doi.org/10.1897/01-171
96. Kempnińska D, Chmiel T, Kot-Wasik A, Mroz A, Mazerska Z, Namieśnik J. State of the art and prospects of methods for determination of lipophilicity of chemical compounds. *TrAC Trends in Analytical Chemistry*. 2019;113:54-73. doi:10.1016/j.trac.2019.01.011
97. Berthod A, Carda-Broch S. Determination of liquid–liquid partition coefficients by separation methods. *Journal of chromatography A*. 2004;1037(1-2):3-14. doi:10.1016/j.chroma.2004.01.001
98. Politeo O, Bektašević M, Carev I, Jurin M, Roje M. Phytochemical composition, antioxidant potential and cholinesterase inhibition potential of extracts from mentha pulegium L. *Chemistry & biodiversity*. 2018;15(12):e1800374. doi.org/10.1002/cbdv.201800374

99. Mannhold R, Poda GI, Ostermann C, Tetko IV. Calculation of molecular lipophilicity: State-of-the-art and comparison of log P methods on more than 96,000 compounds. *Journal of Pharmaceutical Science*. 2009;98(3):861-893. doi:10.1002/jps.21494
100. Pallicer JM, Rosés M, Ràfols C, Bosch E, Pascual R, Port A. Evaluation of log  $P_{o/w}$  values of drugs from some molecular structure calculation software. *ADMET and DMPK*. 2014;2(2):107-114. doi.org/10.5599/admet.2.2.45
101. Poole CF, Atapattu SN. Determination of physicochemical properties of small molecules by reversed-phase liquid chromatography. *Journal of Chromatography A*. 2020;1626(461427):461427. doi:10.1016/j.chroma.2020.461427
102. SINGH A. Lipophilicity profiling on the basic of OECD guideline of haridra hydroalcoholic extract on the basis of its marker compound curcumin. *Innovare Journal of Ayurvedic Science*. 2018; (6). ISSN- 2321-6832
103. Andrés A, Rosés M, Ràfols C, et al. Setup and validation of shake-flask procedures for the determination of partition coefficients (log  $D$ ) from low drug amounts. *European Journal of Pharmaceutical Sciences*. 2015;76:181-191. doi.org/10.1016/j.ejps.2015.05.008
104. Lane S. Chapter 5 coupled chromatography-mass spectrometry techniques for the analysis of combinatorial libraries. *Handbook of Analytical Separations*. 2000;1:127-161. doi: 10.1016/S1567-7192(00)80008-X.
105. Hitzel L, Watt AP, Locker KL. An increased throughput method for the determination of partition coefficients. *Pharmaceutical research*. 2000;17:1389-1395. doi:10.1023/a:1007546905874
106. Dohta Y, Yamashita T, Horiike S, Nakamura T, Fukami T. A system for Log  $D$  screening of 96-well plates using a water-plug aspiration/injection method combined with high-performance liquid

chromatography– mass spectrometry. *Analytical Chemistry*. 2007;79(21):8312-8315.

doi.org/10.1021/ac0709798

107. Alelyunas YW, Pelosi-Kilby L, Turcotte P, Kary M, Spreen RC. A high throughput dried DMSO log *D* lipophilicity measurement based on 96-well shake-flask and atmospheric pressure photoionization mass spectrometry detection. *Journal of Chromatography A*. 2010;1217(12):1950-1955.

doi:10.1016/j.chroma.2010.01.071

108. Low YWI, Blasco F, Vachaspati P. Optimized method to estimate octanol water distribution coefficient (log *D*) in a high throughput format. *European Journal of Pharmaceutical Sciences*. 2016;92:110-116.

doi:10.1016/j.ejps.2016.06.024

109. Wang S, Chen Z, Tang X, Shi L, Zhang L, Yao M. Rapid determination of partition coefficients of pharmaceuticals by phase distribution and microchip capillary electrophoresis with contactless conductivity detection. *Journal of separation science*. 2013;36(21-22):3615-3622. doi:10.1002/jssc.201300720

110. Marine NA, Klein SA, Posner JD. Partition coefficient measurements in picoliter drops using a segmented flow microfluidic device. *Analytical Chemistry*. 2009;81(4):1471-1476. doi:10.1021/ac801673w

111. Ràfols C, Bosch E, Ruiz R, et al. Acidity and hydrophobicity of several new potential antitubercular drugs: Isoniazid and benzimidazole derivatives. *Journal of Chemical & Engineering Data*. 2012;57(2):330-338. doi.org/10.1021/je200827u

112. Clarke FH. Ionization constants by curve fitting: Application to the determination of partition coefficients. *Journal of Pharmaceutical Sciences*. 1984;73(2):226-230. doi:10.1002/jps.2600730221

113. Avdeef A. PH-metric log *P*. part 1. Difference plots for determining ion-pair octanol-water partition coefficients of multiprotic substances. *Quantitative Structure-Activity Relationships*. 1992;11(4):510-517.

doi:10.1002/qsar.2660110408

114. COMER JA, Avdeef A, Box KJ. Limits for successful measurement of  $pK_a$  and  $\log P$  by pH-metric titration. *American laboratory (Fairfield)*. 1995;27(6):36C-36I. doi.org/10.1007/978-94-011-1472-1\_87
115. Valkó K. Application of high-performance liquid chromatography based measurements of lipophilicity to model biological distribution. *Journal of chromatography A*. 2004;1037(1-2):299-310. doi:10.1016/j.chroma.2003.10.084
116. Pagliara A, Khamis E, Trinh A, Carrupt P, Tsai R, Testa B. Structural properties governing retention mechanisms on RP-HPLC stationary phases used for lipophilicity measurements. *Journal of Liquid Chromatography & Related Technologies*. 1995;18(9):1721-1745. doi:10.1080/10826079508010002
117. *OECD Guideline for the Testing of Chemicals*. 117; partition coefficient (n-octanol/water): High performance liquid chromatography (HPLC) method.; 2004. doi.org/10.1787/9789264069824-en
118. Donovan SF, Pescatore MC. Method for measuring the logarithm of the octanol–water partition coefficient by using short octadecyl–poly (vinyl alcohol) high-performance liquid chromatography columns. *Journal of Chromatography A*. 2002;952(1-2):47-61. doi.org/10.1016/s0021-9673(02)00064-x
119. Valko K, Du C, Bevan C, Reynolds DP, Abraham MH. Rapid method for the estimation of octanol/water partition coefficient ( $\log P_{oct}$ ) from gradient RP-HPLC retention and a hydrogen bond acidity term ( $\sigma_{\alpha 2H}$ ). *Current medicinal chemistry*. 2001;8(9):1137-1146. doi.org/10.2174/0929867013372643
120. Wiczling P, Markuszewski MJ, Kaliszan R. Determination of  $pK_a$  by pH gradient reversed-phase HPLC. *Analytical Chemistry*. 2004;76(11):3069-3077. doi.org/10.1021/ac049807q
121. Canals I, Portal JA, Bosch E, Rosés M. Retention of ionizable compounds on HPLC. 4. mobile-phase pH measurement in methanol/water. *Analytical Chemistry*. 2000;72(8):1802-1809. doi.org/10.1021/ac990943i

122. Sarmini K, Kenndler E. Capillary zone electrophoresis in mixed aqueous–organic media: Effect of organic solvents on actual ionic mobilities and acidity constants of substituted aromatic acids: III. 1-propanol. *Journal of Chromatography A*. 1998;818(2):209-215. doi.org/10.1016/s0021-9673(98)00565-2
123. Herbert BJ, Dorsey JG. N-octanol-water partition coefficient estimation by micellar electrokinetic capillary chromatography. *Analytical Chemistry*. 1995;67(4):744-749. doi.org/10.1021/ac00100a009
124. Poole SK, Durham D, Kibbey C. Rapid method for estimating the octanol–water partition coefficient ( $\log P_{o/w}$ ) by microemulsion electrokinetic chromatography. *Journal of Chromatography B: Biomedical Sciences and Applications*. 2000;745(1):117-126. doi.org/10.1016/s0378-4347(00)00072-4
125. Ishihama Y, Oda Y, Uchikawa K, Asakawa N. Evaluation of solute hydrophobicity by microemulsion electrokinetic chromatography. *Analytical Chemistry*. 1995;67(9):1588-1595. doi.org/10.1021/ac00105a018
126. Ishihama Y, Oda Y, Asakawa N. Hydrophobicity of cationic solutes measured by electrokinetic chromatography with cationic microemulsions. *Analytical Chemistry*. 1996;68(23):4281-4284. doi.org/10.1021/ac960447j
127. El Tayar N, Marston A, Bechalany A, Hostettmann K, Testa B. Use of centrifugal partition chromatography for assessing partition coefficients in various solvent systems. *Journal of Chromatography A*. 1989;469:91-99. doi.org/10.1016/s0021-9673(01)96443-x
128. Kubáň P, Hauser PC. Evaluation of microchip capillary electrophoresis with external contactless conductivity detection for the determination of major inorganic ions and lithium in serum and urine samples. *Lab on a Chip*. 2008;8(11):1829-1836. doi.org/10.1039/b802973c
129. Cai Z, Li Y, Li L, Chen Z. Analysis of arecoline in semen arecae decoction pieces by microchip capillary electrophoresis with contactless conductivity detection. *Journal of Pharmaceutical Analysis*. 2012;2(5):356-360. doi.org/10.1016/j.jpha.2012.07.003

130. Kubáň P, Karlberg B, Kubáň P, Kubáň V. Application of a contactless conductometric detector for the simultaneous determination of small anions and cations by capillary electrophoresis with dual-opposite end injection. *Journal of Chromatography A*. 2002;964(1-2):227-241. doi:10.1016/s0021-9673(02)00656-8
131. Kubáň P, Hauser PC. Contactless conductivity detection for analytical techniques: Developments from 2010 to 2012. *Electrophoresis*. 2013;34(1):55-69. doi.org/10.1002/elps.201200358
132. Mayrhofer K, Zemann AJ, Schnell E, Bonn GK. Capillary electrophoresis and contactless conductivity detection of ions in narrow inner diameter capillaries. *Analytical Chemistry*. 1999;71(17):3828-3833. doi:10.1021/ac990019o
133. Kah M, Brown CD. Log *D*: Lipophilicity for ionisable compounds. *Chemosphere*. 2008;72(10):1401-1408. doi.org/10.1016/j.chemosphere.2008.04.074
134. Kralj JG, Sahoo HR, Jensen KF. Integrated continuous microfluidic liquid–liquid extraction. *Lab on a Chip*. 2007;7(2):256-263. doi.org/10.1039/b610888a
135. Stephan K, Saab J, Mokbel I, Goutaudier C, Ferrigno R. Continuous-flow microfluidic method for octanol-water partition coefficient measurement. *Fluid Phase Equilibria*. 2014;380:116-120. doi:10.1016/j.fluid.2014.07.033
136. Payne EM, Wells SS, Kennedy RT. Continuous and automated slug flow nanoextraction for rapid partition coefficient measurement. *Analyst*. 2021;146(18):5722-5731. doi:10.1039/d1an01156a
137. Garstecki P, Fuerstman MJ, Stone HA, Whitesides GM. Formation of droplets and bubbles in a microfluidic T-junction—scaling and mechanism of break-up. *Lab on a Chip*. 2006;6(3):437-446. doi:10.1039/b510841a
138. Zhang Y. Methods for determining n-octanol-water partition constants. *TrAC trends in analytical chemistry*. 1996;15(4):188-196. doi.org/10.1016/0165-9936(96)00003-9

139. Port A, Bordas M, Enrech R, et al. Critical comparison of shake-flask, potentiometric and chromatographic methods for lipophilicity evaluation ( $\log P_{o/w}$ ) of neutral, acidic, basic, amphoteric, and zwitterionic drugs. *European Journal of Pharmaceutical Sciences*. 2018;122:331-340. doi.org/10.1016/j.ejps.2018.07.010
140. Taka K, Avdeel A. Interlaboratory study of  $\log P$  determination by shake-flask and potentiometric methods. *Journal of pharmaceutical and biomedical analysis*. 1996;14(11):1405-1413. doi.org/10.1016/0731-7085(96)01773-6
141. Pallicer JM, Pascual R, Port A, Rosés M, Rafols C, Bosch E. The contribution of the hydrogen bond acidity on the lipophilicity of drugs estimated from chromatographic measurements. *European Journal of Pharmaceutical Sciences*. 2013;48(3):484-493. doi:10.1016/j.ejps.2012.12.008
142. Woo SO, Oh M, Choi Y. Fabricating self-powered microfluidic devices via 3D printing for manipulating fluid flow. *STAR protocols*. 2022;3(2):101376. doi.org/10.1016/j.xpro.2022.101376
143. Mohamed MG, Kumar H, Wang Z, Martin N, Mills B, Kim K. Rapid and inexpensive fabrication of multi-depth microfluidic device using high-resolution LCD stereolithographic 3D printing. *Journal of Manufacturing and Materials Processing*. 2019;3(1):26. doi:10.3390/jmmp3010026
144. Waheed S, Cabot JM, Macdonald NP, et al. 3D printed microfluidic devices: Enablers and barriers. *Lab on a Chip*. 2016;16(11):1993-2013. doi.org/10.1039/c6lc00284f
145. Garrido G, Rafols C, Bosch E. Acidity constants in methanol/water mixtures of polycarboxylic acids used in drug salt preparations: Potentiometric determination of aqueous  $pK_a$  values of quetiapine formulated as hemifumarate. *European journal of pharmaceutical sciences*. 2006;28(1-2):118-127. doi.org/10.1016/j.ejps.2006.01.005
146. Perrin DD, Dempsey B. Buffers for pH and metal ion control. *Journal of the Association of Official Analytical chemistry*. 1975;58(4):864. doi:10.1093/jaoac/58.4.864

147. Ellis KJ, Morrison JF. Buffers of constant ionic strength for studying pH-dependent processes. *Methods Enzymol.* 1982;87:405-426. doi:10.1016/s0076-6879(82)87025-0
148. Khaledi MG. High performance capillary electrophoresis. *John Wiley & Sons, Inc., New York.* 1998;146:303-401.
149. Fuguet E, Ràfols C, Rosés M. A fast high throughput method for the determination of acidity constants by capillary electrophoresis. 3. basic internal standards. *Journal of Chromatography A.* 2011;1218(25):3928-3934. doi.org/10.1016/j.chroma.2011.04.054
150. Longe L, Garnier G, Saito K. Synthesis of lignin-based phenol terminated hyperbranched polymer. *Molecules.* 2019;24(20):3717. doi.org/10.3390/molecules24203717
151. Lim M, Yoon CM, An G, Rhee H. Environmentally benign oxidation reaction of aldehydes to their corresponding carboxylic acids using Pd/C with NaBH<sub>4</sub> and KOH. *Tetrahedron letters.* 2007;48(22):3835-3839. doi.org/10.1016/j.tetlet.2007.03.151
152. Hayun H, Gavrilu I, Silviana S, Siahaan A, Vonna RF, Latifah MI. Synthesis and antioxidant activity study of new mannich bases derived from vanillic acid. *Rasayan J.Chem.* 2020;13(1):131-138. doi.org/10.31788/rjc.2020.1315300
153. Tiemann F. Ueber eine charakteristische reaction des vanillins. *Berichte der deutschen chemischen Gesellschaft.* 1885;18(2):3493-3496. doi:10.1002/cber.188501802336
154. Tiemann F, Haarmann W. Ueber das coniferin und seine umwandlung in das aromatische princip der vanille. *Berichte der deutschen chemischen Gesellschaft.* 1874;7(1):608-623. doi:10.1002/cber.187400701193
155. Li T, Rosazza JP. Biocatalytic synthesis of vanillin. *Applied and Environmental Microbiology.* 2000;66(2):684-687. doi:10.1128/AEM.66.2.684-687.2000

156. Kütt A, Selberg S, Kaljurand I, et al. pKa values in organic chemistry – making maximum use of the available data. *Tetrahedron letters*. 2018;59(42):3738-3748. doi: 10.1016/j.tetlet.2018.08.054.  
doi:10.1016/j.tetlet.2018.08.054
157. Shalaeva M, Kenseth J, Lombardo F, Bastin A. Measurement of dissociation constants ( $pK_a$  values) of organic compounds by multiplexed capillary electrophoresis using aqueous and cosolvent buffers. *Journal of pharmaceutical sciences*. 2008;97(7):2581-2606. doi:10.1002/jps.21287
158. de Nogales V, Ruiz R, Rosés M, Ràfols C, Bosch E. Background electrolytes in 50% methanol/water for the determination of acidity constants of basic drugs by capillary zone electrophoresis. *Journal of Chromatography A*. 2006;1123(1):113-120. doi: 10.1016/j.chroma.2006.05.008.
159. Box KJ, Comer J. Using measured  $pK_a$ ,  $\text{Log}P$  and solubility to investigate supersaturation and predict BCS class. *Current drug metabolism*. 2008;9(9):869-878. doi.org/10.2174/138920008786485155
160. McCalley DV. Influence of sample mass on the performance of reversed-phase columns in the analysis of strongly basic compounds by high-performance liquid chromatography. *Journal of chromatography A*. 1998;793(1):31-46. doi:10.1016/s0021-9673(97)00898-4
161. Buckenmaier SM, McCalley DV, Euerby MR. Overloading study of bases using polymeric RP-HPLC columns as an aid to rationalization of overloading on silica-ODS phases. *Analytical chemistry*. 2002;74(18):4672-4681. doi:10.1021/ac0202381
162. Buckenmaier SM, McCalley DV, Euerby MR. Determination of ionization constants of organic bases in aqueous methanol solutions using capillary electrophoresis. *Journal of Chromatography A*. 2004;1026(1-2):251-259. doi:10.1016/j.chroma.2003.11.007
163. Buckenmaier SM, McCalley DV, Euerby MR. Determination of  $pK_a$  values of organic bases in aqueous acetonitrile solutions using capillary electrophoresis. *Journal of Chromatography A*. 2003;1004(1-2):71-79. doi:10.1016/s0021-9673(03)00717-9

164. Pal'm VA. *Tables of rate and equilibrium constants of heterolytic organic reactions*. Vol 2. Viniti; 1976.
165. Poole CF. Solvent selection for liquid-phase extraction. In: *Liquid-phase extraction*. Elsevier; 2020:45-89. doi.org/10.1016/b978-0-12-816911-7.00002-5
166. Toepke MW, Beebe DJ. PDMS absorption of small molecules and consequences in microfluidic applications. *Lab on a Chip*. 2006;6(12):1484-1486. doi.org/10.1039/b612140c
167. Wang JD, Douville NJ, Takayama S, ElSayed M. Quantitative analysis of molecular absorption into PDMS microfluidic channels. *Annals of biomedical engineering*. 2012;40:1862-1873. doi:10.1007/s10439-012-0562-z
168. Gomez-Sjoberg R, Leyrat AA, Houseman BT, Shokat K, Quake SR. Biocompatibility and reduced drug absorption of sol– gel-treated poly (dimethyl siloxane) for microfluidic cell culture applications. *Analytical chemistry*. 2010;82(21):8954-8960. doi.org/10.1021/ac101870s
169. Grant J, Özkan A, Oh C, Mahajan G, Prantil-Baun R, Ingber DE. Simulating drug concentrations in PDMS microfluidic organ chips. *Lab on a Chip*. 2021;21(18):3509-3519. doi:10.1039/d1lc00348h
170. Ali U, Karim, Khairil Juhanni Bt Abd, Buang NA. A review of the properties and applications of poly (methyl methacrylate)(PMMA). *Polymer Reviews*. 2015;55(4):678-705. doi.org/10.1080/15583724.2015.1031377

